Technical University of Denmark

DTU

Measurement and Modelling of Scaling Minerals

Villafafila Garcia, Ada; Thomsen, Kaj

Publication date:
2005

Document Version
Publisher's PDF, also known as Version of record

[Link back to DTU Orbit](#)

DTU Library
Technical Information Center of Denmark

Measurement and Modeling of Scaling Minerals

Ada Villafáfila García

2005

Ph.D. Thesis

Measurement and Modelling of Scaling Minerals

Ada Villafáfila García

Ph.D. Thesis

31 August 2005

Department of Chemical Engineering
IVC-SEP
Technical University of Denmark
DK-2800 Kgs. Lyngby
Denmark

Preface

This thesis is submitted as partial fulfilment of the requirements for the Ph.D. degree at the Technical University of Denmark.

This work, granted by the IVC-SEP, has been carried out at the Department of Chemical Engineering at the Technical University of Denmark, from October 2002 to September 2005. Associated Professor Kaj Thomsen and Professor Erling H. Stenby have supervised the development of this Ph.D. study. I wish to express my sincere gratitude to my supervisors for their interest, support, quality advice and constructive reviews during these 3 years.

I would like to thank DONGs Jubilæumslegat for financial support for the experimental part of this Ph.D. project. I wish to express my sincere gratitude to Dr. Simon I. Andersen and to technician Povl V. Andersen for their constant help and support during the development of the experimental setup, and for their valuable ideas and challenges.
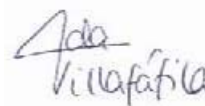
Special mention has to be made to the students Valerie Montel, who searched for some of the information about magnesite, and to Charlotte Coudert and Eduardo Ribeiro, who conducted many of the solubility measurements.

At the Technical University of Denmark, I need to thank all the staff working at IVC-SEP for creating such a nice environment, and especially to the Ph.D. students for their friendship.

I want to show a special mention to my parents, Gonzalo and Mercedes, for their love and support in all the moments of my life. Gracias por todo lo que habéis hecho por mí y por ser como sois. Os quiero.

And last, but not least, I would like to thank Diego for his love, patience, support and friendship during all these years in Denmark, and for making the most out of this experience. Gracias por compartir los mejores años de mi vida, por crear aquellas manos suaves como las uvas. Todo lo llenas tú, todo lo llenas.

<div align="right">Lyngby, September 2005</div>

<div align="right">Ada Villafáfila García</div>

Summary

This Ph.D. project can be divided into two main sections. The first one, covering chapters 2 to 7, deals with the calculation of vapour-liquid, solid-liquid, and speciation equilibria for sparingly soluble salts found in natural waters, under hydrothermal conditions (up to 300ºC and 1000 bar). Chapters 8 and 9 focus on the experimental part of this dissertation, analyzing different experimental procedures to determine salt solubility at high temperature and pressure, and developing a setup to perform those measurements.

The motivation behind both parts of the Ph.D. project is the problem of scale formation found in many industrial processes, and especially in oilfield and geothermal operations. We want to contribute to the study of this problem by releasing a simple and accurate thermodynamic model capable of calculating the behaviour of scaling minerals, covering a wide range of temperature and pressure. Reliable experimental solubility measurements under conditions similar to those found in reality will help the development of strong and consistent models.

Chapter 1 is a short introduction to the problem of scale formation, the model chosen to study it, and the experiments performed.

Chapter 2 is focused on thermodynamics of the systems studied and on the calculation of vapour-liquid, solid-liquid, and speciation equilibria. The effects of both temperature and pressure on the solubility are addressed, and explanation of the model calculations is also given.

Chapter 3 presents the thermodynamic model used in this Ph.D. project. A review of alternative activity coefficient models an earlier work on scale formation is provided. A guideline to the parameter estimation procedure and the number of parameters estimated in the present work are also described.

The prediction of solid-liquid equilibrium of sulphate scaling minerals ($SrSO_4$, $BaSO_4$, $CaSO_4$ and $CaSO_4 \cdot 2H_2O$) at temperatures up to 300ºC and pressures up to 1000 bar is described in chapter 4. Results for the binary systems (M^{2+}, SO_4^{2-})-H_2O; the ternary systems (Na^+, M^{2+}, SO_4^{2-})-H_2O, and (Na^+, M^{2+}, Cl^-)-H_2O; and the quaternary systems (Na^+, M^{2+})(Cl^-, SO_4^{2-})-H_2O, are presented. M^{2+} stands for Ba^{2+}, Ca^{2+}, or Sr^{2+}.

Chapter 5 is devoted to the correlation and prediction of vapour-liquid-solid equilibria for different carbonate systems causing scale problems ($CaCO_3$, $BaCO_3$, $SrCO_3$, and $MgCO_3$), covering the temperature range from 0 to 250ºC and pressures up to 1000 bar. The solubility of CO_2 in pure water, and the solubility of CO_2 in solutions of different salts (NaCl and

Na$_2$SO$_4$) have also been correlated. Results for the binary systems MCO$_3$-H$_2$O, and CO$_2$-H$_2$O; the ternary systems MCO$_3$-CO$_2$-H$_2$O, CO$_2$-NaCl-H$_2$O, and CO$_2$-Na$_2$SO$_4$-H$_2$O; and the quaternary system CO$_2$-NaCl-Na$_2$SO$_4$-H$_2$O are given. M^{2+} stands for Ca^{2+}, Mg^{2+}, Ba^{2+}, and Sr^{2+}. This chapter also includes an analysis of the CaCO$_3$-MgCO$_3$-CO$_2$-H$_2$O system.

Chapter 6 deals with the system NaCl-H$_2$O. Available data for that system at high temperatures and/or pressures are addressed, and sodium chloride solubility calculations are performed up to 2000 bar.

Chapter 7 includes a validation of the model by comparing our predictions to data for real natural waters not used during the parameterization. A very good agreement between our predictions and the field observations is obtained, making us confident about the validity of the model, despite the high temperature, pressure and ionic strength of the tested systems.

In chapter 8, alternative experimental procedures to determine solubility at high temperature and pressure are introduced: Synthetic fluid inclusion technique, electrochemical technique, quartz crystal microbalances, and conductivity measurements.

Chapter 9 describes the experimental procedure followed and the setup employed to determine barite solubility in NaCl solutions at high temperature and pressure. The analytical technique chosen to determine Ba^{2+} concentrations (inductively coupled plasma mass spectrometry) is explained. Few experimental results for the systems NaCl-H$_2$O (used for validation) and BaSO$_4$-NaCl-H$_2$O are reported and analyzed.

Chapter 10 contains the conclusions of the Ph.D. project.

Resume på Dansk

Dette Ph.D. projekt kan inddeles i to hovedsektioner. Den første hovedsektion dækker kapitlerne 2 til 7 og handler om beregning af damp - væske, fast stof – væske og specieringsligevægte for tungt opløselige salte som findes i naturligt forekommende vand under hydrotermiske betingelser (op til 300ºC og 1000 bar). I kapitlerne 8 og 9 fokuseres der på den eksperimentelle del af denne afhandling. Her analyseres forskellige eksperimentelle metoder til bestemmelse af saltopløselighed ved høje temperaturer og tryk. Desuden beskrives udviklingen af en eksperimentel opstilling til at foretage disse målinger.

Motivationen bag begge dele af dette Ph.D. projekt er problemet med aflejring af mineraler fra vandige opløsninger. Det er et problem man møder i mange industrielle processer og ganske særligt inden for olieindvinding og indvinding af geotermisk energi. Vi ønsker at bidrage til studiet af dette problem ved at offentliggøre en simpel, men nøjagtig termodynamisk model der er i stand til at gengive faseforholdene for disse tungt opløselige salte i et bredt temperatur- og trykinterval. Gode eksperimentelle målinger under betingelser, der svarer til de naturlige hydrotermiske betingelser bidrager til at udvikle gode modeller.

Kapitel 1 er en kort introduktion til problemet med aflejring af mineraler samt modellen, der er valgt til at beskrive fænomenet og de eksperimenter, der er blevet udført.

Kapitel 2 fokuserer på den termodynamiske beskrivelse af de pågældende systemer, og på beregning af damp – væske, fast stof – væske og specieringsligevægte. Opløselighedens temperatur- og trykafhængighed beskrives og der gives forklaringer om modelberegningerne.

I kapitel 3 præsenteres den termodynamiske model, der bruges i dette Ph.D. projekt. Der gives et resume af alternative aktivitetskoefficientmodeller og tidligere arbejder om saltaflejringer. Metoden til at bestemme modelparametre beskrives og antallet af parametre diskuteres.

Forudsigelse af fast stof – væske ligevægt for tungt opløselige sulfatmineraler ($SrSO_4$, $BaSO_4$, $CaSO_4$ and $CaSO_4 \cdot 2H_2O$) ved temperaturer op til 300ºC and tryk op til 1000 bar beskrives i kapitel 4. Resultater for de binære systemer (M^{2+}, SO_4^{2-})-H_2O; de ternære systemer (Na^+, M^{2+}, SO_4^{2-})-H_2O, og (Na^+, M^{2+}, Cl^-)-H_2O; samt de kvaternære systemer (Na^+, M^{2+})(Cl^-, SO_4^{2-})-H_2O præsenteres. M^{2+} står for Ba^{2+}, Ca^{2+}, eller Sr^{2+}.

Kapitel 5 indeholder hovedsageligt beskrivelsen af arbejdet med at korrelere og forudsige damp – væske ligevægte for forskellige karbonat systemer, der forårsager problemer med

mineraludfældning ($CaCO_3$, $BaCO_3$, $SrCO_3$, og $MgCO_3$). Korrelationen gælder temperaturintervallet fra 0 til 250ºC and tryk op til 1000 bar. Opløseligheden af CO_2 i rent vand og opløseligheden af CO_2 i forskellige saltopløsninger (NaCl and Na_2SO_4) er også omfattet af denne korrelation. Resultater for de binære systemer MCO_3-H_2O, og CO_2-H_2O; de ternære systemer MCO_3-CO_2-H_2O, CO_2-NaCl-H_2O, og CO_2-Na_2SO_4-H_2O; og det kvaternære system CO_2-NaCl-Na_2SO_4-H_2O rapporteres. M^{2+} står for Ca^{2+}, Mg^{2+}, Ba^{2+}, og Sr^{2+}. Dette kapitel omfatter også en analyse af $CaCO_3$-$MgCO_3$-CO_2-H_2O systemet.

Kapitel 6 drejer sig om NaCl-H_2O systemet. Data for dette system ved høje temperaturer og tryk rapporteres og natriumklorid opløseligheder beregnes op til 2000 bar.

I kapitel 7 valideres den udviklede model ved at sammenligne modelberegninger med data for naturligt forekommende vand, der ikke blev brugt til parameterbestemmelsen. Overensstemmelsen mellem vore forudsigelser og feltobservationerne er udmærket. Da opløsningerne fra disse feltobservationer har høj temperatur, højt tryk og høj ionstyrke styrker disse beregninger vor overbevisning om modellens gyldighed.

I kapitel 8 introduceres alternative eksperimentelle metoder til bestemmelse af opløseligheder ved høj temperatur og tryk: Synthetic fluid inclusion teknikken, den elektrokemiske teknik, metoder med anvendelse af quartz krystal microvægte og ledningsevnemålinger.

Kapitel 9 omhandler den eksperimentelle metode og opstilling der blev anvendt i dette projekt til bestemmelse af barit opløselighed i NaCl opløsninger ved høj temperatur og højt tryk. Den analytiske teknik der blev valgt til bestemmelse af Ba^{2+} koncentrationer (ICP-MS, Inductively Coupled Plasma Mass Spectrometry) forklares. Nogle få eksperimentelle resultater for systemerne NaCl-H_2O og $BaSO_4$-NaCl-H_2O rapporteres og analyseres.

Kapitel 10 indeholder konklusionerne, der kan drages af Ph.D. projektet.

Symbols

Symbol	
α	pressure parameter 1
β	pressure parameter 2
γ	activity coefficient
$\Delta_r{}^0$	standard change in a chemical reaction
μ	chemical potential
ν	stoichiometric coefficient / kinematic viscosity
ϕ	fugacity coefficient / volume fraction
κ	partial molal compressibility
κ	isothermal compressibility
Φ	osmotic coefficient
Θ	constant (200 K) in equation 2-33 / constant (228 K) in equation aI-2
θ	surface area fraction
Ψ	fraction given in equation 3-6 / constant (2600 bar) in equation aI-2
ω	rotational speed
r	volume parameter
q	surface area parameter
u	interaction energy parameter
a	activity
f	fugacity
A	Debye-Hückel parameter / area
b	Debye-Hückel constant
F	Faraday's constant / frequency
N_A	Avogadro's number
N	harmonic
ε_0	vacuum permitivity
d / ρ	density
D	dielectric constant / diffusion coefficient
i_L	limiting current
C	concentration in mol dm^{-3}
	constant (41.84 bar cm3 cal^{-1}) in equation aI-2
c	stiffness
I	ionic stregth
G	Gibbs free energy
H	enthalpy
S	entropy
$H_{i,j}$	Henry's constant of species i in solvent j
C_p	heat capacity
K_e	equilibrium constant
P	pressure
P_0	reference pressure

Symbol	
R	gas constant
s	solubility
T	temperature
T_0	reference temperature
V	partial molar volume
V	volume
x	mole fraction in the liquid phase
y	mole fraction in the vapour phase
M	molar mass / molarity
m	molality
z	coordination number / ionic charge
w	Born coefficient
$\mathring{a}$	ion size parameter in Helgeson's approach
a, b, c, d, e	used in equation 2-42, explained in equation 2-43
$a_{1,j}, a_{2,j}, a_{3,j}, a_{4,j}$	Helgeson's coefficients (equation aI-2)
$c_{1,j}, c_{2,j}$	Helgeson's coefficients (equation aI-2)
b_{il}, b_{ni}, b_{nl}	short-range interaction parameters in Helgeson's approach
Z, Q, Y	solvent Born functions in Helgeson's approach
Γ_γ	mole fraction-molality conversion factor
M^{2+}	$Ba^{2+}, Ca^{2+}, Sr^{2+}, Mg^{2+}$
F	objective function
SD	standard deviation
ASD	average standard deviation
AAD	average absolute deviation
$MAAD$	mean average absolute deviation
RD	residual deviation
CV	variation coefficient
$ndata$	number of data
n	number of moles
l	liquid phase
g	vapor phase
C_{p1}, C_{p2}, C_{p3}	heat capacity coefficients
superscripts	
0	pure component standard state
$*$	solute standard state (mole fraction)
E	excess
IG	ideal gas
∞	infinite dilution
sat	saturation
m	molality scale
subscripts	
w	water
l	liquid phase
c	crystalline

subscripts	
g	vapour phase
dis	disolution reaction
m	molality scale
calc	calculated
exp	experimental
f	formation
r	reaction
q	quartz crystal

1. Introduction

The present Ph.D. project covers both modelling and experimental determinations of the solubility of scaling minerals in natural waters under hydrothermal conditions, in connection with the problem of scale formation. This chapter gives a general introduction to the problem of scale formation, to the model used to estimate the solubility behaviour of scaling minerals, and to the experimental setup developed to determine salt solubility at high temperature and pressure.

1.1 Scale Formation

Scale formation is a common problem in many industrial processes, such as the production of oil (Shams El Din and Mohammed, 1989, Yuan et al., 1994, 1997, Sorbie and Mackay, 2000, Dyer and Graham, 2002) and the production of geothermal energy (Arnorsson, 1989, Gill, 1998, Potapov et al., 2001). It can be defined as hard adherent mineral deposits that precipitate from brine solution. The amount and location of scale depends on different factors, such as the degree of supersaturation, kinetics, solution pH and composition, CO_2 content, temperature and pressure.

In the reservoir, the natural water is in equilibrium with its surroundings at ambient temperature and pressure. As the brine flows up through the well, both temperature and pressure decrease considerably and the equilibrium is disturbed. This will generally lead to solid-phase deposition (Atkinson et al., 1991). The formation of carbonate scale is mainly associated with the pressure and pH changes of the production fluid, while the occurrence of sulphate scale is mainly due to the mixing of incompatible brines.

Carbon dioxide is generally present in large amounts in geothermal and oilfield fluids at reservoir temperature and pressure conditions. The decrease of pressure during the flow path reduces considerably the solubility of carbonate minerals, leading in some cases to the deposit of solid minerals ($CaCO_3$, $MgCO_3$, $BaCO_3$, $SrCO_3$) in the inner wall of the pipe. From all the carbonate minerals, calcite ($CaCO_3$) seems to be the most likely to precipitate (Wat et al., 1992). The most commonly found carbonate scales in the oil industry are the salts of calcium, barium, and strontium (Li et al., 1995). Dyer and Graham (2002) also added magnesium carbonates to that list.

In offshore oilfield developments, mixing of incompatible waters due to water flooding is the main cause of sulphate scale formation. Two waters are incompatible if they interact chemically and precipitate minerals when mixed. When sulphate-rich injection water (often

seawater) is mixed with the Ba^{2+}, Ca^{2+} and Sr^{2+}- rich formation water, it is very likely that barite ($BaSO_4$), celestite ($SrSO_4$), gypsum ($CaSO_4·2H_2O$) and/or anhydrite ($CaSO_4$) precipitation takes place (Sorbie and Mackay, 2000).

Mineral scale deposition causes serious damage in utilization systems and reduces the flow area. Therefore, the production rate (and the re-injection capacity) drops down, with the consequent economical loss: BP looses around 4 million bbls per year in the North Sea (Graham and Mackay, 2003). The cross section decrease caused by solid deposition onto the inner wall of a pipe is shown in figure 1-1. In some cases, the choke of the flow line is so large that the well needs to be closed (Zhang et al., 2001). Scaling can also cause safety problems due to blockage and failure of valves (Graham and Mackay, 2003). According to Dyer and Graham (2002), the future expectations in the oil field in the North Sea are even more alarming, due to the recent development of reservoirs with a very large salinity (total dissolved solids around 300000 ppm), high temperature (more than $175^{o}C$) and high pressure (800-1000 bar) (Eastern Trough Area Project, ETAP).

Figure 1-1. Scale formation in a pipe.

In the geothermal field, mineral deposition limits the degree of utilization of geothermal energy. Geothermal energy has many advantages (it is renewable, clean, safe and flexible) but it is necessary to minimize operation costs in order to make its production competitive with other energy resources.

1.2 Thermodynamic Model

Scale prevention is technically and economically more effective than redissolution once scale has formed. One essential step in scale prevention is scale prediction. Unfortunately, that is a difficult task because the thermodynamics of brines is a sensitive function of their composition, temperature and pressure. These variables change considerably during the flow path of the fluid and can also vary significantly from well to well (even within the

same resource area). Moreover, they can change in a single well over the lifetime of the resource. Therefore, effective prediction of the scaling tendency requires a reliable thermodynamic model. In this Ph.D. project we have focused on the prediction of mineral solubility in natural waters under conditions of varying brine composition, temperature and pressure.

The majority of the programs (He and Morse, 1992, Møller et al., 1998, Zhenhao et al., 1996) employed to predict scale tendency use the framework provided by Pitzer (1991). For multicomponent solutions, Pitzer's approach requires both binary and ternary parameters and thus both binary and ternary experimental data for all the species in the mixture. Unfortunately, such data are not available for some systems of importance in natural waters, and are especially scarce at the high temperature and pressure conditions we are dealing with. In many cases the quantity and quality of experimental data do not justify the use of many parameters. Clearly, a method requiring limited amount of data but leading to accurate predictions for the solid-liquid-vapour equilibrium and crystallization processes for electrolyte solutions would be of great use. This is the case of the extended UNIQUAC model, which is the thermodynamic model selected in the present work to determine the aqueous-phase activity coefficients, while the vapour-phase fugacities are determined by the Soave-Redlich-Kwong (SRK) cubic equation of state.

The extended UNIQUAC model is capable of accurately representing multicomponent systems with common ions, covering a range of temperature and ionic strength large enough to represent the conditions found in geothermal and oil production wells. Using this approach, the number of parameters is considerably lower than the number of parameters required by Pitzer's model (only two parameters per species plus two parameters per species pair are required by the extended UNIQUAC model). At the same time, the temperature dependency is accounted for in the model equations, avoiding the introduction of a new set of parameters. Two additional parameters have been added to the model presented by Thomsen and Rasmussen (1999), in order to account for the pressure dependency. The results obtained through this modification are very satisfactory in the pressure range investigated (1 to 1000 bar).

This work presents the results obtained for some of the major species present in natural waters and some of the most problematic scaling minerals found in oilfield and geothermal operations ($BaSO_4$, $SrSO_4$, $CaSO_4$, $CaSO_4 \cdot 2H_2O$, $CaCO_3$, $BaCO_3$, $SrCO_3$, $MgCO_3$). Parameters for the system CO_2-Na-H-Ca-Mg-Ba-Sr-OH-Cl-SO_4-CO_3-HCO_3 have been estimated on the basis of available experimental SLE data.

1.3 Experimental Determination of Solubilities

There is a general lack of data on the solubility of most of the scaling minerals in water and in NaCl solutions, especially at high temperatures and pressures. Some of the available data are inconsistent, and most of the published data only cover a narrow range of low temperature (around 25ºC) and NaCl concentration, and are measured at atmospheric pressure. The use of such data can lead to weak models and inaccurate predictions. The few sources dealing with high temperature and pressure cannot be cross-checked due to the different conditions measured. Therefore, a larger databank is necessary to understand and predict the causes of precipitation and dissolution of scaling minerals in nature.

During this Ph.D. project, an experimental setup has been developed in order to determine barite solubility in the ternary system $NaCl-BaSO_4-H_2O$ from very diluted solutions to the saturation point. The setup can cover the temperature range from room conditions up to 300ºC, and pressures up to 10000 psi.

1.4 References in Chapter 1

Arnorsson, E., 1989. Deposition of calcium carbonate minerals from geothermal waters. Theoretical considerations. Geothermics 18, 33-39.

Atkinson, G., Oklahoma, U., Raju, K., Aramco, S., Howell R.D., 1991. The thermodynamics of scale prediction. SPE 21021, 209-215.

Dyer, S.J., Graham, G.M., 2002. The effect of temperature and pressure on oilfield scale formation. Journal of Petroleum Science and Engineering 35, 95-107.

Gill, J.S., 1998. Silica scale control. Chemical Treatment, 41-45.

Graham, G.M., Mackay, E.J., 2003. A background to inorganic scaling-mechanisms, formation and control. 5th Intl. SPE Oilfield Scale Symposium. Aberdeen, UK.

He, S., Morse, J.W., 1992. Prediction of halite, gypsum, and anhydrite solubility in natural brines under subsurface conditions. Computer & Geosciences 19, 1-22.

Li, Y.H., Crane, S.D., Coleman, J. R., 1995. Novel approach to predict the co-precipitation of $BaSO_4$ and $SrSO_4$. SPE 29489, 447-461.

Møller, N., Greenberg, J.P., Weare, J.H., 1998. Computer modelling for geothermal systems: Predicting carbonate and silica scale formation, CO_2 breakout and H_2S exchange. Transport in Porous Media 33, 173-204.

Pitzer, K.S., 1991. Activity coefficients in electrolyte solutions, 2nd edition. CRC Press, Boca Raton, pp. 293-422.

Potapov, V.V., Kashpura, V.N., Alekseev, V.I., 2001. A study of the growth of deposits in geothermal power systems. Thermal Engineering 48 (5), 395-400.

Shams El Din, A.M., Mohammed, R.A., 1989. The problem of alkaline scale formation from a study on Arabian Gulf water. Desalination 71, 313-324.

Sorbie, K.S., Mackay, E.J., 2000. Mixing of injected, connate and aquifer brines in water flooding and its relevance to oilfield scaling. Journal of Petroleum Science and Engineering 27, 85-106.

Thomsen, K., Rasmussen, P., 1999. Modeling of vapor-liquid-solid equilibrium in gas-aqueous electrolyte systems. Chemical Engineering Science 54, 1787-1802.

Wat, R.M.S., Sorbie, K.S., Todd, A.C., Chen, P., Jiang, P., 1992. Kinetics of $BaSO_4$ crystal growth and effect in formation damage. SPE 23814, 429-437.

Yuan, M., Todd, A.C., Sorbie, K.S., 1994. Sulfate scale precipitation arising from seawater injection: a prediction study. Marine and Petroleum Geology 11(1), 24-30.

Yuan, M.D., Anderson, M., Jamieson, E., 1997. Investigation and improvement of $BaSO_4$ scale inhibition tests. Society of Petroleum Engineers 37304, 765-768.

Zhang, Y., Shaw, H., Farquhar, R., Dawe, R., 2001. The kinetics of carbonate scaling-application for the prediction of downhole carbonate scaling. Journal of Petroleum Science and Engineering 29, 85-95.

Zhenhao, D., Møller, N., DeRocher, T., Weare, J.H., 1996. Prediction of boiling, scaling and formation conditions in geothermal reservoirs using computer programs. Geothermics 25 (6), 663-678.

2. Thermodynamics

This chapter is intended to explain the thermodynamic basis needed to describe solubility phenomena and calculate solid-liquid, vapour-liquid, and speciation equilibria at various temperatures and pressures.

The condition for chemical equilibrium for a species B at a given temperature T and pressure P in the phases α and β is that the chemical potential of B be equal in the two phases:

$$\mu_B^\alpha(T, P, \mathbf{n}^\alpha) = \mu_B^\beta(T, P, \mathbf{n}^\beta) \tag{2-1}$$

where $\mathbf{n}$ represents the concentrations of the different components in the system and μ_B the chemical potential of B. If more than two phases are present, equation 2-1 is extended to all of them. The chemical potential of component B is the sum of the standard state chemical potential and a concentration dependent term which is calculated in this work by means of the extended UNIQUAC model.

2.1 Standard States

The standard state for solid phases is the pure crystalline component at the system temperature and pressure.

The standard state for vapour species is the pure ideal gas at the reference pressure P_0 (chosen to be 1 bar) and the temperature of the system.

For the liquid phase, two different standard states are used, one for the solvent and another for the ions and molecules. The symmetric convention is used for water, while the unsymmetric convention based on mole fraction is used for all other species.

The chemical potential of water can be written as

$$\mu_w = \mu_w^0 + RT \ln a_w = \mu_w^0 + RT \ln(\gamma_w x_w) \tag{2-2}$$

In equation 2-2, μ_w^0 is the standard state chemical potential of water, which is the chemical potential of pure liquid water at the system temperature and pressure, a_w is the water activity, R is the gas constant (8.314 J mol^{-1} K^{-1}), T is the system temperature in Kelvin, x_w is the mole fraction of water, and γ_w is the symmetric water activity coefficient. According to the symmetric convention, the activity coefficient of water is unity in the pure component state at all temperatures ($\gamma_w \to 1$ as $x_w \to 1$).

For aqueous solutions, the osmotic coefficient (Φ) is usually used as a measure for the activity of water.

$$\Phi = -\frac{\ln a_w}{M_w \sum_j v_{Bj} m_{Bj}} \tag{2-3}$$

where M_w is the molar mass of water in kg mol^{-1}, m_B is the molality of salt B, which dissociates into v_{Bj} moles of ions per mol of salt.

The chemical potential of ion i (or any solute i) can be written as

$$\mu_i = \mu_i^* + RT \ln(\gamma_i^* x_i) \tag{2-4}$$

where μ_i^* is the standard state chemical potential of ion i based on the unsymmetrical convention and mole fraction scale, at the system temperature and pressure. γ_i^* is the rational unsymmetric activity coefficient for ion i, where $\gamma_i^* \to 1$ as $\sum x_i \to 0$. The standard state is the pure component standard state normalized so that solute activity coefficients are equal to unity at infinite dilution.

The unsymmetric activity coefficient can be calculated from the symmetric activity coefficient and the symmetric activity coefficient at infinite dilution (γ^∞):

$$\gamma_i^* = \frac{\gamma_i}{\gamma_i^\infty} \tag{2-5}$$

2.2 Vapour-Liquid Equilibrium

Equilibrium is reached when equation 2-1 is fulfilled for all the components and phases of a system. For a volatile component as H_2O, the vapour-liquid equilibrium (VLE) is represented as

$$H_2O \ (l) \leftrightarrow H_2O \ (g) \tag{2-6}$$

And equation 2-1 becomes

$$\mu_{w,l} = \mu_{w,g} \tag{2-7}$$

where the subscripts l and g refer to liquid and vapour phases, respectively.

For the liquid phase, the chemical potentials of water and CO_2 are given by equations 2-2 and 2-4, respectively.

The chemical potential of the volatile component i (water, carbon dioxide) in the vapour phase can be calculated as

$$\mu_{i,g} = \mu_i^{IG} + RT \ln \frac{\hat{f}_{i,g}}{P_0} \qquad (2\text{-}8)$$

where μ_i^{IG} is the chemical potential of component i in the standard state, P_0 is the reference pressure (1 bar), and $\hat{f}_{i,g}$ is the fugacity of component i in the gas phase at the temperature and pressure of the system, which can be written as

$$\hat{f}_{i,g} = y_i \hat{\phi}_{i,g} P \qquad (2\text{-}9)$$

where y_i refers to the mole fraction of component i in the gas phase, P is the total pressure, and $\hat{\phi}_{i,g}$ is the fugacity coefficient for component i in the gas phase, calculated in this work from the Soave-Redlich-Kwong (SRK) cubic equation of state. For sufficiently low pressures, the fugacity coefficient is close to unity, and the fugacity of species i can be assimilated to the partial pressure of that component.

By combining equations 2-2, 2-7, 2-8 and 2-9, the condition 2-1 for equilibrium between vapour and liquid can be written:

$$\mu_w^0 + RT \ln x_w \gamma_w = \mu_w^{IG} + RT \ln \frac{y_w \hat{\phi}_{w,g} P}{P_0} \qquad (2\text{-}10)$$

and the vapour-liquid equilibrium equation for water can be expressed as:

$$\ln \frac{y_w \hat{\phi}_{w,g} P}{x_w \gamma_w P_0} = \frac{\mu_w^0 - \mu_w^{IG}}{RT} \qquad (2\text{-}11)$$

The approach used in equation 2-11 requires the chemical potentials of liquid (μ_w^0) and vapour (μ_w^{IG}). These potentials are not available at temperatures above the critical. For this reason, a different approach using the Henry's constant and a Poynting correction is chosen for CO_2.

The fugacity of a component i in the liquid phase can be calculated as

$$\hat{f}_{i,l} = H_{i,j} \gamma_i^* x_i \qquad (2\text{-}12)$$

where $H_{i,j}$ is the Henry's law constant of component i in solvent j. It is defined as

$$H_{i,j} = \lim_{x_i \to 0} \left(\frac{\hat{f}_{i,l}}{\gamma_i^* x_i} \right)_{T,P,n_{j \neq i}} \qquad (2\text{-}13)$$

The dependency of fugacity with pressure is given from classical thermodynamics as

$$\left(\frac{\partial \ln \hat{f}_i}{\partial P}\right)_{T,n} = \frac{\overline{V}_i}{RT} \tag{2-14}$$

where $\overline{V}_i$ is the partial molar volume of component i. Integrating equation 2-14 from a reference pressure P_0 to pressure P:

$$\hat{f}_{i,l,P} = \hat{f}_{i,l,P_0} \cdot \exp\left(\frac{\overline{V}_i (P - P_0)}{RT}\right) \tag{2-15}$$

Inserting the definition of fugacity given by equation 2-12 into equation 2-15:

$$\hat{f}_{i,l,P} = H_{i,j,P_0} \gamma_i^* x_i \cdot \exp\left(\frac{\overline{V}_i (P - P_0)}{RT}\right) \tag{2-16}$$

Inserting equation 2-16 in the definition of the Henry's law constant (equation 2-13), the dependency with pressure is obtained:

$$H_{i,j} = \lim_{x_i \to 0} \left[\frac{\hat{f}_{i,l,P_0}}{x_i} \exp\left(\frac{\overline{V}_i (P - P_0)}{RT}\right)\right]_{P,T,n_{i \neq j}} \tag{2-17}$$

At infinite dilution ($x_i \to 0$), the total pressure is the saturation pressure of the solvent, and equation 2-17 may be rewritten as

$$H_{i,j} = H_{i,j,P_j^{sat}} \cdot \exp\left(\frac{\overline{V}_i^* (P - P_j^{sat})}{RT}\right) \tag{2-18}$$

and the Krichevsky-Ilinskaya equation is obtained

$$\hat{f}_{i,l} = H_{i,j,P_j^{sat}} \gamma_i^* x_i \cdot \exp\left(\frac{\overline{V}_i^* (P - P_j^{sat})}{RT}\right) \tag{2-19}$$

At equilibrium, the isofugacity criteria must be fulfilled, and

$$\ln(y_i \hat{\phi}_i P) = \ln\left[H_{i,j,P_j^{sat}} \gamma_i^* x_i \cdot \exp\left(\frac{\overline{V}_i^* (P - P_j^{sat})}{RT}\right)\right] \tag{2-20}$$

Rearranging equation 2-20, the vapour-liquid equilibrium equation for CO_2 can therefore be written as:

$$\ln \frac{y_{CO_2} \hat{\phi}_{CO_2,g} P}{x_{CO_2} \gamma_{CO_2}^*} = \frac{\overline{V}_{CO_2}^* (P - P_w^{sat})}{RT} + \ln H_{CO_2} \tag{2-21}$$

The fugacity coefficients for both H_2O (g) and CO_2 (g) are calculated by the cubic SRK equation of state using classical mixing rules. The Henry's constant for carbon dioxide in water (H_{CO_2}) is calculated according to Rumpf and Maurer (1993):

$$\ln H_{CO_2} = 192.876 - \frac{9624.4}{T} + 1.441 \cdot 10^{-2} T - 28.749 \ln T \tag{2-22}$$

where T is the temperature in Kelvin and H_{CO_2} is given in MPa·mol^{-1}·kg. Equation 2-22 is based on molality scale, so the Henry's law constant value is converted to mole fraction scale before using it. The empirical correlation 2-22 was based on selected literature data for the solubility of carbon dioxide in pure water. The temperature range of applicability of equation 2-22 is from 0 to 200°C. Nevertheless, we applied equation 2-22 up to 250°C obtaining very satisfactory results. The standard state partial molar volume used for calculating the Poynting correction follows a temperature dependency as indicated in equation 2-23 (Rumpf and Maurer, 1993)

$$\overline{V}^{*}_{CO_2} = 77.83350021 - 327.8959231 \cdot 10^{-3} T + 594.8558514 \cdot 10^{-6} T^2 \tag{2-23}$$

In equation 2-23 T is the temperature in Kelvin and $\overline{V}^{*}_{CO_2}$ is given in cm^3·mol^{-1}.

2.3 Solid-Liquid Equilibrium

For a mineral $M_{\nu_M} X_{\nu_X} nH_2O$ consisting of ν_M cations M, ν_X anions X and n molecules of H_2O, the solid-liquid equilibrium can be expressed as

$$M_{\nu_M} X_{\nu_X} nH_2O\,(c) \Leftrightarrow \nu_M M^{zM+}\,(aq) + \nu_X X^{zX-}\,(aq) + nH_2O\,(l) \tag{2-24}$$
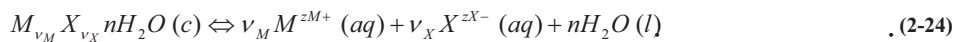
The condition for equilibrium, corresponding to equation 2-1, is:

$$\mu_{M_{\nu_M} X_{\nu_X} nH_2O(c)} = \nu_M \mu_{M^{zM+}(aq)} + \nu_X \mu_{X^{zX-}(aq)} + n\mu_w \tag{2-25}$$

Using the previous definitions for the chemical potentials (equations 2-2 and 2-4), equation 2-25 can be rewritten as

$$(\gamma^{*}_{M^{zM+}} x_{M^{zM+}})^{\nu_M} (\gamma^{*}_{X^{zX-}} x_{X^{zX-}})^{\nu_X} a_w^n = \exp\left(-\frac{\nu_M \mu^{*}_{M^{zM+}} + \nu_X \mu^{*}_{X^{zX-}} + n\mu^{0}_w - \mu^{0}_{M_{\nu_M} X_{\nu_X} \cdot nH_2O}}{RT}\right) \tag{2-26}$$

The chemical potential of the salt $M_{\nu_M} X_{\nu_X} nH_2O$ is equal to its standard state chemical potential since the solid salt is in its standard state: Pure crystalline component at the system temperature and pressure.

The left hand side of equation 2-26 is the solubility product (K_e) of the salt $M_{\nu_M} X_{\nu_x} nH_2O$.
The numerical value of K_e can be calculated from the right hand side of equation 2-26 Solid-liquid equilibrium calculation reduces to the solution of equation 2-26 to obtain the composition of the liquid phase in equilibrium with the solid phase(s). The concentrations on the left-hand side of equation 2-26 can then be adjusted by iteration until the activity product yields the desired value. Therefore, to predict solid-liquid equilibrium, a model for activity coefficients in mixed electrolyte solutions is needed, together with the knowledge of the thermodynamic solubility products of all the possible solid phases formed in the system under consideration, at the system temperature and pressure.

2.4 Speciation Equilibrium

Dissociation equilibrium can be derived in an analogous manner as described for solid-liquid equilibrium. The hydrogen carbonate ion dissociates following reaction 2-27.

$$HCO_3^- \ (aq) \leftrightarrow CO_3^{2-} \ (aq) + H^+ \ (aq) \tag{2-27}$$

Applying the definition of the chemical potential for ions given in equation 2-4 a similar expression to equation 2-26 is obtained:

$$\frac{x_{CO_3^{2-}} \cdot \gamma_{CO_3^{2-}}^* \cdot x_{H^+} \cdot \gamma_{H^+}^*}{x_{HCO_3^-} \cdot \gamma_{HCO_3^-}^*} = \exp\left(-\frac{\mu_{CO_3^{2-}}^* + \mu_{H^+}^* - \mu_{HCO_3^-}^*}{RT}\right) \tag{2-28}$$

Equations 2-26 and 2-28 can be written in a more general way as

$$K_{e,j} = \exp\left(-\frac{\Delta_r G_j^0}{RT}\right) = \prod_i (x_i \gamma_i)^{\nu_{i,j}} \tag{2-29}$$

where $\Delta_r G_j^0$ is the change in standard state Gibbs free energy for equilibrium j at the temperature T and pressure P, and $\nu_{i,j}$ is the stoichiometric coefficient of species i in equilibrium j.

2.5 Standard State Chemical Potentials

Standard state chemical potentials are required by the extended UNIQUAC model in order to perform calculations. These properties can be found at 25ºC and 1 bar in different data compilations (i.e., NIST, 1990). The standard state for solutes reported in thermodynamic tables is based on the hypothetical ideal unit mean molal solution ($\mu_i^{*,m}$). These values in

the molality scale are converted by equation 2-30 to the mole fraction scale prior to their use by the model.

$$\mu_i^* = \mu_i^{*,m} - RT \ln M_w \tag{2-30}$$

When the standard state chemical potentials are not available in literature (as it is the case for $Na_2SO_4 \cdot CaSO_4$ or $BaSO_4 \cdot SrSO_4$, among others) they can be fitted to experimental solubility data.

2.6 Temperature Effect on Solubility

Values for the standard state Gibbs free energy at temperatures other than 25ºC can be calculated using the Gibbs-Helmholtz equation

$$\left[\frac{\partial \left(\Delta_r G^0 / RT \right)}{\partial T} \right]_P = -\frac{\Delta_r H^0}{RT^2} \tag{2-31}$$

The change in standard state enthalpy ($\Delta_r H^0$) by the equilibrium is temperature dependent:

$$\left[\frac{\partial \Delta_r H^0}{\partial T} \right]_P = \Delta_r C_p^0 \tag{2-32}$$

where $\Delta_r C_p^0$ is the variation in standard state heat capacity due to the reaction. For pure crystalline salts, the standard state heat capacity is often nearly constant in a wide temperature range. For ions, on the other hand, the standard state heat capacity cannot be considered temperature independent. It can be eventually calculated by the correlation (Thomsen et al., 1996):

$$C_{pi}^* = C_{p1,i} + C_{p2,i} T + \frac{C_{p3,i}}{T - \Theta} \tag{2-33}$$

where Θ is a constant equal to 200 K. The parameters $C_{p1,i}$, $C_{p2,i}$, and $C_{p3,i}$ can be fitted to experimental heat capacity data or can be taken from data compilations (Kelley, 1960). The standard state heat capacity at 25ºC can also be found in data compilations.

2.7 Pressure Effect on Solid-Liquid Equilibrium

The saturation concentration of a salt can be calculated from equation 2-29. According to equation 2-29, this saturation concentration is a function of the solubility product and the activity coefficients of the ions of the salt. The solubility product and the activity coefficients are temperature and pressure dependent (the activity coefficients are

composition dependent as well). Therefore, in order to estimate scale formation in a well (where pressure changes with depth) the pressure effect on solubility (and thus on the solubility product and activity coefficients) must be taken into consideration.

2.7.1 Pressure Dependence of the Solubility Product

The derivative of K_e with respect to pressure at constant temperature is expressed as

$$\left(\frac{\partial \ln K_e}{\partial P} \right)_T = -\frac{\Delta \overline{V}_{dis}}{RT} \tag{2-34}$$

where $\Delta \overline{V}_{dis}$ is the increment in standard partial molar volume for a mineral dissolution reaction. For example, for the dissolution reaction $BaSO_4(c) \Leftrightarrow Ba^{2+} + SO_4^{2-}$:

$$\Delta \overline{V}_{dis} = \overline{V}_{Ba^{2+}}^* + \overline{V}_{SO_4^{2-}}^* - V_{BaSO_4}^0 \tag{2-35}$$

The isothermal compressibility is defined as

$$\kappa = -\frac{1}{V} \left(\frac{\partial V}{\partial P} \right)_T \tag{2-36}$$

The partial molar compressibility of component i is defined as

$$\overline{\kappa}_i = -\left(\frac{\partial \overline{V}_i}{\partial P} \right)_T \tag{2-37}$$

and for the dissolution reaction 2-35:

$$\left(\frac{\partial \Delta \overline{V}_{dis}}{\partial P} \right)_T = -\Delta \overline{\kappa}_{dis} \tag{2-38}$$

where $\Delta \overline{V}_{dis}$ is defined in equation 2-35 and $\Delta \overline{\kappa}_{dis}$ is the corresponding change in standard partial molar compressibility.

The change in standard partial molar compressibility is considered pressure independent in this work.

Integrating equation 2-34, the correction required to account for the pressure dependency of the solubility product (and therefore, of the standard state chemical potentials of the different species taking place in the dissolution reaction) is obtained:

$$\ln K_{e,P} = \ln K_{e,P_0} - \frac{\Delta \overline{V}_{dis,P_0}}{RT} (P - P_0) + \frac{\Delta \overline{\kappa}_{dis}}{2RT} (P - P_0)^2 \tag{2-39}$$

2.7.2 Pressure Dependence of Activity Coefficients

The pressure effect on the activity coefficient of species i at constant temperature T is described by the thermodynamic relation

$$\left(\frac{\partial \ln \gamma_i}{\partial P}\right)_{T,n} = \frac{\overline{V}_i^E}{RT} \tag{2-40}$$

where $\overline{V}_i^E$ is the excess partial molar volume of component i.

Equation 2-40 is valid for water and ions (symmetric and unsymmetric standard states). Integrating equation 2-40, the pressure effect on the activity coefficient is obtained as

$$\ln \gamma_{i,P} = \ln \gamma_{i,P_0} + \frac{\overline{V}_{i,P_0}^E}{RT}(P-P_0) - \frac{\overline{\kappa}_i^E}{2RT}(P-P_0)^2 \tag{2-41}$$

By substituting equation 2-39 and equation 2-41 into equation 2-29 the following relation is obtained:

$$\ln K_{e,P} = \ln K_{e,P_0} - a(P-P_0) + b(P-P_0)^2 = c + \sum_{i=1}^{m} \nu_i \left[\ln \gamma_{i,P_0} + d(P-P_0) - e(P-P_0)^2\right] \tag{2-42}$$

where

$$
\begin{aligned}
a &= \frac{\Delta \overline{V}_{dis,P_0}}{RT} \\
b &= \frac{\Delta \overline{\kappa}_{dis}}{2RT} \\
c &= \sum_{i=1}^{m} \nu_i \ln x_i \\
d &= \frac{\overline{V}_{i,P_0}^E}{RT} \\
e &= \frac{\overline{\kappa}_i^E}{2RT}
\end{aligned}
\tag{2-43}
$$

In equations 2-42 and 2-43, m is the number of species (ions and water) that constitute the mineral $M_{\nu_M} X_{\nu_X} nH_2O$ and ν refers to the stoichiometric coefficient of the SLE reaction.

Equations 2-42 and 2-43 show the corrections that must be applied to both the solubility product and the residual and combinatorial terms of the activity coefficients to introduce the pressure effect in the solubility calculations. The Debye-Hückel term for the activity coefficient is calculated at the system pressure, and therefore, correction 2-41 is not required for this term. The Debye-Hückel parameter A given by equation 3-10 is a function of the density and dielectric constant, both of them evaluated at the system temperature and pressure.

In the present work, we have included two additional parameters (α and β) to the extended UNIQUAC thermodynamic model presented by Thomsen and Rasmussen (1999) to account for pressure dependence:

$$\ln K_{e,P} = \ln K_{e,P_0} + \alpha(P - P_0) + \beta(P - P_0)^2 \tag{2-44}$$

No further corrections to account for pressure are applied, apart from α and β (except for the calculation of the A Debye-Hückel parameter). Thus, the residual and combinatorial terms of the activity coefficients are calculated at the reference pressure, so that equation 2-42 becomes:

$$\ln K_{e,P_0} + \alpha(P - P_0) + \beta(P - P_0)^2 = c + \sum_{i=1}^{m} v_i \left[\ln \gamma_{i,P_0} \right] \tag{2-45}$$

For equation 2-45 to be consistent with equation 2-42, it is necessary that

$$\alpha = -\frac{\Delta \overline{V}_{dis,P_0}}{RT} - \sum_{i=1}^{m} v_i \frac{\overline{V}_{i,P_0}^E}{RT} = -a - \sum_{i=1}^{m} v_i d \tag{2-46}$$

$$\beta = \frac{\Delta \overline{\kappa}_{dis}}{2RT} + \sum_{i=1}^{m} v_i \frac{\overline{\kappa}_i^E}{2RT} = b + \sum_{i=1}^{m} v_i e \tag{2-47}$$

Using two fitting parameters to correct for the pressure effect is preferred over evaluating α and β from the physical properties (equations 2-46 and 2-47), because of the lack of accurate experimental data for both the partial molar volume and compressibility.

Most of the experimental measurements of partial molar volumes are limited to simple ions and are reliable at low temperatures only. The interpolations performed in some cases to calculate $\overline{V}_i$ at temperatures different from the experimental values, show differences as large as 0.3 cm^3 mol^{-1} (Millero, 1981). Yousef et al. (2001) demonstrated that an accurate value for the standard partial molar volume is critical for a reliable prediction of solubility at high pressures. Such values are generally overestimated by the equations of state (Millero, 1981).

In the case of compressibility, the situation is even worse and reliable data are very difficult to find. The derivation of $\overline{\kappa}_i$ from compressibility studies is experimentally difficult (Lown et al., 1968). The number of ions studied is also small, especially in the marine environment, and a large divergence can be found among the various authors. There are no compressibility data for mixed electrolyte solutions and it is impossible nowadays to make a precise calculation of the change in standard partial molar compressibility for natural highly concentrated brines (Krumgalz et al., 1999). Even the error introduced by neglecting this

term cannot be defined with any precision. Very limited data are available for the effect of temperature on $\bar{\kappa}_i$ and the effect of pressure is neglected. The effect of pressure has nevertheless not been studied in detail and seems to be more important for low temperatures. Lown et al. (1968) demonstrated that the molar compressibility for different acid-base equilibria could be assumed pressure independent in the range 1-2000 bar. According to Millero (1981), such a dependence should be accounted for above 700 bar (the error introduced at 1000 bar is around 4%). For $SrSO_4$ at 1000 bar, neglecting the change in partial molar compressibility with pressure leads to an overestimation of the ratio $K_{e,T,P} / K_{e,T,P_0}$ by as much as 39% (Millero, 1981). The error caused by uncertainties in both molar volume and compressibility should also be added to the latter percentage (around 6% for seawater, according to Millero, 1981). By estimating the values of the pressure parameters α and β from experimental solubility data we will avoid these inaccuracies.

2.8 Model Calculations

The calculations performed to achieve the final solution are explained based on the specific system $CaCO_3$-CO_2-H_2O. The following equilibrium processes are taken into account for that system:

Vapour-liquid equilibria:

$$CO_2(g) \Leftrightarrow CO_2(aq) \tag{2-48}$$

$$H_2O(g) \Leftrightarrow H_2O(l) \tag{2-49}$$

Speciation equilibria:

$$CO_2(aq) + H_2O(l) \Leftrightarrow HCO_3^- + H^+ \tag{2-50}$$

$$HCO_3^- \Leftrightarrow CO_3^{2-} + H^+ \tag{2-51}$$

$$H_2O(l) \Leftrightarrow H^+ + OH^- \tag{2-52}$$

Except for the carbonate/bicarbonate system, all the other electrolytes are considered strong electrolytes and therefore completely dissociated. The formation of association products such as $CaCO_3^0$ or $CaHCO_3^+$ is not considered (the same criteria is applied to all the systems studied in the present work).

Liquid-solid equilibrium:

$$Ca^{2+} + CO_3^{2-} \Leftrightarrow CaCO_3(c) \tag{2-53}$$

Each of the equilibrium processes 2-48 to 2-53 can be expressed in a form similar to equation 2-29. To calculate the equilibrium phase compositions of a mixture of CO_2, $CaCO_3$ and H_2O, equations 2-48 to 2-53, together with the electroneutrallity condition and the condition that the sum of the mole fractions in the gas phase and the sum of the mole fractions in the liquid phase is equal to unity, is solved with respect to the mole fractions of the n components in the liquid phase (H_2O, Ca^{2+}, CO_3^{2-}, HCO_3^-, H^+, OH^-, $CO_2(aq)$), the mole fractions of the n' components in the gas phase (H_2O (g) and CO_2 (g)) and the bubble point pressure, by adjusting the amounts of the n'' solid phases ($CaCO_3$ (c)). At equilibrium, equation 2-54 must be fulfilled

$$K_{CaCO_3} = a_{Ca^{2+}} a_{CO_3^{2-}} \tag{2-54}$$

In general, a s-salt saturation point has to fulfil equation 2-55 for all s salts:

$$K_k = \prod_i a_i^{v_{k,i}} \quad k = 1...s \tag{2-55}$$

while for the rest of the salts potentially formed by the system

$$K_k > \prod_i a_i^{v_{k,i}} \quad k > s \tag{2-56}$$

Equation 2-55 is solved by a Newton-Raphson method using analytical composition derivatives of the activity coefficients.

For the calculation of the bubble point pressure of the solution, an initial guess of both pressure and composition is introduced in the program. Then, all the speciation equilibria equations are solved simultaneously. The fugacities of the vapour phase components appear in the equations for the vapour-liquid equilibria 2-48 and 2-49, which can be expressed as in equation 2-29. From those equations the mole fractions of the components forming the vapour phase can be calculated. If the sum of those mol fractions is different from unity, a new pressure is guessed. The procedure is repeated until a final solution is found.

2.9 References in Chapter 2

Kelley, K.K., 1960. High-temperature heat-content, heat-capacity, and entropy data for the elements and inorganic compounds. Bulletin/Bureau of Mines 584, 1-211.

Krumgalz, B.S., Starinsky, A., Pitzer, K.S., 1999. Ion-interaction approach: pressure effect on the solubility of some minerals in submarine brines and seawater. Journal of Solution Chemistry 28 (6), 667-692.

Lown, D.A., Thirsk, H.R., Lord W.J., 1968. Effect of pressure on ionization equilibria in water at 25ºC. Trans. Faraday Soc. 64, 2073-2080.

Millero, F.J., 1981. The effect of pressure on the solubility of minerals in water and seawater. Geochimica et Cosmochimica Acta 46, 11-22.

NIST Chemical Thermodynamics Database Version 1.1, 1990. U.S. Department of Commerce, National Institute of Standards and Technology, Gaithesburg MD 20899.

Rumpf B., Maurer G., 1993. An experimental and theoretical investigation on the solubility of carbon dioxide in aqueous solutions of strong electrolytes. Ber. Bunsenges. Phys. Chem. 97(1), 85-97.

Thomsen, K., Rasmussen, P., Gani, R., 1996. Correlation and prediction of thermal properties and phase behaviour for a class of electrolyte systems. J. Chem. Eng. Science 51, 3675-3683.

Thomsen, K., Rasmussen, P., 1999. Modeling of vapor-liquid-solid equilibrium in gas-aqueous electrolyte systems. Chemical Engineering Science 54, 1787-1802.

Yousef, A.M., Elkanzi, E.M., Singh, H., 2001. Prediction of supercritical CO_2 solubility using the Krichevsky-Ilinskaya equation with v2 as an Adjustable Parameter. J. of Supercritical Fluids 20, 105-112.

3. Extended UNIQUAC Model

In the present work, aqueous phase activity coefficients are calculated by means of the extended UNIQUAC model, improved with the addition of two pressure parameters to account for the pressure dependency of solubility. The gas phase fugacity for volatile components in the system is calculated by the Soave-Redlich-Kwong (SRK) cubic equation of state, using classical mixing rules.

The extended UNIQUAC model was chosen due to its simplicity and at the same time good accuracy to represent solid-liquid-vapour equilibria for multicomponent electrolyte solutions up to high ionic strengths and temperatures. The model only requires two parameters per species, plus two parameters per pair of interacting species, reducing the amount of experimental data required (scarce for the systems of interest in the present work, especially for multicomponent solutions at high temperature and pressure). Bromley's and Helgeson's models were also studied, but the extended UNIQUAC model was preferred due to its higher capability to perform calculations in multicomponent electrolyte solutions with common ions. A closer view to Bromley's and Helgeson's model is included in Appendix I.

3.1 Activity Coefficient Models

One of the first studies devoted to describe the thermodynamic behaviour of electrolyte solutions was performed by Lewis and Randall in 1921. Their motivation was the inaccuracy obtained for strong electrolytes when applying models derived from Arrhenius' theory of electric dissociation. Such models were adequate for weak electrolytes, but not for strong electrolytes. They proposed several methods to determine activity coefficients from measurements of the electromotive force, the freezing point, and the vapour pressure. One year later (in 1922), Brønsted postulated that there would only be specific interactions between ions of the opposite sign, while interactions between ions of the same sign would only depend on the electrical charges. In 1923, Debye and Hückel developed the first successful model (the Debye-Hückel limiting law) for the activity coefficients of dilute aqueous electrolytes. They considered the solvent to be a continuous dielectric. The ions interact following Coulomb's law, and the effect of all other ions on a given ion is calculated by the Poisson-Boltzmann equation. The Debye-Hückel (D-H) limiting law is a simplification of the Debye-Hückel equation where ions are considered to be point charges. The limiting law is reliable up to ionic strengths of 0.001 m. When ions are considered as

hard spheres instead, the limiting law is transformed into the extended Debye-Hückel law, reliable for ionic strengths up to 0.1 m.

Since the Debye-Hückel limiting law, many authors have proposed modifications to that model in order to extend its range of applicability. Bjerrum (1926) attributed the differences between experimental data and the Debye-Hückel theory to ionic association of ions of opposite charge. Guggenheim (1935) combined the extended D-H law with the principles of Brønsted (1922) and suggested an expression for the mean activity coefficient with one solute-specific parameter. The expression is valid up to ionic strengths of 0.1 m. Stokes and Robinson (1948) modified the D-H model introducing the ion-solvent interactions in terms of hydration, obtaining a two parameters equation to calculate the activity coefficients in electrolyte solutions. They assumed that ions were surrounded by solvent molecules and their ionic character was shielded. The behaviour of the solution is then determined by the free solvent molecules. Their model was applicable to 1:1 and 1:2 electrolyte solutions up to 4 m. In 1962, Davies added the term "aI" (I being the ionic strength and a a constant) to the original Debye-Hückel expression. His equation was frequently used in geochemical modelling, but only for temperatures close to 25°C and ionic strengths of a few tenths molal (Sahai et al., 1998). Hamer and Wu (1972) added to the D-H equation a serial function of the ionic strength, improving the correlation results due to the additional parameters.

Bromley (1973) modified the D-H model introducing an additional term that was dependent on the ionic strength. His one-parameter equation was found empirically from fitting experimental data. Bromley's model only uses one interaction parameter for each salt, which can be calculated as the sum of contributions from cation and anion. Many of those parameters are reported in literature (Zemaitis et al., 1986, Iliuta et al., 1999, Borge et al., 1996, Raposo et al., 1998, Belaustegi et al., 1999). According to Chen et al. (1998), the model had an accuracy of 5% for 1:1 electrolytes up to 6 m, but was limited to only 1 m solutions for other types of electrolytes. The properties of multicomponent electrolyte solutions are very often determined within the framework provided by Pitzer (1973, 1975, 1991), who developed one of the most popular virial expansion models. Using the pressure equation of statistical thermodynamics, Pitzer pointed out that the interaction coefficient is a function of the ionic strength. The general formulation of Pitzer's model is principally made up of two parts in terms of excess Gibbs energy. The first corresponds to the Debye-Hückel model, and the second is an empirical expression for the second and third virial coefficients that takes into account the binary and ternary interactions neglected in the first part. Third virial coefficients for three ions of the same charge have been neglected as they are assumed to be very small. According to Pérez-Villaseñor and Iglesias-Silva (2002), the main

disadvantage when using Pitzer's equations is that the concentration range normally cannot exceed a molality of 6. Other authors have also realized the same problem (Pitzer and Mayorga, 1973, Chen et al., 1982, Haghtalab and Vera, 1988, Marshall et al., 1995, Renon, 1996). Pitzer's formalism requires both binary and ternary experimental data for all components in the mixture. Some attempts to reduce the number of parameters used in Pitzer's model have also been made. Krop (1999) used a modified Pitzer's excess Gibbs free energy in which binary and ternary interaction parameters relate to the interactions of electrolytes in a solution rather than to the interactions of real species in a solution (i.e., cations, anions and non dissociated molecules). This approach reduces the number of parameters significantly. Pérez-Villaseñor and Iglesias-Silva (2002) assumed the double ion interactions to be independent of the ionic strength, therefore reducing the number of parameters. To achieve a similar accuracy, they also optimized the value of the b Debye-Hückel parameter for each electrolyte solution. Lietzke et al. (1975) presented a two-structure model to predict activity coefficients of each component in a mixed electrolyte solution. The model incorporated the ion atmosphere description of Debye-Hückel at low concentrations, and a function of ionic stregth at high concentrations. The contribution of each term was weighted by a partition function. The model needs three parameters for each electrolyte. Helgeson (Helgeson and Kirkham, 1974a, b, 1976, Helgeson et al., 1981, Shock and Helgeson, 1988, Johnson et al., 1992) developed equations to calculate the standard molal thermodynamic properties of minerals, gases, aqueous species, and reactions as a function of temperature and pressure. He proposed an equation to calculate activity coefficients for electrolyte solutions which is a simple extension by a term dependent on the ionic strength of the D-H model. Helgeson calculated successfully thermodynamic and transport properties of aqueous species at temperatures up to $1000^{o}C$ and pressures up to 5 kbar (Shock and Helgeson, 1988). He studied a huge amount of binary systems at different temperature and pressure conditions, and their results were in agreement with the experimental data (Helgeson et al., 1981). Lin et al. (1998) developed a characteristic-parameter correlation model for the aqueous strong electrolyte solutions. The model consists of the long range ion-ion interaction described by Pitzer-Debye-Hückel and short range ion-solvent molecule interaction attributed to solvation effect. This model contains three parameters of physical significance.

The Debye-Hückel model has also been combined with different local-composition models, such as UNIQUAC or NRTL. For instance, Cruz and Renon (1978) combined the Debye-Hückel expression with the NRTL model and a Born model contribution. They considered the changes in the dielectric constant with the salt concentration. To describe a system

formed by one salt and one solvent, four adjustable parameters are needed. A similar approach is followed by Ball et al. (1985), who used a different Born contribution, resulting in a reduced number of adjustable parameters (two for a binary system). Chen et al. (1982) and Chen and Evans (1986) used the electrostatic function of the Pitzer's model with a local composition term, which is an extension of the NRTL equation for electrolyte solutions. With this model, the number of interaction parameters to describe a binary system is reduced to two. They obtained good results for mixtures below concentrations of 6 m. Their model requires pair interaction parameters for each binary mixture. A very similar approach to Chen's et al. (1982) is followed by Haghtalab and Vera (1988), using the original expression given by D-H to account for the long range interactions. Sander (1984) added the Debye-Hückel equation to the UNIQUAC model (extended UNIQUAC), allowing the latter to be used for electrolyte solutions. Nicolaisen et al. (1993) simplified Sander's version of the extended UNIQUAC model in order to contain only binary parameters with no concentration dependency. This latter model is the one used in this work, with a different procedure to estimate parameters to that followed by Nicolaisen et al. (1993). The temperature dependency of the parameters is included in the model equations. Also, the model can be applied for mixed solvents. Liu et al. (1989) used an approach including the D-H term and a three-parameter Wilson equation derived by Renon and Prausnitz (1969). The D-H term only accounts for the long range interactions between the central ion and all ions outside the first coordination shell. The Wilson term accounts for the short range interactions, where the interactions between the ions within the first coordination shell are included. The model parameters are ion specific. Polka et al. (1994) proposed a new expression for the excess Gibbs energy formed by three contributions: A Debye-Hückel term to account for long range electrostatic interactions, the UNIQUAC equation for the description of short range interactions between all particles, and a middle range contribution to include all indirect effects of the charge interactions. The model needs four parameters for each electrolyte present in the solution. According to Polka et al. (1994), their results are comparable to the models of Sander et al. (1986a, b, c), Macedo et al. (1990), Pitzer and Mayorga (1973), Bromley (1973) and Chen et al. (1982) for the 362 binary and 185 ternary (two solvents and one salt) systems studied. A very similar model to extended UNIQUAC is the one used by Lu et al. (1996), where physical interactions between all species are taken into account combining the D-H law and the UNIQUAC model. The expression employed for the D-H law and the value of the b Debye-Hückel parameter differs from the ones in the extended UNIQUAC model.

Apart from modifications to the D-H law, many other activity coefficient models not including the D-H term have also been developed (Rasaiah and Friedman, 1968, Meissner et al., 1972, Tan, 1987, 1990, Pal et al., 1991, Kolker and De Pablo, 1995, Zuo and Fürst, 1998, Vanderbeken et al., 1999, Clegg and Simonson, 2001).

3.2 Previous Work on Scale Formation

Scale formation has been a problem for the development of the geothermal power and for the oil industry for a long time. The prediction of salt deposition during production is an important tool to fight against scale formation, and has been widely investigated during the last decades. Numerous saturation indexes and computer algorithms have been developed to determine when and where scale will occur.

Some of the first models predicting scale formation have important shortcomings, and as a result large errors in scale prediction may occur. This is the case of Helgeson (1970) and Miller et al. (1977), who did not consider the pressure effect on scaling. The effect of pressure on solubility is relatively small compared to that of temperature. In geothermal energy and oil production, however, the pressure change is of the order of hundreds of bars through the injection, reservoir, and production system, and the effect on solubility change may be significant.

Some models assume the solubility in natural waters is comparable to that in sodium chloride solutions of the same total ionic strength, neglecting the effect of all other ions present in the system. (Millero, 1979, Jacques and Bourland, 1983, Raju and Atkinson, 1988, 1989, Battistelli et al., 1997). In many cases, the possibility of co-precipitation of different scaling minerals is not taken into account, and simple empirical predictions (generally limited to pure water, CO_2-water, or NaCl solutions) for the formation of a particular precipitate as a function of temperature, pressure and ionic strength are used. Jacobson and Langmuir (1974) reported temperature dependent dissociation constants of calcite ($CaCO_3$) from 0 to 50ºC at 1 atm, based on conductance measurements and using the extended Debye-Hückel equation. Millero (1979) developed an empirical temperature, salinity, and pressure dependent equation to determine the solubility product of calcite in seawater. The equation includes two adjustable parameters, and the pressure dependency is taken into account by the partial molar volume and compressibility changes. Plummer and Busenberg (1982) reported empirical temperature dependent equations to calculate the solubility product of calcite, aragonite and varetite in CO_2-H_2O solutions, based on their 350 experimental measurements from 0 to 90ºC at 1 atm. Individual ion activity coefficients

were determined from the equations of Truesdell and Jones (1974), which are modifications from the Debye-Hückel equations. A similar approach is followed by Jacques and Bourland (1983) based on their own experimental results. They presented a predictive equation for the solubility of celestite ($SrSO_4$) in water containing up to 200 g L^{-1} NaCl, at temperatures from 38 to 149ºC and pressures from 7 to 207 bar. Reardon and Armstrong (1986) reported a temperature dependent equation to calculate celestite solubility product, and used Pitzer's formalism to calculate the activity coefficient and fit their experimental results. No pressure correction is included since the experimental data used were all measured at atmospheric pressure. Raju and Atkinson (1988, 1989) developed equations to calculate thermodynamic properties and equilibrium constants as a function of temperature and ionic strength, based on their experimental data for $SrSO_4$ and $BaSO_4$. The activity coefficients were calculated from Pitzer's equations. The heat capacity value reported for Sr^{2+} at 25ºC is -7.4 J K^{-1} mol^{-1}, extremely different from the value of -106 J K^{-1} mol^{-1} reported by Marcus (1997), and used as initial guess in this work. Howell et al. (1992) derived an equation to calculate the solubility product of $SrSO_4$ in NaCl solutions as a function of temperature and pressure, based on their experimental results. Also, an equation to determine the mean activity coefficient as a function of temperature, pressure and ionic strength is reported. Duan et al. (1996) used Pitzer's approach to calculate the liquid phase activity coefficients, while an EOS developed by Duan et al. (1992a, b) was used to represent the vapour phase. Their model was implemented only for $CaCO_3$ solubility in NaCl solutions, and gases CO_2 and CH_4. Battistelli et al. (1997) modelled mixtures of water, sodium chloride, and a slightly soluble non condensable gas (air, CO_2, CH_4, H_2, or N_2) in connection to geothermal reservoirs. The system is modelled by an equation of state developed by Battistelli et al. (1993) and includes precipitation and dissolution of solid salt. The concentration of solutions that are both vapour and halite (NaCl) saturated was calculated using an equation by Potter quoted in Chou (1987). The applicability of the model ranges from 100 to 350ºC and up to a partial CO_2 pressure of 100 bar. Satman et al. (1999) studied the effect of calcite deposition in geothermal wells performance. The solubility of calcite in CO_2-H_2O solutions up to high temperature and pressure was obtained through a simple correlation derived from experimental data.

Some investigators prefer the use of solubility indices to determine whether or not precipitation of a certain mineral will take place at given conditions of temperature and pressure. Oddo and Tomson (1994) compared the Langelier (1936), and Oddo and Tomson (1994) saturation indices relative to calcium carbonate scale. They also introduced a new saturation index for barium, strontium, and calcium sulphate scale formation. The

equilibrium constants required to obtain the saturation index were derived from literature data as a function of temperature, pressure, and ionic strength, by performing a non-linear least-squares fit of the data sets. For $CaCO_3$, the saturation index was improved by the addition of the CO_2 fugacity, calculated by the Peng-Robinson equation of state. Marshall (1989) calculated the saturation index for calcite from the reconstructed reservoir water composition at Dixie Valley (Nevada, EEUU) geothermal field. The ion-association type model EQ3NR developed by Wolery (1983) and the specific-interaction model EQUIL developed by Weare (1987) were used to determine activity coefficients in the Na-Ca-Cl-CO_2-H_2O system and to calculate the distribution of elements in the reservoir and production water.

All the previous models are focused on a single mineral or couple of minerals, and therefore cannot be applied to determine real concentrations in natural waters, where many different species coexist and interact with each other. Models accounting for all the possible reactions taking place simultaneously are scarcer. Among them, we can mention Harvie and Weare (1980), who used Pitzer's formalism to study the solubility of solid phases in the system Na-K-Ca-Mg-Cl-SO_4-H_2O at 25ºC and 1 atm. This study has been later extended by different authors to cover wider ranges of temperature, pressure, and to include additional species present in connate and injection waters. In general, to determine salt solubility at high temperature and pressure, the dissociation constants are described as a function of temperature and pressure. Then, the saturated concentration is calculated by the use of Pitzer's activity coefficient model. However, the studies disagree about the temperature dependency of Pitzer parameters. Harvie et al. (1984) considered new carbonate species, modelling the system Na-K-Ca-Mg-Cl-SO_4-HCO_3-CO_3-CO_2-H_2O at 25ºC and 1 atm. Møller (1988) constructed a variable temperature model for the Na-Ca-Cl-SO_4-H_2O system from 25 to 250ºC. Greenberg and Møller (1989) extended the seven component seawater model developed by Harvie and Weare (1980) from 0 to 250ºC and from zero to high ionic strength (around 18 m). The pressure is considered to be 1 atm up to 100ºC and the saturation pressure of water above 100ºC. Spencer et al. (1990) parameterized the same system as Greenberg and Møller (1989) at low temperatures (from -60 to 25ºC). Spencer et al. (1990) had some problems when predictions were carried in sulphate-dominated systems, and a new re-parameterization of those systems was performed by Marion and Farren (1999). Additionally, they consider five new sulphate minerals (gypsum – $CaSO_4\cdot2H_2O$- among them) allowing a more complete treatment of the system. He and Morse (1993) predicted the solubility of halite, gypsum and anhydrite ($CaSO_4$) in Na-K-H-Ca-Mg-Cl-OH-SO_4-H_2O solutions of varying composition as a function of temperature

(from 0 to 200ºC) and pressure (from 1 to 1000 bar). In 1998, Møller et al. predicted carbonate scale formation in the Na-K-H-Ca-Cl-SO$_4$-H$_2$O system up to 250ºC, and silica scale formation in the Na-Mg-Cl-SO$_4$-SiO$_2$-H$_2$O system up to 320ºC. The gas phase is modelled by using an equation of state (Duan et al., 1992a).

Pitzer's approach has also been used by many investigators to include new species of great importance in connection to scale formation in the oil and geothermal industry (as Ba^{2+} and Sr^{2+}). Monnin and Galinier (1988) proposed a predictive model for the solubility of barite (BaSO$_4$) and celestite in the Na-H-K-Ca-Mg-Ba-Sr-Cl-OH-SO$_4$-H$_2$O system at 25ºC based on Pitzer's ion interaction model, and in the parameterization performed by Harvie et al. (1984). The model fails for highly concentrated waters, but the accuracy for barite and celestite solubility calculations in the low to moderate concentration region is better than ±10%. The previous model was later extended by Monnin (1999), covering temperatures from 0 to 200ºC, and pressures up to 1 kbar. Pressure correlations are evaluated through partial molar volume calculations within Pitzer's formalism. The compressibility effects have been neglected due to the lack of experimental data. Haarberg (1989) developed a scale prediction model for the minerals CaCO$_3$, BaSO$_4$, CaSO$_4$ and CaSO$_4$·2H$_2$O. He compared some of the results obtained using Pitzer's formalism whit results from Sander's (1984) model, and concluded the former model gives the best description of experimental data. Gas phase fugacities for carbon dioxide were calculated according to Houghton et al. (1957). Activity coefficients for aqueous CO$_2$ were determined from the equations of Weiss (1974) or Naumov et al. (1974), depending on the temperature of the system. The model predictions are reliable up to 175ºC and 400 bar. Yuan and Todd (1991) developed a model to predict sulphate scaling tendency in oilfield operations, taking into account the possible co-precipitation of BaSO$_4$, SrSO$_4$ and CaSO$_4$. The model is based on Pitzer's formalism to calculate activity coefficients, but does not use the parameterization reported by Harvie et al. (1984). Instead, they determined new parameters and thermodynamic solubility products based on solubility data. According to Yuan and Todd (1991), the limited number of published data makes Pitzer's approach to take into account the pressure effect impractical. Instead, they developed empirical equations from the correlation of solubility with pressure. The model was used to predict sulphate scaling potential of mixing injection water and formation water in the North Sea, and the predictions were substantiated by field observations. Nonetheless, some of the predictions by Yuan and Todd (1991) and Yuan et al. (1994) do not agree with those by Vetter et al. (1982) and Atkinson et al. (1991). Kaasa (1998) presented a model than can predict pH and mineral solubility (CaSO$_4$, CaSO$_4$·2H$_2$O, BaSO$_4$, SrSO$_4$, CaCO$_3$, FeCO$_3$, FeS and NaCl) together with multiphase equilibria and the

phase distribution for CO_2, H_2S and hydrocarbon components. The equation of state given by Vonka et al. (1995) is used to describe the volumetric behaviour of the gas phase and the phase equilibrium between gas and oil. That equation is linked to the Pitzer's model and solved simultaneously. Carrier et al. (1998) combined two thermodynamic models to describe salt solubility in the system Na-K-Ca-Ba-Sr-Cl-SO_4-H_2O. Helgeson, Kirkman and Flowers (HKF) modified equations of state (Helgeson et al., 1981) are used to calculate the dissociation constants of mineral species, while Pitzer ionic interaction model is used to calculate activity coefficients for the ions. The model was applied in the temperature range from 25 to 350ºC, and pressures from 1 to 160 bar. Pátzay et al. (1997) developed an equilibrium simulation algorithm to represent $CaCO_3$, $CaSO_4$, $BaSO_4$, and SrSO4 scale formation in a Na-K-Mg-Ca-H-Ba-Sr-Cl-Br-SO_4-OH-HCO_3-CO_3-CO_2-H_2O system using Davies and Pitzer models. The predicted results using Pitzer's activity coefficients fitted the literature data well.

Pitzer's framework is probably the most widely used to determine solubility of scaling minerals in natural waters at high temperature and pressure. Nevertheless, some investigators opted for other approaches. Arnórsson et al. (1982) calculated the composition and aqueous speciation of geothermal reservoir waters from 0 to 370ºC. The species considered were SiO_2, B, Na, K, Ca, Mg, Fe, Al, NH_3, CO_2, SO_4, H_2S, Cl, F, N_2, O_2, H_2, and CH_4. The equilibrium constants for the different reactions taking place were calculated as a function of temperature from experimental data on thermodynamic properties, following the methods described by Helgeson (1967, 1969), and Helgeson et al. (1978). Individual activity coefficients for ions were also calculated following Helgeson's framework, with the required parameters taken from Helgeson and Kirkhan (1974a, b). Potapov et al. (2001) studied the possibility and efficiency of chemical treatment of the geothermal separate prior to reinjection under conditions of the Verkhne-Mutnovsk (Russia) geothermal power station. They simulated the chemical equilibrium in the multicomponent aqueous solution and calculated the activity coefficients from the semi-empirical formula of Helgeson quoted in Kaz'min (1983).

Some of the later models coupled thermodynamics and kinetics to obtain a more reliable prediction of scale formation (Wat et al., 1992, Zhang et al., 2001); and others consider fluid dynamics and flow in porous media (Bertero et al., 1988, Li et al., 1995). Wat et al. (1992) performed experiments on kinetics of $BaSO_4$ crystal growth and concluded the rate of growth of barite can be represented by a second order rate equation. Zhang et al. (2001) used a thermodynamic model (Kharaka et al., 1988) coupled to a kinetic model to predict $CaCO_3$ deposition downhole. The model has been applied to predict the scale formed on the

internal surface of a tube, and the predicted results are in good agreement with the real scale profile. Bertero et al. (1988) presented a numerical model coupling a reservoir-fluid-flow/thermal-equilibrium simulator with a chemical-equilibrium computer code. The output of the model is the evolution with time of the amount of scale formed when changes in the injection water temperature occur or when there is mixing of incompatible waters. Li et al. (1995) developed a model to predict co-precipitation of $BaSO_4$ and $SrSO_4$ in oil fields. The computer model simulates reactive flow through porous media. Dissolved ions move in the aqueous phase by convection and diffusion, while the solid phase does not move with the fluid.

There are also several commercial programs to determine mineral scaling potential in oil and gas production. OLI (http://www.olisystems.com/oliscale.htm) is a software that computes gas-liquid-oil-solid equilibria up to 316ºC, 1517 bar and $7 \cdot 10^5$ TDS. The model uses a revised Helgeson's equation of state to consider the temperature and pressure effects on the brine, while the SRK equation of state is used to account for the temperature and pressure effects both in the vapour and in the organic phase. Different activity coefficient models are implemented (Bromley, Zemaitis, Pitzer and Setschnow).

3.3 The Extended UNIQUAC Model

In this work, the extended universal quasichemical (extended UNIQUAC) model, as presented by Thomsen and Rasmussen (1999), is used to model solutions containing electrolytes, covering wide ranges of concentration, temperature, and pressure. The model was originally developed to represent vapour-liquid equilibrium in mixed solvents where salts were present. Since then, it has been applied to describe solid-liquid, liquid-liquid, and vapour-liquid equilibria in a wide range of system with good accuracy (Nicolaisen et al., 1993, Thomsen, 1997, Thomsen et al., 1996, 2004, Thomsen and Rasmussen, 1999).

The extended UNIQUAC model is a local composition model derived from the original UNIQUAC model (Abrams and Prausnitz, 1975, Maurer and Praustniz, 1978) by adding a Debye-Hückel term (Sander, 1984, Sander et al., 1986a, b) to take into account the presence of ionic species in the solution. The UNIQUAC term, which is subdivided into a combinatorial or entropic term and a residual or enthalpic term, takes into account the short range ion-ion, ion-solvent and solvent-solvent interactions. The Debye-Hückel term was originally derived for an ideal solution of charged particles, and takes into account long range, electrostatic ion-ion interactions. For salt-free solutions, the model reduces to the original UNIQUAC equation.

Hence, the excess Gibbs energy expression by the extended UNIQUAC model consists of three terms:

$$G^E = G^E_{Combinatorial} + G^E_{Residual} + G^E_{Debye-Hückel} \tag{3-1}$$

where G^E is the molar excess Gibbs energy. The combinatorial and residual terms are identical to the terms used in the original UNIQUAC equation. These terms are based on the rational, symmetric activity coefficient convention, while the Debye-Hückel term is based on the rational, symmetric convention for water, and the rational, unsymmetric convention for ions.

The combinatorial, entropic term takes into account the deviation from ideality due to differences in size and shape of the species forming the system. It is expressed as:

$$\frac{G^E_{Combinatorial}}{RT} = \sum_i x_i \ln\left(\frac{\phi_i}{x_i}\right) - \frac{z}{2}\sum_i q_i x_i \ln\left(\frac{\phi_i}{\theta_i}\right) \tag{3-2}$$

where R is the gas constant (8.314 J K^{-1} mol^{-1}), T is the temperature in Kelvin, x_i is the mole fraction of species i, z is the coordination number (the number of nearest neighbours, arbitrarily fixed at 10), ϕ_i is the volume fraction of species i, and θ_i is the surface area fraction of species i, expressed as:

$$\phi_i = \frac{x_i r_i}{\sum_l x_l r_l} \tag{3-3}$$

$$\theta_i = \frac{x_i q_i}{\sum_l x_l q_l} \tag{3-4}$$

where r_i and q_i are the volume and surface area parameters for species i.

The residual, enthalpic term takes into account the short-range molecular energetic interactions, and it is calculated as:

$$\frac{G^E_{Residual}}{RT} = -\sum_i x_i q_i \ln\left(\sum_k \theta_k \psi_{ki}\right) \tag{3-5}$$

where ψ_{ki} is given by

$$\psi_{ki} = \exp\left(-\frac{u_{ki} - u_{ii}}{T}\right) \tag{3-6}$$

In equation 3-6, u_{ki} ($= u_{ik}$) and u_{ii} are the interaction energy parameters. They are temperature dependent:

$$u_{ki} = u_{ki}^0 + u_{ki}^t(T - 298.15) \tag{3-7}$$

The Debye-Hückel contribution to the excess Gibbs energy of the extended UNIQUAC model is given by the expression:

$$\frac{G_{Debye-Hückel}^E}{RT} = -x_w M_w \frac{4A}{b^3}\left[\ln(1 + bI^{1/2}) - bI^{1/2} + \frac{b^2 I}{2}\right] \tag{3-8}$$

where M_w is the molar mass of water (0.01801534 kg mol^{-1}), x_w is the mole fraction of water, A is a temperature and pressure dependent Debye-Hückel parameter, b is a constant equal to 1.5 (kg mol^{-1})$^{1/2}$, and I is the ionic strength based on molality, calculated as:

$$I = 0.5\sum_i m_i z_i^2 = 0.5\frac{\sum_i x_i z_i^2}{x_w M_w} \tag{3-9}$$

In equation 3-9, z_i is the charge of ion i and m_i is the molality (mol (kg H$_2$O)$^{-1}$) of ion i. Equation 3-8 is a simplification by Fowler and Guggenheim (1949) of the excess Gibbs energy given by Debye and Hückel (1923).

The parameter A is calculated as

$$A = \frac{F^3}{4\pi N_A}\left[\frac{d}{2(\varepsilon_0 DRT)^3}\right]^{1/2} \tag{3-10}$$

F is the Faradays constant (96484.6 C mol^{-1}), N_A is the Avogadro's number (6.023·10^{23} mol^{-1}), ε_0 is the vacuum permittivity (8.8542·10^{-12} C^{2}J^{-1}m^{-1}), d is the density of the solution (kg m^{-3}), and D is the dielectric constant (relative permittivity) of the solution (dimensionless). Both d and D are functions of temperature and pressure, and are calculated according to Wagner and Pruss (1993).

The extended Debye-Hückel law is based on the assumption of infinite dilution. Therefore, it can describe the non-ideal behaviour caused by electrostatic forces in very dilute electrolyte solutions. As the ionic strength increases, the accuracy of the extended Debye-Hückel law decreases, and it is not accurate for ionic strengths higher than 0.1 m. Therefore, the Debye-Hückel parameter A is only valid in very dilute solutions, where the density and relative permittivity of the solution are very close to the properties of pure water. For this reason, the parameter A for aqueous solutions is calculated according to the density and dielectric constant of pure water, instead of the properties of the real solution. According to Thomsen (1997), the value of the Debye-Hückel contribution to the activity coefficient is only changed a few percent when the density of pure water at 25°C is used instead of the density of a saturated solution of NaCl. Regarding the relative permittivity, the values for

pure water and real solutions may be rather different, especially in the high concentration region. Nevertheless, the ions only "see" pure water around them, and thus it is the property of water and not the solution the one needed in the A parameter.

The activity coefficient for species i is obtained by partial molar differentiation:

$$\ln \gamma_i = \left[\frac{\partial \left(\dfrac{nG^E}{RT} \right)}{\partial n_i} \right]_{P,T,n_{j \neq i}} \tag{3-11}$$

Using equation 3-11 and the correspondent excess Gibbs free energy equations (equations 3-2, 3-5 and 3-8), the different contributions to the activity coefficient can be obtained:

$$\ln \gamma = \ln \gamma^{Debye-Hückel} + \ln \gamma^{Combinatorial} + \ln \gamma^{Residual} \tag{3-12}$$

It is necessary at this point to take into account that the different terms in equation 3-1 are not based on the same conventions. The combinatorial and residual UNIQUAC terms are based on the rational, symmetrical activity coefficient convention, while the Debye-Hückel term is based on the rational, symmetric convention for water, and the rational, unsymmetric convention for ions. The unsymmetric activity coefficient for ion i (γ_i^*) ca be obtained from the symmetric activity coefficient using the relationship

$$\ln \gamma_i^* = \ln \gamma_i - \ln \gamma_i^\infty \tag{3-13}$$

Therefore, the equation for the unsymmetric activity coefficient of ion i is transformed into equation 3-14, while for water it is reduced to the form of equation 3-12.

$$\ln \gamma_i^* = \ln \gamma_i^{Combinatorial} - \ln \gamma_i^{\infty,Combinatorial} + \ln \gamma_i^{Residual} - \ln \gamma_i^{\infty,Residual} + \ln \gamma_i^{*,Debye-Hückel} \tag{3-14}$$

The combinatorial and residual parts of the rational, symmetric activity coefficients are

$$\ln \gamma_i^{Combinatorial} = \ln \left(\frac{\phi_i}{x_i} \right) + 1 - \frac{\phi_i}{x_i} - \frac{z}{2} q_i \left[\ln \left(\frac{\phi_i}{\theta_i} \right) + 1 - \frac{\phi_i}{\theta_i} \right] \tag{3-15}$$

$$\ln \gamma_i^{Residual} = q_i \left[1 - \ln \left(\sum_k \theta_k \psi_{ki} \right) - \sum_k \frac{\theta_k \psi_{ik}}{\sum_l \theta_l \psi_{lk}} \right] \tag{3-16}$$

where i can be applied to both water and ions.

The infinite dilution terms of the combinatorial and residual parts of the activity coefficient can be obtained by setting the mole fraction of water equal to one (infinite dilution for ion i)

$$\ln \gamma_i^{\infty,Combinatorial} = \ln\left(\frac{r_i}{r_w}\right) + 1 - \frac{r_i}{r_w} - \frac{z}{2}q_i\left[\ln\left(\frac{r_i q_w}{r_w q_i}\right) + 1 - \frac{r_i q_w}{r_w q_i}\right]$$ (3-17)

$$\ln \gamma_i^{\infty,Residual} = q_i\left[1 - \ln\psi_{wi} - \psi_{iw}\right]$$ (3-18)

Where γ_i^{∞} is the infinite dilution activity coefficient of ion i in pure water.

By partial molal differentiation of equation 3-8, the contribution to the activity coefficient by the Debye-Hückel term is obtained, both for water and for ions:

$$\ln \gamma_w^{Debye-Hückel} = M_w \frac{2A}{b^3}\left[1 + bI^{1/2} - \frac{1}{1+bI^{1/2}} - 2\ln(1+bI^{1/2})\right]$$ (3-19)

$$\ln \gamma_i^{*,Debye-Hückel} = -z_i^2 \frac{AI^{1/2}}{1+bI^{1/2}}$$ (3-20)

Finally, the symmetric, rational activity coefficient for water can be expressed as

$$\ln \gamma_w = \ln\left(\frac{\phi_w}{x_w}\right) + 1 - \frac{\phi_w}{x_w} - \frac{z}{2}q_w\left[\ln\left(\frac{\phi_w}{\theta_w}\right) + 1 - \frac{\phi_w}{\theta_w}\right] +$$
$$q_w\left[1 - \ln\left(\sum_k \theta_k\psi_{kw}\right) - \sum_k \frac{\theta_k\psi_{wk}}{\sum_l \theta_l\psi_{lk}}\right] +$$ (3-21)
$$M_w \frac{2A}{b^3}\left[1 + bI^{1/2} - \frac{1}{1+bI^{1/2}} - 2\ln(1+bI^{1/2})\right]$$

The unsymmetric, rational activity coefficient for ion i is:

$$\ln \gamma_i^* = \ln\left(\frac{\phi_i}{x_i}\right) + 1 - \frac{\phi_i}{x_i} - \frac{z}{2}q_i\left[\ln\left(\frac{\phi_i}{\theta_i}\right) + 1 - \frac{\phi_i}{\theta_i}\right]$$
$$- \ln\left(\frac{r_i}{r_w}\right) + 1 - \frac{r_i}{r_w} - \frac{z}{2}q_i\left[\ln\left(\frac{r_i q_w}{r_w q_i}\right) + 1 - \frac{r_i q_w}{r_w q_i}\right]$$
$$+ q_i\left[1 - \ln\left(\sum_k \theta_k\psi_{ki}\right) - \sum_k \frac{\theta_k\psi_{ik}}{\sum_l \theta_l\psi_{lk}}\right]$$ (3-22)
$$- q_i\left[1 - \ln\psi_{wi} - \psi_{iw}\right] - z_i^2 \frac{AI^{1/2}}{1+bI^{1/2}}$$

The activity coefficients for water and ion i as expressed in equations 3-21 and 3-22 are rational (mole fraction based) activity coefficients. They can be converted to molal activity coefficients ($\gamma_{i,m}^*$) using equation 3-23.

$$\gamma_{i,m}^* = \gamma_i^* \left(1 - \sum_j x_j \right)$$

(3-23)

where the summation is over all ionic species. In the case of water, $\gamma_{i,m}^*$ and γ_i^* are replaced

by $\gamma_{w,m}$ and γ_w, respectively.

3.4 Gas Phase Fugacities

The only two volatile solutes considered in this work are water and carbon dioxide. Ions are considered non volatile species and kept in the aqueous solution in the whole range of temperature and pressure investigated. Therefore, only the fugacity of vapour water and gaseous carbon dioxide are required by the model.

At low pressure the vapour phase behaves almost like a perfect gas and the vapour phase fugacity coefficient is approximately one. Therefore, at low pressures, equation 2-9 for fugacity is simplified to:

$$\hat{f}_{i,g} = y_i P$$

(3-24)

The pressure range covered in the present work goes up to 1000 bar, and thus it is necessary to take into account the non-ideal behaviour of aqueous solutions of gases as CO_2 at high pressures. To do so, the gas phase fugacity coefficients are calculated by the Soave-Redlich-Kwong cubic equation of state, using classical mixing rules.

3.5 Model Parameters

The parameters required by the Debye-Hückel contribution to the extended UNIQUAC model are A and b in equation 3-8. The A parameter is calculated as a function of temperature and pressure as shown by equation 3-10. The b parameter can be explained in terms of specific short-range interactions between the ions and water or each other, but is best regarded as an empirical parameter. In this work, b is given the constant value 1.5 (kg $(mol^{-1}))^{\frac{1}{2}}$.

The parameters required by the SRK cubic equation of state are derived from the critical properties of the volatile species. The critical properties for water are taken from Wagner and Pruss (1993).

The UNIQUAC model requires the volume and surface area parameters for each species (r_i and q_i, respectively, in equations 3-3 and 3-4), and the interaction energy parameters for

each pair of interacting species (u_{ki} and u_{ii} in equation 3-6). No ternary parameters are required.

In the UNIQUAC model presented by Abrams and Prausnitz (1975) the volume and surface area parameters for non-electrolytes (but for water) were calculated based on the geometry of the species. This calculation is not reliable for electrolyte systems, since the dimension of an ion in a crystal lattice differs from the real dimension in an aqueous solution as consequence of hydration. Therefore, both r_i and q_i are fitted to experimental data (Thomsen, 1997).

Due to the constraint of electroneutrality, the properties of ions must be measured relative to the properties of a "reference ion". The hydrogen ion was taken as that reference ion. Its thermodynamic properties (Gibbs free energy of formation, enthalpy of formation and heat capacity) in its standard state (hypothetical ideal one molal solution) are by convention all fixed at zero at all temperatures. If the standard chemical potential is given in a different standard state (and therefore not necessarily equal to zero), equation 3-25 can be applied:

$$\mu_i^{*,m} = \mu_i^0 + RT\ln(M_w\gamma_i^\infty) = \mu_i^* + RT\ln M_w \qquad\qquad \textbf{(3-25)}$$

The natural logarithm of the infinite dilution activity coefficient for the hydrogen ion ($\ln\gamma_{H^+}^\infty$) is taken to be zero at any temperature. Using this convention the infinite dilution activity coefficient of ion i can be calculated relative to H^+. The value for the volume parameter for the hydrogen ion is obtained from equation 3-17, fixing q_{H^+} at zero and using the r and q parameters for water given by Abrams and Prausnitz (1975) (Thomsen, 1997). The interaction energy parameters between the hydrogen ion and the rest of the species were fixed to 10^{10} K and 0, meaning no interaction between the hydrogen ion and the other components. With this convention, the contribution of the hydrogen ion to the residual excess Gibbs energy is null, and thus the activity coefficient for H^+ is mainly determined by the Debye-Hückel term at all concentrations and temperatures (Thomsen et al., 1996).

Some of the u_{ki}^0 and u_{ki}^t parameters have been assigned the values 2500 K and 0, respectively. This is the case for the interaction parameters between aqueous CO_2 and CO_3^{2-}. Solutions containing CO_3^{2-} are characterized by containing an insignificant amount of aqueous CO_2. Therefore, the interaction between those two species can be considered negligible. The same explanation is followed by the interaction parameter between Ba^{2+} and SO_4^{2-}. The solubility of $BaSO_4$ in all the systems studied is so low, that the interaction between those two ions may be considered negligible. In other cases, the lack of

experimental data for certain salts makes it difficult to estimate some parameters. This is the case for the binary interaction energy parameters between Sr^{2+} or Ba^{2+} and OH^-. Moreover, those interactions are not considered relevant for the aim of the present work and are assumed to be low. As done by Thomsen et al. (1996), the water-water and the like cation interaction energy parameters have been fixed at zero to reduce the total number of parameters. This will influence the numerical value of the other parameters, but not the value of the binary interactions (ψ_{ki} in equation 3-6), which is calculated from the difference between interaction energy parameters.

Many of the UNIQUAC parameters required in the present work have already been estimated or given a fixed value and can be found in Thomsen (1997) or Thomsen et al. (1999). This is the case for volume and surface area parameters for H_2O, H^+, Na^+, Ca^{2+}, Mg^{2+}, Cl^-, SO_4^{2-}, OH^-, CO_3^{2-} and HCO_3^-. Table 3-1 shows all the possible binary interactions between the different species considered in the present work. Cells in light grey represent parameters that have already been determined or given a fixed value. Cells in blue represent parameters to be estimated (or fixed) in the present work.

The unknown r_i, q_i, u_{ki}^0 and u_{ki}^t parameters are determined on the basis of experimental data from the IVC-SEP databank for electrolyte solutions (http://www.ivc-sep.kt.dtu.dk/databank/databank.asp).

The low number of parameters required by the extended UNIQUAC model to perform solid-liquid, liquid-liquid, vapour-liquid and speciation equilibria calculations is one of the main advantages of the model. The total number of parameters needed by the extended UNIQUAC model is similar to that required by the NRTL model, but considerably lower than the number required by Pitzer's approach. According to Krop (1999), the complete thermodynamic description of the three component system NH_3-CO_2-H_2O using Pitzer's approach requires as many as 248 parameters (128 of them of binary and 120 of ternary interactions) assuming the symmetry of the ternary interaction parameters. Otherwise, the number of total parameters is furthermore increased. If the same system is described by the extended UNIQUAC model, the total number of parameters is decreased to 52: 16 volume and surface area parameters for the eight species considered by Krop (1999) (H^+, OH^-, $NH_3(aq)$, NH_4^+, $CO_2(aq)$, CO_3^{2-}, HCO_3^- and NH_2COO^-), and 36 binary interaction energy parameters. Of those, fixed values would be given to the interaction energy parameters between the hydrogen ion and any other species, and for the interaction NH_4^+-NH_4^+. Therefore, the number of unknown parameters is reduced to 43. If the temperature dependency needs to be included in the model, the number of parameters required by

Pitzer's approach would increase by a factor of 4-5, while only 120 parameters would be needed by the extended UNIQUAC model.

Table 3-1.
Binary interaction energy parameters for the multicomponent system considered in the present work

	CO_2	H_2O	H^+	Na^+	Ca^{2+}	Ba^{2+}	Sr^{2+}	Mg^{2+}	HCO_3^-	OH^-	Cl^-	CO_3^{2-}	SO_4^{2-}
CO_2													
H_2O		(1)											
H^+		(1)	(1)										
Na^+		(1)	(1)	(1)									
Ca^{2+}		(2)	(2)		(2)								
Ba^{2+}													
Sr^{2+}													
Mg^{2+}		(2)	(2)	(2)	(2)			(2)					
HCO_3^-		(1)	(1)	(1)					(1)				
OH^-		(1)	(1)	(1)	(2)				(1)	(1)			
Cl^-		(1)	(1)	(1)	(2)			(2)	(1)	(1)	(1)		
CO_3^{2-}		(1)	(1)	(1)					(1)	(1)	(1)	(1)	
SO_4^{2-}		(1)	(1)	(1)	(2)			(2)	(1)	(1)	(1)	(1)	(1)

(1) Parameters taken from Thomsen et al. (1999).
(2) Unpublished parameters

3.6 Parameter Estimation

All the parameters required are estimated on the basis of experimental data, mainly solid-liquid equilibrium data, in the temperature range from -10°C to 300°C , pressures up to 1000 bar and concentrations from infinite dilution to saturation. Binary, ternary and quaternary data sets for mixtures with solvent water; cations Na^+, Ca^{2+}, Mg^{2+}, Sr^{2+} and Ba^{2+}; and anions Cl^-, CO_3^{2-}, HCO_3^- and SO_4^{2-} were used. Also, VLE and SLE experimental data containing carbon dioxide were employed.

All data were analyzed before being used. The first data check is done within each source of data, analyzing the tendency followed by the solubility with increasing temperature, pressure and/or salt concentration. For all the salts analyzed at high pressure in the present work, solubility increases with increasing pressure. Regarding the temperature and salt concentration, the behaviour varies from one system to another (e.g., $CaSO_4$ solubility in pure water decreases with increasing temperature, while $BaSO_4$ solubility in pure water

increases with temperature up to around 125°C, and behaves in the opposite way for higher temperatures). The trend followed by each system studied is generally well known and should be easily observed in the experimental data used. Also, the experimental procedure and device used to perform the measurements can be studied in order to find out methodological errors. Finally, data from different sources at the same conditions can be compared and those points considerably far away from the main tendency can be rejected. Note that for certain systems, the amount of data at high temperature and pressure are scarce and such comparison is difficult or even impossible. The problem is enhanced when the experiments are performed in solutions containing a second salt instead of pure water. The number of points that can be compared in this case is reduced drastically.

The parameter estimation procedure varied depending on the system and number of unknown parameters. For example, for the system $NaCl$-$SrSO_4$-H_2O, the unknown parameters were the volume and surface area parameters for Sr^{2+}, and the binary interaction energy parameters between Sr^{2+} and H_2O, H^+, Na^+, Sr^{2+}, Cl^-, SO_4^{2-}, and OH^-. As mentioned previously, some of these parameters are fixed due to the lack of available experimental data or to reduce the total number of parameters. Thus, $u^0_{Sr^{2+}-Sr^{2+}} = 0\ K$, $u^t_{Sr^{2+}-Sr^{2+}} = 0$, $u^0_{Sr^{2+}-H^+} = 10^{10}\ K$, $u^t_{Sr^{2+}-H^+} = 0$, $u^0_{Sr^{2+}-OH^-} = 2500\ K$ and $u^t_{Sr^{2+}-OH^-} = 0$. The final set of parameters to be estimated was $r_{Sr^{2+}}$, $q_{Sr^{2+}}$, $u^0_{Sr^{2+}-H_2O}$, $u^t_{Sr^{2+}-H_2O}$, $u^0_{Sr^{2+}-Na^+}$, $u^t_{Sr^{2+}-Na^+}$, $u^0_{Sr^{2+}-Cl^-}$, $u^t_{Sr^{2+}-Cl^-}$, $u^0_{Sr^{2+}-SO_4^{2-}}$, and $u^t_{Sr^{2+}-SO_4^{2-}}$. The volume and surface area parameter for Sr^{2+}, together with the interaction energy parameters between Sr^{2+}-H_2O, Sr^{2+}-Cl^- and Sr^{2+}-Na^+ were estimated on the basis of experimental data for the binary system $SrCl_2$-H_2O and for the ternary system $SrCl_2$-$NaCl$-H_2O. These parameters were determined simultaneously in order to differentiate between the interaction Sr^{2+}-H_2O and the other interactions. Once these parameters are estimated, the Sr^{2+}-SO_4^{2-} binary interaction energy is obtained from experimental solubility data for the binary system $SrSO_4$-H_2O at low pressure (atmospheric pressure or the saturation pressure of the solution at the given temperature) and the ternary system $SrSO_4$-Na_2SO_4-H_2O. The pressure parameters for the salt $SrSO_4$ were determined on the basis of experimental solubility data for celestite in pure water at high pressure. Finally, experimental data on the quaternary system $NaCl$-$SrSO_4$-H_2O are added to the database and all parameters are estimated simultaneously.

To estimate the parameters values, a non-linear, least squares minimization is performed in order to minimize the difference between calculated and experimental data. Such difference

was calculated in different ways according to the type of data and the system being studied. For the majority of the systems, the objective function to minimize was:

$$F = \sum_{i=1}^{ndata} \left| \frac{\left| \sum_{j=1}^{n} (s_{j,calc} - s_{j,exp}) \right|}{\sum_{j=1}^{n-1} s_{j,exp} + 0.04} \right| \cdot 100 \tag{3-26}$$

where the summation is over the data points and *s* is the solubility in mass percentage. *Calc* and *exp* in equation 3-26 refer to calculated and experimental data, respectively. The summation in the numerator of equation 3-26 is over all the species present in the system (water, ions and molecules), while the summation in the denominator includes all the species but water. Most of the salts we are dealing with have a very low solubility in water and using solubility in the denominator of the objective function would magnify the error, even though the agreement between experimental points and the model is good. The problem was solved by introducing 0.04 in the denominator of equation 3-26. The constant 0.04 was found to give low deviations if the experimental points were well represented by the extended UNIQUAC model and vice versa.

When estimating parameters for the NaCl-H$_2$O system, the large solubility of sodium chloride in water allows the use of the residual deviation (equation 3-27) as the objective function:

$$F_{NaCl-H_2O} = \sum_{i=1}^{ndata} \left| \frac{\left| \sum_{j=1}^{n} (s_{j,calc} - s_{j,exp}) \right|}{\sum_{j=1}^{n} s_{j,exp}} \right| \cdot 100 \tag{3-27}$$

3.7 References in Chapter 3

Abrams, D.S., Prausnitz, J.M., 1975. Statistical thermodynamics of liquid mixtures: A new expression for the excess gibbs energy of partly or completely miscible systems. AIChE Journal 21, 116-128.

Arnórsson, S., Sigurdsson, S., Svavarsson, H., 1982. The chemistry of geothermal waters in Iceland. I. Calculation of aqueous speciation from 0° to 370°C. Geochimica et Cosmochimica Acta 46, 1513-1532.

Atkinson, G., Raju, K., Howell, R.D., 1991. The thermodynamics of scale prediction. Proceedings of the SPE Interantional Symposium on Oilfield Chemistry, 20-22, Anaheim, CA, USA, Society of Petroleum Engineers, Dallas, 209-215.

Ball, F.X., Planche, H., Fürst, W., Renon, H., 1985. Representation of deviation from ideality in concentrated aqueous solutions of electrolytes using a mean sperical approximation molecular model. AIChE Journal 31, 1233-1240.

Battistelli, A., Calore, C,. Pruess, K., 1993. A fluid property module for the TOUGH2 simulator for saline brines with non-condensible gas. Proceedings 18th Workshop on Geothermal Reservoir Engineering, Stanford, CA, pp. 249-259.

Battistelli, A., Calore, C., Pruess, K., 1997. The simulator TOUGH2/EWASG for modelling geothermal reservoirs with brines and non-condensible gas. Geothermics 26 (4), 437-464.

Belaustegi, Y., Olazabal, M. A., Madariaga, J. M., 1999. Development of a Modified Bromley's Methodology for the estimation of ionic media effects on solution equilibria. Part 4. The chemical model of Fe(III) with the halide ligands in aqueous solution at 25ºC Fluid Phase Equilibria 155, 21-31.

Bertero, L., Chierici, G.L., Gottardi, G., Mesini, E., Mormino, G., 1988. Chemical equilibrium models: Their use in simulating the injection of incompatible waters. SPE Reservoir Engineering 14126, 288-294.

Bjerrum, N., 1926. Untersuchungen über ionenassoziation. Mat. Fys. Medd., Kgl. Danske Videnskabernes Selskab 7 (9), 3-48.

Borge, G., Castaño, R., Carril, M. P., Corbillón, M. S., Madariaga, J. M., 1996. Development of a Modified Bromley's Methodology (MBM) for the estimation of ionic media effects on solution equilibria Part 1. Calculation of the interaction parameters in the molar and molal scales at 25ºC Fluid Phase Equilibria, 121, 85-98.

Bromley, L.A., 1973. Thermodynamic properties of strong electrolytes in aqueous solutions. AIChE Journal 19, 313-320.

Brønsted, J. N, 1922. Studies on solubility. IV. Principle of the specific interaction of ions. Journal of the Americal Chemical Society 44, 877-898.

Carrier, H., Ye, S., Vanderbeken, I., Li, J., Xans, P., 1998. Salt solubility under high pressure and high temperature. High Temperature-High Pressure 30, 629-634.

Chen, C., Britt, H., Boston, J., Evans, L., 1982. Local composition model for the excess Gibbs energy of aqueous electrolyte systems. AIChE. J. 28, 588.

Chen, C.C., Evans, L.B., 1986. A local composition model for the excess Gibbs energy of aqueous electrolyte systems. AIChE Journal 32, 444-454.

Chou, I.M., 1987. Phase relations in the system NaCl-KCl-H_2O. III. Solubilities of halite in vapor-saturated liquids above 445°C and redetermination of phase equilibrium properties in the system NaCl-H_2O. Geochimica et Cosmochimica Acta 51, 1965-1975.

Clegg, S.L., Simonson, J.M., 2001. A BET model of the thermodynamics of aqueous multicomponent solutions at extreme concentration. J. Chem. Thermodynamcis 33, 1457-1472.

Cruz, J.L., Renon, H., 1978. A new thermodynamic representation of binary electrolyte solutions nonideality in the whole range of concentrations. AIChE Journal 24, 817-830.

Davies, C.W., 1962. Ion association. Butterworths, London.

Debye, P., Hückel, E., 1923. Zur Theorie der Elektrolyte. I. Gefrierpunktserniedrigung und verwandte Erscheinungen. Physikalische Zeitschrift 24, 185-206.

Duan, Z., Møller, N, Weare, J.H., 1992a. An equation of state for the CH_4-CO_2-H_2O systems: I. Pure systems from 0 to 1000ºC and 0 to 8000 bar. Geochimica et Cosmochimica Acta 56, 2605-2617.

Duan, Z., Møller, N, Weare, J.H., 1992b. An equation of state for the CH_4-CO_2-H_2O systems: II. Mixtures from 50 to 1000ºC and 0 to 1000 bar. Geochimica et Cosmochimica Acta 56, 2619-2631.

Duan, Z., Møller, N., DeRocher, T., Weare, J.H., 1996. Prediction of boiling, scaling and formation conditions in geothermal reservoirs using computer programs TEQUIL and GEOFLUIDS. Geothermics 25 (6), 663-678.

Fowler, S.R., Guggenheim, E.A., 1949. Statistical thermodynamics. University Press, Cambridge, 1965

Greenberg, J.P., Møller, N., 1989. The prediction of mineral solubilities in natural waters: A chemical equilibrium model for the Na-K-Ca-Cl-SO_4-H_2O system to high concentration from 0 to 250ºC. Geochimica et Cosmochimica Acta 53, 2503-2518.

Guggenheim, E.A., 1935. The specific thermodynamic properties of aqueous solutions of strong electrolytes. Philosphical Magazine 19, 588-643.

Haarberg, T., 1989. Mineral deposition during oil recovery. An equilibrium model. Ph.D. Thesis. Instittut for Uorganisk Kjemi, Norges Tekniske Høgskole, Trondheim, Norway.

Haghtalab, A., Vera, J., 1988. A non-random factor model for the excess Gibbs energy of electrolyte solutions. AIChE J. 34, 803-813.

Hamer, W.J., Wu, Y.C., 1972. Osmotic coefficients and mean activity coefficients of uni-univalent electrolytes in water at 25ºC. J. Phys. Chem. Ref. Data 1, 1047-1099.

Harvie, C.E., Weare, J.H., 1980. The prediction of mineral solubilities in natural waters.. Geochim. et Cosmochim. Acta 44, 981-997.

Harvie, C.E., Möller, N., Weare, J.H., 1984. The prediction of mineral solubilities in natural waters: The Na-K-Mg-Ca-H-Cl-SO_4-OH-HCO_3-CO_3-CO_2-H_2O system. Geochimica et Cosmochimica Acta 48, 723-751.

He, S., Morse, J.W., 1993. Prediction of halite, gypsum, and anhydrite solubility in natural brines under subsurface conditions. Computer & Geosciences 19, 1-22.

Helgeson, H.C., 1967. Thermodynamics of complex dissociation in aqueous solutions at elevated temperatures. J. Phys. Chem. 71, 3121-3136.

Helgeson, H.C., 1969. Thermodynamics of hydrothermal systems at elevated temperatures and pressures. Amer. J. Sci. 267, 729-804.

Helgeson, H.C., 1970. Calculation of mass transfer in geochemical process involving aqueous solutions. Geochimica et Cosmochimica Acta 34, 569-592.

Helgeson, H.C., Kirkham, D.H., 1974 a. Theoretical prediction of the thermodynamic behaviour I. American Journal of Science 274, 1089-1198.

Helgeson, H.C., Kirkham, D., 1974 b. Theoretical prediction of the thermodynamic behaviour of aqueous electrolytes at high pressures and temperatures: II. Debye-Hückel parameters for activity coefficients and relative partial molal properties. Amer. J. Sci. 274, 1199-1261.

Helgeson, H.C., Kirkham, D.H., 1976. Theoretical prediction of the thermodynamic behaviour III American Journal of Science 276, 97-240.

Helgeson, H.C., Delany, J.M., Nesbitt, H., Wayne; B., Dennis, K., 1978. Summary and critique of the thermodynamic properties of rock-forming minerals. Pp 229

Helgeson H.C., Kirkham D.H., Flowers G.C., 1981. Theoretical prediction of the thermodynamic behaviour IV. American Journal of Science 281, 1249-1516.

Houghton, G., McLean, A.M., Ritchie, P.D., 1957. Compressibility, fugacity, and water-solubility of carbon dioxide in the region 0-36 atm. and 0-100ºC. Chemical Engineering Science 6, 132-137.

Howell, R.D., Raju, K., Atkinson, G., 1992. Thermodynamics of "Scale" mineral solubilities 4. $SrSO_4$. J. Chem. Eng.

Data 37, 464-469.

Iliuta, M., Rasmussen, P., Thomsen, K., 1999. Electrolyte solutions continuing education course, IVC-SEP, Technical University of Denmark, Lyngby, Denmark.

Jacques, D.C., Bourland, B.I., 1983. A study of solubility of strontium sulphate. SPEJ, 292-300.

Jacobson, R.L., Langmuir, D., 1974. Dissociation constants of calcite and $CaHCO_3^+$ from 0 to 50ºC. Geochimica et

Cosmochimica Acta 33, 301-318.

Johnson, J.W., Oelkers, E.H., Helgeson, H.C., 1992. SUPCRT92: A software package for calculating the standard molal thermodynamic properties of minerals, gases, aqueous species, and reactions from 1 to 5000 bar and 0 to 1000ºC. Computers and Geosciences 18, 899-947.

Kaasa, B., 1998. Prediction of pH, mineral precipitation and multiphase equilibria during oil recovery. Ph.D. thesis. Institutt for Uorganisk Kjemi. Norges Teknisk-Naturvitenskapelige Universitet, Trondheim, pp. 5-272.

Kharaka, Y.K., Gunter, W.D., et al., 1988. Solmineq 88: A computer program for geochemical modelling of water-rock interactions. U.S. Geological Survey, Water-Resources Investigations Report, California, pp. 88-4221.

Kaz'min, L.A., 1983. Computer-based methods of physicochemical simulation of water-rock interaction in Geochemistry. Cand. Sci. (Geol.-Min.) Dissertation, Irkutsk.

Kolker, A., de Pablo, J.J., 1995. Thermodynamic modeling of concentrated aqueous electrolyte. AIChE Journal 41, 1563-1571.

Krop, J., 1999. New approach to simplify the equation for the excess Gibbs free energy of aqueous solutions of electrolytes applied to the modelling of the NH_3-CO_2-H_2O vapour-liquid equilibria. Fluid Phase Equilibria 163, 209-229.

Langelier, W.G., 1936. The analytical control of anti-corrosion water treatment. J. AWWA 25, 1500-1521.

Lewis, G.N., Randall, M., 1921. The activity coefficient of strong electrolytes. J. Am. Chem. Soc. 43, 1112-1154.

Li, Y-H., Crane, S. D., Coleman, J. R., 1995. Novel approach to predict the co-precipitation of $BaSO_4$ and $SrSO_4$. SPE 29489, 447-461.

Lietzke, M.H., Stoughton, R.W., 1975. Extension of a two-structure model for electrolyte solutions to aqueous mixed electrolyte systems. J. Inorg. Nucl. Chem. 37, 2503-2506.

Lin, C., Tseng, H., Lee, L., 1998. A three-characteristic-parameter model for strong electrolytes. Fluid Phase Equilibria 152, 169-185.

Liu, Y., Harvey, A.H., Prausnitz, J.M., 1989. Thermodynamics of concentrated electrolyte solutions. Chem. Eng. Comm. 77, 43-66.

Lu, X., Zhang, L., Wang, Y., Shi, J., 1996. Simultaneous prediction of activity coefficients and enthalpy for aqueous electrolyte solutions at high temperature Fluid Phase Equilibria 116, 201-208.

Macedo, E. A., Skovborg, P., Rasmussen, P., 1990. Calculation of phase equilibria for solutions of strong electrolytes in solvent-water mixtures. Chem. Eng. Sci. 45, 875-882.

Marcus, Y., 1997. Ion Properties. Marcel Dekker, Inc.

Marion, G.M., Farren, R.E., 1999. Mineral solubilities in the Na-K-Mg-Ca-Cl-SO_4-H_2O system: A re-evaluation of the sulphate chemistry in the Spencer-Møller-Weare model. Geochimica et Cosmochimica Acta 63 (9), 1305-1318.

Marshall J.R., 1989. Thermodynamic calculations of calcium carbonate scaling in geothermal wells, Dixie Valley geothermal field, U.S.A. Geothermics 18 (1-2), 269-277.

Marshall, S., May, P., Hefter, G., 1995. Least square analysis of osmotic coefficient data at 25ºC according to Pitzer's equation, 1:1 electrolytes. J. Chem. Eng. Data 40, 1041-1052.

Maurer, G., Prausnitz, J.M., 1978. On the derivation and extension of the UNIQUAC equation. Fluid Phase Equilibria 2, 91-99.

Meissner, H.P., Kusik, C.L., Tester, J.W., 1972. Activity coefficients of strong electrolytes in multicomponent aqueous solution. AIChE Journal 18, 294-298.

Miller, D.G., Piwinskii, A.J., Yamauchi, R., 1977. Geochemical equilibrium codes: A means of modelling precipitation and reinjection phenomena in the Salton Sea geothermal field. SPE 6604.

Millero, F.J., 1979. The thermodynamics of the carbonate system in seawater. Geochimica et Cosmochimica Acta 43 (10), 1651-1661.

Monnin, C., Galinier, C., 1988. The solubility of celestite and barite in electrolyte solutions and natural waters at 25ºC: A thermodynamic study. Chemical Geology 71, 283-296.

Monnin, C., 1999. A thermodynamic model for the solubility of barite and celestite in electrolyte solutions and seawater to 200ºC and to 1 kbar. Chemical Geology 153, 187-209.

Møller, N., 1988. The prediction of mineral solubilities in natural waters: A chemical equilibrium model for the system to high temperature and concentration. Geochimica et Cosmochimica Acta 52, 821-837.

Møller, N., Greenberg, J.P., Weare, J.H., 1998. Computer modelling for geothermal systems: Predicting carbonate and silica scale formation, CO_2 breakout and H_2S exchange. Transport in Porous Media 33, 173-204.

Naumov, V.B., Khakimov, A.K., Khodakovskiy, I.L., 1974. Solubility of carbon dioxide in concentrated chloride solutions at high temperatures and pressures. Geokhimiya 1, 45-55.

Nicolaisen, H., Rasmussen, P., Sørensen, J.M., 1993. Correlation and predicition of mineral solubilities in the reciprocal salt system $(Na^+, K^+)(Cl^-, SO_4^{2-})$-$H_2O$ at 0-100ºC Chemical Engineering Science 48, 3149-3158.

Oddo, J.E., Tomson, M.B., 1994. Why scale forms and how to predict it. SPE Production and Facilities, 47-54.

Pal, K., Mahapatra, P., Sengupta, M., 1991. Activity measurements in aqueous mixed electrolyte solutions. 5. Ternary mixtures of (i) hydrochloric acid, (ii) mono-, di-, or trimethylammonium chloride, and (iii) water of constant total molality. J. Chem. Eng. Data 36, 440-446.

Pátzay, G., Stáhl, G., Kármán, F.H., Kálmán, E., 1997. Modeling of scale formation and corrosion from geothermal water. Electrochimica Acta 43 (1-2), 137-147.

Pérez-Villaseñor, F., Iglesias-Silva, G.A., 2002. Osmotic and activity coefficients using a modified Pitzer equation for strong electrolytes 1:1 and 1:2 at 298.15 K. I&EC Res. 41, 1031-1037.

Pitzer, K., 1973. Thermodynamics of electrolytes I. Theoretical basis and general equations. Journal of Physical Chemistry 77 (2), 268-277.

Pitzer, K.S., Mayorga, G., 1973. Thermodynamics of electrolytes II. J. Phys. Chem. 77, 2300.

Pitzer, K.S., 1975. Thermodynamics of electrolytes. V. Effects of higher-order electrostatic terms. Journal of Solution Chemistry 4 (3), 249-265.

Pitzer, K.S., Simonson, J.M., 1991. Thermodynamics of multicomponent, miscible, ionic systems: theory and equations. Journal of Physical Chemistry 95 (17), 6746.

Plummer, L.N., Busenberg, E., 1982. The solubilities of calcite, aragonite and vaterite in CO_2-H_2O solutions between 0 and 90ºC, and an evaluation of the aqueous model for the system $CaCO_3$-CO_2-H_2O. Geochimica et Cosmochimica Acta 46, 1011-1040.

Polka, H. M., Li, J., Gmehling, J., 1994. A g^E model for single and mixed solvent electrolyte systems. Fluid Phase Equilibria 94, 115-127.

Potapov, V.V., Kashpura, V.N., Alekseev, V.I., 2001. A study of the growth of deposits in geothermal power systems.
Thermal Engineering 48 (5), 395-400.

Raju, K.U.G., Atkinson, G., 1988. Thermodynamics of scale mineral solubilities. 1. $BaSO_4$ (s) in H_2O and aqueous NaCl. J. Chem. Eng. Data 33, 490-495.

Raju, K.U.G., Atkinson, G., 1989. Thermodynamics of scale mineral solubilities. 2. $SrSO_4$ (s) in aqueous NaCl. J. Chem. Eng. Data 34, 361-364.

Raposo, J. C., Sanz, J., Borge, G., Olazábal, M. A., Madariaga, J. M., 1998. Fluid Phase Equilibria 155, 1-19.

Rasaiah, J.C., Friedman, H.L., 1968. Charged square-well model for ionic solutions. J. Chem. Phys. 48, 2724-2749.

Reardon, E.J., Armstrong, D.K., 1987. Celestite (SrSO4(s)) solubility in water, seawater and NaCl solution.
Geochimica et Cosmochimica Acta 51, 63-72.

Renon, H., Prausnitz, J.M., 1969. Derivation of the three-parameter Wilson equation for the excess Gibbs energy of liquid mixtures. AIChE Journal 15 (5), 785.

Renon, H., 1996. Models for excess properties of electrolyte solutions: Molecular bases and classification, needs and trends for new developments. Fluid Phase Equilibria 116, 217.

Sahai, N., Sverjensky, D.A., 1998. GEOSURF: A computer program for modeling adsorption on mineral surfaces from aqueous solution. Computers and Geosciences 24 (9), 853-873.

Sander, B., 1984. Extended UNIFAC/UNIQUAC models for gas solubility calculations and electrolyte solutions. Ph.D. Thesis, Technical University of Denmark, Lyngby, Denamrk.

Sander, B. Fredenslund, Aa., Rasmussen, P., 1986a. Calculation of vapour-liquid equilibria in mixed solvent/salt systems using an extended UNIQUAC equation. Chemical Engineering Science 41, 1171-1183.

Sander, B., Rasmussen, P. Fredenslund, Aa., 1986b. Calculation of vapour-liquid equilibria in nitric acid-water-nitrate salt systems using an extended UNIQUAC equation. Chemical Engineering Science 41, 1185-1195.

Sander, B., Rasmussen, P., Fredenslund, Aa., 1986c. Calculation of solid-liquid equilibria in aqueous solutions of nitrate salts using an extended UNIQUAC equation. Chemical Engineering Science 41, 1197-1202.

Satman, A., Ugur, Z., Onur, M., 1999. The effect of calcite deposition on geothermal well inflow performance. Geothermics 28, 425-444.

Shock, E.L., Helgeson, H.C., 1988. Calculation of the thermodynamic and transport properties. Geochimica et Cosmochimica Acta 52, 2009-2036.

Spencer, R.J., Møller, N., Weare, J.H., 1990. The prediction of mineral solubilities in natural waters: A chemical equilibrium model for the $Na-K-Ca-Mg-Cl-SO_4-H_2O$ system at temperatures below 25ºC. Geochimica et Cosmochimica Acta 54, 575-590.

Stokes, R.H., Robinson, R.A., 1948. Ionic hydration and activity in electrolyte solutions. J. Am. Chem. Soc. 70, 1870-1878.

Tan, T.C., 1987. Model for predicting the effect of dissolved salt on the vapour liquid equilibrium of solvent mixtures. Chem. Eng. Res. Des. 65, 355-365.

Tan, T.C., 1990. A modified NRTL model for predicting the effect of dissolved solute on the vapour-liquid equilibrium of solvent mixtures. Chem. Eng. Res. Des. 68, 93-103.

Thomsen, K., Rasmussen, P., Gani, R., 1996. Correlation and prediction of thermal properties and phase behaviour for a class of electrolyte systems. Chemical Engineering Science 51, 3675-3683.

Thomsen, K., 1997. Aqueous electrolytes: model parameters and process simulation. Ph.D. thesis. Technical University of Denmark, Denmark.

Thomsen, K., Rasmussen, P., 1999. Modeling of vapor-liquid-solid equilibrium in gas-aqueous electrolyte systems. Chemical Engineering Science 54, 1787-1802.

Thomsen, K., Iliuta, M., Rasmussen, P., 2004. Extended UNIQUAC model for correlation and prediction of vapor-liquid-liquid-solid equilibria in aqueous salt systems containing non-electrolytes. Part B. Alcohol (ethanol, propanols, butanols) - water - salt systems. Chemical Engineering Science 59, 3631-3647.

Truesdell, A.H., Jones, B.F., 1974. WATEQ, a computer program for calculating chemical equilibria of natural waters. U.S. Geol. Survey J. Res. 2, 233-248.

Vanderveken, I, Suyu, Y., Bouyssiere, B., Carrier, H., Xans, P., 1999. Ability of the MHV2 mixing rule to describe the effect of salt on gas solubility in brines at high temperature and high pressure. High Temperatures-High Pressures 31, 653-663.

Vetter, O.J., Kandarpa, V., Harouaka, A., 1982. Prediction of scale problems due to injection of incompatible waters. JPT, 273-284.

Vonka, P., Løvland, J., Prokes, T., 1995. Describing vapor-liquid equilibria in methanol $PLU n-alkane systems by means of an equation of state with association. Int. J. of Thermophysics 16 (1), 227-236.

Wagner, W., Pruss, A., 1993. International equations for the saturation properties of ordinary water substance. J. Phys. Chem. Ref. Data 22, 783-787.

Wat, R.M.S., Sorbie, K.S., Todd, A.C., Chen, P., Jiang, P., 1992. Kinetics of $BaSO_4$ crystal growth and effect in formation damage. SPE 23814, 429-437.

Weare, J.H., 1987. Models of mineral solubility in concentrated brines with application to field observations. Chap. 5. Rev. in Mineralogy 17. Mineral Soc. Of Amer., 143-176.

Weiss, R.F., 1974. Carbon dioxide in water and seawater: The solubility of a non-ideal gas. Marine Chemistry 2, 203-215.

Wolery, T.J., 1983. EQ3NR a computer program for geochemical aqueous speciation-solubility calculations: User's guide and documentation. Lawrence Livermore Nat. Lab. Rpt., pp. 191.

Yuan, M.D., Todd, A.C., 1991. Prediction of sulfate scaling tendency in oilfield operations. SPE 18484, 237-250.

Yuan, M., Todd, A.C., Sorbie, K.S., 1994. Sulfate scale precipitation arising from seawater injection: a prediction study. Marine and Petroleum Geology 11(1), 24-30.

Zemaitis, J. F. Jr., Clark, D. M., Rafal, M., Scrivner, N. C., 1986. Handbook of aqueous electrolyte thermodynamics, design institute for physical property data, New York.

Zhang, Y., Shaw, H., Farquhar, R., Dawe, R., 2001. The kinetics of carbonate scaling – application for the prediction of downhole carbonate scaling. Journal of Petroleum Science and Engineering 29, 85-95.

Zuo, Y.X., Fürst, W., 1998. Use of an electrolyte equation of state for the calculation of vapour-liquid equilibria and mean activity coefficients in mixed solvent electrolyte systems. Fluid Phase Equilibria 150-151, 267-275.

4. Sulphate Scaling Minerals

This chapter covers the modelling work performed on sulphate scaling minerals, and it has been published with the title "Prediction of mineral scale formation in geothermal and oilfield operations using the extended UNIQUAC model. Part I. Sulfate scaling minerals" in Geothermics 34 (2005), 61-97 (authors: Ada Villafáfila García, Kaj Thomsen and Erling H. Stenby).

The literature contains little information on most of the systems studied in this chapter at temperatures and pressures different from 25°C and 1 bar. Some of the data present in the literature are, moreover, highly suspected of being erroneous and comparisons among the results reported by different authors show an unacceptable variation in many cases. Reliable and accurate solubility measurements covering a wide range of thermodynamic conditions are necessary in order to accurately determine scale formation, otherwise, false predictions could be produced, such as over-or underestimates of scale formation or even negligence of the same (Vetter et al., 1983). So far the data on $BaSO_4$ and $SrSO_4$ solubilities in the high temperature and pressure range are somewhat incomplete.

Of special concern is any system containing barite, as the solubilities are extremely low and therefore difficult to measure accurately.

According to Vetter et al. (1983), the celestite solubilities determined by atomic absorption spectroscopy (which is a common experimental technique used for this purpose) can have a relative deviation as high as 16%. This value is expected to be even larger for barite.

In the following, it will be demonstrated that the extended UNIQUAC model is able to give a very good representation of the solid-liquid phase equilibria in the binary and ternary systems, over the entire temperature, pressure and concentration range investigated. It will be shown that the model correlates the appearance and disappearance of the different solids very nicely. In all cases, the absolute deviation between extended UNIQUAC calculations and the experimental data is within experimental accuracy. A more detailed explanation about the procedure for calculating the experimental standard deviation is given in section 4.1.

The high accuracy of the extended UNIQUAC model seems to decrease when four different ions are present in the solution, which may be explained in part by the very large scatter in data for these kinds of systems. In most of the cases, the lack of experimental measurements at the same conditions (especially at high temperatures and pressures) makes it impossible

to detect inaccurate data by comparison. For example, figure 4-1 shows the inconsistencies between different data sets for the quaternary $SrSO_4$-NaCl-H_2O system at 25ºC and 1 bar. In this case, the fact that a large number of investigators have studied the same system makes it easy to identify the unreliable data sets. As temperature and pressure increase, however, the number of sources reporting measurements of this type of system at the same conditions generally drops to one or two and no comparison is possible.

This being the case, most of the data containing four ions and water were used for parameter regression, even though some data sets were in clear disagreement. We discarded only the data sets that followed a wrong tendency when varying temperature, pressure and salt concentration.
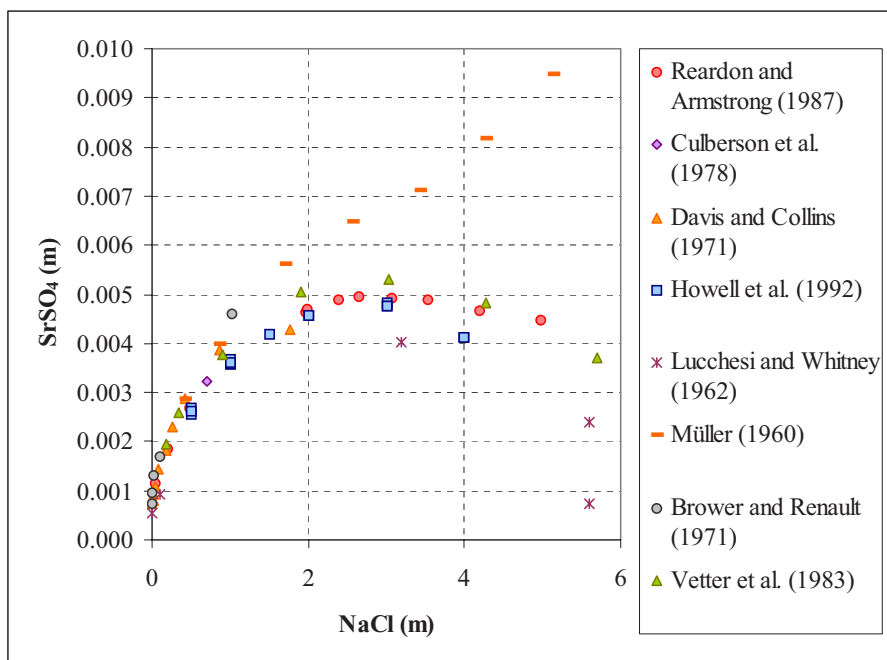
Figure 4-1. Experimental solid-liquid phase diagram for the $SrSO_4$-NaCl-H_2O system at 25ºC and 1 bar.

The surface area and volume parameters obtained from the present work, together with the values required for other species obtained by Thomsen and Rasmussen (1999) are given in table 5-15 in Chapter 5. The binary energy interaction parameters for the extended UNIQUAC model are shown in table 5-16 and table 5-17. Finally, the two new pressure parameters added to the extended UNIQUAC model to account for the pressure dependency are given in table 5-18. The parameters obtained from the present work are marked in bold.

The values for the standard state Gibbs free energy, enthalpy and heat capacity for the different crystalline phases analyzed are taken (whenever it was available) from the NIST Chemical Thermodynamics Database (1990). Those values are also reported in table 4-20.

4.1 Calculation of the Mean Absolute Deviation

Because of the different pressure and temperature conditions used by the different authors, it was not possible to include all the experimental measurements in the standard deviation (SD) calculation. In order to use as much information as possible, we calculated a weighted average standard deviation (ASD) from the SD of experiments carried out at the same conditions of temperature and pressure.

$$SD = \sqrt{\frac{\sum_{i=1}^{n}(m - m_{average})^2}{n-1}}$$

(4-1)

$$ASD = \frac{\sum_i n_i \cdot SD_i}{\sum n_i}$$

(4-2)

Thus, in equation 4-1, n represents the number of experimental data at the same T and P and the standard deviation is calculated for all the available experimental data sets at constant conditions. These SD values are introduced in equation 4-2, where the summation is over all the different data sets. All the calculations are performed in molality units (m).

For ternary systems, the standard deviation for each salt is assumed to be similar to the SD for the binary system salt-H_2O, as the real value could not be calculated because of a complete lack of data at the same conditions of temperature, pressure and salt concentration. This calculation was possible for the system $CaSO_4$-Na_2SO_4-H_2O only, because different authors performed experiments at the same conditions.

All data were analyzed prior to their use. Any data found to be inconsistent were not used for the parameter estimation and were not included in the standard deviation calculation.

When the same investigator reports more than one experimental point at the same conditions, we calculated the average value and used it as m in equation 4-1. In this way, no great weight is given to a single source.

For a given system, the ASD obtained for all the experimental data used is compared to the average absolute deviation (AAD) between the results calculated by the extended UNIQUAC model and the values reported by each reference.

$$AAD = \frac{\sum_{i=1}^{ndata} \left| m_{experimental} - m_{Extended\ UNIQUAC} \right|}{ndata}$$

(4-3)

These AAD values for each reference used in the present work are given in table 4-3 to table 4-19. The mean AAD ($MAAD$) for all the references dealing with each system used is given at the bottom of each table. In most cases the AAD for each data set is lower than the ASD so that the difference between experimental and calculated solubilities is within experimental accuracy.

In equation 4-3, $ndata$ stands for the number of experimental data used from each reference. Table 4-1 shows the values of the standard deviation for the different data sets at constant temperature and pressure for the system $SrSO_4$-H_2O. The calculated average standard deviation is also given in table 4-1.

Table 4-2 shows the values for the ASD for all the binary systems studied in this paper and for the ternary system $CaSO_4$-Na_2SO_4-H_2O. As mentioned previously, the ASD could not be calculated for the rest of the ternary and the quaternary systems.

Table 4-1
Experimental data used to calculate the SD for the system $SrSO_4$-H_2O

Number of data	T (°C)	P (bar)	SD (m)
8	25	1	3.6E-05
2	30	1	5.7E-05
3	50	1	9.5E-05
2	75.5	1	1.1E-05
2	89.5	1	4.1E-06
2	100	1	5.0E-05
2	150.5	5	1.0E-04
2	200	15.6	2.8E-07
2	250	40	1.1E-06
		ASD (m):	4.1E-05

Table 4-2
Calculated ASD values for different systems

System	ASD (m)	
BaSO$_4$-H$_2$O	2.1E-06	
BaCl$_2$-H$_2$O	4.0E-02	
NaCl-H$_2$O	1.8E-01	
SrSO$_4$-H$_2$O	4.1E-05	
SrCl$_2$-H$_2$O	4.0E-02	
CaSO$_4$-H$_2$O	7.8E-04	
Na$_2$SO$_4$-CaSO$_4$-H$_2$O	1.8E-02	Na$_2$SO$_4$
	3.8E-04	CaSO$_4$

4.2 Systems Containing Barium

The results of the SLE-data correlation containing barium, performed in this work, are illustrated in tables 4-3 to 4-9 and figures 4-2 to 4-9. Experimental data are plotted along with calculated curves.

4.2.1 BaSO$_4$-H$_2$O System

The experimental and calculated phase diagrams for the system BaSO$_4$-H$_2$O at a constant pressure of 500 bar and a constant temperature of 200ºC are shown in figures 4-2 and 4-3, respectively. Barite solubility increases with temperature up to around 100-125ºC and starts decreasing for higher temperatures. Regarding pressure, a considerable increase from $8 \cdot 10^{-6}$ to $2.4 \cdot 10^{-5}$ mol BaSO$_4$ (kg H$_2$O)$^{-1}$ (m) is observed when the pressure is increased from 1 to 1000 bar. Of all the systems containing barite studied in the present work, only the BaSO$_4$-H$_2$O and BaSO$_4$-NaCl-H$_2$O systems have been studied at high pressures and temperatures, as they are the ones with scale deposition problems. The rest of the systems will be shown at atmospheric pressure and temperatures up to around 100ºC. The same applies to the other systems investigated in the present chapter; only SrSO$_4$-H$_2$O, SrSO$_4$-NaCl-H$_2$O, CaSO$_4$-H$_2$O and CaSO$_4$-NaCl-H$_2$O are considered relevant for scale formation and are studied at high temperature and pressure.
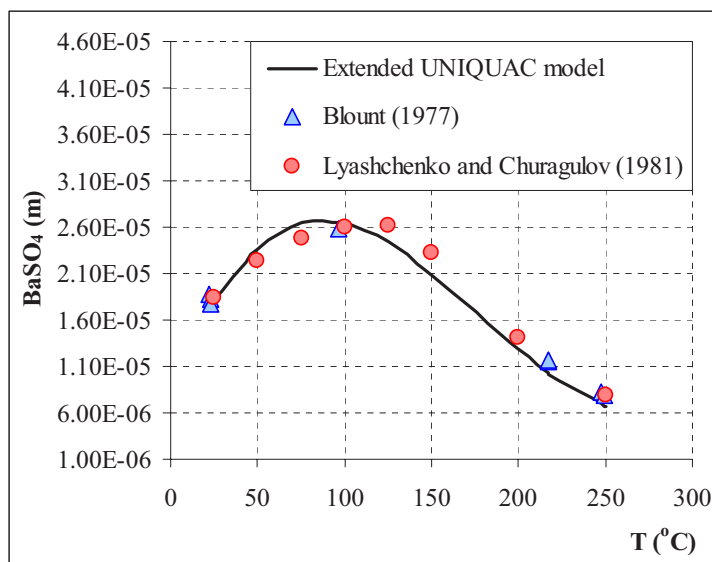
Figure 4-2. Experimental and calculated solid-liquid phase diagram for the BaSO$_4$-H$_2$O system at 500 bar
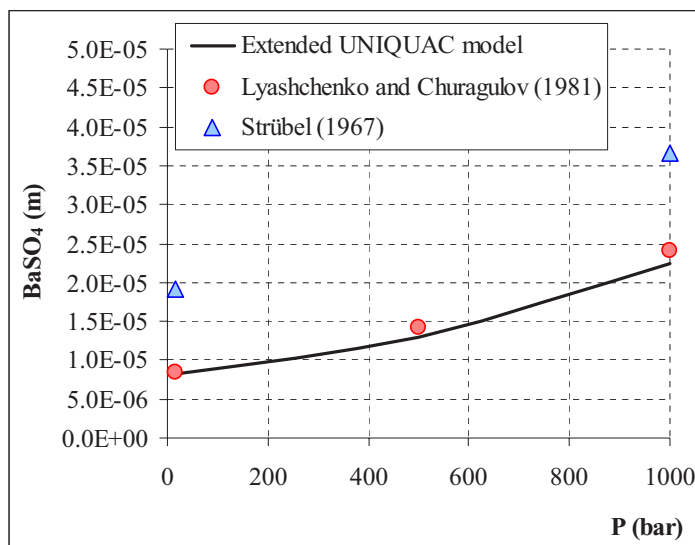
Figure 4-3. Experimental and calculated solid-liquid phase diagram for the $BaSO_4$-H_2O system at 200ºC

The representation by the extended UNIQUAC model of the solubility curves shown in figure 4-2 and figure 4-3 is very good, with a mean absolute deviation (*MAAD*) of $1.6 \cdot 10^{-6}$ m, well below the average experimental standard deviation (*ASD*: $2.1 \cdot 10^{-6}$ m). These values, together with a list of references for the experimental data used for parameter estimation, are presented in table 4-3. The total number of data found in the reference is given, together with the number of data chosen for parameter estimation in this work (in brackets).

Table 4-3
Experimental binary $BaSO_4$-H_2O SLE data sets used for parameter estimation

T (ºC)	P (bar)	Number of data	AAD (m)	Reference
25	1	1 (1)	1.8E-06	Trendafelov et al. (1994)
25	1	1 (1)	1.4E-06	Brower and Renault (1971)
25/95	1	6 (6)	5.5E-07	Templeton (1960)
23/279	36/1406	40 (32)	1.1E-06	Blount (1977)
25/300	1/1000	27 (27)	2.2E-06	Lyashchenko and Churagulov (1981)
99.8/600	4.8/2100	18 (0)		Strübel (1967)
			MAAD (m):	**1.6E-06**

Strübel (1967) and Blount (1977) report data (11 and 8 points, respectively) at temperatures and pressures outside the range correlated in this work (up to 300ºC and 1000 bar).

The data of Strübel (1967) show very large deviations from model calculations and from other experimental data. Figure 4-3 shows the large disagreement when the data of Strübel

(1967) are compared to those of Lyashchenko and Churagulov (1981). The same disagreement is also found at other temperatures and pressures, when compared to other references from table 4-3. Moreover, in some of Strübel's (1967) measurements, a decrease in barite solubility is observed for increasing pressure. Strübel's (1967) data were not used for the evaluation of model parameters because of this apparent lack of reliability.

4.2.2 BaCl₂-H₂O System

The experimental data and the correlation results for the binary $BaCl_2$-H2O system are given in table 4-4 and plotted in figure 4-4. The *MAAD* between experimental and calculated solubilities is within experimental accuracy (*ASD* of 0.04 m).

Although the mean absolute deviation for this system is lower than the average experimental standard deviation, there are three references (Schreinemakers, 1911, Uspenskaya et al., 1955 and Moshinskii and Tikhomirova, 1973) for which the mean absolute deviation between calculated and experimental data is slightly higher than the average experimental standard deviation. Figure 4-4 shows that these three references seem to over- and under-estimate barium chloride solubility, when compared to the other ten references in table 4-4. This disagreement justifies the larger absolute deviation, although its value is low enough to keep these data sets.
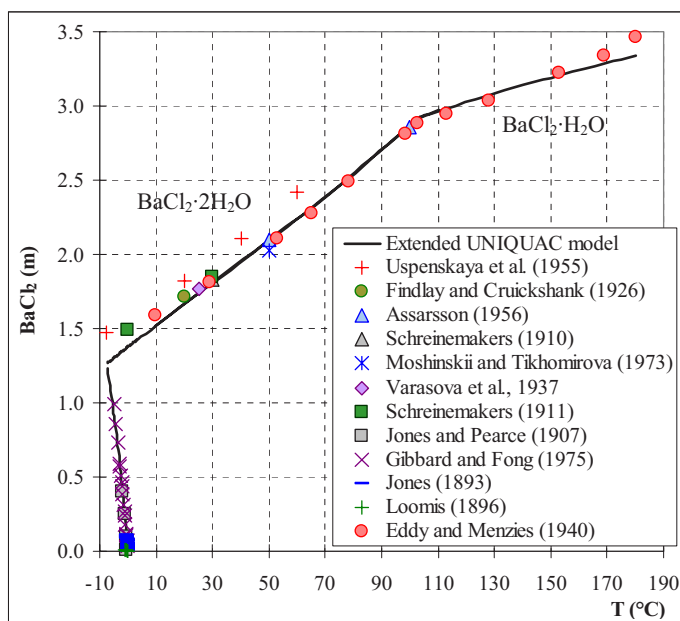
Figure 4-4. Experimental and calculated solid-liquid phase diagram for the $BaCl_2$-H₂O system at 1 bar.

Table 4-4
Experimental binary BaCl$_2$-H$_2$O SLE data sets used for parameter estimation

T (°C)	P (bar)	Number of data	AAD (m)	Reference
-7.6/60	1	4 (4)	1.2E-01	Uspenskaya et al. (1955)
-5/-0.1	1	17 (17)	1.3E-02	Gibbard and Fong (1975)
-1.9/-0.5	1	6 (6)	9.5E-03	Jones and Pearce (1907)
-0.9/0	1	5 (4)	1.1E-03	Loomis (1896)
-0.5/0	1	39 (39)	1.1E-02	Jones (1893)
0/30	1	2 (2)	7.8E-02	Schreinemakers (1911)
9.7/180	1/8.15	12 (12)	4.1E-02	Eddy and Menzies (1940)
20	1	1 (1)	4.0E-02	Findlay and Cruickshank (1926)
25	1	1 (1)	3.0E-02	Varasova et al., 1937
30	1	1 (1)	2.2E-02	Schreinemakers and de Baat (1909)
30	1	1 (1)	2.2E-02	Schreinemakers (1910)
50	1	1 (1)	6.9E-02	Moshinskii and Tikhomirova (1973)
50/100	1	2 (2)	4.9E-03	Assarsson (1956)
			$MAAD$ (m):	**2.2E-02**

4.2.3 Na$_2$SO$_4$-BaSO$_4$-H$_2$O System.

We found only one reference (Jiang, 1996) dealing with the ternary system Na$_2$SO$_4$-BaSO$_4$-H$_2$O. Lieser (1965) and Felmy et al. (1990) also studied the latter system at 20 and 25°C, respectively, but unfortunately they reported their data only as plots. The accuracy of these measurements is questionable as the disagreement among the sources is large. The problem is aggravated by the fact that barite solubility in Na$_2$SO$_4$-H$_2$O solutions is considerably lower than in pure water, because of the common-ion effect. Measurement of such low concentrations (of the order of $10^{-7}/10^{-8}$ m) becomes very difficult and likely to include large errors. In his paper, Jiang (1996) made no comparison with other sources with the result that it is impossible to determine the reliability of such measurements. The aqueous solutions were determined by atomic absorption spectroscopy and Jiang (1996) claims that the error is between ± 0.05%. According to Vetter et al. (1983), this technique can lead to relative deviations that are much larger than the value reported by Jiang (1996).

The range of temperatures and pressures covered for this system and the number of experimental data are given in table 4-5. The average absolute deviation between calculated and experimental data is also shown. The average experimental standard deviation for that reference could not be calculated as different measurements at the same conditions (temperature, pressure and Na$_2$SO$_4$ concentration) were not available.

The representation of the extended UNIQUAC model for the ternary system BaSO$_4$-Na$_2$SO$_4$-H$_2$O at 20°C and 1 bar is shown in figure 4-5.

Table 4-5
Experimental ternary $BaSO_4$-Na_2SO_4-H_2O SLE data sets used for parameter estimation

T (°C)	P (bar)	Number of data	AAD_{BaSO4} (m)	Reference
0/80	1	60 (60)	5.0E-08	Jiang (1996)
			***MAAD* (m):**	**5.0E-08**
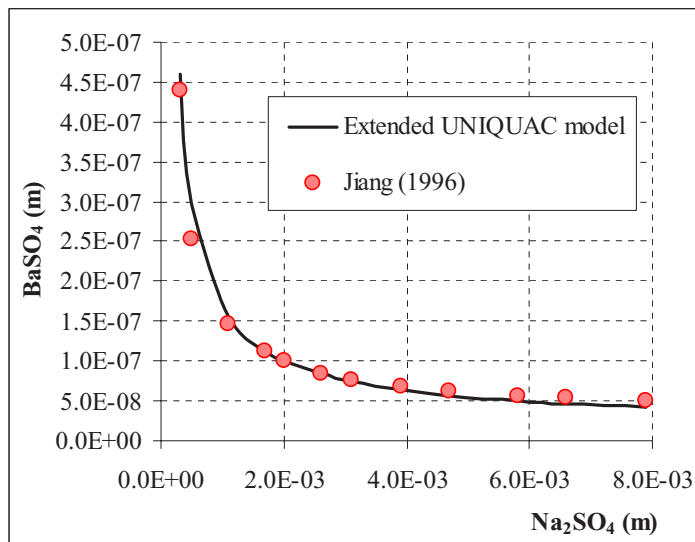
Figure 4-5. Experimental and calculated solid-liquid phase diagram for the $BaSO_4$-Na_2SO_4-H_2O system at 20°C and 1 bar.

4.2.4 BaCl₂-NaCl-H₂O System

The extended UNIQUAC model is also able to accurately represent the ternary system $BaCl_2$-NaCl-H_2O, presented in table 4-6 and figure 4-6. As mentioned previously, no experimental standard deviation could be calculated because of the lack of measurements carried out at the same experimental conditions.

Table 4-6
Experimental ternary $BaCl_2$-NaCl-H_2O SLE data sets used for parameter estimation

T (°C)	P (bar)	Number of data	AAD_{BaCl2} (m)	Reference
-6.4/-0.2	1	21 (21)	5.3E-03	Gibbard and Fong (1975)
0/50	1	2 (2)	1.3E-01	Speranskaya (1954)
20	1	7 (7)	9.3E-02	Findlay and Cruickshank (1926)
30	1	10 (10)	8.3E-02	Schreinemakers and de Baat (1909)
			***MAAD* (m):**	**9.2E-02**

Speranskaya (1954) reports two measurements at 0 and 50ºC that deviate considerably from the model calculations. As no additional data for the ternary system are given at those conditions, it is not possible to compare these points with other measurements and determine their accuracy. The rest of the 38 points used are in close agreement with the extended UNIQUAC model and the system is satisfactorily represented by the model.
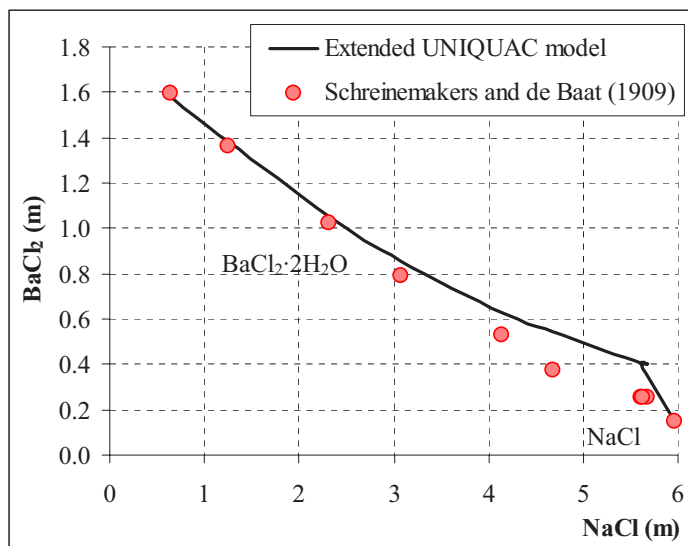
Figure 4-6. Experimental and calculated solid-liquid phase diagram for the $BaCl_2$-NaCl-H_2O system at 30ºC and 1 bar.

4.2.5 $BaSO_4$-NaCl-H_2O System

Table 4-7 presents an overview of the data used for evaluation of the model parameters for the system $BaSO_4$-NaCl-H_2O is given. The temperature and pressure range of each data set are listed, along with the average absolute deviation between calculated and experimental data for $BaSO_4$. The number of data points found and used from each set of data is also given in table 4-7. A more detailed review about the different experimental procedures employed in the different studies is given in Chapter 9.

Many of the data are shown to be inaccurate and most of them could not be tested for their reliability. It is clear, at certain conditions, the measurements are erroneous, as two sources report rather different values. Because of the lack of data at the same conditions it is impossible to determine which sources can be trusted. The extended UNIQUAC model is able, however, to accurately correlate experimental NaCl-$BaSO_4$-H_2O data, as shown in figures 4-7 and 4-8. The accuracy of the model is very good even for very high NaCl

concentrations (up to 5 m NaCl), and also at high temperatures and pressures. Figure 4-8 shows the change in the solubility tendency with temperature depending on the NaCl concentration. For high ionic strengths, barite solubility increases constantly with temperature, while for low ionic strengths a maximum solubility is observed around 100-150ºC.

Table 4.7
Experimental quaternary NaCl-BaSO$_4$-H$_2$O SLE data sets used for parameter estimation

T (ºC)	P (bar)	Number of data	AAD_{BaSO4} (m)	Reference
20/350	1/165	41 (40)	2.9E-05	Strübel (1967)
25/95	1	108 (108)	1.6E-05	Templeton (1960)
25	1	8 (8)	3.2E-05	Davis and Collins (1971)
80/120	1/414	34 (0)		Schulien (1987)
94/253	5/560	35 (35)	3.4E-05	Blount (1977)
95/340	1/165.4	84 (71)	2.2E-04	Uchameyshvili et al. (1966)
			MAAD (m):	7.5E-05
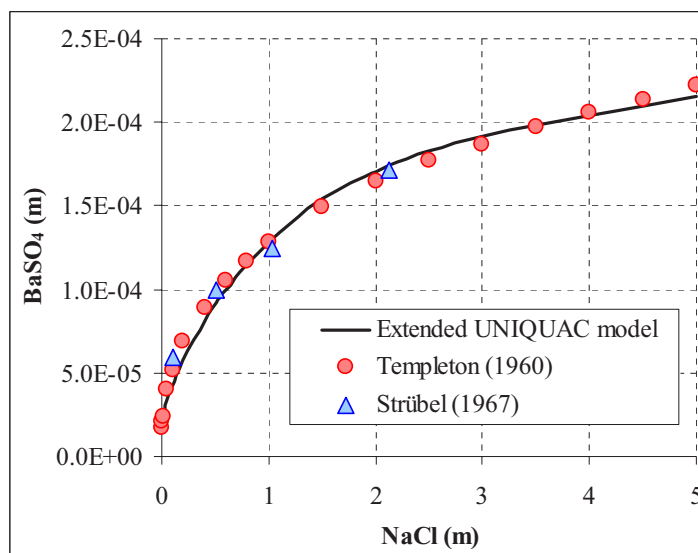
Figure 4-7 Experimental and calculated solid-liquid phase diagram for the BaSO$_4$-NaCl-H$_2$O system at 50ºC and 1 bar.

Uchameyshvili et al. (1966) and Strübel (1967) performed measurements outside the temperature range of interest in this work.

Uchameyshvili et al. (1966) data show a relatively large scatter at some conditions (i.e., barite solubilities at 0.25 m NaCl and 170ºC varied from 8.66·10^{-5} to 9.77·10^{-5} m). When compared to Templeton (1960), the values reported by Uchameyshvili et al. (1966) are

considerably lower, being the measurements by Templeton (1960) at 95°C comparable to the values given by Uchameyshvili et al. (1966) at 140°C. The latter investigators suggest such difference may be due to the different particle size employed (Uchameyshvili et al. (1966) used a single crystal while Templeton (1960) used finely crystalline powder).
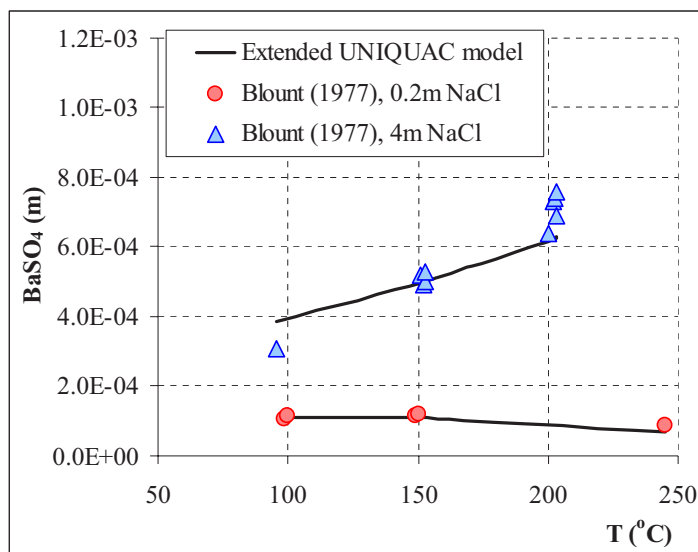
Figure 4-8 Experimental and calculated solid-liquid phase diagram for the BaSO$_4$-NaCl-H$_2$O system at 500 bar.

The data reported by Strübel (1967) at 90 and 100°C are consistent with those by Uchameyshvili et al. (1966) at 95°C, and also quite lower than the values by Templeton (1960). In general, the measurements performed by Strübel (1967) agree very well with the ones by Templeton (1960) for low temperatures (from 20 to 50°C). For higher temperatures, the disagreement is large, being more pronounced the larger the temperature is. Templeton (1960) shows a very large increase on barite solubility with increasing temperature from 65 to 95°C, while the influence of this temperature range is less pronounced (and practically negligible from 60 to 80°C) for the data reported by Strübel (1967). For example, similar solubility values are obtained by Templeton (1960) at 65°C and by Strübel (1967) at 80°C, under the same NaCl concentration.

At temperatures above 100°C and pressures equal to the saturation pressure of the solution, the data reported by Uchameyshvili et al. (1966) and Blount (1977) are in agreement in the region of overlap. Nevertheless, that agreement is lost for the high pressure (100 to 500 bar) range, where Blount (1977) reports low solubilities compared to Uchameyshvili et al. (1966) (the measurements by Uchameyshvili et al. (1966) at the saturation pressure of the

solution are comparable to Blount's (1977) values at 500bar). As it happened for Uchameyshvili et al. (1966), a large scatter is also observed for Blount's (1977) data, especially at 150 and 200°C, where solubility values may vary from $6.4 \cdot 10^{-4}$ to $7.6 \cdot 10^{-4}$ m BaSO$_4$. Results obtained by Templeton (1960) and Strübel (1967) are considerably higher than those obtained by Blount (1977). The latter results show smoother variations with temperature, pressure and NaCl concentration. Blount (1977) calculated solubility values for barite in NaCl solutions at 25°C from the values of the solubility product and the activity coefficients from a modified Debye-Hückel equation. The results he obtained are below those reported by Templeton (1960) and Strübel (1967), and agree with the data reported by Puchelt (1967)[1]. Calculated thermodynamic quantities from Blount (1977) measurements closely agree with those calculated from thermal and solution density data.

Davis and Collins (1971) measurements are slightly lower than those by Templeton (1960) and Strübel's (1967) at 20, 25 and 30°C, but the general agreement is good.

According to Uchameyshvili et al. (1966), barite solubility increases steadily with increasing temperature for 2 m NaCl solutions, while it passes through a maximum for 0.25 m NaCl solutions, and it bends for 1 m NaCl solutions. The same monotically positive increase in barite solubility with increasing temperature was observed by Templeton (1960) for NaCl concentrations higher than 1 M, and by Blount (1977) for NaCl concentrations of 4 m. Contrary to this behaviour, Schulien (1987) reports a maximum in barite solubility between 100 and 120°C, independently of the NaCl content of the solution. The results given by Schulien (1987) are extremely low when compared to any other source in table 4.7. Moreover, the tendency followed by barite solubility with pressure seems to be wrong. No real changes are noticed in the solubility value when the pressure is increased from 1 to 414 atm. In some experiments, a slight reduction in barite solubility is observed when the pressure is increased to 414 bar, and a maximum is obtained at 200 bar.

Monnin (1999) developed a model for the solubility of barite in electrolyte solutions to 200°C and 1000 bar. The results predicted by his model at 80°C are in full agreement with Templeton's (1960) data, but that agreement is lost (10% RD) at 100°C when the results are compared to the experimental values determined by Strübel (1967) and Blount (1977) in the 1 to 3 M NaCl concentration range. Monnin's (1999) results are also systematically higher than Schulien's (1987) measurements at 80, 100, and 120°C and at 1, 200 and 400 bar.

---

[1] Puchelt (1967) reported his measurements only in plots, and therefore his values could not be used for parameter estimation. They were used, nevertheless, for comparison with other sources.

We can conclude there is a general disagreement among the different solubility measurements reported by the sources in table 4-7, especially at high temperatures and pressures. As a general tendency, it seems Templeton (1960) reports the highest values of solubility, followed by Uchameyshvili et al. (1966), Strübel (1967), and finally Blount (1977). Schulien's (1987) data are notably lower than the previous sources for any experimental condition.

4.2.6 BaCl₂-SrCl₂-Na₂SO₄ System

In order to estimate the interaction energy parameter between Ba^{2+} and Sr^{2+} the data by Qadirie (1990) were used. Qadirie (1990) performed solubility measurements in solutions containing BaCl₂, SrCl₂ and Na₂SO₄ at 20, 40 and 60°C and 1 atm. He analyzed both the concentration in the liquid phase and the composition of the solid phase, which was reported as a solid solution $(Ba^{2+}, Sr^{2+})SO_4^{2-}$. Nevertheless, the ratio $Ba^{2+}/(Ba^{2+} + Sr^{2+})$ in the solid solution was equal to 0.5 for most of the cases and could correspond to the formation of the double salt BaSO₄·SrSO₄ instead of a solid solution. Thus, the system was modelled assuming the double salt Ba·Sr(SO₄)₂ as the solid phase. Whenever the ratio $Ba^{2+}/(Ba^{2+} + Sr^{2+})$ was different from 0.5, two different solid phases were assumed to appear: the double salt Ba·Sr(SO₄)₂ together with a pure salt BaSO₄ [for ratios $Ba^{2+}/(Ba^{2+} + Sr^{2+})$ higher than 0.5] or SrSO₄ [for ratios $Ba^{2+}/(Ba^{2+} + Sr^{2+})$ lower than 0.5]. The accuracy of the results obtained led us to conclude that the assumptions done are correct. Table 4-8 shows the average absolute deviation between the extended UNIQUAC model and the experimental data for the solubility of BaCl₂ and SrCl₂.

Table 4-8
Experimental BaCl₂-SrCl₂-Na₂SO₄-H₂O SLE data sets used for parameter estimation

T (°C)	P (bar)	Number of data	AAD_{Ba++} (m)	AAD_{Sr++} (m)	Reference
20/60	1	112 (112)	2.8E-03	3.0E-03	Qadirie (1990)
		MAAD (m):	**2.8E-03**	**3.0E-03**	

4.2.7 Ba^{2+}-Mg^{2+} and Ba^{2+}-Ca^{2+} Interaction Energy Parameters

The binary energy interaction parameters for the pairs Ba^{2+}-Mg^{2+} and Ba^{2+}-Ca^{2+} were estimated on the basis of experimental SLE data for the ternary systems BaCl₂-MCl₂-H₂O, and the quaternary systems MCl₂-BaSO₄-H₂O and Ca(NO₃)₂-BaCl₂-H₂O, where M represents Ca and Mg. The sources employed, number of experimental data used and ranges

of temperature and pressure covered are reported in table 4-9. The average absolute deviation between calculated and experimental data is given for Ba^{2+}.

Table 4-9
Experimental SLE data sets used for parameter estimation

T (^{o}C)	P (bar)	Number of data	AAD_{Ba2+} (m)	Reference
25	1	8 (8)	8.0E-06	Davis and Collins (1971)[a]
25	1	12 (12)	8.9E-07	Neuman (1933) [a]
110/275	1/60	18 (18)	2.1E-04	Uchameyshvili et al. (1966)[a]
45/100	1	27 (27)	5.6E-02	Assarsson (1956)[b]
25	1	10 (10)	5.1E-05	Davis and Collins (1971)[c]
100/255	1/44	36 (36)	4.9E-04	Uchameyshvili et al. (1966)[c]
-17.5/60	1	97 (97)	7.3E-02	Uspenskaya et al. (1955)[d]
80/120	1	63 (63)	6.0E-02	Uspenskaya and Bergman (1955)[d]
25	1	7 (7)	2.5E-01	Varasova et al. (1937)[e]

[a] Quaternary $MgCl_2$-$BaSO_4$-H_2O system   [d] Quaternary $Ca(NO_3)_2$-$BaCl_2$-H_2O system
[b] Ternary $MgCl_2$-$BaCl_2$-H_2O system   [e] Ternary $CaCl_2$-$BaCl_2$-H_2O system
[c] Quaternary $CaCl_2$-$BaSO_4$-H_2O system

Puchelt (1967) measured barite solubility data in $MgCl_2$ and $CaCl_2$ solutions, but unfortunately he reported his measurements only in plots, and therefore his values could not be used for parameter estimation. They were used, nevertheless, for comparison with other sources. There is a very large discrepancy between the tendency followed by Puchelt (1967) and that given by Davis and Collins (1971) for the $CaCl_2$-$BaSO_4$-H_2O system. Davis and Collins (1971) obtained a maximum barite solubility ($7.8 \cdot 10^{-5}$ m) for $CaCl_2$ concentrations around 0.2 m, while Puchelt (1967) obtained the maximum solubility (around $2 \cdot 10^{-4}$ m) for a 1.8 m $CaCl_2$ solution. For the $MgCl_2$-$BaSO_4$-H_2O system, both Puchelt (1967) and Davis and Collins (1971) got a maximum in barite solubility for similar $MgCl_2$ concentrations (around 1.8 m), but the former investigator reports higher $BaSO_4$ values. For this system, there is a very good agreement between Neuman's (1933) and Davis and Collins' (1971) data in the region of overlap.

The data given by Uchameyshvili et al. (1966) for both $MgCl_2$-$BaSO_4$-H_2O and $CaCl_2$-$BaSO_4$-H_2O systems cannot be compared to the previous sources due to the different temperature and pressure ranges covered. Nonetheless, the tendency reported by Uchameyshvili et al. (1966) for barite solubility with increasing chloride concentration is much more pronounced than that shown by Puchelt (1967) and Davis and Collins (1971).

Figure 4-9 shows the calculations performed by the extended UNIQUAC model for the systems $CaCl_2$-$BaSO_4$-H_2O and $MgCl_2$-$BaSO_4$-H_2O. The model is able to fit experimental

data fairly accurately, even at relatively high chloride concentrations. Further experimental data are needed to clarify barite behaviour in $CaCl_2$ and $MgCl_2$ solutions.
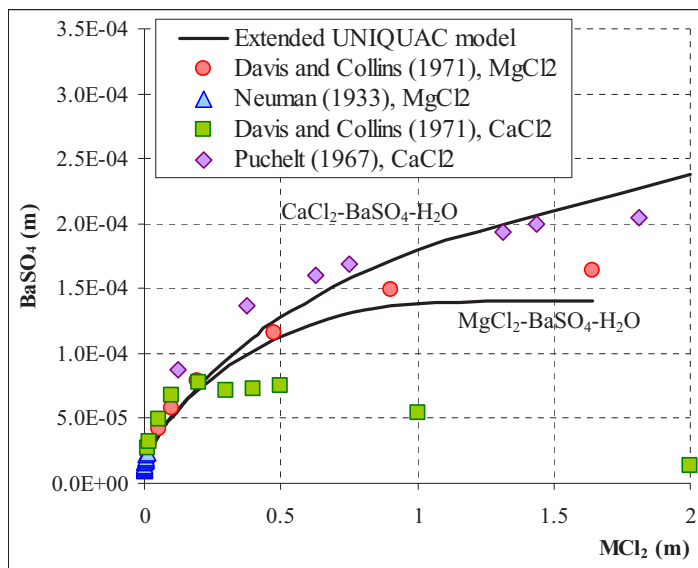
Figure 4-9. Experimental and calculated solid-liquid phase diagram for the $MgCl_2$-$BaSO_4$-H_2O and $CaCl_2$-$BaSO_4$-H_2O systems at 25ºC and 1 bar

The formation of anhydrite ($CaSO_4$) or gypsum ($CaSO_4 \cdot 2H_2O$) for high chloride concentrations in the $CaCl_2$-$SrSO_4$-H_2O system has been reported by Uchameyshvili et al. (1966) and Monnin (1999). For barite, $CaSO_4$ precipitation is less documented than in the previous system due to the lower barite solubility (one order of magnitude lower than that of celestite). Thus, the sulphate content is not high enough to allow gypsum to precipitate. Uchameyshvili et al. (1966) observed, nevertheless, the formation of $CaSO_4$ for temperatures higher than 230ºC. According to Monnin (1999), the anhydrite stability field is reached for solutions containing 0.165 m $CaCl_2$ at 210ºC, and 0.5 m $CaCl_2$ at 165ºC. When anhydrite precipitates from barite saturated solutions, the aqueous sulphate content decreases and the barium concentration increases. Even though anhydrite formation is reported by Uchameyshvili et al. (1966), their data do not follow that behaviour and are better modeled when equilibrium with only barite is considered (Monnin, 1999).

4.3 Systems Containing Strontium

4.3.1 SrSO$_4$-H$_2$O System

The experimental and calculated phase diagrams for the system SrSO$_4$-H$_2$O at a constant pressure of 200 bar and at constant temperatures of 25, 100 and 200°C are shown in figures 4-10 and 4-11, respectively. Both diagrams are simple, with only one solid phase (SrSO$_4$). The decrease of celestite solubility with increasing temperature from 25°C is very large, dropping from 7.5·10^{-4} m at 25°C to 6·10^{-5} m at 250°C. The calculated solubility compares well with the experimental data, which are presented in table 4-10, together with the temperature and pressure range covered and the average absolute deviation between the extended UNIQUAC results and the experimental data. The value of the *MAAD* (1.6·10^{-5} m) is below the average experimental standard deviation of the data used for parameter estimation, which was found to be 4.1·10^{-5} m.

Table 4-10
Experimental binary SrSO$_4$-H$_2$O SLE data sets used for parameter estimation

T (^{o}C)	*P* (bar)	Number of data	*AAD* (m)	Reference
0/98	1	7 (0)		Wolfmann (1896)
2/35	1/1013	18 (0)		MacDonald and North (1974)
2.8/32.3	1	3 (3)	1.6E-05	Kohlrausch (1908)
5/95	1	11 (0)		Gallo (1935)
10.3/89.3	1	19 (19)	6.3E-06	Reardon and Armstrong (1987)
20	1	1 (0)		Lieser (1965)
20	1	1 (1)	2.7E-05	Belfiori (1940)
22/600	1/1990	28 (12)	1.6E-05	Strübel (1966)
24.4/250	1/600	72 (72)	1.7E-05	Howell et al. (1992)
25/125	1/2.3	4 (0)		Vetter et al. (1983)
25	1	1 (1)	4.5E-05	Müller (1960)
25	1	1 (1)	7.9E-07	Campbell and Nancollas (1969)
25	1	1 (0)		Selivanova and Zubova (1956)
25	1	2 (2)	1.9E-05	Culberson et al. (1978)
25	1	1 (1)	1.5E-05	Brower and Renault (1971)
25	1	1 (0)		Marden (1916)
30	1	1 (1)	5.7E-05	Campbell and Cook (1935)
85.5/154.4	5.6/211.5	10 (3)	2.4E-05	Jacques and Bourland (1983)
194/426	13.7/343	13 (0)		Booth and Bidwell (1950)
			MAAD (m):	**1.6E-05**

At 86°C, some of the measurements of celestite solubility reported by Jacques and Bourland (1983) decrease considerably with pressure (from 7·10^{-4} m to 4.7·10^{-4} m when pressure increases from 1 to 200 bar). Additionally, the data are very scattered, with solubility values ranging from 5.6.10^{-4} m to 8.3.10^{-4} m at 38°C and 100 bar. Nevertheless, some other data

reported for the binary system (at 149.4°C and 80.7 bar, and at 154.4°C and 108.2 and 109.4 bar) do not show any irregularity and are close to other measurements at similar conditions reported by different authors. Only some of the solubility values given by Jacques and Bourland (1983) were therefore used in the present work.

Gallo (1935) reported celestite solubilities in pure water in clear disagreement with the general tendency followed by most of the references shown in table 4-10. The same lack of reliability is shown for the measurements done by Marden (1916), Lieser (1965), and Selivanova and Zubova (1956). These authors report higher solubilities than the rest of the data sets analyze, being possible that surface poisoning effects contributed to the enhancement of the solubility (Reardon and Armstrong, 1987). The presence of adsorbed substances (particularly phosphates) at the surface of strontium sulphate crystals markedly affects the critical supersaturation and the rates of spontaneous precipitation and dissolution of that mineral (Campbell and Nancollas, 1969).
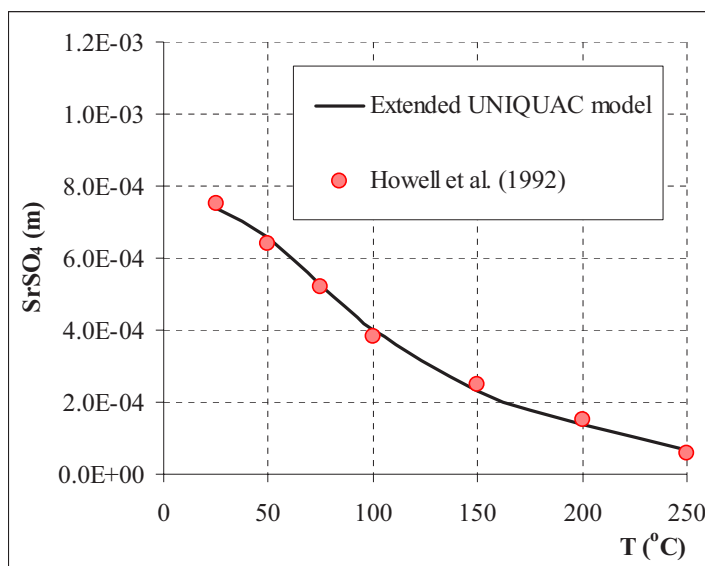
Figure 4-10. Experimental and calculated solid-liquid phase diagram for the $SrSO_4$-H_2O system at 200 bar.

The data of Wolfmann (1896) display, by far, the greatest discrepancies with respect to the other studies (as large as $6 \cdot 10^{-4}$ m). Furthermore, his data do not follow the expected trend of increasing solubility with pressure.

The only measurement from MacDonald and North (1974) that could be compared to other sources was the one at 2°C and 1 bar (the other experimental conditions were unique). The solubility reported at those conditions by MacDonald and North (1974) disagrees

considerably with the values reported by the different authors in table 4-10 at similar conditions. Thus, this source was not considered reliable.

Vetter et al. (1983) performed measurements in pure water and in NaCl solutions at 25, 75, 95 and 125°C. They adopted a radioactive tracer technique using ^{90}Sr and some of the results were cross-checked using ^{35}S instead of [90]Sr. Both methods led to relative deviations as large as 30%.

The data of Booth and Bidwell (1950) are of relatively low precision as they deviate systematically from the majority of other studies.
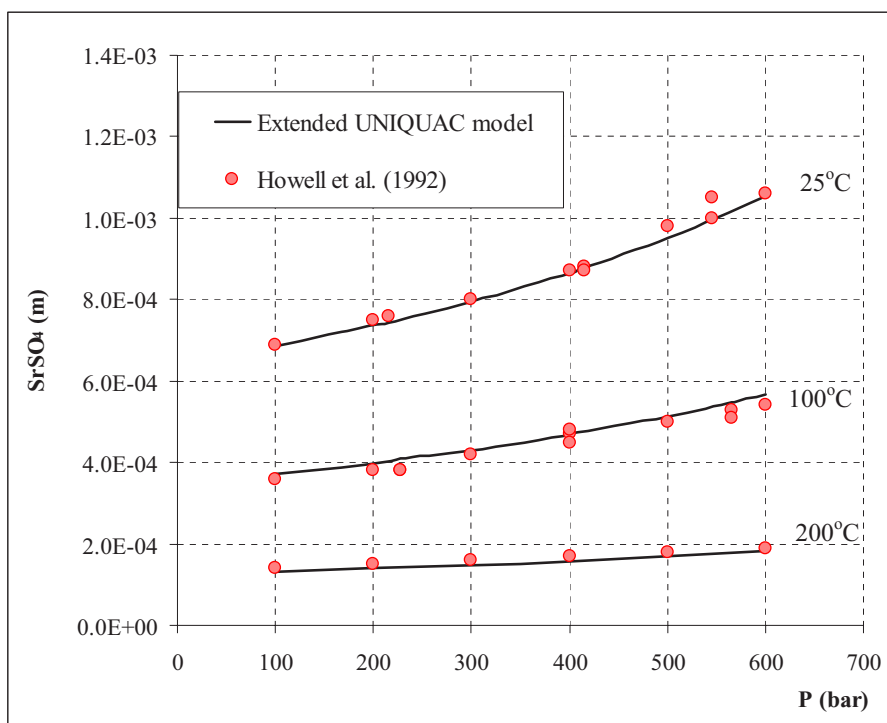
Figure 4-11. Experimental and calculated solid-liquid phase diagram for the SrSO$_4$-H$_2$O system at 25, 100 and 200 ^{o}C.

4.3.2 SrCl$_2$-H$_2$O System

The binary phase diagram for the system SrCl$_2$-H$_2$O is shown in figure 4-12. The extended UNIQUAC model can represent the experimental data for this system with high accuracy and the agreement between the calculated and experimental eutectic point and peritectic points is good. The results for the SrCl$_2$ salt with reference to the experimental data are given in table 4-11. Due to the lack of experimental data at the same conditions, the

calculated experimental *ASD* value is not very reliable. It is only based on the difference between the data reported by Assarsson (1953) and Moshinskii and Tikhomirova (1973) at 50ºC. The value for the mean average absolute deviation between experimental data and extended UNIQUAC calculations is low compared to the solubility values (*MAAD* of 0.1 m for solubilities in the range of 3 to 7 m).

Table 4-11
Experimental binary $SrCl_2$-H_2O SLE data sets used for parameter estimation

T (ºC)	*P* (bar)	Number of data	*AAD* (m)	Reference
-6/-0.05	1	10 (10)	6.5E-02	Jones and Pearce (1907)
18/114	1	18 (18)	1.1E-01	Assarsson (1953)
25	1	1 (1)	1.2E-01	Rard and Miller (1982)
50	1	1 (1)	2.8E-01	Moshinskii and Tikhomirova (1973)
			MAAD (m):	1.0E-01
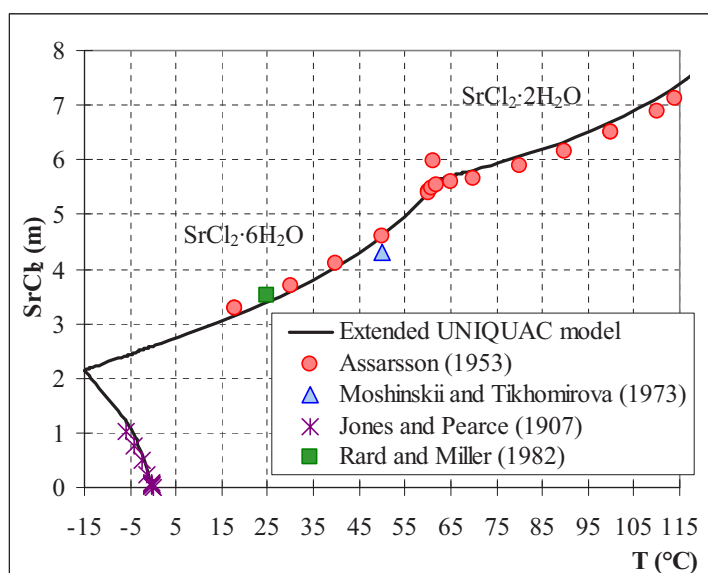
Figure 4-12. Experimental and calculated solid-liquid phase diagram for the $SrCl_2$-H_2O system at 1 bar.

4.3.3 SrSO₄-Na₂SO₄-H₂O and SrCl₂-NaCl-H₂O Systems

As mentioned previously for the case of barite, the average experimental standard deviation for the ternary systems $SrSO_4$-Na_2SO_4-H_2O and $SrCl_2$-$NaCl$-H_2O could not be calculated, because of the lack of experimental measurements at the same temperature, pressure and solution composition. The experimental standard deviation for the binary systems $SrSO_4$-

H_2O ($4.1 \cdot 10^{-5}$ m) and $SrCl_2$-H_2O ($4.0 \cdot 10^{-2}$ m) was therefore taken as reference. Note that, as mentioned previously, the *ASD* for the system $SrCl_2$-H_2O is only based on two experimental values.

Tables 4-12 and 4-13 show the data sets used for these two ternary systems and the average absolute deviation between calculated and experimental data. The *MAAD* is in both cases lower than the average experimental standard deviation for the binary systems, demonstrating the ability of the model to represent the systems.

Table 4-12
Experimental ternary $SrSO_4$-Na_2SO_4-H_2O SLE data sets used for parameter estimation

T (°C)	P (bar)	Number of data	AAD_{SrSO4} (m)	Reference
0/25	1	8 (8)	2.7E-05	Lucchesi and Whitney (1962)
25	1	1 (1)	4.8E-05	Brower and Renault (1971)
			MAAD (m):	**3.0E-05**

Table 4-13
Experimental ternary $SrCl_2$-$NaCl$-H_2O SLE data sets used for parameter estimation

T (°C)	P (bar)	Number of data	AAD_{SrCl2} (m)	Reference
18/114	1	27 (27)	1.7E-01	Assarsson (1953)
			MAAD (m):	**1.7E-01**
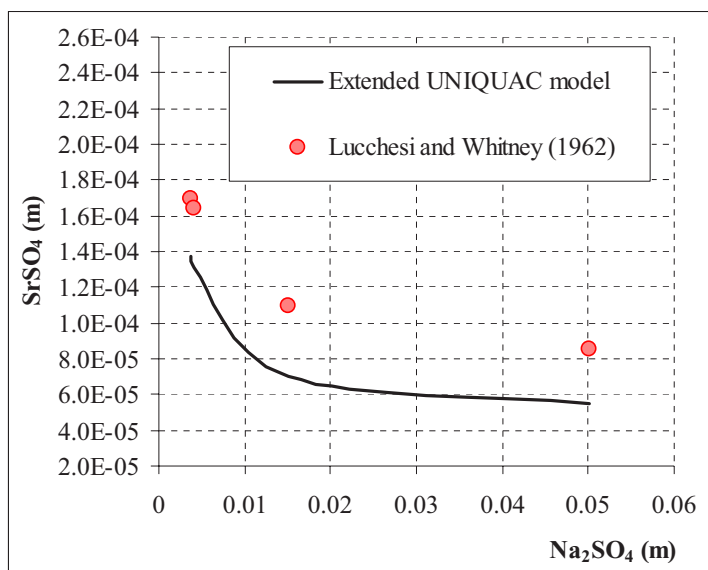
Figure 4-13. Experimental and calculated solid-liquid phase diagram for the $SrSO_4$-Na_2SO_4-H_2O system at -0.05°C and 1 bar.

Figure 4-13 shows the model calculations for the ternary system $SrSO_4$-Na_2SO_4-H_2O at - 0.05ºC and 1 bar. The calculated values are lower than the experimental ones, but the shape of the curve agrees with the experimental tendency. Moreover, the value for the *MAAD* between experimental and calculated data is lower than that for the binary system $SrSO_4$-H_2O, and the difference shown in figure 4-13 may be regarded as experimental inaccuracy (only one source was used for the ternary system, and therefore comparison to other sources was not possible).

Figure 4-14 shows the extended UNIQUAC calculations for the ternary system $SrCl_2$-NaCl-H_2O at 60ºC and 1 bar. For low NaCl concentrations, the solid phases are $SrCl_2 \cdot 6H_2O$ and $SrCl_2 \cdot 2H_2O$, while NaCl appears for higher concentrations. The appearance and disappearance of these salts is well correlated by the model.
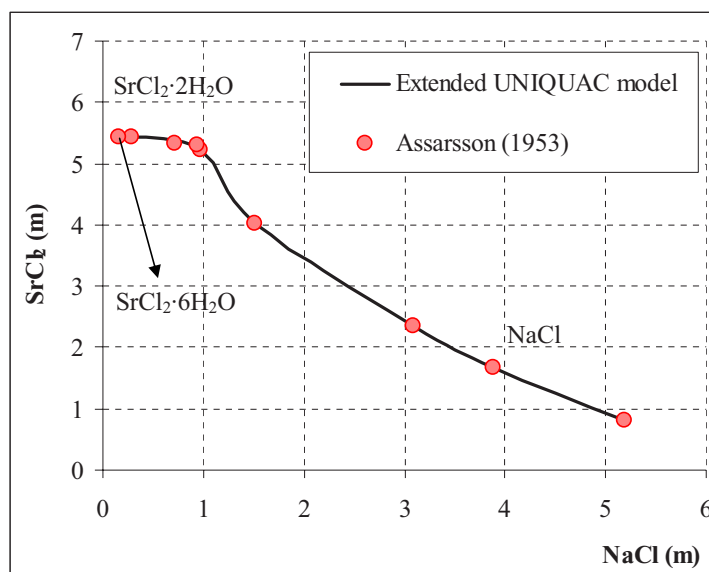
Figure 4-14. Experimental and calculated solid-liquid phase diagram for the $SrCl_2$-NaCl-H_2O system at 60ºC and 1 bar.

4.3.4 SrSO₄-NaCl System

Table 4-14 shows the different data used for the system $SrSO_4$-NaCl-H_2O. The temperature and pressure ranges for each data set are listed, as well as the average absolute deviation between the calculated and experimental data. A more detailed explanation about the different experimental procedures used and possible sources of error is presented in Chapter 9.

As mentioned previously and shown in figure 4-1, there is a large disagreement among the different authors as regards experimental celestite solubility data in NaCl solutions. This disparity is aggravated at high temperature and pressure conditions. This variability may be related to the experimental difficulties associated to this mineral. According to Campbell and Cook (1935), supersaturated solutions of celestite are characterized by long term stability. Campbell and Nancollas (1969) aware of the propensity of this mineral for surface poisoning effects, while Enüstün and Turkevich (1960) assure the solubility of $SrSO_4$ depends on the particle size. Most of the studies on celestite solubility do not consider these experimental problems and so the available solubility data in the literature are sometimes unreliable and inaccurate.

Table 4-14
Experimental quaternary $SrSO_4$-NaCl-H_2O SLE data sets used for parameter estimation

T (^{o}C)	P (bar)	Number of data	AAD_{SrSO4} (m)	Reference
-0.05/25	1	10 (0)		Lucchesi and Whitney (1962)
9/20	1	2 (2)	1.3E-03	Gallo (1935)
10.3/40	1	36 (36)	1.8E-04	Reardon and Armstrong (1987)
20/60	1	26 (26)	5.4E-04	Qadirie (1990)
20/90	1	32 (32)	2.2E-04	Strübel (1966)
25	1	10 (10)	1.2E-04	Davis and Collins (1971)
25	1	5 (5)	3.3E-04	Brower and Renault (1971)
25	1	1 (1)	2.9E-04	Culberson et al. (1978)
25	1	8 (0)		Müller (1960)
25/253.5	1/600	436 (436)	4.4E-04	Howell et al. (1992)
25/125	1/2.3	24 (0)		Vetter et al. (1983)
80/120	1/414	49 (0)		Schulien (1987)
100/305	0.2/165	41 (41)	5.1E-04	Jacques and Bourland (1983)
			MAAD (m):	**4.2E-04**

A relatively good agreement is found in figure 4-1 for low NaCl concentrations (up to less than 1m NaCl). From that concentration, there are two sources (Müller, 1960 and Lucchesi and Whitney, 1962) reporting measurements that disagree considerably with the main tendency. For the first reference, even the solubility curve shape is different. Müller (1960) measured solubility values at 25°C and 1 atm in different NaCl solutions from 0.4 to 5.1 m. His data show a much higher solubility value and do not show a reversal in the solubility behaviour between 2 and 5 m NaCl, as observed by the other sources performing measurements at the same conditions. These unreliable data may be the result of an inadequate analytical technique (titration) to determine very low Sr^{2+} concentrations

Celestite solubility decreases with increasing temperature from 25ºC (from 0 to 25ºC celestite solubility increases with increasing temperature). This tendency is not clearly followed by the data reported by Schulien (1987) at atmospheric pressure. Schulien (1987) concluded that additional measurements are required to determine whether that deviation from the probable trend is due to analytical errors or inhomogeneities in the solutions. Regarding the trend followed with pressure, Schulien (1987) data show some inconsistencies. For some temperatures and NaCl concentrations, the solubility increases continuously from 1 to 400 bar. For other conditions the effect of pressure is negligible, and in other cases the effect is reversed, and the highest solubilities are found for the lowest pressures. According to Schulien (1987), this inconsistency is due to the small changes in solubility values with pressure, which lie within the variability of the experimental technique. As mentioned for barite measurements, the results given by Schulien (1987) for $SrSO_4$ show a large scatter for some experimental conditions (e.g., at 80°C), and disagree with most of the sources given in table 4-14. Such disagreement may result as a consequence of the low time waited before performing analysis, and aggravated by the lack of agitation of the sample.

Howell et al. (1992) agrees with Strübel (1966), Davis and Collins (1971), Culberson et al. (1978) and Reardon and Armstrong (1987) in the regions of overlap, for low sodium chloride concentrations (up to around l.5 m NaCl). For higher concentrations, the agreement is not so good, and Howell et al. (1992) report lower solubility data than the other sources. Moreover, there are some inconsistencies for some of the measurements reported by Howell et al. (1992). At the highest temperatures reported (200 and 250°C) the trend followed by the data for increasing pressures is wrong, and the values reported at 600 bar are lower than at 500 bar, and in some cases even lower than values at 200 bar. Also, scatter in the experimental data is found for the high temperature (T > 200°C) and high sodium chloride concentrations (3 m and higher).

Vetter et al. (1983) report solubility values at 25ºC in relatively good agreement with many other sources. Nonetheless, that agreement is lost at higher temperatures, where Vetter et al. (1983) report very low values when compared to Strübel (1966), Jacques and Bourland (1983) or Howell et al. (1992). Also, the shape of the solubility curve reported by Vetter et al. (1983) at constant NaCl concentration differs from the ones followed by the rest of the sources. Vetter et al. (1893) used a radioactive tracer technique using ^{90}Sr to determine Sr^{2+} concentrations. In some measurements, they cross-checked the results by using ^{35}S as well. The two methods lead to solubility values differing as much as 30%.

Brower and Renault (1971) data agree with the majority of the sources reporting solubility data at 25°C and 1 atm when the NaCl concentration is lower than 1 m. For 1 m, the solubility reported by Brower and Renault (1971) is considerably larger than the values measured by Davis and Collins (1971), Vetter et al. (1983) and Howell et al. (1992).

Finally, it seems that Davis and Collins (1971) report higher solubility values than Reardon and Armstrong (1987) for some similar conditions, while Strübel (1966) data are larger than Jacques and Bourland (1983) data, in the region of overlap. No further conclusions about the reliability of these sources can be taken due to the lack of additional information.
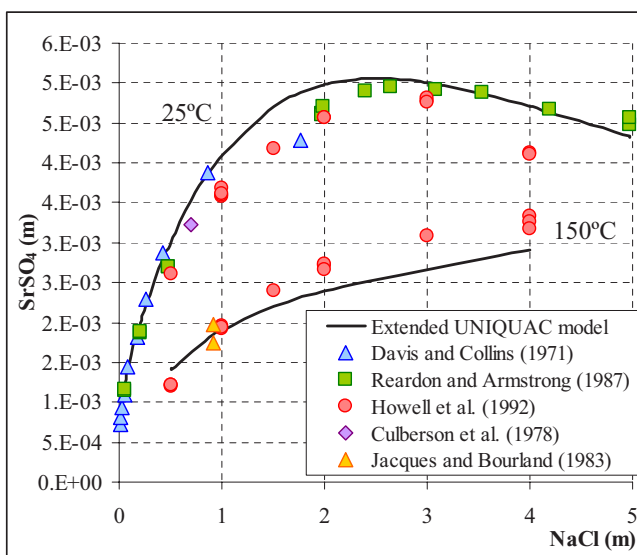
Figure 4-15. Experimental and calculated solid-liquid phase diagram for the SrSO₄-NaCl-H₂O system at 25°C and 1 bar, and 150°C and 5 bar.
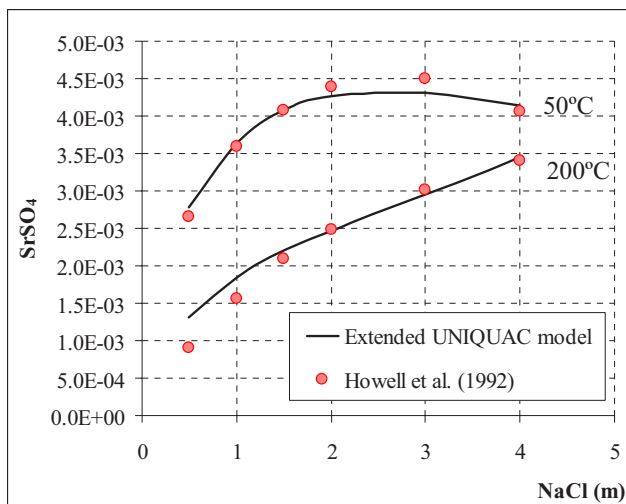
Figure 4-16. Experimental and calculated solid-liquid phase diagram for the SrSO$_4$-NaCl-H$_2$O system at 100 bar.

The experimental and calculated phase diagrams for the system SrSO$_4$-NaCl-H$_2$O at 25ºC and 1 bar, and at 150ºC and the saturation pressure of the solution are shown in figure 4-15. The phase diagram at 50 and 200ºC and a constant pressure of 100 bar is shown in figure 4-16. The effect of NaCl concentration on celestite solubility depends on temperature. For low temperatures (0-75ºC), SrSO$_4$ solubility reaches a maximum for NaCl concentrations around 2-3 m, and then starts decreasing for higher concentrations. For high temperatures (100-300ºC), celestite solubility increases constantly with NaCl concentration.

4.3.5 Sr^{2+}-Mg^{2+} and Sr^{2+}-Ca^{2+} Interaction Energy Parameters

The value of the binary energy interaction parameters between Sr^{2+} and Mg^{2+} or Ca^{2+} was estimated on the basis of experimental SLE data for the ternary system MSO$_4$-SrSO$_4$-H$_2$O, and the quaternary systems MCl$_2$-SrSO$_4$-H$_2$O, where M stands for Ca and Mg. The sources found, the total number of data reported, and the temperature and pressure ranges covered by each source are presented in table 4-15. The average absolute deviation between calculated and experimental data is given for Sr^{2+}.

Celestite solubility increases with the CaCl$_2$ concentration and, at a certain chloride amount, the solid calcium sulphate stability field is reached (Monnin and Galinier, 1988). Then, gypsum or anhydrite will be the phases precipitating and controlling the sulphate content in the solution. According to Monnin (1999), gypsum forms at 25ºC in solutions containing more than 0.75 m CaCl$_2$. At 75ºC anhydrite is the stable solid calcium sulphate phase, and it

will appear for $CaCl_2$ concentrations above 0.5 m. That value decreases to 0.24 and 0.06 m $CaCl_2$ when the temperature is raised to 95 and 125ºC, respectively. Analyzing the data reported by Brower and Renault (1971), Davis and Collins (1971), Culberson et al. (1978), and Vetter et al. (1983), it seems clear neither gypsum nor anhydrite did precipitate in any of the experiments reported, although their stability fields were reached.

Table 4-15
Experimental SLE data sets used for parameter estimation

T (ºC)	P (bar)	Number of data	AAD_{Sr2+} (m)	Reference
25	1	1	1.5E-04	Culberson et al. (1978)[a]
25	1	4	1.8E-03	Brower and Renault (1971)[a]
25	1	9	3.0E-04	Davis and Collins (1971)[a]
25/125	1	27	2.0E-04	Vetter et al. (1983)[a]
25	1	2	1.9E-04	Brower and Renault (1971)[b]
25	1	1	4.2E-04	Culberson et al. (1978)[c]
25	1	2	8.0E-04	Brower and Renault (1971)[c]
25	1	9	7.6E-04	Davis and Collins (1971)[c]
25-125	1	27	3.5E-04	Vetter et al. (1983)[c]
25	1	1	2.8E-04	Brower and Renault (1971)[d]

[a] Quaternary $MgCl_2$-$SrSO_4$-H_2O system   [c] Quaternary $CaCl_2$-$SrSO_4$-H_2O system
[b] Ternary $MgSO_4$-$SrSO_4$-H_2O system   [d] Ternary $CaSO_4$-$SrSO_4$-H_2O system
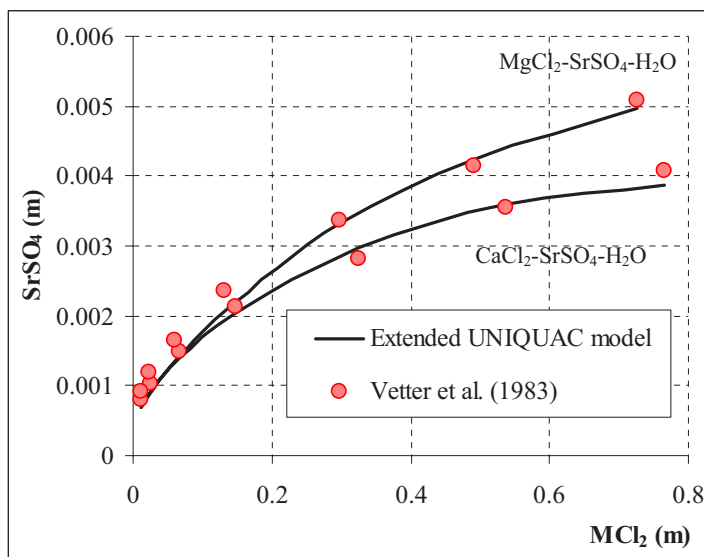
Figure 4-17. Experimental and calculated solid-liquid phase diagram for the $MgCl_2$-$SrSO_4$-H_2O and $CaCl_2$-$SrSO_4$-H_2O systems at 95ºC and 1 bar.

Figure 4-17 shows the calculations performed by the extended UNIQUAC model for the systems CaCl$_2$-SrSO$_4$-H$_2$O and MgCl$_2$-SrSO$_4$-H$_2$O. The representation of the model for the quaternary systems is very good. Figure 4-17 shows than an increasing chloride concentration results in a salting-in effect, increasing the solubility of celestite.

4.4 Systems Containing Calcium

4.4.1 CaSO$_4$-H$_2$O System

The r and q parameters for Ca^{2+} and the interaction parameters between Ca^{2+} and H$_2$O, Cl$^-$ and SO$_4^{2-}$ were determined from a large number of experimental solubility data of salts containing the mentioned ions. Therefore, only the interaction parameter between Ca^{2+} and Na$^+$ and the pressure parameters α and β need to be regressed in the present work from experimental SLE data.

Many studies on the solubility of anhydrite and gypsum in pure water are available in literature, although, at high temperatures and pressures, the number of experimental measurements decreases dramatically. The references used in this work for the binary CaSO$_4$-H$_2$O system, the temperature and pressure ranges covered, and the number of experimental data are given in table 4-16.

The experimental and calculated phase diagram for the system CaSO$_4$-H$_2$O at a constant pressure of 1000 bar is shown in figure 4-18. Extended UNIQUAC calculations are in very good agreement with the experimental data and the average absolute deviation between the model calculations and the experimental measurements is within experimental accuracy. A thorough analysis of the data was performed prior to the parameter estimation because the solubility data reported by numerous workers were not in agreement, perhaps because of the high instability of some of the forms of calcium sulphate. Solubility determinations by the usual isothermal method are rather difficult or may even be impossible (Zdanovskii and Spiridonov, 1967).

Table 4-16
Experimental binary CaSO$_4$-H$_2$O SLE data sets used for parameter estimation

T ($^{\circ}$C)	P (bar)	Number of data	AAD (m)	Reference
0/80	1	5 (3)	1.8E-04	Kydynov and Druzhinin (1957)
0/92	1	9 (9)	4.7E-04	Posnjak (1938)
0/100	1	5 (2)	1.4E-04	Zdanovskii and Spiridonov (1967)
0.5/25	1	2 (2)	1.0E-04	Culberson et al. (1978)
14	1	1 (0)		D'Anselme (1903)
18	1	1 (0)		Kohlrausch and Rose (1893)

Table 4-16 (continuation)
Experimental binary CaSO$_4$-H$_2$O SLE data sets used for parameter estimation

T (^{o}C)	P (bar)	Number of data	AAD (m)	Reference
18/218	1/22.1	6 (4)	1.6E-04	Melcher (1910)
20	1	1 (1)	5.1E-04	Kuznetsov (1946)
22/26	1	3 (3)	1.7E-04	Cameron and Seidell (1901)
25	1	1 (0)		Cameron and Bell (1907)
25	1	1 (1)	1.5E-04	Dietrich (1916)
25	1	1 (1)	1.9E-04	Kolosov (1958)
25	1	1 (1)	1.9E-04	Kolosov (1959)
25	1	2 (2)	1.5E-04	Rza-Zade and Rustamov (1963)
25	1	1 (1)	1.5E-04	Shternina and Frolova (1949)
25	1	1 (1)	1.8E-04	Seidell and Smith (1904)
25	1	1 (1)	1.9E-04	Jones (1939)
25	1	2 (0)		Kruchenko and Beremzhanov (1976)
25/26	1	2 (2)	4.1E-05	Rza-Zade and Rustamov (1961)
25/35	1	3 (2)	1.5E-04	Madgin and Swales (1956)
25/50	1	8 (5)	5.5E-04	Bock (1961)
25/75	1	4 (2)	1.4E-04	Hill and Wills (1938)
25/80	1	5 (0)		Taperova (1940)
25/100	1	6 (3)	2.8E-04	Hill and Yanick (1935)
26/82	1	2 (0)		Cameron (1901)
30/50	1/290	15 (10)	7.1E-03	Manikhin (1966)
35	1	1 (1)	1.3E-04	Lepeshkov and Fradkina (1959)
35	1	1 (1)	1.3E-04	Valyashko and Petrova (1952)
35	1	1 (1)	1.3E-04	Novikola (1957)
35	1	1 (1)	1.3E-04	Lepeshkov and Novikova (1958)
35/60	1	3 (2)	1.6E-04	Dobberstein (1991)
35/65	1	4 (3)	5.1E-04	Hill (1937)
40	1	1 (1)	1.4E-04	Barba et al. (1984)
40/100	1	4 (3)	2.1E-04	Hill (1934)
40/125	1	6 (2)	1.4E-04	Marshall et al. (1964)
50/83.5	3/1010	32 (2)	8.4E-04	Blount and Dickson (1973)
55	1	5 (0)		Bodaleva and Lepeshov (1956)
55	1	1 (1)	1.7E-03	Sveshnikova (1952)
73/202.5	118/1410	17 (8)	1.2E-03	Blount and Dickson (1969)
96/263	2/1010	54 (54)	7.9E-04	Dickson et al. (1963)
100/195	1/13.8	53 (53)	6.2E-04	Hall et al. (1926)
100/200	1/15.6	12 (8)	1.3E-04	Gardner and Glueckauf (1970)
100/220	1/23.2	13 (13)	1.0E-04	Partridge and White (1929)
100/300	1/1000	15 (15)	3.6E-04	Lyashchenko and Churagulov (1981)
110	1	1 (0)		Gromova (1960)
141/408	3.7/287.2	22 (13)	3.3E-04	Booth and Bidwell (1950)
			MAAD (m):	7.6E-04

The phase diagram for the binary system $CaSO_4$-H_2O contains a peritectic point at about 45^oC, where the stable solid phase changes from gypsum to anhydrite. At temperatures higher than 45^oC, gypsum will therefore become a metastable phase and its dissolution will be suppressed by anhydrite crystallization, which is a more stable solid phase at those conditions. The same applies to anhydrite if the temperature is lower than 45^oC, in which case gypsum will be the solid phase with the lowest solubility. Finally, a third, metastable solid phase, hemihydrate ($CaSO_4 \cdot 0.5H_2O$), may appear in the binary $CaSO_4$-H_2O system.

Many investigators measured both anhydrite and gypsum solubilities in pure water for temperature conditions where these solid phases are metastable and many other references also report $CaSO_4 \cdot 0.5H_2O$ as the solid phase, which is unstable at all temperatures. As we are only interested in the equilibrium phases at a given temperature and composition, all the experimental data concerning anhydrite below 40^oC, gypsum above 45^oC and the salt $CaSO_4 \cdot 0.5H_2O$ at any temperature were not used for parameter estimation. Both anhydrite and gypsum measurements in the temperature interval 40-45^oC are used in the present work, because of the disagreement found in literature concerning the temperature of the peritectic point.
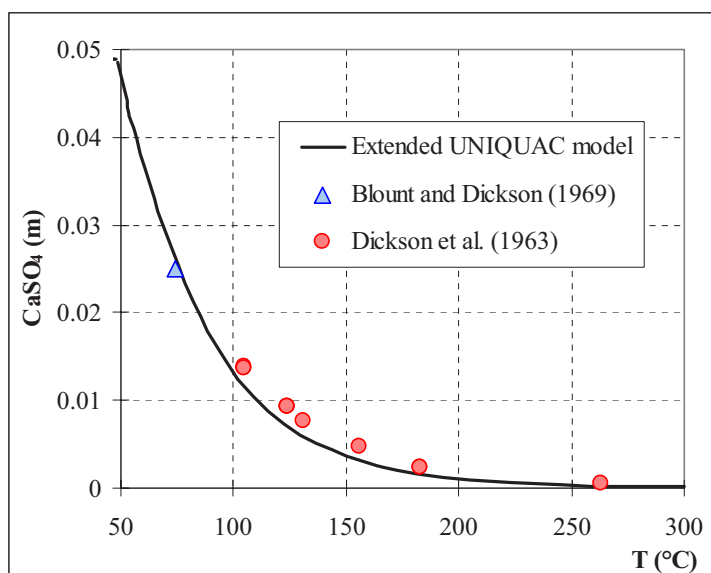
Figure 4-18. Experimental and calculated solid-liquid phase diagram for the $CaSO_4$-H_2O system at 1000 bar.

The sources reporting experimental measurements where a metastable phase is the solid phase are: Kohlrausch and Rose (1893), Melcher (1910), Hill (1934, 1937), Hill and Yanick

(1935), Hill and Wills (1938), Taperova (1940), Bodaleva and Lepeshov (1956), Madgin and Swales (1956), Bock (1961), Marshall et al. (1964), Manikhin (1966), Zdanovskii and Spiridonov (1967), Gardner and Glueckauf (1970), Blount and Dickson (1973), Kruchenko and Beremzhanov (1976) and Dobberstein (1991). Some of the references cited also report measurements in which the solid phase is stable. Such experimental data will be used unless they disagree with the tendency followed by the majority of the sources, which is the case for the stable phases reported by Taperova (1940), Bodaleva and Lepeshov (1956) and Kruchenko and Beremzhanov (1976).

When comparing the different available sources at atmospheric pressure, some measurements were found to be in disagreement with the tendency followed by the majority of the experimental data reported in table 4-16. Such data sets were not used for parameter estimation: Cameron (1901), D'Anselme (1903), Cameron and Bell (1907), and Gromova (1960).

The Kydynov and Druzhinin (1957) measurements at temperatures higher than 60°C seem to be inaccurate when compared to others.

Hall et al. (1926) report very scattered data at all the conditions analyzed. For example, the anhydrite solubility at 122°C and 2.11 bar varies from 0.0033 m to 0.005 m. Nevertheless, all data from this source were used because it was not possible to distinguish between the good and bad data.

4.4.2 CaSO$_4$-Na$_2$SO$_4$ System

The solubility diagram for the ternary system CaSO$_4$-Na$_2$SO$_4$-H$_2$O at 35°C and 1 bar is shown in figure 4-19, where the solid phase gypsum up to about 24 wt.% of Na$_2$SO$_4$; at this point the solid phase changes to glauberite (Na$_2$SO$_4$·CaSO$_4$) and thenardite (Na$_2$SO$_4$) when the Na$_2$SO$_4$ concentration increases to about 32 wt.%. The gypsum curve shows a maximum and a minimum, which is a shape that is well represented by the extended UNIQUAC model. Nevertheless, when the temperature increases the calculations performed by the model lose some accuracy, probably because of the difficulty encountered by any model in following curves with such large tendency changes. Table 4-17 shows the data sources used for the ternary system CaSO$_4$-Na$_2$SO$_4$-H$_2$O, together with the average absolute deviation between the model calculations and the experimental data. The mean absolute deviation *MAAD* is larger than the average experimental standard deviation *ASD*. The results are fairly accurate, considering that only one parameter was used (the rest had already been

determined). A further study of such a system, with the possibility of modifying additional parameters, would very probably lead to much more accurate results.

Many of the solubility measurements performed by Hill and Wills (1938) correspond to metastable phases, and therefore where not used for parameter estimation. The same criterion is applied to the data reported by Cameron et al. (1907) and Kydynov and Druzhinin (1957).

Table 4-17
Experimental ternary $CaSO_4$-Na_2SO_4-H_2O SLE data sets used for parameter estimation

$T\,(^oC)$	$P\,(bar)$	Number of data	$AAD_{CaSO4}\,(m)$	Reference
0/80	1	31 (15)	6.8E-03	Kydynov and Druzhinin (1957)
18	1	2 (2)	5.3E-03	Mecke (1935)
22	1	8 (8)	1.6E-03	Cameron and Seidell (1901)
25	1	1 (1)	2.9E-03	Nikolskaya and Moshkina (1958)
25	1	1 (0)		Cameron et al. (1907)
25	1	4 (2)	1.2E-03	Madgin and Swales (1956)
25	1	11 (11)	1.7E-03	Cameron and Breazeale (1904)
25	1	12 (12)	1.7E-03	Kolosov (1959)
25/75	1	144 (45)	3.8E-04	Hill and Wills (1938)
35/55	1	7 (5)	2.2E-03	Lepeshkov and Fradkina (1959)
40	1	11 (11)	7.0E-04	Barba et al. (1984)
110	1	13 (13)	6.2E-04	Gromova (1960)
			MAAD (m):	1.6E-03
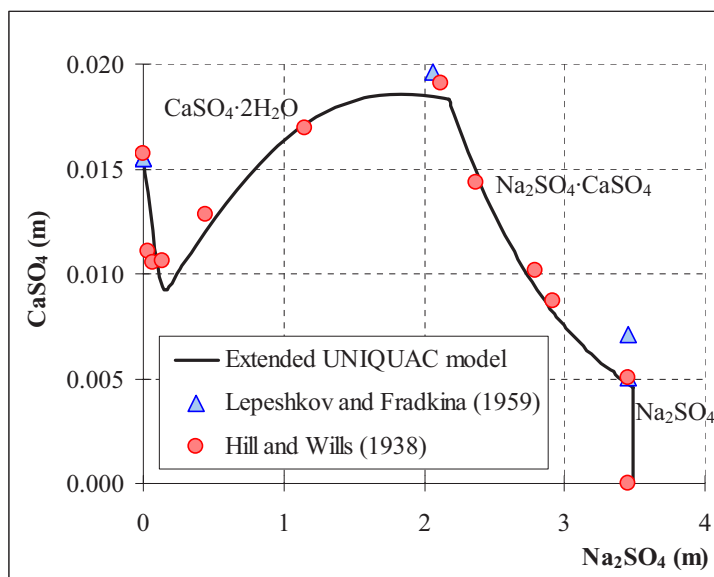
Figure 4-19. Experimental and calculated solid-liquid phase diagram for the $CaSO_4$-Na_2SO_4-H_2O system at 35ºC and 1 bar

4.4.3 CaSO₄-CaCl₂-H₂O and CaSO₄-NaCl-H₂O Systems

As mentioned before, the additional parameters required for the Na-Ca-SO$_4$-Cl-H$_2$O system were already known. The experimental data sets given in table 4-18 for the ternary system CaSO$_4$-CaCl$_2$-H$_2$O and in table 4-19 for the quaternary system CaSO$_4$-NaCl-H$_2$O were therefore not used for parameter estimation. The references dealing with these two systems, the conditions of temperature and pressure covered, and the number of experimental measurements are given in these two tables. The values of the *AAD* between experimental data and the extended UNIQUAC model are also presented.

Table 4-18
Experimental ternary CaSO$_4$-CaCl$_2$-H$_2$O SLE data sets used for parameter estimation

T (°C)	P (bar)	Number of data	AAD_{CaSO4} (m)	Reference
0/55	1	17	3.0E-03	Sveshnikova (1949)
20	1	5	6.3E-04	Kuznetsov (1946)
25	1	13	6.3E-04	Rza-Zade and Rustamov (1963)
25	1	13	6.3E-04	Rza-Zade and Rustamov (1961)
25	1	1	6.4E-04	Perova (1957)
25	1	9	3.8E-04	Cameron and Seidell (1901)
55	1	11	2.0E-03	Sveshnikova (1952)
55	1	13	2.3E-03	Campbell and Marsh (1959)
110	1	8	7.1E-04	Gromova (1960)
			MAAD (m):	**1.5E-03**

Table 4-19
Experimental quaternary CaSO$_4$-NaCl-H$_2$O SLE data sets used for parameter estimation

T (°C)	P (bar)	Number of data	AAD_{CaSO4} (m)	Reference
-21.2/-3	1	40	2.8E-01	Korolev (1937)
-4.5/-1.5	1	5	4.8E-01	Semenchenko and Zavada (1931)
14	1	17	1.7E-02	D'Anselme (1903)
15/82	1	55	1.7E-02	Cameron (1901)
18	1	2	4.0E-03	Mecke (1935)
19	1	9	1.8E-02	Foret (1943)
20	1	9	1.2E-02	Orlov (1902)
25	1	15	1.6E-02	Shternina and Frolova (1949)
25	1	26	1.4E-02	Rza-Zade and Rustamov (1963)
25	1	35	7.6E-03	Melnikova and Moshkina (1973)
25	1	16	8.7E-02	Cameron et al. (1907)
25/35	1	67	1.0E-02	Madgin and Swales (1956)
25/50	1	48	3.0E-02	Bock (1961)
40/200	1/15.5	134	2.1E-02	Marshall et al. (1964)
94/302	1/1063	77	1.1E-01	Blount and Dickson (1969)
100/200	1/15.4	19	9.2E-02	Il'inskii and German (1936)
110	1	7	1.5E-01	Gromova (1960)
			MAAD (m):	**5.8E-02**

Table 4-20

Thermodynamic properties (NIST, 1990) and related parameters

	$\Delta_r G_f^0$ (kJ mol^{-1})	$\Delta_r H_f^0$ (kJ mol^{-1})	C_{p1} (J mol^{-1}K^{-1})	C_{p2} (J mol^{-1}K^{-2})
Sr^{2+}	-559.48	-545.8	-1124.756[a]	3.450446[a]
$BaCl_2 \cdot H_2O$	-1055.669	-1160.79	120	0
$BaCl_2 \cdot 2H_2O$	-1296.32	-1460.13	161.96	0
$BaSO_4$	-1361.866[a]	-1467.929[a]	104.0038	0
$SrSO_4$	-1341.538[a]	-1452.955[a]	100	0
$SrCl_2 \cdot 2H_2O$	-1284.587[a]	-1456.694[a]	160.2	0
$SrCl_2 \cdot 6H_2O$	-2240.92	-2623.8	320	0
$BaSO_4 \cdot SrSO_4$	-2714.505[a]	-2954.863[a]	201.75	0
$CaSO_4$	-1321.8	-1436.132[a]	70.21[b]	0.009874[b]
$CaSO_4 \cdot 2H_2O$	-1797.407[a]	-2026.294[a]	91.38[b]	0.318[b]
$Na_2SO_4 \cdot CaSO_4$	-2594.808	-2816.396	140.25[b]	0.2907[b]
Na_2SO_4	-1270.16	-1387.08	128.2	0
$CaCl_2$	-748.1	-795.8	72.59	0
$CaCl_2 \cdot 2H_2O$	-1253.87	-1402.9	153	0
$CaCl_2 \cdot 4H_2O$	-1738.434	-2014.119	233	0
$CaCl_2 \cdot 6H_2O$	-2219.378	-2607.658	313	0

[a] Values estimated from experimental SLE data.
[b] Values taken from Kelley, 1960.

4.5 References in Chapter 4

Archer, D.G., 1992. Thermodynamic properties of NaCl+H$_2$O system II. Thermodynamic properties of NaCl (aq), NaCl·2H$_2$O (c), and phase equilibria. J. Phys. Chem. Ref. Data 21, 793-829.

Arnorsson, E., 1989. Deposition of calcium carbonate minerals from geothermal waters. Theoretical considerations. Geothermics 18, 33-39.

Assarsson, G.O., 1953. Equilibria in aqueous systems containing Sr, K, Na and Cl. J. Phys. Chem. 57, 207-210.

Assarsson, G.O., 1956. Equilibria in the ternary system MgCl$_2$-BaCl$_2$-H$_2$O between 18 and 100°C. Phys. Chem. 60, 1436-1439.

Atkinson, G., Oklahoma, U., Raju, K., Aramco, S., Howell R.D., 1991. The thermodynamics of scale prediction. SPE 21021, 209-215.

Barba, D., Brandani, V., Di Giacomo, G., 1984. Solubility of calcium sulfate dihydrate in the system Na$_2$SO$_4$. J. Chem. Eng. Data 29, 42-45.

Belfiori, P., 1940. The effect of alkali nitrites on several difficulty soluble sulfates. Ann. Chim. Applicata 30, 233-237.

Blount, C.W., Dickson, F.W., 1969. The solubility of anhydrite (CaSO$_4$) in NaCl-H$_2$O from 100 to 450°C and 1 to 1000 bars. Geochimica et Cosmochimica Acta 33, 227-245.

Blount, C.W., Dickson, F.W., 1973. Gypsum-anhydrite equilibria in systems CaSO$_4$-H$_2$O and CaSO$_4$-NaCl-H$_2$O. American Mineralogist 58, 323-331.

Blount, C.W., 1977. Barite solubilities and thermodynamic quantities up to 300 ^{o}C and 1400 bars. American Mineralogist 62, 942-957.

Bock, E., 1961. On the solubility of anhydrous calcium sulphate and of gypsum in concentrated solutions of sodium chloride at 25°C. Can. J. Chem. 39, 1746-1751.

Bodaleva, N.V., Lepeshov, I.N., 1956. Investigation of phase equilibria in the system K$_2$SO$_4$-MgSO$_4$-CaSO$_4$-H$_2$O at 55°C. Zh. Neorgan. Khim. 1 (5), 995-1007.

Booth, H.S., Bidwell, R.M., 1950. Solubilities of salts in water at high temperatures. J. Amer. Chem. Soc. 72, 2567-2575.

Brower, E., Renault, J., 1971. Solubility and enthalpy of the barium strontium sulfate solid solution series. New Mexico State Bureau of Mines and Mineral Resources, Circular 116.

Cameron, F.K., 1901. Solubility of gypsum in aqueous solutions of sodium chloride. J. Phys. Chem. 5, 556-576.

Cameron, F.K., Seidell, A., 1901. Solubility of gypsum in aqueous solutions of certain electrolytes. J. Phys. Chem. 5, 643-655.

Cameron, F.K., Breazeale, J.F., 1904. Calcium sulphate in aqueous solutions of potassium and sodium sulphates. J. Phys. Chem. 8, 335-340.

Cameron, F., Bell, J., 1907. The action of water and aqueous solutions upon soil phosphates. U. S. Dept. Agr., Bull. 41.

Cameron, F.K., Bell, J.M., Robinson, W.O., 1907. The solubility of certain salts present in alkali soils. J. Phys. Chem. 11, 396-420.

Campbell, A.N., Cook, E.J.R., 1935. A study of precipitation from supersaturated solutions of strontium sulfate. J. Amer. Chem. Soc. 57, 387-390.

Campbell, J.A., Marsh, F.L., 1959. The system magnesium bromide, ammonium bromide, and water at 25^oC. J. Phys. Chem. 63, 316-317.

Campbell, J.R., Nancollas, G.H., 1969. The crystallization and dissolution of strontium sulfate in aqueous solution. J. Phys. Chem. 73, 1735-1740.

Culberson, C.H., Lathman, G., Bates, R.G., 1978. Solubilities and activity coefficients of calcium and strontium sulfate in synthetic seawater at 0.5^oC and 25^oC. J. Phys. Chem. 82, 2693-2699.

D'Anselme, A., 1903. Bull. Soc. Chim. 29 (3), 373.

Davis, J.W., Collins, A.G., 1971. Solubility of barium and strontium sulfates in strong electrolyte solutions. Environmental Science & Technology 5, 1039-1043.

Dickson, F.W., Blount, C.W., Tunell, G., 1963. Use of hydrothermal solution equipment to determine the solubility of anhydrite in water from 100^oC to 275^oC and from 1 bar to 1000 bars pressure. American Journal of Science 261, 61-78.

Dietrich, 1916. Kaminer Handbuch der Balneologie Vol.1, pp.205.

Dobberstein, K.U., 1991. Dichte und Viskositätsmessungen in ternäre Elektrolytlösungen. Dissertation, Martin-Luther-Universität Halle Wittenberg.

Dyer, S.J., Graham, G.M., 2002. The effect of temperature and pressure on oilfield scale formation. Journal of Petroleum Science and Engineering 35, 95-107.

Eddy, R.D., Menzies, A.W.C., 1940. The solubilities of certain inorganic compounds in ordinary water and in deuterium water J. Phys. Chem. 44, 207-235.

Enüstün, B.V., Turkevich, J., 1960. Solubility of fine particles of strontium sulfate. J. Amer. Chem. Soc. 82, 4502-4509.

Felmy, A.R., Rai, D., Amonette, J.E., 1990. The solubility of barite and celestite in sodium sulfate: evaluation of thermodynamic data. J. Sol. Chem. 19 (2), 175-185.

Findlay, A., Cruickshank, J., 1926. The reciprocal salt pair (Na, Ba)-(Cl, NO_3) in aqueous solution at 20^oC. J. Chem. Soc., 316-318.

Foret, J., 1943. Nonexistence of the paradox claimed to exist in the solubility of gypsum in aqueous solutions of NaCl. Compt. Rend. 217, 264-266.

Gallo, G., 1935. Equilibrium of strontium sulfate and water at various temperatures. Ann. Chim. Applicata 25, 628-631.

Gardner, A.W., Glueckauf, E., 1970. Thermodynamic data of the $CaSO_4$ solution process. Trans. Faraday Soc. 66, 1081-1086.

Gibbard, H.F., Fong, S.L., 1975. Freezing points and related properties of electrolyte solutions III. The systems $NaCl-CaCl_2-H_2O$ and $NaCl-BaCl_2-H_2O$. J. Sol. Chem. 4, 863-872.

Gill, J.S., 1998. Silica scale control. Chemical Treatment, 41-45.

Graham, G.M., Mackay, E.J., 2003. A background to inorganic scaling-mechanisms, formation and control. 5th Intl. SPE Oilfield Scale Symposium. Aberdeen, UK.

Gromova, E.T., 1960. The solubility isotherm of the $Na-Ca-Cl-SO_4-H_2O$ system at 110^oC. Russian Journal of Inorganic Chemistry 5, 1244-1247.

Hall, R.E., Robb, J.A., Coleman, C.E., (1926). The solubility of calcium sulfate at boiler-water temperatures. J. Am. Chem. Soc., 927-938.

Harvey, A.H., Perskin, A.P., Klein, S.A., 1996. NIST/ASME steam properties formulation for general and scientific use.

He, S., Morse, J.W., 1992. Prediction of halite, gypsum, and anhydrite solubility in natural brines under subsurface conditions. Computer & Geosciences 19, 1-22.

Hill, A.E., 1934. Ternary Systems XIX. Calcium sulfate, potassium sulfate and water. J. Am. Chem. Soc. 56, 1071-1078.

Hill, A.E. and Yanick, N.S., 1935. Ternary system. Calcium sulfate, ammonium sulfate and water. J. Am. Chem. Soc. 57, 645-651.

Hill, A.E., 1937. The transition temperature of gypsum to anhydrite. J. Am. Chem. Soc. 59, 2242-2244.

Hill, A.E., Wills, J. H., 1938. Ternary systems XXIV. Calcium sulfate, sodium sulfate and water. J. Am. Chem. Soc. 60, 1647-1655.

Howell, R.D., Raju, K., Atkinson, G., 1992. Thermodynamics of "Scale" mineral solubilities 4. $SrSO_4$. J. Chem. Eng. Data 37, 464-469.

Il'inskii, V.P., German, N.A., 1936. Tr. Vses. Nauch.-Issled. Inst. Gal.

Jacques, D.C., Bourland, B.I., 1983. A study of solubility of strontium sulphate. SPEJ, 292-300.

Jiang, C., 1996. Solubility and solubility constant of barium sulfate in aqueous sodium sulfate solutions between 0 and 80°C. J. Sol. Chem. 25 (1), 105-111.

Jones, H.C., 1893. Über die Bestimmung des Gefrierpunktes sehr verdünnter Salzlösungen. Z. Phys. Chem. 11, 529-551.

Jones, H.C., Pearce, J.N., 1907. Dissociation as measured by freezing point lowering and by conductivity-bearing on the hydrate theory. The approximate composition of the hydrates formed by a number of electrolytes. Am. Chem. J. 38, 683-743.

Jones, F.E., 1939. The quaternary system $CaO-Al_2O_3-CaSO_4-H_2O$ at 25°C. Trans. Faraday Soc. 35, 1484-1510.

Juranek, J., Skollova, Z., Harnova, J., 1987. MINEQUA-Part I. A program for computing the chemistry of calcium carbonate in mineralized and thermal waters. Geothermics 16, 263-270.

Kaasa, B., 1998. Prediction of pH, mineral precipitation and multiphase equilibria during oil recovery. Ph.D. thesis. Institutt for Uorganisk Kjemi. Norges Teknisk-Naturvitenskapelige Universitet, Trondheim, pp. 5-272.

Keevil, N. B., 1942. Vapor pressures of aqueous solutions at high-temperatures. J. Am. Chem. Soc. 64, 841-850.

Kelley, K.K., 1960. High-temperature heat-content, heat-capacity, and entropy data for the elements and inorganic compounds. Bulletin/Bureau of Mines 584, 1-211.

Kohlrausch, F., Rose, F., 1893. Die Löslichkeit einiger schwer löslicher Körper in Wasser, beurteilt aus der elektrischen Leitfähigkeit. Z. Physik. Chemie 12, 234-243.

Kohlrausch, F., 1908. Über gesättigte wässerige Lösungen schwerlöslicher Salze. II. Teil: Die gelösten Mengen mit ihrem Temperaturgang. Z. Physik. Chemie 64, 129-169.

Kolosov, A.S., 1958. Isotherm in the system MgSO4-CaSO4 at 25°C. Akad. Nauk SSSR 12, 29-38.

Kolosov, A.S., 1959. The system Na, Mg, Ca, SO_4, H_2O at 25°C. Izv. Sib. Otd. Akad. Nauk SSSR 3, 67-75.

Korolev, V.F., 1937. Akad. Nauk SSSR 15, 28.

Kruchenko, V.P., Beremzhanov, V.A., 1976. The solubilities of the salts in the calcium sulphate-hydrochloric acid-water system at 25°C. Russian Journal of Inorganic Chemistry 21, 152-153.

Krumgalz, B.S., Starinsky, A., Pitzer, K.S., 1999. Ion-interaction approach: pressure effect on the solubility of some minerals in submarine brines and seawater. Journal of Solution Chemistry 28 (6), 667-692.

Kuznetsov, A.M., 1946. On the solubility of $CaSO_4$ in the system $CaCl_2-HCl-H_2O$. Zh. Prikl. Khim. 19 (12), 1335-1339.

Kydynov, M., Druzhinin, I.G., 1957. The solubility of the system of the sulfates of calcium and sodium at 0, 20, 40, 60, and 80°C and the glauberite rocks of Tien-Shan. Izv. Akad. Nauk Kirg. SSSR 4, 89-117.

Lepeshkov, I.N., Novikova, L.V., 1958. Physico-chemical investigation of the system $K_2SO_4-MgSO_4-CaSO_4-H_2O$ at 35°C. Zh. Neorgan. Khim. 3 (10), 2395-2407.

Lepeshkov, I.N., Fradkina, Kh. B., 1959. Salt solubilities in the $CaSO_4-Na_2SO_4-NaCl-H_2O$ system at 35 and 55°C. Russian Journal of Inorganic Chemistry 4, 1297-1301.

Lieser, K.H., 1965. Radiochemische messung der löslichkeit von erdalkalisulfaten in wasser und in natriumsulfatlösungen. Z. Anorg. Allg. Chem. 335 (5-6), 225-231.

Loomis, E.H., 1896. Über den Gefrierpunkt verdünnter wässeriger Lösungen. Physical Review 3, 270-292.

Lown, D.A., Thirsk, H.R., Lord W.J., 1968. Effect of pressure on ionization equilibria in water at 25°C. Trans. Faraday Soc. 64, 2073-2080.

Lucchesi, P.J., Whitney, E.D., 1962. Solubility of strontium sulphate in water and aqueous solutions of hydrogen chloride, sodium chloride, sulphuric acid and sodium sulphate by the radiotracer method. J. Appl. Chem. 12, 277-279.

Lyashchenko, A.K., Churagulov, B.R., 1981. Influence of pressure on the temperature coefficients of the solubility of electrolytes in water. Russ. J. Inorg. Chem. 26, 642-644.

MacDonald, R.W., North, N.A., 1974. The effect of pressure on the solubility of $CaCO_3$, CaF_2 and $SrSO_4$ in water. Can. J. Chem. 52, 3181-3186.

Madgin, W.M., Swales, D.A., 1956. Solubilities in the system $CaSO_4-NaCl-H_2O$ at 25°C and 35°C. J. Appl. Chem. 6, 482-487.

Manikhin, V.I., 1966. Solubility of calcium sulfate under high pressures. Gidrokhim. Mater 41, 192-196.

Marden, J.W., 1916. Solubilities of the sulfates of barium, strontium, calcium and lead in ammonium acetate solutions at 25°C and a criticism of the presents methods for the separation of these substances by means of ammonium acetate solution. J. Amer. Chem. Soc. 38, 310-316.

Marshall, W.L., Slusher, R., Jones, E.V., 1964. Aqueous systems at high temperature XIV. J. Chem. Eng. Data 9, 187-191.

Mecke, P., 1935. Über die Löslichkeit von calciumsulfat und calciumhydroxyd. Zement 24 (48), 764-766.

Melcher, A.C., 1910. The solubility of silver chloride, barium sulphate, and calcium sulphate at high temperatures. J. Am. Chem. Soc. 32, 50-66.

Melnikova, Z.M., Moshkina, I.A., 1973. The solubility of anhydrite and gypsum in the system Na,Mg,Ca,Cl,SO$_4$-H$_2$O at 25°C. Ser. Khim. Nauk. 2, 18-26.

Millero, F.J., 1981. The effect of pressure on the solubility of minerals in water and seawater. Geochimica et Cosmochimica Acta 46, 11-22.

Monnin, C., Galinier, C., 1988. The solubility of celestite and barite in electrolyte solutions and natural waters at 25°C: A thermodynamic study. Chemical Geology 71, 283-296.

Monnin, C., 1999. A thermodynamic model for the solubility of barite and celestite in electrolyte solutions and seawater to 200°C and to 1 kbar. Chemical Geology 153, 187-209.

Moshinskii, A. S., Tikhomirova, K. A., 1973. Equilibrium between zinc chloride and alkaline earth metal chlorides in an aqueous medium at 50°C. Russ. J. Inorg. Chem. 18, 431-433.

Møller, N., Greenberg, J.P., Weare, J.H., 1998. Computer modeling for geothermal systems: Predicting carbonate and silica scale formation, CO$_2$ breakout and H$_2$S exchange. Transport in Porous Media 33, 173-204.

Müller, G., 1960. Die Löslichkeit von Coelestin (SrSO$_4$) in wässerigen NaCl- und KCl-Lösungen. Neues Jahrb. Mineral. Mon., 237-239.

Neuman, E.W., 1933. Solubility relations of barium sulfate in aqueous solutions of strong electrolytes. J. Am. Chem. Soc. 55, 879-884.

Nikolskaya, Y.P., Moshkina, I.A., 1958. The Na, Ca, SO$_4$, HCO$_3$ - H$_2$O system at 25°C and 1 atm. CO$_2$ pressure. Zh. Neorgan. Khim. 3 (2), 498-500.

NIST Chemical Thermodynamics Database Version 1.1, 1990. U.S. Department of Commerce, National Institute of Standards and Technology, Gaithesburg MD 20899.

Novikola, L.V., 1957. Study of solubility in the equilibrium in the system CaSO$_4$-MgSO$_4$-H$_2$O at 35°C by the method of labelled atom. Zh. Neorgan. Khim. 2 (3), 662-668.

Orlov, N.A., 1902. Obshchest. Chast. Khim. 34, 951.

Partridge, E., White, A.H., 1929. The solubility of calcium sulfate from 0 to 200°C. J. Am. Chem. Soc. 51, 360-370.

Perova, A.P., 1957. Solubility isotherms in the aqueous magnesium chloride calcium sulfate system at 25 and 55°C. Sb. Tr. Voronezh. Otd. Vses. Khim. Obshch. im Mendeleva 1, 155-163.

Pitzer, K.S., 1991. Activity coefficients in electrolyte solutions, 2nd edition. CRC Press, Boca Raton, pp. 293-422.

Posnjak, E., 1938. The system CaSO$_4$-H$_2$O. American Journal of Science 35, 247-272.

Potapov, V.V., Kashpura, V.N., Alekseev, V.I., 2001. A study of the growth of deposits in geothermal power systems. Thermal Engineering 48 (5), 395-400.

Puchelt, H., 1967. Zur Geochemie des Bariums im exogenen Zyklus. Sitzungsberichte der Heidelberger Akademie der Wissenschaften, Heidelberg (Germany).

Qadirie, A.R., 1990. Experimente zum Fällungsverhalten im System Barium-Strontium-Sulfat und Vergleich mit natürlichen Ausfällungen. Diplomarbeit (Teil 2), Mathematisch-Naturwissenschaftlichen Fakultät der Christian-Albrechts-Universität zu Kiel.

Rard, J.A., Miller, D.G., 1982. Isopiestic determination of the osmotic and activity coefficients of aqueous CsCl, SrCl$_2$, and mixtures of NaCl and CsCl at 25°C. J. Chem. Eng. Data 27, 169-173.

Reardon, E.J., Armstrong, D.K., 1987. Celestite (SrSO$_4$(s)) solubility in water, seawater and NaCl solution. Geochimica et Cosmochimica Acta 51, 63-72.

Rza-Zade, P.F., Rustamov, P.G., 1961. Isotherms in the system MgCl$_2$-CaCl$_2$-CaSO$_4$-H2O at 25°C. Azerb. Khim. Zh. 4, 127-131.

Rza-Zade, P.F., Rustamov, P.G., 1963. Solubility isotherm in the system NaCl-CaCl$_2$-CaSO$_4$-H$_2$O at 25°C. Azerb. Khim. Zh. 1, 57-63.

Schreinemakers, F.A.H., de Baat, W.C., 1909. Gleichgewichte in quaternaren Systeme. Z. Physik. Chem. 65, 586-594.

Schreinemakers, F.A.H., 1910. Gleichgewicht in quaternären Systemen. Das System: Natriumoxyd - Baryumoxyd - Salzsäure und Wasser. Zeitschrift für Physikalische Chemie 68, 83-103.

Schreinemakers, F.A.H., 1911. Le point de transformation de sels doubles. Archives Néerlandaises des Sciences Exactes et Naturelles 15, 396-402.

Schroeder, W.C., Gabriel, A., Partridge, E.P., 1935. Solubility equilibria of sodium sulfate at temperatures of 150 to 350°C. I. Effect of sodium hydroxide and sodium chloride. J. Am. Chem. Soc. 57, 1539-1546.

Schulien, S., 1987. High-temperature/high-pressure solubility measurements in the systems $BaSO_4$-NaCl-H_2O and $SrSO_4$-NaCl-H_2O in connection with scale studies. SPE symposium (SPE 16264), San Antonio, Texas.

Seidell, A., Smith, J.G., 1904. The solubility of calcium sulphate in solutions of nitrates. J. Phys. Chem. 8, 493-499.

Selivanova, N.M., Zubova, G.A., 1956. Polarography and thermodynamics IV. Thermodynamic properties and solubility of strontium sulfate. Trudy Moskov. Khim.-Teknol. Inst. im. D.I. Mendeleeva, 38-46.

Semenchenko, V.K., Zavada, E.A.. 1931. Krioskopija vodnykh rastvorov smesej jelektrolitov. Zhurnal obshchei khimii 1, 1121-1931.

Shams El Din, A.M., Mohammed, R.A., 1989. The problem of alkaline scale formation from a study on Arabian Gulf water. Desalination 71, 313-324.

Shternina, E.B., Frolova, E.V., 1949. Akad. Nauk SSSR 17, 354.

Sorbie, K.S., Mackay, E.J., 2000. Mixing of injected, connate and aquifer brines in waterflooding and its relevance to oilfield scaling. Journal of Petroleum Science and Engineering 27, 85-106.

Speranskaya, E.I., 1954. Reactions of nitrates and chlorides of sodium and barium in melts and in aqueous solutions. Akad. Nauk. SSSR 24, 212-221.

Strübel, G., 1966. Die hydrothermale Löslichkeit von Cölestin im System $SrSO_4$-NaCl-H_2O. Neues Jahrb. Mineral. Mon., 99-107.

Strübel, V.G., 1967. Zur Kenntnis und genetischen Bedeutung des Systems $BaSO_4$-NaCl-H_2O. Neues Jahr. Miner. Monatsh., 223-234.

Sveshnikova, V.N., 1949. Solubility isotherms in the system $CaSO_4$-$CaCl_2$-H_2O at 25 and 55°C and $CaSO_4$-KCl-H_2O at 25°C. Izv. Sektora Fiz.-Khim. Anal. Akad. Nauk SSSR 17, 345-351.

Sveshnikova, V.N., 1952. Phase equilibria in the reciprocal system $CaSO_4$-KCl-H_2O at 55°C. Otd. Khim. Nauk 1, 44-51.

Taperova, A.A., 1940. L'analyse physicochimique dans le domaine du traitement des phosphates par l'acide sulfurique. Zhurnal Prikladnoi Khimii 13 (5), 643-52.

Templeton, C.C., 1960. Solubility of barium sulfate in sodium chloride solutions from 25° to 95°C. Journal of Chemical and Engineering Data 5 (4), 515-516.

Thomsen, K., Rasmussen, P., Gani, R., 1996. Correlation and prediction of thermal properties and phase behaviour for a class of electrolyte systems. J. Chem. Eng. Science 51, 3675-3683.

Thomsen, K., Rasmussen, P., 1999. Modeling of vapor-liquid-solid equilibrium in gas-aqueous electrolyte systems. Chemical Engineering Science 54, 1787-1802.

Trendafelov, D., Balarew, C., Zlateva, I., Keremidtchieva, B., Gradinarov, S., 1994. Investigations of the $BaSO_4$ conversion to $BaCO_3$ in the quaternary reciprocal water-salt system $BaSO_4$+K_2CO_3 = $BaCO_3$+K_2SO_4. Comptes Rendus de l'Academie Bulgare des Science 47 (1), 47-50.

Uchameyshvili, N.Y., Malinin, S.D., Khitarov, N.I., 1966. Solubility of barite in concentrated chloride solutions of some metals at elevated temperatures in relation to problems of the genesis of barite deposits. Geochem. Int. 10, 951-963.

Uspenskaya, L.N., Bergman, A.G., 1955. Solubility in the reciprocal salt system Barium, Calcium, Nitrate, Chloride at 80, 100 and 120°C. Zh. Obshch. Khim. 25, 1277-1284.

Uspenskaya, L.N., Glushkova, N.P., Bergman, A.G., 1955. Solubility in the reciprocal salt system Barium, Calcium, Nitrate, Chloride from the freezing point to 60°C. Zh. Obshch. Khim. 25 (9), 1658-1673.

Valyashko, M.G., Petrova, V.M., 1952. Tr. Vses Nauch.-Issled. Inst. Galurgii 23, 162.

Varasova, E.N., Mischenko, K.P., Frost, O.I., 1937. Investigation of the thermodynamic properties of saturated water-salt systems (heat capacity and vapor pressure for the system $BaCl_2$-$CaCl_2$-H_2O at 25°C. Zh. Obshch. Khim. 7, 1284-1291.

Vetter, O.J.G., Vandenbroeck, I., Nayberg, J., 1983. $SrSO_4$: the basic solubility data. Society of Petroleum Engineers, 271-281.

Wolfmann, I., 1896. Studium über die Löslichkeitsverhältnisse einiger Strontiumsalze. Besonders des Strontiumsulfates. Österr. Ungar. Z. Zuckerind. 25, 986-997.

Yousef, A.M., Elkanzi, E.M., Singh, H., 2001. Prediction of supercritical CO_2 solubility using the Krichevsky-Ilinskaya equation with v2 as an adjustable parameter. J. of Supercritical Fluids 20, 105-112.

Yuan, M., Todd, A.C., Sorbie, K.S., 1994. Sulfate scale precipitation arising from seawater injection: a prediction study. Marine and Petroleum Geology 11(1), 24-30.

Yuan, M.D., Anderson, M., Jamieson, E., 1997. Investigation and improvement of $BaSO_4$ scale inhibition tests. Society of Petroleum Engineers 37304, 765-768.

Zdanovskii, A.B., Spiridonov, F.P., 1967. Polytherm for the solubilities of various forms of $CaSO_4 \cdot xH_2O$ in water between 0 and 100°C. Zhurnal Prikladnoi Khimii 40, 1152-1154.

Zhang, Y., Shaw, H., Farquhar, R., Dawe, R., 2001. The kinetics of carbonate scaling-application for the prediction of downhole carbonate scaling. Journal of Petroleum Science and Engineering 29, 85-95.

Zhenhao, D., Møller, N., DeRocher, T., Weare, J.H., 1996. Prediction of boiling, scaling and formation conditions in geothermal reservoirs using computer programs. Geothermics 25 (6), 663-678.

5. Carbonate Scaling Minerals

This chapter is devoted to the calculation of the solubility of different carbonate minerals by means of the extended UNIQUAC model. It has been submitted with the title "Prediction of mineral scale formation in geothermal and oilfield operations using the extended UNIQUAC model. Part II. Carbonate scaling minerals" in Geothermics (authors: Ada Villafáfila García, Kaj Thomsen and Erling H. Stenby). In the following, it will be demonstrated that the extended UNIQUAC model is able to give a very good representation of the solid-liquid-vapour phase equilibria for carbonate systems, in the whole temperature, pressure and concentration range investigated. In most of the cases, the absolute deviation between extended UNIQUAC calculations and the experimental data is within experimental accuracy. Table 5-1 shows the values for the *ASD* calculated from the experimental data reported for the different systems studied in this paper.

Table 5-1
Calculated *ASD* values for different systems

System	*ASD* (m)
CO_2-H_2O	4.1E-02
CO_2-$NaCl$-H_2O	2.2E-02
CO_2-Na_2SO_4-H_2O	2.7E-02
$CaCO_3$-CO_2-H_2O	1.3E-03
$BaCO_3$-CO_2-H_2O	2.3E-04
$SrCO_3$-CO_2-H_2O	
$MgCO_3$-CO_2-H_2O	1.8E-02

The surface area and volume parameters obtained from the present work together with the values required for other species obtained by Thomsen and Rasmussen (1999) are given in table 5-15. The binary energy interaction parameters for the extended UNIQUAC model are shown in table 5-16 and table 5-17. Finally, the two new pressure parameters added to the extended UNIQUAC model to account for the pressure dependency are given in table 5-18. The parameters obtained from the present work are marked in bold.

The values for the standard state Gibbs free energy, enthalpy and heat capacity for the different crystalline phases analyzed are taken (whenever it was available) from the NIST Chemical Thermodynamics Database (1990). Those values are also reported in table 5-19.

5.1 CO₂ Solubility

5.1.1 CO₂ Solubility in Pure Water

Most of the papers dealing with calcite ($CaCO_3$) solubility in CO_2-saturated water do not report the CO_2 concentration in the liquid, but only the $CaCO_3$ solubility and the partial pressure of CO_2. In order to be able to use those data, the amount of CO_2 in the solution at the experimental conditions is needed. Therefore, a program calculating CO_2 solubility in water as a function of temperature and pressure was developed. The extended UNIQUAC model was used to calculate activity coefficients in the liquid phase, while gas phase fugacities were calculated according to the Soave-Redlich-Kwong equation of state, using classical mixing rules.

It was assumed that the CO_2 solubility in $CaCO_3$ solutions is very close to the CO_2 solubility in pure water at the same conditions. This assumption is based on the fact that calcite solubility in water is so low that it will not influence the gas solubility significantly. This assumption is supported by table 5-2, where CO_2 solubility values in the $CaCO_3$-H_2O solutions reported by Malinin (1963) are compared to the values obtained from the program. The highest relative deviation is found to be 5.7%, and the average relative deviation is 3.1%. These values are low enough and demonstrate that the influence of calcite on CO_2 solubility in the liquid phase can be neglected without leading to large errors.

Diamond and Akinfiev (2003) reviewed 25 experimental studies on CO_2 solubility in pure water in the temperature range from -1.5 to 100°C, and pressures from 1 to 1000 bar. Different criteria were used to analyze the references, giving them a different weight factor depending on their reliability. All the points with the highest accuracy (according to Diamond and Akinfiev, 2003): Wiebe and Gaddy (1939, 1940), Bartholome and Friz (1956), Matous et al. (1969), Zawisza and Malesinska (1981), Müller et al. (1988), Bamberger et al. (2000), and Anderson (2002)) were used in this work for parameter estimation. Some of the points with very low accuracy (according to Diamond and Akinfiev, 2003) were rejected (Wroblewski (1883), Sander (1912), Hähnel (1920), Kritschewsky et al. (1935), Vilcu and Gainar (1967), Stewart and Munjal (1970), Teng et al. (1997), and Servio and Englezos (2001)).

Table 5-3 shows all the publications used for the system CO_2-H_2O, the ranges of temperature and pressure covered by them, the number of data points reported by each publication, the number of data points used in the present work (in brackets), and the average absolute deviation between our calculations and the experimental data. The calculated CO_2 solubilities in pure water compare well with the experimental data, with a mean absolute deviation of

$3.6 \cdot 10^{-2}$ m CO_2, while the average standard deviation for the experimental data is $4.1 \cdot 10^{-2}$ m

CO_2.

Table 5-2
Calculated versus experimental CO_2 solubility in $CaCO_3$-H_2O solutions.

T	*P*	CO_2 solubility in pure water (m)		*RD*
(°C)	(bar)	**Malinin (1963)**	**Our model**	(%)
150	10.9	0.053	0.056	5.66
150	20.2	0.133	0.138	3.76
150	21.7	0.146	0.151	3.42
150	35.1	0.262	0.263	0.38
150	54.2	0.409	0.411	0.56
150	54.3	0.410	0.414	0.98
150	57.5	0.443	0.437	-1.35
150	59.2	0.457	0.450	-1.53
150	145.1	0.955	0.973	1.88
150	200.1	1.192	1.228	3.02
225	57.9	0.318	0.337	5.97
225	80.4	0.523	0.553	5.74
225	131.4	0.955	1.002	4.92
225	135.3	0.978	1.034	5.73
225	199.1	1.458	1.518	4.12
225	200.1	1.468	1.525	3.88
225	398.2	2.660	2.767	4.02
225	402.1	2.680	2.788	4.03

Table 5-3
Experimental CO_2-H_2O VLE data sets used for parameter estimation.

T (°C)	*P* (bar)	Number of data	*AAD* (m)	Reference
0/12.4	5/30.4	12 (0)		Wroblewski (1883)
0/15	5/45.6	14 (0)		Hähnel (1920)
0/25	0.1/1	19 (19)	5.3E-04	Morgan and Maass (1931)
0/25	1	3 (3)	1.7E-03	Kiss et al. (1937)
0/25	10/45	12 (0)		Stewart and Munjal (1970)
0/50	1.00E+00	18 (18)	6.0E-04	Harned and Davis (1943)
0/60	1/9	65 (65)	8.7E-03	Wasmund and Bultmann (1980)
0/100	1/96	95 (95)	2.8E-02	Zelvenskii (1937)
0.2/40	1.00E+00	3 (3)	7.2E-04	Markham and Kobe (1941a)
1/5	9/21	9 (9)	9.6E-03	Malegaonkar et al. (1997)
1/15	1/22	53 (53)	8.2E-03	Anderson (2002)
1/35	1.00E+00	8 (8)	1.1E-03	Murray and Riley (1971)
100/200	3/81	49 (49)	3.6E-02	Müller et al. (1988)
3.9/10	20/42	9 (0)		Servio and Englezos (2001)

Table 5-3 (continuation)
Experimental CO_2-H_2O VLE data sets used for parameter estimation.

T (°C)	P (bar)	Number of data	AAD (m)	Reference
5/20	64.4/295	24 (0)		Teng et al. (1997)
5/65	0.5/0.8	10 (10)	3.0E-04	Zheng et al. (1997)
10/30	1/20	15 (15)	1.6E-02	Bartholome and Friz (1956)
10/70	10/160	23 (0)	1.7E-02	Oleinik
11.5/40	0.1/0.9	24 (24)	1.2E-03	Novak et al. (1961)
12/40	50/506	42 (42)	1.0E-01	Wiebe and Gaddy (1940)
13.3/74.7	1	19 (19)	1.9E-03	Morrison and Billett (1952)
15/25	1.00E+00	2 (2)	1.2E-03	Geffcken (1904)
15/55	1	5 (5)	1.4E-03	Postigo et al. (1978)
15.6/93.3	6.9/202.7	16 (16)	2.8E-02	Gillespie and Wilson (1982)
20/30	4.8/29	40 (0)		Kritschewsky et al. (1935)
20/34	1	8 (8)	6.9E-04	Kunerth (1992)
20/35	25/76	20 (0)		Vilcu and Gainar (1967)
20/60	24/167	34 (0)		Sander (1912)
21.2/21.8	1	4 (4)	2.1E-03	Curry and Hazelton (1938)
22.8/25.5	1	6 (6)	3.9E-04	Van Slyke (1939)
25	1	1 (1)	3.8E-04	Markham and Kobe (1941b)
25	21.7/53.3	7 (7)	4.0E-02	Yang et al. (2000)
25/45	1.00E+00	4 (4)	1.0E-03	Yeh and Peterson (1964)
25/75	48	20 (20)	8.9E-03	Malinin and Savel'eva (1972)
25/150	48	10 (10)	1.5E-02	Malinin and Kurovskaya (1975)
30/80	9.3/39.3	13 (13)	8.8E-03	Matous et al. (1969)
33/213	8/5.8	7 (6)	2.0E-02	Cramer (1982)
40/120	1/92.6	39 (0)		Kiepe et al. (2002)
5.00E+01	10.6/58	7 (7)	2.2E-03	Rumpf et al. (1994)
50/80	40/141	29 (29)	1.1E-02	Bamberger et al. (2000)
50/100	25/709	29 (29)	6.6E-02	Wiebe and Gaddy (1939)
50/100	100/800	9 (0)		Shagiakhmetov and Tarzimanov (1981
50/200	1.5/54	33 (33)	9.2E-03	Zawisza and Malesinska (1981)
50/350	200/3500	108 (14)	1.4E-01	Tödheide and Franck (1963)
80/198	20.4/102	33 (33)	2.2E-02	Nighswander et al. (1989)
101/120	23.3/703	26 (26)	9.9E-02	Prutton and Savage (1945)
110/350	100/1500	121 (39)	2.2E-01	Takenouchi and Kennedy (1964)
114/348	5/162	36 (23)	6.0E-03	Ellis (1959b)
150/350	100/1400	39 (0)		Takenouchi and Kennedy (1965)
177/334	25/199	15 (6)	3.7E-02	Ellis and Golding (1963)
			$MAAD$ (m):	**3.6E-02**

The original papers of Oleinik (unknown year) and Shagiakhmetov and Tarzimanov (1981) were not found. The data were taken from Diamond and Akinfiev (2003), who also obtained these measurements quoted in references different from the original publications. Although

the measurements reported by both sources compare well with the majority of the references analyzed, the lack of the original sources led us to discard the data for parameter estimation. The same criteria is followed for the CO_2 solubilities in pure water given by Takenouchi and Kennedy (1965). They measured the solubility of CO_2 in 6 and 20 wt% NaCl solutions, and they also included in their work data for the solubility of CO_2 in pure water. Nevertheless, it is not explained where the latter data were taken from.

Some of the references rejected by Diamond and Akinfiev (2003) were used in the present work for parameter estimation, as they are believed to be accurate enough, and the agreement among those sources and the ones considered reliable is rather good.

The weight factor given by Diamond and Akinfiev (2003) to the data reported by Gillespie and Wilson (1982) is 0.33. Diamond and Akinfiev (2003) claim that those points deviate systematically from the majority of other studies, but we think the deviation is small enough to consider the source reliable. Figure 5-1 shows all the CO_2-H_2O data used in the present work at 30°C and the correlation by the extended UNIQUAC model. The agreement between the data reported by the reference mentioned above and Wiebe and Gaddy (1940), Bartholome and Friz (1956) and Matous et al. (1969) is quite good even at high pressures. The same agreement is also found at other temperatures. The latter references were all given a weight factor of one, and therefore it was decided to use the measurements reported by Gillespie and Wilson (1982) for parameter estimation.

Only one out of the seven measurements performed by Cramer (1982) was analyzed by Diamond and Akinfiev (2003) (the other six points were out of the T/P range of interest in that source). Cramer's (1982) work was discarded by Diamond and Akinfiev (2003) due to its "deviation from the assumption of $\gamma_{CO2} \rightarrow 1$ at low solubility". Figure 5-1 compares the rejected point with the measurements performed by Bartholome and Friz (1956), which was given a weight factor of unity. It is clearly observed that both sources agree very well, and therefore the tendency followed by the activity coefficient in both cases should be the same. When comparing the other six points to reliable sources, a good agreement is found in most of the cases. The highest deviation is found at 146°C. This point was therefore not used for parameter estimation.

The solubilities reported by Yang et al. (2000) agree rather well with many other sources, and therefore it was decided to use those points for parameter estimation.

The solubility values measured by Zelvenskii (1937) agree remarkably well with the majority of other studies. Diamond and Akinfiev (2003) claim that at temperatures above 50°C the CO_2 activity coefficient does not tend to zero for low concentrations. But the values reported by Zelvenskii (1937) at temperatures higher than 50°C are remarkably close to those from

Wiebe and Gaddy (1940), and Müller et al. (1988), both sources with a weight factor of unity. Therefore, if the temperature and pressure conditions coincide, and the solubility values are so close, the value of the activity coefficient should be similar. If two of the sources are considered reliable, the third one should also be given credibility.
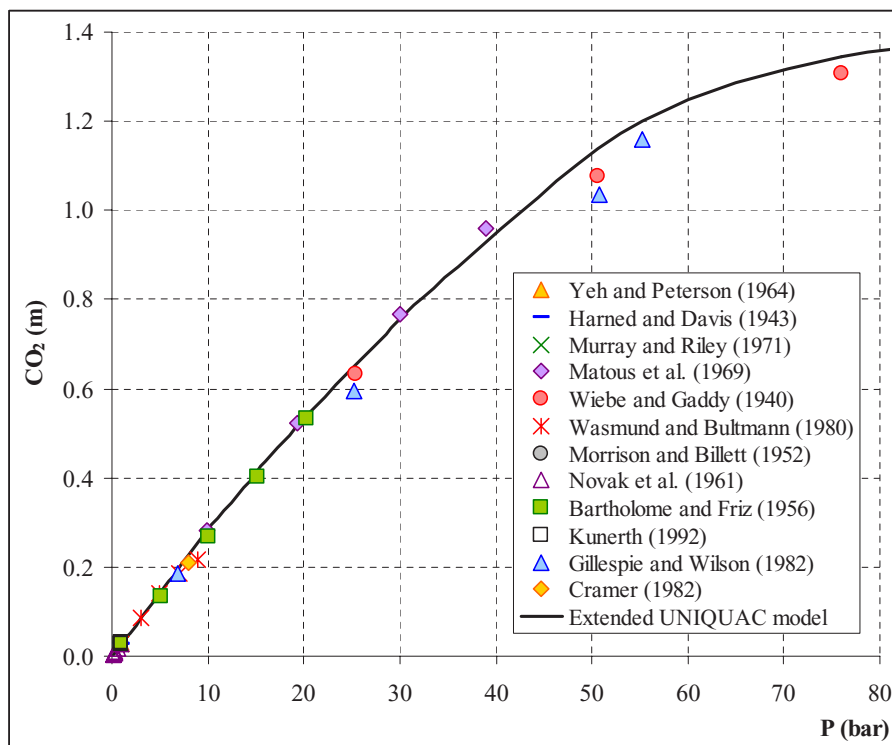
Figure 5-1. Experimental and calculated vapour-liquid phase diagram for the CO_2-H_2O system at 30°C

Finally, measurements performed by Malinin and Kurovskaya (1975) were also used for parameter estimation, as they agreed with most of the reliable sources.

Some sources report experimental data at temperatures and/or pressures out of the range of interest in the present work. That is the case of Ellis (1959b), Ellis and Golding (1963), Tödheide and Franck (1963) and Takenouchi and Kennedy (1964). The number of experiments performed by these authors under the conditions of interest in the present work is 23, 6, 14 and 39, respectively.

The other references given in table 5-3 and not analyzed by Diamond and Akinfiev (2003) were all used for parameter estimation, as they agreed very well with the trusted sources. Only the values reported by Kiepe et al. (2002) were discarded, as they deviate considerably from the main tendency, especially at pressures higher than 50 bar.

The calculated and experimental CO_2 solubility in pure water at 150°C is shown in figure 5-2, where the good agreement between the extended UNIQUAC model and the data is observed even at very large pressures. Only data up to 1000 bar were used for parameter estimation, but figure 5-2 shows that predictions performed by our model at larger pressures (up to 1500 bar) are very accurate. Carbon dioxide solubility increases considerably with pressure, changing from 0.028 m CO_2 at 7.7 bar to 2.8 m CO_2 at 1500 bar.

Figure 5-3 shows the solubility of carbon dioxide in water at a constant pressure of 100 bar. CO_2 solubility in water decreases very steeply with temperature from 25 to 100°C, while the influence of temperature becomes almost negligible in the temperature range from 100 to 200°C. For higher temperatures, the carbon dioxide solubility decreases again with increasing temperature. The shape of the experimental curve is very well represented by the extended UNIQUAC model. Table 5-3 shows the value of the mean average absolute deviation between the model calculations and the experimental data used in this work. This value, $3.6 \cdot 10^{-2}$ m CO_2, is lower than the experimental *ASD* ($4.1 \cdot 10^{-2}$ m CO_2), and therefore it can be concluded that the calculations and predictions for the CO_2-H_2O system are within experimental accuracy.
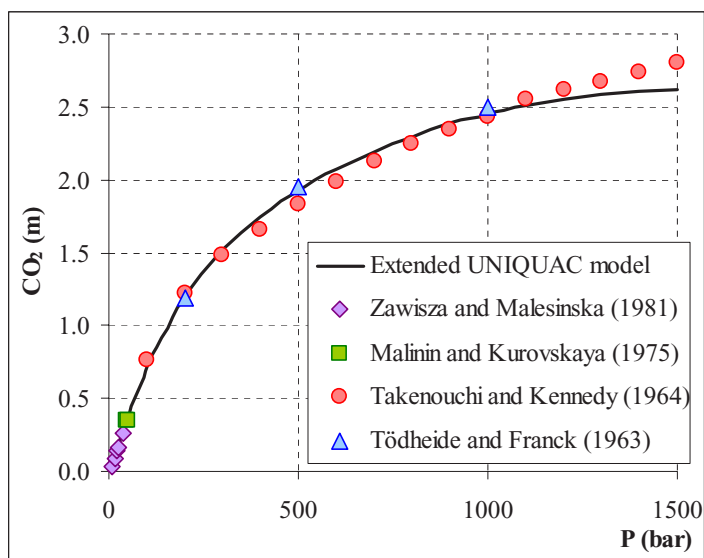
Figure 5-2. Experimental and calculated vapour-liquid phase diagram for the CO_2-H_2O system at 150°C
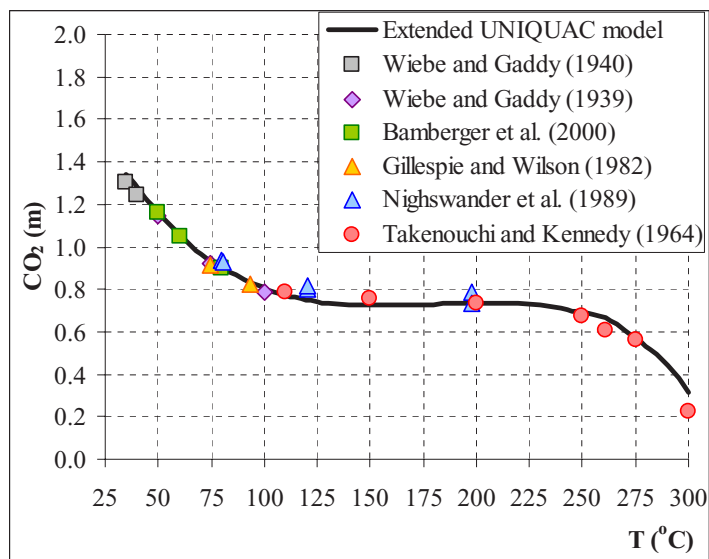
Figure 5-3. Experimental and calculated vapour-liquid phase diagram for the CO_2-H_2O system at 100 bar

5.1.2 CO_2 Solubility in Aqueous Solutions of NaCl and Na_2SO_4

In order to be able to apply our model to the calculation of vapour-liquid-solid equilibria in natural waters, the main constituents of such kind of waters have to be accounted for. For this reason, we found necessary to study and model the carbon dioxide solubility in different electrolyte solutions, such as solutions containing NaCl and Na_2SO_4. The interaction parameters between CO_2, HCO_3^-, CO_3^{2-} and Na^+, Cl^- and SO_4^{2-} have been previously determined by Thomsen and Rasmussen (1999) on the basis of VLE and SLE data. The temperature and pressure range covered by them is from 0 to 100°C and from 1 to 100 atm, respectively. Those ranges are not enough for the purposes of the present work. Extrapolation to higher temperatures and pressure did not give accurate results, and therefore parameter estimation was carried out on the basis of VLE data covering a wider range of both temperature and pressure.

The VLE behaviour in aqueous solutions may be quite different than in pure water. The thermodynamic properties of the solution can vary significantly as a consequence of the interactions between molecules and ionic species. Depending on the kind of salt, the gas solubility may be raised (salting-in effect) or decreased (salting-out effect). For carbon dioxide solubility in NaCl and Na_2SO_4 solutions, a large salting-out effect is noticed.

However, the general form and trend of the solubility curves is approximately the same as for the system CO_2-H_2O (Takenouchi and Kennedy, 1965).

5.1.2.1 CO_2 Solubility in NaCl Solutions

Table 5-4 shows the sources found in the literature reporting carbon dioxide solubility in sodium chloride solutions at different temperatures and pressures. The number of experimental determinations for each source and the number of data used in the present paper (in brackets) is also given there.

Table 5-4
Experimental CO_2-NaCl-H_2O VLE data sets used for parameter estimation.

$T(°C)$	$P(atm)$	Number of data	AAD (m)	Reference
0/50	1	90 (90)	9.7E-04	Harned and Davis (1943)
0/90	1	31 (0)		He and Morse (1993)
0.2/40	1	15 (15)	1.3E-03	Markham and Kobe (1941a)
15/35	1	27 (27)	1.3E-03	Yasunishi and Yoshida (1979)
20/35	1	16 (16)	1.7E-03	Vazquez et al. (1994)
25	1	8 (8)	1.5E-03	Onda et al. (1970)
25/150	48.9	27 (27)	2.5E-02	Malinin and Kurovskaya (1975)
25/75	48	13 (13)	4.3E-02	Malinin and Savel'eva (1972)
40/160.8	4.6/96.4	63 (63)	1.5E-02	Rumpf et al. (1994)
80/200.5	21.1/100.3	34 (0)		Nighswander et al. (1989)
172/334	25/213.6	59 (0)		Ellis and Golding (1963)
25	1	7 (7)	1.9E-03	Yasunishi et al. (1979)
250/450	100/1400	86 (30)	1.3E-01	Takenouchi and Kennedy (1965)
100/500	200/2500	178 (32)	1.2E-01	Naumov et al. (1974)
5/65	0.5/0.9	18 (0)		Zheng et al. (1997)
			$MAAD$ (m):	3.1E-02

Rumpf et al. (1994) developed a model using Pitzer's (1973) equations to predict CO_2 solubility in sodium chloride solutions based on their experimental determinations. The results obtained by them agree very well with Markham and Kobe (1941a), Malinin and Savel'eva (1972), and Yasunishi and Yoshida (1979). The average relative deviation for the total pressure between the model given by Rumpf et al. (1994) and the previous sources is 2.4%, 1.7% and 1.5%, respectively (values calculated by Rumpf et al., 1994). On the other hand, the dataset by Ellis and Golding (1963) disagrees with the model of Rumpf et al. (1994), with an average relative deviation of 5.7%. Therefore, it will not be used for parameter estimation. The data by Nighswander et al. (1989) agree only fairly with the model of Rumpf et al. (1994), and they also disagree with Takenouchi and Kennedy (1965). Both

Takenouchi and Kennedy (1965) and Nighswander et al. (1989) determined carbon dioxide solubility at 200°C and at comparable pressures, but at different NaCl concentrations of 1 and 0.17 m, respectively. Even though the salt concentrations are different, the measurements gave similar results for the CO_2 solubility, indicating that there is no salting-out effect. Thus, the data by Nighswander et al. (1989) were not used for parameter estimation.

The shape of the carbon dioxide solubility curve in NaCl solutions obtained from the data of He and Morse (1993) and Zheng et al. (1997) differs from the curves obtained by the different datasets shown in table 5-4. The decrease in carbon dioxide solubility as a consequence of increasing concentration is much flatter for the data of He and Morse (1993) and Zheng et al. (1997) than claimed by the rest of the sources employed. He and Morse (1993) compared the value for the second dissociation constant for CO_2 they obtained from their measurements to literature. A clear disagreement is found when compared to Thurmond and Millero (1982) and Patterson et al. (1982, 1984). Their pK values seem to agree with those by Harned and Bonner (1945). The data of He and Morse (1993) and Zheng et al. (1997) were therefore not used in the present work.

The effect of pressure on the carbon dioxide solubility in NaCl solutions reported by Naumov et al. (1974) does not agree with the data of Malinin and Kurovskaya's (1975). The first source reports solubility values at 100°C and 100 bar very close to the values given by Malinin and Kurovskaya (1975) at 100°C and 48 bar, covering a NaCl concentration range from 0.5 to 6 m. The latter source is in good agreement with Malinin and Savel'eva (1972), which was mentioned previously due to its agreement with many other sources in table 5-4. On the other hand, Naumov et al. (1974) agrees quite well with Takenouchi and Kennedy (1965), especially at high temperatures (250 and 300°C). At lower temperatures (150 and 200°C) the influence of NaCl concentration on CO_2 solubility reported by both sources is somehow different. The values given by Naumov et al. (1974) at 0.5 and 5 m are very close to those by Takenouchi and Kennedy (1965) at 1 and 4.3 m, respectively. After analyzing all these data sets it seems clear that a general disagreement is found among the different sources. Nevertheless, the regions of overlap of the different studies are rather narrow, and a clear conclusion about the reliability of the sources cannot be achieved. Therefore, it was decided to employ them all in the present work. Both Takenouchi and Kennedy (1965) and Naumov et al. (1974) performed measurements at higher temperatures and pressures than the range of interest in this work (56 and 146 measurements, respectively).

At 30 and 35°C and 1 atm total pressure, there is some scatter among the data reported by three sources: Harned and Davis (1943), Yasunishi and Yoshida (1979), and Vazquez et al.

(1994). Nevertheless, the differences are not so large and they can be regarded as reasonable experimental standard deviations.

The experimental and calculated phase diagram for the system CO_2-NaCl-H_2O at a constant temperature of 160°C and NaCl concentrations of 4 and 6 m is shown in figure 5-4. Carbon dioxide solubility increases with increasing pressure, while it decreases for increasing salt concentration.

Figure 5-5 shows experimental data in the pressure range from 60 to 70 bar, together with the model calculations, at both 4 and 6 m NaCl. The reason why data from a pressure range were used instead of isobaric data is the lack of isobaric data. Figure 5-5 includes calculations performed by the model at the experimental conditions (grey dots and triangles) together with the calculations at a constant pressure of 60 bar (lines). As already mentioned for figure 5-4, the salting-out effect can also be observed in figure 5-5. CO_2 solubility decreases considerably with increasing temperature, passing from 0.53 m at 40°C to 0.22 m at 160°C, for 4 m NaCl solutions.
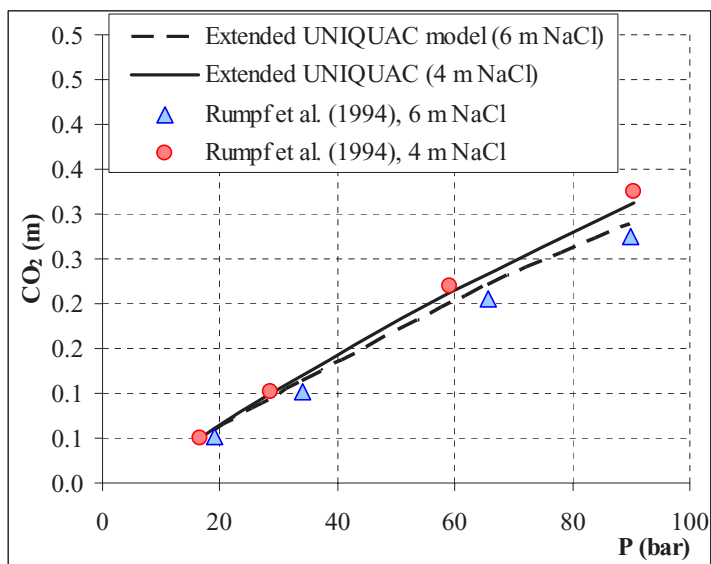
Figure 5-4. Experimental and calculated vapour-liquid phase diagram for the CO_2-NaCl-H_2O system at 160°C.

The representation by the extended UNIQUAC model of the solubility of carbon dioxide in NaCl solutions is very good, even for very concentrated solutions (close to the saturation of NaCl). The mean absolute deviation between the model calculations and the experimental points is $3.1 \cdot 10^{-2}$ m, while the average standard deviation for the experimental points is

$2.2 \cdot 10^{-2}$ m. The latter value is mainly based on data at atmospheric conditions, due to the lack of experimental measurements at the same NaCl concentration, temperature and pressure. If only data at pressures larger than 1 atm are considered in the calculation of *ASD*, the value is increased to $1.5 \cdot 10^{-1}$ m.
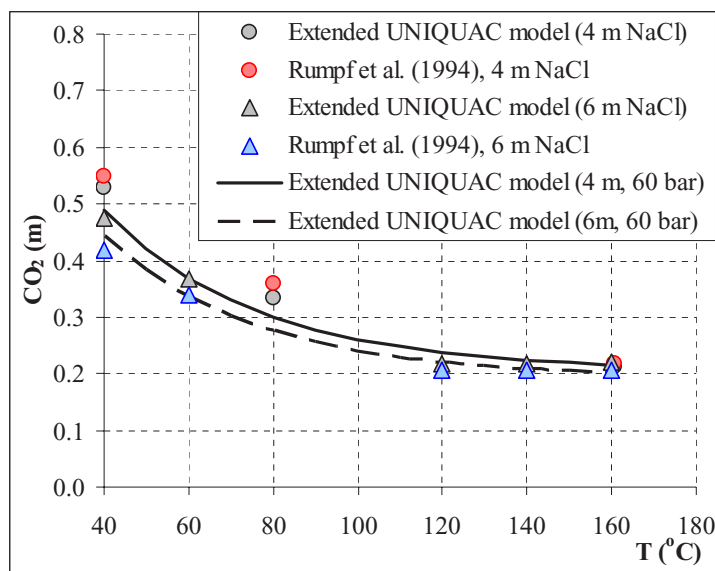
Figure 5-5. Experimental and calculated vapour-liquid phase diagram for the CO_2-NaCl-H_2O system at 60-70bar. Lines represent calculations at a constant pressure of 60 bar, while grey dots and triangles represent calculations at the experimental pressure (in the range from 60 to 70 bar), which are compared to the experimental data (red and blue dots and triangles).

Table 5-4 shows the *AAD* for each one of the CO_2-NaCl-H_2O sources employed in the present work. There, it can be seen that the value of *AAD* for all the sources at atmospheric pressure is lower than $2.2 \cdot 10^{-2}$ m. For some sources dealing with higher pressures (Malinin and Kurovskaya, 1975 and Rumpf et al., 1994) the value is lower or very close to $2.2 \cdot 10^{-2}$ m. Only for the investigations at high pressure conditions the average absolute deviation between the extended UNIQUAC calculations and the experimental data is larger than $2.2 \cdot 10^{-2}$ m (but always lower than 0.15 m). Therefore, it can be concluded that extended UNIQUAC calculations are within experimental accuracy, and the model is able to represent correctly the salting-out effect and the temperature and pressure dependence of the carbon dioxide solubility in NaCl solutions (from very dilute solutions to almost the saturation point).

5.1.2.2 CO_2 solubility in Na_2SO_4 solutions

Sodium sulphate also produces a relatively large salting-out effect for aqueous CO_2 solutions, reducing the gas solubility in the solution when compared to that in pure water.

Literature data on the solubility of carbon dioxide in aqueous solutions of sodium sulphate is scarce. Furthermore, most of the available data were measured at pressures around 1 atm and not very high temperatures. The sources found in literature reporting CO_2 solubility in Na_2SO_4 solutions are given in table 5-5. The range of temperature and pressure covered, and the number of measurements performed and used in this work (in brackets) for parameter estimation can also be found there.

Table 5-5
Experimental CO_2-Na_2SO_4-H_2O VLE data sets used for parameter estimation.

T(°C)	P(atm)	Number of data	AAD (m)	Reference
0/90	0.3/1	24 (0)		He and Morse (1993)
15/35	1	26 (26)	1.3E-03	Yasunishi and Yoshida (1979)
25	1	3 (3)	3.7E-04	Onda et al. (1970)
25	1	5 (5)	7.9E-04	Yasunishi et al. (1979)
25/40	1	8 (8)	8.8E-04	Markham and Kobe (1941a)
40/160	4.2/93.8	102 (102)	7.0E-03	Rumpf and Maurer (1993)
50/75	1/200	26 (0)		Corti et al. (1990b)
			MAAD (m):	5.3E-03

As observed for the CO_2 solubility in NaCl solutions, the shape of the carbon dioxide solubility curve in Na_2SO_4 solutions obtained from the data of He and Morse (1993) differs from the curves shown by the sources given in table 5-5. The decrease in carbon dioxide solubility as a consequence of increasing concentration is much flatter for He and Morse's (1993) data than claimed by the rest of the sources employed. Moreover, when He and Morse's (1993) data were compared to others at similar conditions, a disagreement for the former dataset was always found. Therefore, these data were not used for parameter estimation.

As done for NaCl solutions previously, Rumpf and Maurer (1993) also used Pitzer's (1973) equations to predict CO_2 solubility in sodium sulphate solutions based on their experimental determinations. The agreement between the model by Rumpf and Maurer (1993) and the datasets reported by Markham and Kobe (1941a) is very good, with an average relative deviation in the partial pressure of carbon dioxide of 2.6% (value calculated by Rumpf and Maurer, 1993). The agreement is also good when comparing to Onda et al. (1970), Yasunishi and Yoshida (1979) and Yasunishi et al. (1979). On the other hand, quite large deviations

were obtained when comparing to Corti et al. (1990b), with an average relative deviation of 14.2%, and a maximum relative deviation as large as 37%. Thus, it was decided not to use the latter source in the present work.

The experimental and calculated phase diagrams for the system CO_2-Na_2SO_4-H_2O at a constant temperature of 140°C, and at pressures in the range of 80-90 bar are shown in figure 5-6 and figure 5-7, respectively. CO_2 solubility in Na_2SO_4 solutions behaves in a very similar way as in NaCl solutions. A salting-out effect is observed in both figures. Regarding temperature, carbon dioxide solubility decreases quite fast with increasing temperature in the range 0-100°C, while the slope of the curve is much flatter for higher temperatures. The solubility of CO_2 in 1 m Na_2SO_4 solution decreases from 0.6 m at 50°C to 0.4 m at 160°C.
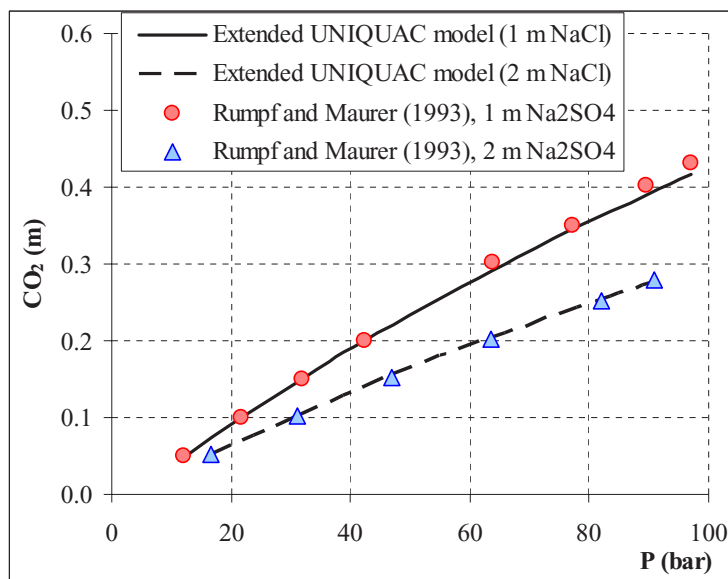
Figure 5-6. Experimental and calculated vapour-liquid phase diagram for the CO_2-Na_2SO_4-H_2O system at 140°C.

The calculated solubility compares very well with the experimental data presented in table 5-5. The value of *MAAD* ($5.3 \cdot 10^{-3}$ m) is well below the *ASD* ($2.7 \cdot 10^{-2}$ m). The latter value was calculated taking into account all the experimental points, and not only those coming from different sources, due to the lack of data at the same conditions.
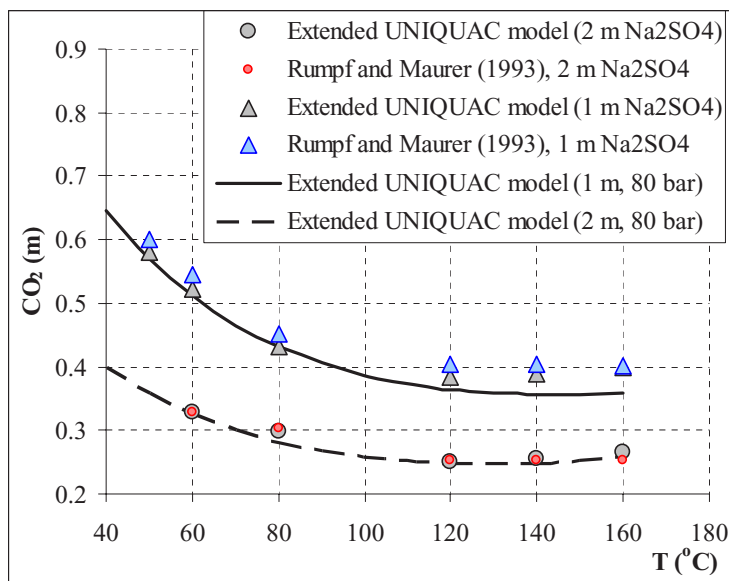
Figure 5-7. Experimental and calculated vapour-liquid phase diagram for the CO_2-Na_2SO_4-H_2O system at 80-90bar. Lines represent calculations at a constant pressure of 80 bar, grey dots and triangles represent calculations at the experimental pressure (in the range from 80 to 90 bar), which are compared to the experimental data (red and blue dots and triangles)

5.1.2.3 CO₂ Solubility in NaCl-Na₂SO₄ Solutions

Only one source (Yasunishi et al., 1979) studying the quaternary system CO_2-NaCl-Na_2SO_4-H_2O has been used for parameter estimation. Yasunishi et al. (1979) performed 15 measurements of carbon dioxide solubility in solutions of NaCl and Na_2SO_4 at 25°C and 1 atm. The results obtained for this quaternary systems are also very satisfactory, with a *MAAD* of $9.3 \cdot 10^{-4}$ m. Figure 5-8 shows experimental and calculated CO_2 solubilities in NaCl-Na_2SO_4 solutions as a function of the ionic strength of the solution, at 25°C and 1 atm.
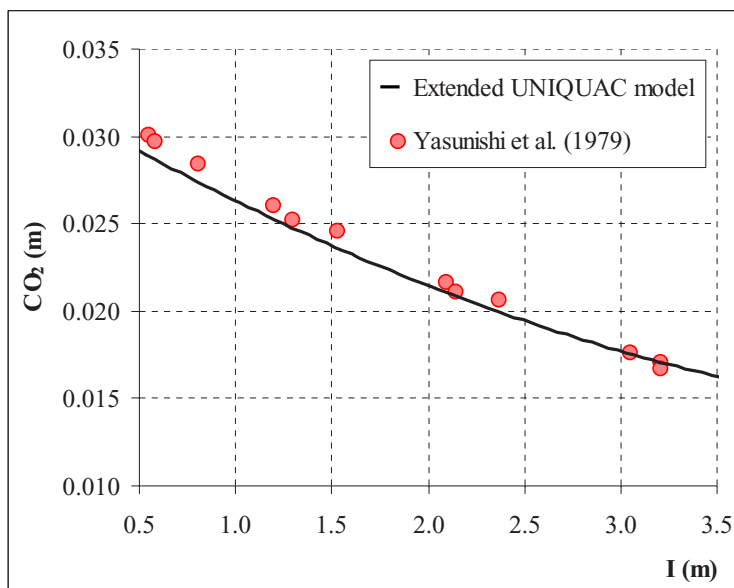
Figure 5-8. Experimental and calculated CO_2 solubility in NaCl-Na_2SO_4-H_2O solutions of ionic strength I, at 25°C and 1 bar.

5.2. CaCO$_3$-H$_2$O and CaCO$_3$-CO$_2$-H$_2$O systems

The solubility of calcite is highly influenced by the amount of carbonic acid present in the solution ($CaCO_3$ solubility increases with CO_2 concentration). In that sense, calcite solubility studies (and, in general, any carbonate mineral study) can be divided into different groups according to the amount of carbon dioxide employed. In most of the cases, pure CO_2 is bubbled into the solution, and therefore the amount of CO_2 in the liquid phase corresponds to the gas solubility in the calcite-water solution, at the experimental temperature and pressure. A second line of studies deals with calcite solubility in pure water, freed of CO_2. To achieve that purpose, all the CO_2 dissolved in the water is expelled previous to its use by vigorous boiling. Finally, some authors perform experiments adding a given amount of CO_2 which is kept constant, while the temperature and/or pressure are changed.

Table 5-6 shows the sources reporting calcite solubility in pure water, and in CO_2-H_2O solutions, together with the range of temperatures and pressures investigated, and the number of experimental points.

Kendall (1912), Kindyakov et al. (1958), Morey (1962), MacDonald and North (1974) and Lyashchenko and Churagulov (1981) used water freed of carbon dioxide in their experiments. Kendall (1912) performed several experiments under atmospheric conditions. In three of his measurements, the CO_2 was removed from the air by passing it through a column and

washing the air. None of these sources was used for parameter estimation, as very large discrepancies are found among the different investigators, and the tendency followed for increasing temperatures varies from one source to another. According to the data reported by Kendall (1912), calcite solubility increases with temperature from 25 to 100°C. MacDonald and North (1974) reported data from 1 to 25°C where the temperature influence on the solubility is practically negligible, and in most of the cases the lowest value is obtained for the lowest temperature used. For Morey's (1962) data, the temperature influence on the solubility of calcite is negligible from 25 to 165°C, while decreasing solubilities were obtained for temperatures increasing from 165 to 350°C.

Table 5-6
Experimental $CaCO_3$-H_2O SLE and $CaCO_3$-CO_2-H_2O SLVE data sets used for parameter estimation.

T (°C)	P (bar)	Number of data	AAD (m)	Reference
0/55	1	2 (2)	8.4E-04	Yanat'eva (1955a)
0/102	1/101	98 (98)	1.6E-03	Miller (1952)
0.1/89.7	1	141 (133)	3.8E-04	Plummer and Busenberg (1982)
1/23	1	5 (0)		Wells (unknown year)
1/25	25.3/962.6	32 (0)		MacDonald and North (1974)
10/60	1	8 (4)	8.3E-05	Wolf et al. (1989)
10/70	1	30 (30)	1.1E-04	Weyl (1959)
11/14	1	10 (0)		Treadwell and Reuter (1898)
15/40	1	49 (49)	4.9E-04	Leather and Sen (1909)
16	1	7 (7)	5.3E-04	Johnston (1915)
16	1	12 (12)	4.4E-11	Schloesing (1872)
16	1/6	4 (4)	2.2E-04	Engel (1889)
25	1/24	13 (0)		Mitchell (1923)
25	1	9 (9)	9.3E-04	Frear and Johnston (1929)
25	1/1000	3 (0)		Lyashchenko and Churagulov (1981)
25/75	1	2 (0)		Kindyakov et al. (1958)
25/100	1	6 (2)	3.7E-03	Kendall (1912)
25/350	200	10 (0)		Morey (1962)
30/80	3.4/179	51 (51)	1.6E-03	Sippel and Glover (1964)
70	1	1 (1)	4.0E-04	Yanat'eva (1960)
75/200	5.5/68.2	260 (254)	4.9E-04	Segnit et al. (1962)
98/302	1.9/142.3	59 (59)	6.1E-04	Ellis (1959a)
100/300	2/150	34 (34)	4.9E-04	Ellis (1963)
150/225	10.9/402	18 (18)	3.3E-04	Malinin (1963)
197/300	20/1000	48 (0)		Sharp and Kennedy (1965)
		MAAD (m):		**7.4E-04**

The solubility value reported by Kindyakov et al. (1958) at 25°C is around five times larger than the average measurement given by the other sources at the same conditions. The

disagreement could be due to the presence of a gas phase containing carbon dioxide, in equilibrium with the solution, and enhancing calcite solubility. Nevertheless, the amount of CO_2 employed in the measurements (if any) is not mentioned, and thus this source was not used for parameter estimation.

Engel (1889), Treadwell and Reuter (1898), Mitchell (1923), Miller (1952), Yanat'eva (1955a), Ellis (1959a), Yanat'eva (1960), Segnit et al. (1962), Ellis (1963) and Malinin (1963) used a gas phase over the solution formed by pure carbon dioxide (plus the water vapour corresponding to the experimental conditions).

Schloesing (1872), Leather and Sen (1910), Kendall (1912), Johnston (1915), Wells (1915a), Frear and Johnston (1929), Weyl (1959), Sippel and Glover (1964), Sharp and Kennedy (1965), Plummer and Busenberg (1982) and Wolf et al. (1989) measured calcite solubility in CO_2-H_2O solutions, where the amount of CO_2 was smaller than the one corresponding to the saturation value. Most of these studies used a gas phase over the solution formed by air, or mixtures of carbon dioxide and N_2 or air in different proportions.

At 25°C, the solubility values reported by Wolf et al. (1989) are considerably lower than the average value given by many other sources at the same conditions, and therefore these points are not included in the parameter estimation. Also, low solubility values for calcite are reported by Plummer and Busenberg (1982) at 10°C, when compared to the data by Schloesing (1872) at 16°C or the data by Frear and Johnston (1929) at 25°C, all of them using very similar CO_2 amounts in the liquid phase.

None of the measurements performed by Sharp and Kennedy (1965) has been used in the present study, because their scatter is extremely large. At 200°C and a free CO_2 content of 0.73 m, calcite solubility varies from $2.6 \cdot 10^{-3}$ to $6.7 \cdot 10^{-3}$ m. Moreover, many points also show a wrong solubility tendency with temperature.

The datasets by Treadwell and Reuter (1898) and Mitchell (1923) were not used for parameter estimation. The latter source does not show any influence of pressure on the solubility for pressures higher than 15 bar (and up to 25 bar). Treadwell and Reuter (1898) disagree considerably when compared to other sources at similar conditions. According to Leather and Sen (1910) and Johnston (1915), Treadwell and Reuter (1898) did not attain equilibrium, a fact resulting in a lack of constancy of the calculated solubility product.

Segnit et al. (1962) measurements show a very large scatter, especially at 100°C, where $CaCO_3$ solubility varies from $8.5 \cdot 10^{-3}$ to $11.2 \cdot 10^{-3}$ m. They state their results agree satisfactorily with Ellis (1959a), but disagree somewhat with those obtained by Miller (1952) at 75 and 100°C at pressures above 10 atm. Nevertheless, the disagreement among all these sources was not extreme and all of them were used to estimate the required parameters (with

the exception of 4 points given by Segnit et al. (1962) showing the largest disagreement with the main tendency).

The experimental and calculated phase diagrams for the $CaCO_3$-CO_2-H_2O system at a constant temperature of 100°C and at a constant pressure of 40 bar are shown in figure 5-9 and figure 5-10, respectively. The gas phase over the solution employed for all the measurements reported in figures 5-9 and 5-10 was pure carbon dioxide saturated with water vapour. Therefore, the increase of calcite solubility with increasing pressure also manifests the higher solubility of that mineral for higher CO_2 concentrations. Regarding temperature, a very sharp decrease of calcite solubility is observed for increasing temperature.

The large scatter in the experimental data can be observed in figure 5-9. The experimental standard deviation was calculated from data coming from different sources. When more than one point is given by the same author at the same conditions, the average of the values reported is calculated and compared to the rest of the sources reporting data at the same temperature and pressure. Therefore, the scatter shown in figure 5-9 for the measurements of Segnit et al. (1962) is not included in the calculation of the standard deviation.

Even though in most of the cases the CO_2 content in the system was calculated instead of being experimental, the results obtained for the calcite solubility are very close to the experimental data. The mean absolute deviation between the calculations using extended UNIQUAC and the experimental measurements ($7.4 \cdot 10^{-4}$ m) is lower than the experimental standard deviation, which was calculated to be $1.3 \cdot 10^{-3}$ m. It is confirmed, therefore, that the model is also applicable to the system $CaCO_3$-CO_2-H_2O.

Some authors reported the CO_2 concentration in the liquid phase, as well as the calcite solubility: Ellis (1959a) and Malinin (1963). In both cases, the experimental values were used instead of our calculations (and in both cases the difference between the reported values and the ones calculated by our program was very small).

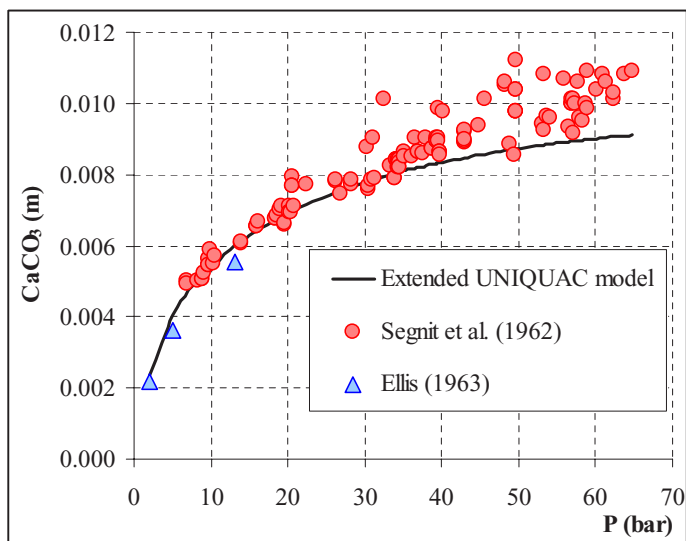**Figure 5-9**. Experimental and calculated solid-liquid phase diagram for the $CaCO_3$-CO_2-H_2O system at 100°C. Gas phase formed by CO_2 (g) and H_2O (g).
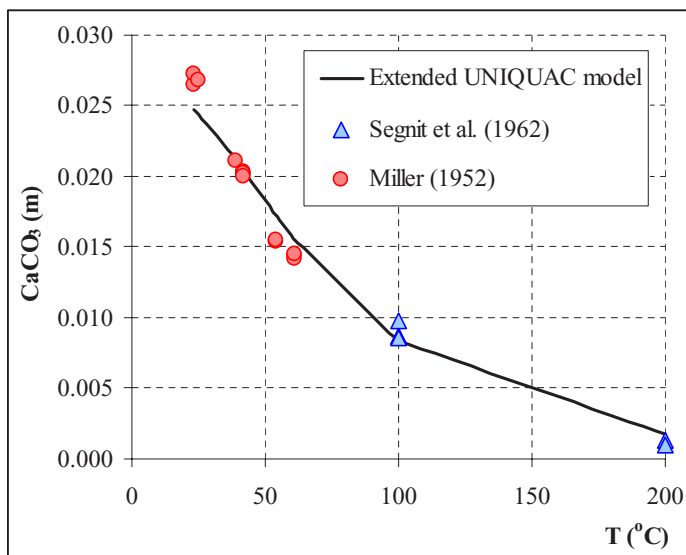

Figure 5-10. Experimental and calculated solid-liquid phase diagram for the $CaCO_3$-CO_2-H_2O system at 40 bar. Gas phase formed by CO_2 (g) and H_2O (g).

5.3 BaCO₃-H₂O and BaCO₃-CO₂-H₂O systems

Very few studies on the solubility of witherite ($BaCO_3$) in pure water and in pure water under various CO_2 partial pressures have been found in literature. Among them, only a couple report solubility values at temperatures higher than 25°C or pressures larger than atmospheric. The list of experimental data used for parameter estimation is presented in table 5-7. The total number of data found in each source is given, together with the number of data chosen for parameter estimation in this work (in brackets). Information about the ranges of temperature and pressure covered is also included.

The experiments performed by Kohlrausch and Rose (1893), McCoy and Smith (1911), Townley et al. (1937), and Trendafelov et al. (1994) used water freed of CO_2. The rest of the experimental data were determined under different CO_2 partial pressures. Malinin (1963) and Busenberg and Plummer (1986) used pure CO_2 saturated with water vapour as the gas phase. The latter authors also reported five experimental points where mixtures of N_2 and CO_2 in different proportions replaced the pure CO_2 in the gas phase. Schloesing (1872) used mixtures of air and CO_2 as the gas phase, with CO_2 partial pressures ranging from 0.0005 to 0.98 atm. From the latter references, only Malinin (1963) reported the amount of CO_2 contained in the liquid phase, while the rest of the sources only measured the partial pressure of CO_2. For such cases, we made similar assumptions to calculate the free carbon dioxide content in the solution as done previously for calcite: The CO_2 amount was calculated from the parameters estimated for the CO_2-H_2O system in the present work. In this case we assumed CO_2 solubility in witherite solutions is approximately equal to that in pure water. $BaCO_3$ is a sparingly soluble salt in water, and it is reasonable to believe it will not influence carbon dioxide solubility to a large extent. When comparing our calculations with the CO_2 contents reported by Malinin (1963) in $BaCO_3$-H_2O solutions (see table 5-8), the assumption made seems to be accurate.

Table 5-7
Experimental BaCO₃-H₂O and BaCO₃-CO₂-H₂O SLVE experimental data sets used for parameter estimation.

T(°C)	P(atm)	Number of data	AAD (m)	Reference
-2/90	1	150 (150)	9.5E-05	Busenberg and Plummer (1986)
16	1	12 (12)	7.5E-04	Schloesing (1872)
18	1	1 (1)	9.7E-06	Kohlrausch and Rose (1893)
25	1	1 (1)	4.7E-05	McCoy and Smith (1911)
25	1	2 (2)	4.2E-05	Trendafelov et al.(1994)
25/40	1	2 (0)		Townley et al. (1937)
100/225	17/107	15 (0)		Malinin (1963)
		MAAD (m):	1.4E-04	

A significant disagreement is observed among some of the data sources listed in table 5-7. The recalculated values for the equilibrium constant for different sources in table 5-7 vary over three orders of magnitude, and the temperature dependence of the equilibrium constant cannot be determined from these data (Busenberg and Plummer, 1986). For example, the value of -8.8 given by Townley et al. (1937) for $\log K_{BaCO_3}$ is too low when compared to many other sources dealing with the same system. On the other hand, the value of -5.5 reported by Benes and Selecká (1973) for $\log K_{BaCO_3}$ is too large compared to data from the sources shown in table 5-7.

Table 5-8
Calculated versus experimental CO_2 solubility in $BaCO_3$-H_2O solutions.

T (°C)	P (bar)	CO_2 solubility in pure water (m)		RD (%)
		Malinin (1963)	**Our model**	
100	16.7	0.161	0.163	1.24
100	32.4	0.308	0.313	1.62
100	52.0	0.482	0.480	-0.41
150	14.8	0.087	0.091	4.60
150	19.5	0.127	0.132	3.94
150	27.2	0.193	0.198	2.59
150	35.5	0.264	0.266	0.76
150	53.3	0.405	0.406	0.25
150	55.4	0.421	0.422	0.24
150	83.7	0.625	0.621	-0.64
150	107.1	0.750	0.767	2.27
225	27.2	0.025	0.028	12.00
225	42.8	0.173	0.187	8.09
225	79.4	0.519	0.544	4.82
225	98.8	0.693	0.720	3.90

Most of Malinin's (1963) solubility data cannot be compared to other sources given in table 5-7, as he is the only author who used temperatures above 100°C. The value of the equilibrium constant for $BaCO_3$ calculated from Malinin's (1963) data at 100°C and various CO_2 pressures is about 0.5 log units smaller than the value calculated by Busenberg and Plummer (1986) (Busenberg and Plummer, 1986).

The equation reported by Busenberg and Plummer (1986) for the equilibrium constant of $BaCO_3$ agrees with many other sources (Schloesing, 1872, Holleman, 1893, McCoy and Smith, 1911, Millero et al., 1984). Their value at 25°C ($\log K_{BaCO_3} = -8.562$) is also very similar to the one reported by the NIST Chemical Thermodynamics Database (1990). This agreement, and the fact that Busenberg and Plummer (1986) report the most detailed study on

witherite solubility, covering a wide range of temperatures, makes us take their work as the reference for the modelling of the system $BaCO_3$-CO_2-H_2O.

The heat capacity of witherite as a function of temperature was experimentally studied by Gurevich et al. (1999) at very low temperatures, -253.12 – 65.66°C. Busenberg and Plummer (1986) derived a relation to calculate the equilibrium constant as a function of temperature, in the temperature range -2 to 90°C. From this relation, a temperature dependent C_p value can be derived. There is, however, a change in the sign of C_p for temperatures larger than 100°C (which is above the temperature range analyzed by them). Extrapolation of that relation to temperatures above the interval studied (-2 to 90°C) is therefore not possible. For this reason, we chose to use the value reported by the NIST Chemical Thermodynamics Database (1990). As the temperature range covered is small enough, the heat capacity may be considered constant with temperature.

Table 5-7 shows the agreement between the experimental data and the extended UNIQUAC model calculation is excellent. The *MAAD* ($1.4 \cdot 10^{-4}$ m) is well below the *ASD* ($2.3 \cdot 10^{-4}$ m). Due to the lack of measurements performed at the same temperature, pressure and CO_2 partial pressure, the *ASD* was mainly calculated from the standard deviation found in the data by Busenberg and Plummer (1986).
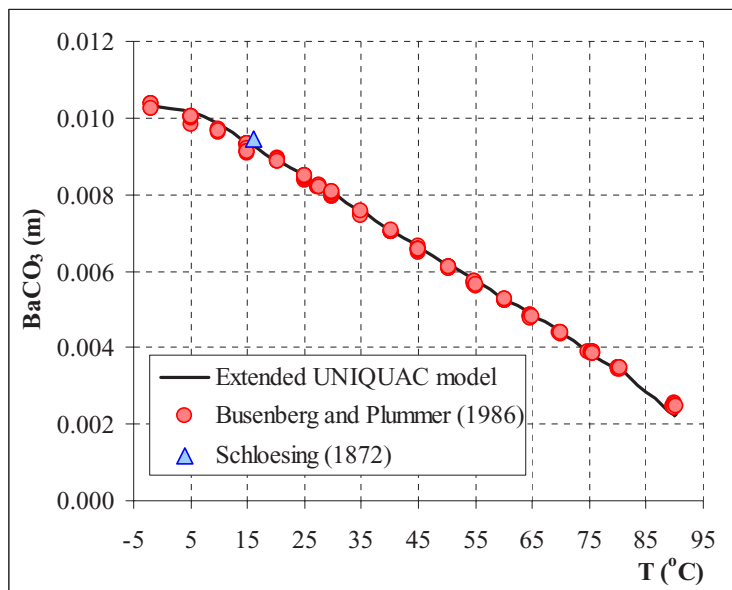

Figure 5-11. Experimental and calculated solid-liquid phase diagram for the $BaCO_3$-CO_2-H_2O system at atmospheric pressure. Gas phase formed by CO_2 (g) and H_2O (g).

The experimental and calculated SLE phase diagram for the system $BaCO_3$-CO_2-H_2O at constant atmospheric pressure is shown in figure 5-11. The gas phase is formed by CO_2 (g) and H_2O (g) (in amounts corresponding to the saturation pressure of the solution at the given temperature). As it can be observed from figure 5-11, witherite solubility decreases with increasing temperature in the range -2 to 90°C.

5.4 $SrCO_3$-H_2O and $SrCO_3$-CO_2-H_2O systems

According to Kapustinsky and Dezideryeva (1946), the research on the thermodynamics of strontium and its compounds is far from exhaustive. This lack of research is even more noticeable for the case of strontianite ($SrCO_3$). Large disagreements are found when comparing calorimetric data and calculations from the equilibrium constants, and the heat of reaction is calculated in most of the cases from quite old determinations. This problem is manifested in the heat of formation of strontianite from the elements given by two different studies carried out at practically the same time: Kelley and Anderson (1935) and Rossini and Bichowsky (1936). The values reported are -1168.2 and -1215 kJ/mol, respectively.

Table 5-9
Experimental $SrCO_3$-H_2O and $SrCO_3$-CO_2-H_2O SLVE experimental data sets used for parameter estimation.

T (°C)	P (atm)	Number of data	AAD (m)	Reference
2/91.2	1	60 (60)	5.7E-05	Busenberg et al. (1984)
5/25	1	4 (0)		Miles and Burton (1972)
18	1	1 (0)		Kohlrausch and Rose (1893)
18	1	1 (0)		Haehnel (1924)
25	1	1 (1)	9.9E-06	Kapustinsky and Dezideryeva (1946)
25	1	7 (0)		Wattenberg and Timmermann (1937)
25	1	1 (0)		McCoy and Smith (1911)
25/40	1	2 (2)	5.8E-06	Townley et al. (1937)
50/200	1/50	66 (0)		Helz and Holland (1965)
			MAAD (m):	5.5E-05

The few sources studying strontianite solubility in pure water and in CO_2-H_2O solutions are shown in table 5-9, together with the number of experimental data reported and the range of temperature and pressure covered. Kohlrausch and Rose (1893), McCoy and Smith (1911), Townley et al. (1937), and Kapustinsky and Dezideryeva (1946) performed experiments in CO_2-free water. Miles and Burton (1972) reported three solubility points in water previously freed of CO_2, and one value using a solution in equilibrium with air. Haehnel (1924), Helz and Holland (1965), and Busenberg et al. (1984) used pure CO_2 saturated with water vapour

as the gas phase, while Wattenberg and Timmermann (1937) used CO_2-H_2O solutions with different carbon dioxide amounts.

None of the sources using CO_2-H_2O solutions measured the carbon dioxide concentration in the liquid phase. Therefore, it was calculated from our CO_2 parameters as explained previously for the case of calcite.

Wattenberg and Timmermann (1937) did not report the partial pressure for carbon dioxide, but instead they gave the solution pH, the concentration of carbonate ions and the value of the second dissociation constant for CO_2. From those values and the first dissociation constant it was possible to calculate the free CO_2 in the solution.

Some of the studies given in table 5-9 show discrepant results. McCoy and Smith (1911) performed nine measurements of strontianite solubility at 25°C and CO_2 partial pressures ranging from 0.05 to 1.1 atm. They did not report those data, but only the average solubility product (defined as the product of the concentrations of Ba^{2+} and CO_3^{2-} ions). The solubility value calculated from it differs considerably from the rest of the sources in table 5-9. Other sources that were not used for parameter estimation due to their disagreement when compared to other experiments at the same conditions are Kohlrausch and Rose (1893) and Haehnel(1924).

Helz and Holland (1965) used natural strontianite in their experiments containing as much as 5 mole percent $CaCO_3$. This impurity of the original solid phase may lead to erroneous solubility values. Their data show a high scatter and a poor reproducibility at the higher pressures, which probably results from experimental difficulties in the hydrothermal bomb method (Busenberg et al. 1984).

According to Busenberg et al. (1984), the experimental data by Miles and Burton (1972) in CO_2-free water show a much larger temperature dependency between 5 and 25°C than observed by them. That could indicate failure to achieve equilibrium at lower temperatures. This may be perfectly the case as the authors only ran the experiments for 6 hours. They used both radiometric and flame emission spectrophotometric methods to determine strontianite solubility. The results obtained from both methods agree very well. Nevertheless, their results in every case disagree with other sources and were not used for parameter estimation in the present work.

The data reported by Wattenberg and Timmermann (1937) could only be compared to those by Busenberg et al. (1984). A very large disagreement is observed, but the lack of additional data makes it difficult to determine the most reliable source. We chose to use Busenberg et al. (1984) because they report 60 solubility measurements covering a wide range of temperature

(from 2 to 91.2°C), while Wattenberg and Timmermann (1937) only reported 7 experimental data at a constant temperature of 25°C. Apart from the wider temperature range of the solubility study performed by Busenberg et al. (1984), their results are also supported by the close agreement[1] with the calculations of Garrels et al. (1960) at 25°C in CO_2 saturated water, Townley et al. (1937) at 25 and 40°C, and Sonderegger et al. (1976) at 30, 40 and 50°C in CO_2 saturated water, although in the latter case, insufficient data were available to correct the equilibrium constants to Busenberg et al. (1984) aqueous model (Busenberg et al. 1984).

The values found in the NIST Chemical Thermodynamics Database (1990) for the standard state enthalpy and Gibbs free energy of $SrCO_3$ are very similar to the ones reported by Busenberg et al. (1984), and are the ones used in the present work. The value of the standard state heat capacity as a function of temperature was taken from Busenberg et al. (1984). Due to the relatively low number of experimental data (63) only the binary interaction parameter between Sr^{2+} and CO_2 was estimated, while the parameters Sr^{2+}-HCO_3^- and Sr^{2+}-CO_3^{2-} were fixed.

The experimental and calculated strontianite solubility in water saturated with CO_2 at different temperatures and 1 atm total pressure is shown in figure 5-12. It can be observed that our results agree exceptionally well with the experimental data. Values for the mean average absolute deviation between our calculations and the experimental data are shown in table 5-9. The *MAAD* for all the data used is as low as $5.5 \cdot 10^{-5}$ m $SrCO_3$. Such value cannot be compared to the *ASD* as the lack of experimental data at similar conditions makes it impossible to determine a reliable average experimental standard deviation. Nevertheless, the value of *MAAD* is very low, especially taking into account the solubility reported by Busenberg et al. (1984) is of the order of 10^{-3} m $SrCO_3$.

---

[1] The comparison is performed by Busenberg et al. (1984). They recalculate the equilibrium constants reported in different sources according to the model employed by them.
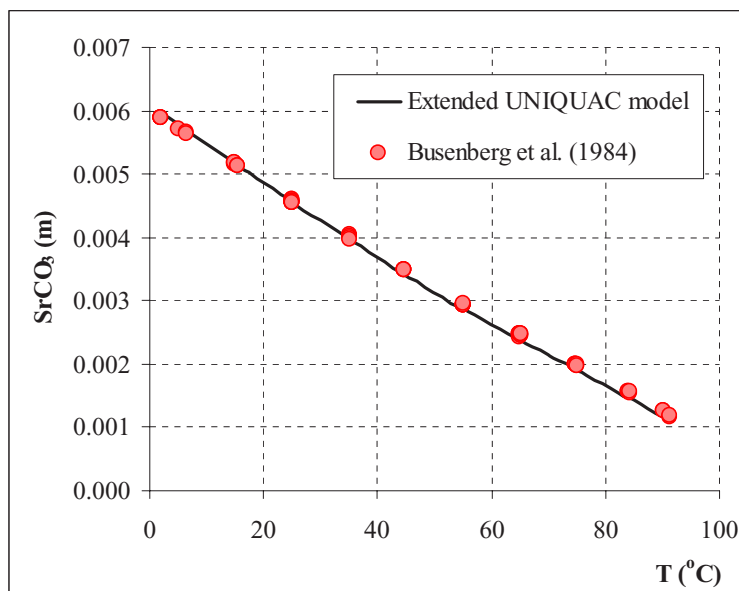
Figure 5-12. Experimental and calculated solid-liquid phase diagram for the $SrCO_3$-CO_2-H_2O system at atmospheric pressure. Gas phase formed by CO_2 (g) and H_2O (g).

5.5 MgCO$_3$-H$_2$O and MgCO$_3$-CO$_2$-H$_2$O

Magnesium is one of the common species found in natural waters. Therefore, the study of magnesium carbonate solubility in pure water and in CO_2-H_2O solutions is of great importance in the present work. Unfortunately, the system $MgCO_3$-CO_2-H_2O is characterized by tremendous experimental chaos. Dismaying discrepancies are found regarding solubility values, stable solid phases at given temperature and pressure conditions, chemical formulae for the different solids, values for the standard state Gibbs free energy, enthalpy and heat capacity, etc. Moreover, most of the data are very old, and recent studies on this system are very scarce. Cameron and Briggs (1901) assured "every investigator who has attempted to study magnesium carbonate in solution has experienced very great experimental difficulties". According to Christ and Hostetler (1970) "no carbonate mineral has proven more difficult to investigate experimentally than magnesite." Königsberger et al. (1999) assure the situation did not improve in the 30 years period which separates their work from Christ and Hostetler's (1970). More reliable experimental data on the $MgCO_3$-CO_2-H_2O system are obviously needed.

Before showing some of the results obtained by the extended UNIQUAC model for this system, a more detailed explanation about the different problems encountered when trying to model it will be addressed.

5.5.1 Chemical Formula for Hydromagnesite

The chemical formula for hydromagnesite is a source of disagreement among different investigators. In general, most of the published formulae for this mineral can be divided into two groups, although additional suggestions in disagreement with both of the main two tendencies are also available in the literature.

Baron and Favre (1958), Kazakov et al. (1959), Yanat'eva and Rassonskaya (1961), Morandi (1969), Riesen (1969), Raade (1970), Robie and Hemingway (1972, 1973), Sayles and Fyfe (1973), Dandurand and Schott (1977) and Königsberger et al. (1999) agree on the chemical formula $5MgO \cdot 4CO_2 \cdot 5H_2O$. On the other hand, Moressée and Cesaro (1910), Palache et al. (1951), Carpenter (1963), Hostetler (1964) and Langmuir (1965a) support the formula $4MgO \cdot 3CO_2 \cdot 4H_2O$.

Leitmeier (1915) studied the composition of the basic magnesium carbonate which forms in CO_2-saturated solutions at temperatures between 60 and 100°C. His 37 analyses correspond to the formula $4MgO \cdot 3CO_2 \cdot XH_2O$, where X is between 4 and 6. Therefore, his study was closer to the second group.

Takahashi (1927) used in his study the chemical formula $5MgO \cdot 4CO_2 \cdot 7H_2O$ for hydromagnesite, very close to the first group, but with additional water molecules.

The disagreement on the hydromagnesite chemical formula may be due to the relative similarity in the mole proportions for the different alternatives, which makes it difficult to use chemical analysis alone to differentiate them (Davies and Bubela, 1973).

The consequence of the use of different hydromagnesite type phases of varying composition is a great variety of contradicting solubility data. The solubility behaviour of the different phases may be rather different. Königsberger et al. (1999) assure that the formula $5MgO \cdot 4CO_2 \cdot 7H_2O$ has a relatively larger solubility than $4MgO \cdot 3CO_2 \cdot 4H_2O$.

Hydromagnesite is the most problematic mineral in the $MgCO_3$-CO_2-H_2O system regarding its chemical formula, but some discrepancies are also found for other minerals. The accepted formula for lansfordite by the majority of the investigators is $MgCO_3 \cdot 5H_2O$. Nevertheless, completely different expressions, such as $4MgO \cdot 3CO_2 \cdot 22H_2O$ (Moressée and Cesaro, 1910) can be found in the literature.

5.5.2 Stability

The solubility product for magnesite at 25°C varies according to the publication from $10^{-5.10}$ to $10^{-10.3}$ (Christ and Hostetler, 1970). These values correspond to a free energy of formation of magnesite, at 25°C, ranging from -1012.5 to -1042.2 kJ/mol. The consequence of such a large variation is completely different relative stabilities for the various minerals in the system $MgCO_3$-CO_2-H_2O. For example, if we accept as true the activity product of $10^{-5.1}$ given by Langmuir (1965a), the solid phases periclase (MgO), brucite ($Mg(OH)_2$), magnesite ($MgCO_3$), hydromagnesite, nesquehonite ($MgCO_3 \cdot 3H_2O$), and lansfordite ($MgCO_3 \cdot 5H_2O$) will all have stability fields at different values of temperature, carbon dioxide partial pressure and activity of water. On the other hand, if we consider as true the activity product of $10^{-8.1}$ reported by Rossini et al. (1961) and Robie and Waldbaum (1965), only magnesite and brucite will be stable phases at surface and near-surface conditions, while hydromagnesite, nesquehonite and lansfordite will be highly metastable.

Even though many different solubility diagrams for the system $MgCO_3$-CO_2-H_2O may be found in the literature, most of the investigations follow either Langmuir's (1965a) or Rossini's et al. (1961) approaches, whose stability relations as function of temperature and CO_2 pressure are given in figures 5-13 and 5-14, respectively. In the following section, we will try to compile the available information regarding both approaches, and the arguments given by the investigators in order to support their chosen stability diagrams.
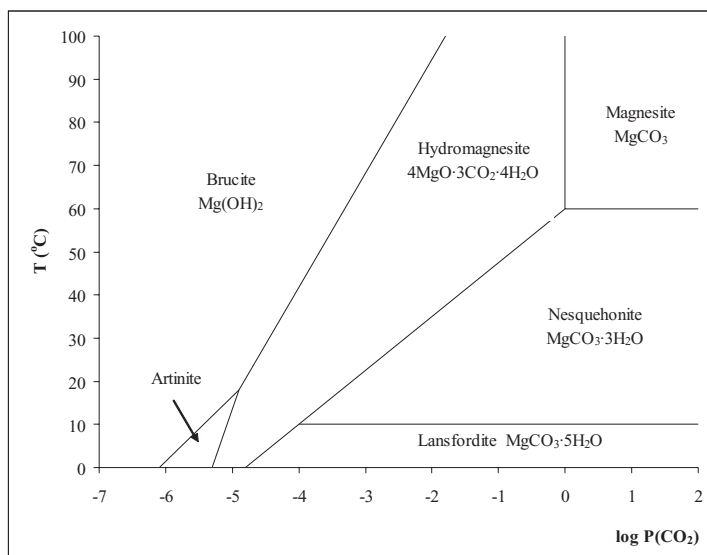
Figure 5-13. Solid-liquid phase diagram for the $MgCO_3$-CO_2-H_2O system according to Langmuir (1965a).
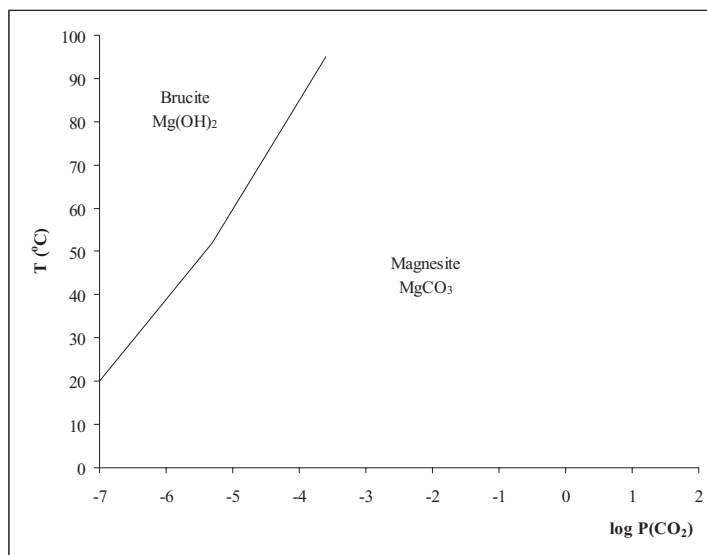
Figure 5-14. Solid-liquid phase diagram for the $MgCO_3$-CO_2-H_2O system according to Rossini et al. (1961).

5.5.2.1 Langmuir's (1965a) Approach

Langmuir (1965a) determined phase relationships based upon free energies of formation estimated from entropy. His first argument to support his study is the agreement with geological evidences. He assures the scarcity of magnesium carbonates under surface conditions may be well explained due to their great solubility (at 25°C and 1 atm, nesquehonite solubility is 24 times larger than calcite solubility). Solid phases that are considered metastable by Rossini's et al. (1961) approach are present in several locations. Both lansfordite and nesquehonite are found in caves and coal mines where temperatures are low and CO_2 pressures ten or more times greater than atmospheric. Nesquehonite has been found in Sounion, in the Lavrion mining district in Greece (Giester et al. 2000). Lansfordite appears in the hydromagnesite deposits of British Columbia (Langmuir, 1965a). Both nesquehonite and lansfordite are present in stalactites from an anthracite mine at Nesquehoning, USA (Genth, 1888, Genth and Penfield, 1890). The natural occurrences of these minerals have also been reported by Cesaro (1910), Poitevin (1924) and Fenoglio (1930, 1933, 1935, 1936). On the other hand, hydromagnesite occurrences have been listed by Palache et al. (1951) and by Alderman and Von der Borch (1961). The formation of magnesite is favoured at high ionic strength, high CO_2 pressure and high temperature (larger than 60°C). These conditions are easier to achieve in evaporate deposits, where magnesite is

reported (Schaller and Henderson, 1932, Stewart, 1949). Also, this mineral is formed through the desiccation of hydromagnesite in warm or dry climates (Alderman and Von der Borch, 1961, Graf et al., 1961, Kinsman, 1964).

According to Langmuir (1965a), the synthesis of magnesite in aqueous solutions has only been achieved at temperatures above 50°C (Pfaff, 1894, D'Ans and Gloss, 1938, Schloemer, 1952, Baron and Favre, 1958, Kazakov et al., 1959). Many times, as in the case of Pfaff (1894), such synthesis is carried out in high ionic strength solutions to favour it. Christ and Hostetler (1970) suggested that the ion Mg^{2+} has a highly hydrated nature, and hence it is relatively unreactive. Therefore, saline conditions (for which the activity of water will be lowered) should favour magnesite crystallization. However, in natural environments at surface temperatures, both nesquehonite and hydromagnesite will precipitate directly from solution, whereas it has not yet been definitively established that magnesite can form in this way (Hostetler, 1964). Even some investigators rejecting Langmuir's (1965a) solubility diagram assure that magnesite is found generally associated with hyper saline environments (Sayles and Fyfe, 1973).

In his paper, Langmuir (1965a) also lists the reasons why he thinks the stability relations given by Rossini et al. (1961) are inaccurate. The Gibbs free energy value reported by Rossini et al. (1961) was largely based on a thermal decomposition study by Marc and Simek (1913). The latter authors based their calculations on a reaction which was not determined reversibly. The same technique was also used by other authors but the agreement among them is not good, and there is no agreement either when comparing the results to other different methods.

The value reported by Rossini et al. (1961) is also supported by Harker and Tuttle (1955) and Stout and Robie (1963), but Langmuir (1965a) assures the experimental evidence is suspect in both studies because the possibility of complexing between magnesium ion and carbonate and bicarbonate has not been taken into account.

Christ and Hostetler (1970) also rejected Langmuir's (1965a) approach after performing solubility measurements at 90°C over different periods of time. The longest period of time was 163 days, but it is not clear whether or not the equilibrium was attained. From the data reported it can be seen that the pH is still not constant, and neither is the Mg^{2+} concentration (which changes from 0.160 after 140 days to 0.174 m after 163 days). Christ and Hostetler (1970) assure equilibrium was almost achieved after 4, 8 and 20 days (depending on the sample).

The Gibbs free energy value for magnesite reported by Rossini et al. (1961) is very similar to that of calcite given by Langmuir (1964), with activity products for those minerals of $10^{-8.4}$

and $10^{-8.1}$, respectively. Therefore, it would be expected a similar behaviour for both salts, but this is not the case. Magnesite is not formed in the oceans where $a_{Mg^{2+}} \cdot a_{CO_3^{2-}} \approx 10^{-7.1}$ and $a_{Ca^{2+}} \cdot a_{CO_3^{2-}} \approx 10^{-7.9}$, although calcite forms easily under these conditions (Garrels and Thompson, 1962). Another large difference in the behaviour of both minerals is related to their hydrates. The hydrates of magnesium carbonate are formed in water below 100°C at CO_2 pressures around 1 atm. On the other hand, the calcium carbonate does not form hydrates under the same conditions (Langmuir, 1964). Langmuir (1965a) rejects the kinetic argument in order to explain the disagreement between Rossini's et al. (1961) solubility diagram and geological evidences. According to him, kinetic arguments should not be valid unless a reliable free energy value is determined, which does not seem to be the case.

Langmuir's (1965a) stability relations are accepted by many investigators, as Schott and Dandurand (1975), and Dandurand and Schott (1977), who established their diagram on the basis of enthalpy of formation. They recalculated the values correcting with more recent and precise free enthalpies of formation and entropies of oxides and ions in the solution, and included the variation of the entropy with temperature. According to the values obtained, magnesite, nesquehonite, lansfordite, hydromagnesite, artinite and brucite all have stability fields.

Leitmeier (1915) studied magnesium carbonate solubility in pure water, and concluded lansfordite is the stable solid phase below 10°C, nesquehonite is the stable phase in the temperature range from 10 to 55-65°C, and hydromagnesite is obtained for higher temperatures. The same stability relations are found in solubility studies in the $MgCO_3$-CO_2-H_2O system performed by Dell and Weller (1959), Kazakov et al. (1959) and Yanat'eva and Rassonskaya (1961).

Ponizovskii et al. (1960) obtained lansfordite as solid phase in their solubility measurements at 0°C and CO_2 pressures varying from 2 to 10 atm.

Ming and Franklin (1985) synthesized both lansfordite and nesquehonite from CO_2-saturated $Mg(HCO_3)_2$ solutions by degassing with air. They concluded lansfordite is unstable when exposed to the atmosphere at temperatures larger than 10°C.

López Gómez (1975) assures brucite is the solid phase in equilibrium with the $MgCO_3$-CO_2-H_2O solution up to a carbon dioxide pressure of $3.85 \cdot 10^{-4}$ atm. For higher CO_2 partial pressures, the stable phase at 25°C is nesquehonite.

Several investigators reported magnesite solubility (Engel, 1889, Leitmeier, 1915, Wells, 1915b, Bär, 1932, Leick, 1932, Halla and Ritter, 1935, Yanat'eva, 1954, 1955a, 1955b, 1957a, 1957b, Garrels et al., 1960, Morey, 1962, Stout and Robie, 1963, Halla and Van

Tassel, 1964, Christ and Hostetler, 1970, Levchenko et al., 1970, Kittrick and Peyrea, 1986). Most of them used natural magnesite as the starting solid phase, instead of a pure solid, and attained equilibrium only from undersaturation. There is a general discordance among these data, which could be explained as a consequence of the different impurities encountered in natural rocks. Also, the disagreement could suggest that equilibrium is not reached in some studies. This is the case of Wells (1915b), who measured concentrations over different periods of time, up to 60 days. It is obvious from those results that equilibrium was not attained, as a constant solubility value was not obtained. He compared his results to waters containing a high amount of magnesium and total carbonate, and concluded "either the waters are all supersaturated with respect to magnesite, or else the solubility found for magnesite had not yet reached its maximum value". The same behaviour is observed in the experiments performed by Leick (1932). He obtained two different solid phases according to the time waited before the analysis. For the shorter periods, he did not report the formula of the solid, although we believe it is magnesite as he used this mineral as starting material, and the time was in all the cases shorter than 5 hours. For longer periods of time (from 16 to 48 hours) he reported a solid phase which did not contain any CO_2 (brucite). From those results, it seems clear that magnesite is only obtained at the beginning, when the equilibrium is not attained, and a change to brucite is obtained afterwards. In the present work, only the data measured after the longest period of time will be used.

In general, it is not very clear in the literature whether artinite becomes a stable phase, but in case it does, the field of stability should be at low temperatures, and between the fields of brucite and hydromagnesite. Baron and Wyart (1958) considered this mineral stable at lower temperatures than nesquehonite. Kazakov et al. (1959) found both artinite and brucite at 20°C. Palache et al. (1951) found artinite deposits associated with hydromagnesite and brucite. The chemical formula used for this mineral by Palache et al.(1951), Langmuir (1965a), Robie and Hemingway (1972, 1973) and Königsberger et al. (1999) is $Mg_2(OH)_2CO_3\cdot3H_2O$.

Langmuir's (1965a) approach is also supported by the study performed by Chase (1998). The value reported by Chase (1998) is the one reported in the NIST Standard Reference Database Number 69.

5.5.2.2 Rossini's et al. (1961) Approach

Rossini's et al. (1961) determination of the Gibbs free energy for magnesite is in very good agreement with the corresponding value determined by Robie and Waldbaum (1965).

According to these values, the only stable phases in the temperature range from 0 to 100°C are brucite (at low CO_2 pressures) and magnesite. Many investigators follow the stability relations derived from Rossini's et al. (1961) approach (Stout and Robie, 1963, Hostetler, 1964, Robie, 1965, Christ and Hostetler, 1970, Sayles and Fyfe, 1973, Kittrick and Peyrea, 1986, Robie and Hemingway, 1995, Königsberger et al., 1999, Giles, 2001). Nevertheless, the agreement on the Gibbs free energy value among all these sources is not always good. There is also a large disagreement with respect to the values of the free enthalpy of formation of magnesite found in literature. These enthalpy values are based on the determinations of solubility at room temperature performed by Leick (1932), Halla and Ritter (1935), Yanat'eva (1955b), Morey (1962), and Halla and Van Tassel (1964); or are derived from calorimetric studies by Robie and Waldbaum (1965) and Robie and Hemingway (1973), confirmed by the solubility measurements at 90°C performed by Christ and Hostetler (1970).

Königsberger et al. (1999) modelled the system Na_2CO_3-$MgCO_3$-$CaCO_3$-H_2O at low temperatures, and derived a value for the Gibbs free energy for magnesite which was very close to the one reported by Rossini's et al. (1961) and Robie and Waldbaum (1965). Nevertheless, when these values are compared to the ones listed by Christ and Hostetler (1970) and Kittrick and Peyrea (1986), it is observed the latter are 2.5 and 4.5 kJ mol^{-1} more positive, respectively, than Königsberger's et al. (1999) value.

Giles (2001) assures magnesite is the only stable phase in a magnesium carbonate solution, from the eutectic point up to 25°C, and in the CO_2 pressure range from $1 \cdot 10^{-4}$ to 1 atm. According to her, the stability order is magnesite > hydromagnesite > nesquehonite (for temperatures above 8.5°C) or lansfordite (for temperature lower than 8.5°C). Giles's (2001) conclusions are in accordance with the calorimetric study on hydromagnesite by Robie and Hemingway (1972, 1973). These investigators concluded hydromagnesite is the stable phase, and not nesquehonite. This idea is also supported by additional studies (D'Ans and Gloss, 1938, Latimer, 1952, Garrels et al., 1960) that assure nesquehonite is an unstable phase. The explanation they give to the fact that nesquehonite appears at certain conditions for large periods of time is that the transformation from nesquehonite to hydromagnesite may become kinetically possible only at high temperatures. According to Davies and Bubela (1973), hydromagnesite is more common in nature than nesquehonite, even though natural conditions of temperature would favour the precipitation of nesquehonite. They concluded nesquehonite transforms into hydromagnesite through an intermediate hydrate. Königsberger et al. (1999) also support the reasoning of nesquehonite being an unstable phase. They used a Gibbs free energy for this mineral 1 kJ mol^{-1} lower than the value reported by Robie and Hemingway (1972, 1973), and managed to reproduce very well hydromagnesite solubility in CO_2-H_2O

and in 3 m $NaClO_4$ and $KHCO_3$ solutions. Their model does not predict that nesquehonite becomes more stable than hydromagnesite at 1 atm CO_2 pressure.

According to Christ and Hostetler (1970), the natural occurrence of magnesite is much more common than nesquehonite or hydromagnesite. They claim that in the hydromagnesite deposits of the Kamloops, Atlin, and Cariboo districts of British Columbia, magnesite is forming at the expense of hydromagnesite.

Additional data on magnesium carbonate stability and solubility are obviously needed, in order to throw some light into the rather complex matrix created for this system. The use of different techniques and newer approaches (note that most of the studies are around 30-40 years old) could help to develop a clearer idea about the real stability relations and the solubility behaviour at different conditions of temperature, pressure and CO_2 concentration. It is also important to mention that any condition introducing a possible source of error must be avoided. In that sense, natural minerals should not be used to perform experiments. Such minerals will always contain different amounts and kinds of impurities, which will obviously influence the solubility behaviour to some extent. It seems clear analyzing the sources mentioned before that the time required to attain equilibrium in the $MgCO_3$-CO_2-H_2O system is very large. Therefore, experimental conditions favouring a shorter time should be encouraged (small particle size, agitation, etc.).

In the present work we have chosen to follow Langmuir's (1965a) stability relations, even though there is no clear evidence that this choice is more reliable. We do think the arguments given by Langmuir (1965a) and his followers are somehow stronger than Rossini's et al. (1961). Moreover, the value given by the NIST Chemical Thermodynamics Database (1990) for the Gibbs free energy for magnesite is very close to Langmuir's (1965a). This is the same source of standard thermodynamic data that was used for all other components in this work. Even if the approach by Rossini et al. (1961) is the correct one, it seems clear that kinetic impediments control the deposition/dissolution of magnesite. Thus, in the context of scale formation in oil and geothermal wells, it is more convenient to model the solubility of the different minerals likely to precipitate on the inner walls of pipes and equipment within a reasonable period of time.

The NIST Chemical Thermodynamics Database (1990) did not report any value for the Gibbs free energy of lansfordite, nesquehonite, and brucite. Starting guesses for those values were calculated from the value reported for magnesite and for water as:

$$G_f^0(MgCO_3 \cdot nH_2O) \cong G_f^0(MgCO_3) + nG_f^0(H_2O) \qquad \textbf{(5-1)}$$

These values were later fitted to experimental data. The same procedure was also used for the calculation of the standard state enthalpy and heat capacity.

Contrary to the assumptions made for other carbonate minerals, the effect of magnesium carbonate on CO_2 solubility cannot be neglected. The solubility of nesquehonite is rather large when compared to carbonates such as calcite, strontianite or witherite. Therefore, in order to determine the interaction parameters between Mg^{2+} and $CO_2/HCO_3^{2-}/CO_3^{2-}$ we were limited to the use of those sources reporting both the salt solubility and the CO_2 concentration in the liquid phase. The references used, together with the ranges of temperature and pressure covered, and the number of experimental determinations carried out and used in the present work (in brackets), are given in table 5-10. Table 5-11 shows additional studies on the $MgCO_3$-CO_2-H_2O system, where the amount of CO_2 in the liquid phase is unknown.

Only a few sources dealing with lansfordite solubility were found in literature: Beckurts (1881), Merkel (1924), Ponizovskii and Vladimirova (1959), Ponizovskii et al. (1960), Yanat'eva and Rassonskaya (1961) and Corti et al. (1990a). All these sources used pure CO_2 saturated with water vapour as the gas phase.

Table 5-10
Experimental $MgCO_3$-H_2O and $MgCO_3$-CO_2-H_2O SLVE experimental data sets used for parameter estimation (CO_2 concentration in the liquid phase reported).

T(°C)	P(atm)	Number of data	AAD (m)	Reference
0	1	1 (1)	1.2E-04	Gothe (1915)
0/80	6/64	20 (0)		López Gómez (1975)
12.1/16	1	17 (0)		Treadwell and Reuter (1898)
12.5	1/6	8 (0)		Seyler and Lloyd (1917)
20	1	12 (0)		Wells (1915b)
20/39	1	27 (27)	2.9E-03	Leather and Sen (1914)
20/158		45 (0)		Corti et al. (1990a)
25	1	23 (23)	6.0E-03	Wattenberg and Timmermann (1937)
25	6/21	6 (6)	1.3E-02	Mitchell (1923)
25/290	200	12 (0)		Morey (1962)
35/200	0.06/15.4	10 (8)	1.9E-05	Travers and Nouvel (1929)
100	1	4 (1)	4.1E-06	Leick (1932)
			MAAD (m): 4.2E-03	

Brucite solubility in pure water, freed of carbon dioxide, was determined by Gothe (1915), Travers and Nouvel (1929), Leick (1932) and Morey (1962). Brucite solubility in CO_2-H_2O solutions was measured by Kline (1929) and Corti el al. (1990a.). The former used mixtures of air and carbon dioxide, in different proportions, as the gas phase. The latter author used

pure CO_2 in the gas phase, previously saturated with $MgCO_3$ solution. To obtain low carbon dioxide pressures (required for the stability of brucite) vacuum was used.

Table 5-11
Experimental $MgCO_3$-CO_2-H_2O SLVE experimental data sets where the CO_2 concentration in the liquid phase is unknown.

T(°C)	P(atm)	Number of data	Reference
0	4	1	Ponizovskii and Vladimirova (1959)
0	4/10	4	Ponizovskii et al. (1960)
0/55	1	2	Yanat'eva (1955a)
0/55	1	3	Yanat'eva (1957a)
0/60	2/56	15	Haehnel (1924)
0/90	1	18	Yanat'eva and Rassonskaya (1961)
3.5/50	1/9	26	Engel (1889)
5	1/6	6	Merkel (1924)
10/40	1/5	7	Beckurts (1881)
17	1	1	Bär (1932)
20	1	1	Leitmeier (1915)
21	1	1	Halla and Van Tassel (1964)
25	1	23	Kline (1929)
25	1	6	Kittrick and Peyrea (1986)
25	1	1	Yanat'eva (1957b)
25	1	2	Yanat'eva (1955b)
25	1	1	Levchenko et al. (1970)
25	1	1	Yanat'eva (1954)
25	1	1	Halla and Ritter (1935)
25	1	1	Garrels et al. (1960)
25	1	1	Stout and Robie (1963)
90	1	48	Christ and Hostetler (1970)

Nesquehonite solubility in CO_2-H_2O solutions was determined by Beckurts (1881), Engel (1889), Treadwell and Reuter (1898), Leather and Sen (1914), Wells (1915b), Seyler and Lloyd (1917), Mitchell (1923), Haehnel (1924), Kline (1929), Bär (1932), Wattenberg and Timmermann (1937), Yanat'eva and Rassonskaya (1961), López Gómez (1975) and Corti et al. (1990a). Most of these sources used pure CO_2 saturated with water vapour in the gas phase. Leather and Sen (1914) and Wells (1915b) used air, while Treadwell and Reuter (1898), Kline (1929) and Wattenberg and Timmermann (1937) used mixtures of air and CO_2, containing different amounts of the latter gas.

Hydromagnesite solubility determinations under a pure CO_2 gas phase were carried out by Engel (1889), Yanat'eva and Rassonskaya (1961) and Corti et al. (1990a).

Literature on experimental determination of magnesite solubility in water and in CO_2-H_2O solutions is mentioned in a previous paragraph of this chapter. Most of the sources cited

employed carbon dioxide saturated with water vapour in the gas phase. Christ and Hostetler (1970) also used mixtures of CO_2 and N_2 (same procedure as followed by Levchenko et al., 1970), while Kittrick and Peyrea (1986) employed air. According to Langmuir (1965a), magnesite should not be stable for the majority of the experimental conditions employed by the sources studying the solubility of this mineral. Only experiments at temperatures above 60°C and 1 atm carbon dioxide pressure may be concordant with the stability relations followed here.

Some of the sources mentioned in table 5-10 did not explicitly report the solid phase obtained in their equilibrium measurements (Beckurts, 1881, Treadwell and Reuter, 1898, Leather and Sen, 1914 and Merkel, 1924). In those cases we assumed the solid phase is the stable one at the experimental temperature and CO_2 pressure.

Many of the data in table 5-10 were not used in the present work for parameter estimation as they included some kind of error: The reported solid phase at the experimental conditions is not stable according to Langmuir (1965a); the data disagree with the majority of the sources; etc.

Nesquehonite solubility in CO_2-H_2O solutions increases with the total CO_2 amount. Such behaviour is followed by all the sources given in table 5-10, but for Treadwell and Reuter (1898), where for some solubility measurements at the highest carbon dioxide concentrations, constant nesquehonite solubility is observed for increasing CO_2 amounts. As mentioned before for calcite, Treadwell and Reuter's (1898) experiments were conducted under imperfect conditions, and supersaturation is to be expected (Leather and Sen, 1914).

Travers and Nouvel (1929) determined brucite solubility in pure water. Two out of the ten measurements performed contained a very low amount of $Mg(OH)_2$ which could not be determined by the analytical technique used. As a consequence, they reported zero as the solubility value. Those two points were therefore not used in the present work.

Morey (1962) determined $MgCO_3$ solubility in water freed of CO_2 at 200 atm total pressure. After X-ray study, he concluded magnesite was the stable solid phase from 25 to 150°C, and this mineral was completely changed to brucite for temperatures higher than 150°C (and up to 290°C). He also found some sepiolite crystals ($Mg_4Si_6O_{15}(OH)_2{\cdot}6H_2O$), which must appear due to the use of natural rock containing impurities. For some temperatures, Morey (1962) obtained mixtures of magnesite and brucite, and he claimed that magnesite would have been completely replaced by brucite if he had waited longer. Thus, maybe his data are affected by the fact that equilibrium was not attained, and magnesite did not have enough time to convert into brucite. This could explain the appearance of magnesite when the only stable phase in the absence of carbon dioxide in the solution is brucite.

As mentioned previously, it is believed that the measurements reported by Wells (1915b) do not correspond to equilibrium, and thus they were not used in the present work. Moreover, he measured the solubility of both magnesite and nesquehonite in water at the same conditions (20°C and 1 atm). Following Langmuir's (1965a) approach, the first phase should not be stable at those conditions.

Seyler and Lloyd (1917) concluded "crystallized magnesium carbonate has no definite solubility in pure water. It decomposes into basic carbonates and magnesium hydrogen carbonate, whilst a certain amount of carbonate is also dissolved". Under the same experimental conditions, they obtained different $MgCO_3$ concentrations depending on the ratio of water to solid employed. When equilibrium is attained, a unique solubility value should be obtained independently of the initial amounts of solid and solvent used. Therefore, Seyler and Lloyd's (1917) data were not used in the present work.

Corti et al. (1990a) report neither the partial pressure of carbon dioxide nor the total pressure used in the experiments. After analyzing the experimental procedure employed, it is clear they performed experiments with different CO_2 quantities, which are sometimes achieved by removing carbon dioxide from the gas phase applying vacuum. But the vacuum pressure is unknown, and therefore the data could not be used.

Wattenberg and Timmermann (1937) did not report the amount of carbon dioxide contained in the liquid phase, but they gave the values of the solution pH and the bicarbonate concentration. From those values, together with the equilibrium constant, the amount of CO_2 was calculated following the same procedure as in the case of $SrCO_3$, where the same source is also used.

López Gómez (1975) presented in his paper several plots for the solubility in the ternary system MgO-CO_2-H_2O at various temperatures and carbon dioxide pressures. He also reports the CO_2 solubility in saturated $MgCO_3$ solutions at 25°C. He mentions he used data from different investigators to draw the solubility curves, but it is not clear which data are his and which are from other sources. He did not analyze the solid phase in equilibrium with the solution at the experimental conditions. When data from this source are compared to others (mainly to Mitchell (1923) at pressures larger than 1 atm, and to available sources in table 5-10 at 25°C and atmospheric pressure) it is clear the solubility of both the salt and carbon dioxide is very much overestimated in that paper.

The experimental and calculated $MgCO_3$ solubility as a function of the CO_2 concentration in the solution at 39°C and 1 atm total pressure is shown in figure 5-15. As expected from Langmuir's (1965a) phase diagram at 39°C, only one solid phase, nesquehonite, is formed in the whole range of CO_2 concentration presented. Nesquehonite solubility increases with the

amount of carbon dioxide, from 0.015 m $MgCO_3 \cdot 3H_2O$ at 0.007 m total CO_2 to 0.08 m $MgCO_3 \cdot 3H_2O$ at 0.17 m total CO_2. The calculated solubility compares very well with the experimental data. Due to the lack of data at the same conditions, it was impossible to calculate a reliable value for the average experimental standard deviation for nesquehonite. To get at least an idea about the order of magnitude of *ASD*, a determination was done considering the only two experimental points at very similar conditions (25°C, 0.52 m total CO_2, and 13.2 atm total pressure; and 25°C, 0.54m total CO_2 and 16.2 atm total pressure, respectively). The obtained *ASD* is $1.8 \cdot 10^{-2}$ m $MgCO_3 \cdot 3H_2O$. When such value is compared to the *MAAD* between our model calculations and the experimental data ($4.2 \cdot 10^{-3}$ m) it is clear extended UNIQUAC calculations are remarkably good.
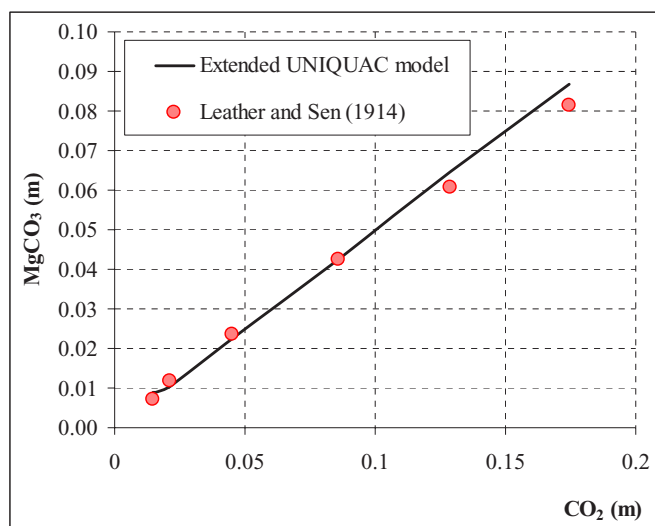
Figure 5-15. Experimental and calculated $MgCO_3$ solubility as a function of the CO_2 concentration in solution, at 39°C and 1 atm total pressure. Gas phase formed by CO_2 (g) and H_2O (g).

For the case of brucite, the same problem was encountered when trying to calculate the *ASD*. If we follow the same procedure as before and use the only two experiments carried out at similar conditions (100°C, $7.2 \cdot 10^{-5}$ m CO_2, and 1 atm; and 100°C, $7.5 \cdot 10^{-5}$ m CO_2, and 1 atm, respectively) the value obtained for the *ASD* is $4.3 \cdot 10^{-6}$ m $Mg(OH)_2$. For this salt, extended UNIQUAC calculations are less accurate than for nesquehonite, and the *MAAD* between the model and the data is $1.7 \cdot 10^{-5}$ m $Mg(OH)_2$.

The binary phase diagram for the system $MgCO_3$-H_2O covering a temperature range from 100 to 158°C, at the saturation pressure, is shown in figure 5-16. The only solid phase encountered at those conditions is brucite, its solubility decreases with increasing pressure.
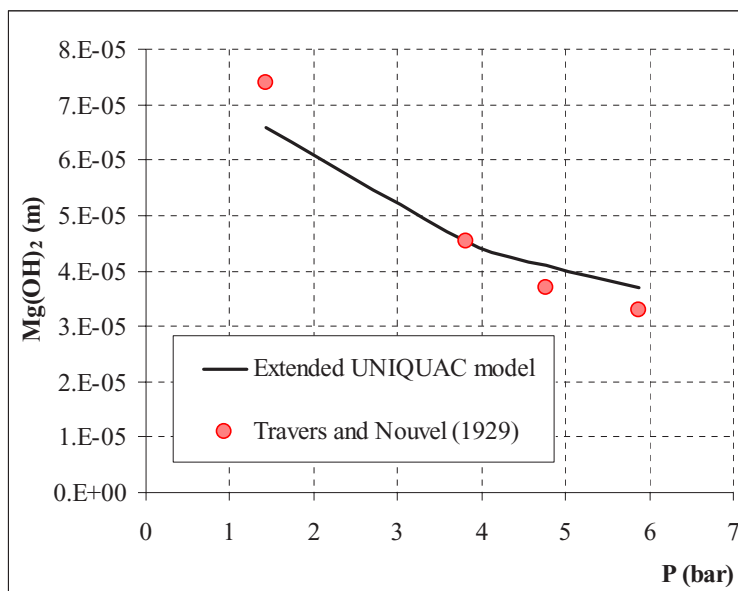
Figure 5-16. Experimental and calculated solid-liquid phase diagram for the binary $MgCO_3$-H_2O system at the saturation pressure.

Once the parameters required for the system $MgCO_3$-CO_2-H_2O were obtained on the basis of the VLSE experimental data reported in table 5-10, they can be used to perform some calculations for the data sets where the amount of carbon dioxide in the liquid phase is unknown (data reported in table 5-11). The solubility of CO_2 in the $MgCO_3$ solution at the experimental temperature and carbon dioxide pressure can be calculated by means of the new parameters. Once the amount of carbon dioxide is estimated, the experimental points could be added to the original VSLE database and refit the parameters based on a larger experimental study. Nevertheless, such improvement of the experimental $MgCO_3$-CO_2-H_2O database and of the parameters was not possible, as the experimental determinations reported in table 5-11 are also characterized by a tremendous lack of agreement. Many of them do not follow the stability field followed by Langmuir (1965a) and report magnesite as the only stable phase at temperatures and CO_2 pressures where lansfordite or nesquehonite should form and be stable. That is the case for all the data reported by Leitmeier (1915), Bär (1932), Halla and Ritter (1935), Yanat'eva (1954, 1955a, 1955b, 1957a, 1957b), Garrels et al. (1960), Stout and Robie

(1963), Halla and Van Tassel (1964), Christ and Hostetler (1970), Levchenko et al. (1970), Kittrick and Peyrea (1986). Several authors agree on the fact that Kline's (1929) work is not precise (Kazakov et al., 1959, Langmuir, 1965a, Harvie et al., 1984). The greatest shortness of his work is the extremely low aging period, which varied between 3 and 5 days. Therefore, it is very unlikely that the solutions Kline (1929) measured had achieved equilibrium. According to Kazakov et al. (1959), this could well explain some of the incongruences found in Kline's (1929) work, as the formation of different solid phases under very similar conditions. Harvie et al. (1984) tried to fit Kline's (1929) results, but they did not succeed, even though different attempts were done, including complexes such as $MgHCO_3^+$. They realized in order to explain those data, it was needed to assume that enormous changes in the interactions occur over a very small concentration range. Kline (1929) was not congruent either when he determined the solubility product of nesquehonite based on a graphic extrapolation to infinite dilution, even though solubility measurements of that mineral cannot be extended below an ionic strength about 0.05 due to the formation of brucite (Langmuir, 1965a).

The aging time measured by Engel (1889) (9 hours) is extremely low for the system considered and it is very unlikely that equilibrium was reached. In his paper he shows the amounts of HCl employed in the titration of different solutions at the same temperature and carbon dioxide pressure, according to the starting solid phase (magnesite or nesquehonite). The amounts of acid employed are completely different, proving that equilibrium was not attained, at least for one of the solutions.

Some of the solid phases reported by Yanat'eva and Rassonskaya (1961) are not stable at the given conditions, according to Langmuir's (1965a) stability diagram.

Haehnel (1924) obtained the same solubility value for nesquehonite at 18°C and CO_2 pressures changing from 18 to 56 atm, which makes his determinations rather suspect. In the experimental procedure followed, samples were taken at atmospheric pressure and analyzed afterwards. Decreasing the carbon dioxide partial pressure from a few atmospheres (up to 56 atm) to room conditions will very likely result in erroneous solubility determinations, as part of the CO_2 will evaporate from the liquid phase.

Large discrepancies are found between the data reported by Beckurts (1881) and Merkel (1924). None of these datasets were taken from the original sources, but from Haehnel (1924), who did not mention the solid phase obtained. Thus, the differences could be due to different solids being involved in the equilibrium. When Beckurts' (1881) data at 20°C are compared to those by Mitchell (1923) at 25°C, the agreement seems good. The experimental

CO_2 pressure is larger for Mitchell (1923), but the tendencies followed by both sources are in good agreement. An additional problem of both sources is the choice of units to characterize the system. The solubility is expressed as weight percent of $MgCO_3$ (the same unit as used by Ponizovskii and Vladimirova, 1959). As the total amount of CO_2 is unknown, the exact composition of the solution is unknown. Therefore, calculations could only be approximate, assuming the percentage is referring only to the amount of water and salt, and excluding the CO_2 (aq). Due to the lack of the original sources, the antiquity of the data, and the imprecision of at least one of the two datasets mentioned, those sources were not used for parameter estimation in the present work.

5.6 $MgCO_3$-$CaCO_3$-CO_2-H_2O System

The binary interaction parameter for the interaction between Ca^{2+} and Mg^{2+} has already been fitted to ternary data containing both calcium and magnesium together with chloride or nitrate. Thus, the analysis of dolomite ($CaCO_3 \cdot MgCO_3$) studies and the system $CaCO_3$-$MgCO_3$-CO_2-H_2O is not necessary for the purpose of parameter estimation. Nonetheless, due to the complexity found for the ternary system $MgCO_3$-CO_2-H_2O, it was considered relevant to study this system in detail.

Similar to the magnesium carbonate system, the system $CaCO_3$-$MgCO_3$-CO_2-H_2O is also characterized by large experimental discrepancies regarding solubility values, stability relations, and values for the standard state Gibbs free energy and enthalpy. The experimental difficulties mentioned before for the $MgCO_3$-CO_2-H_2O system are also found in the present case. Dolomite has not been successfully obtained in laboratory near room conditions because of an extremely slow kinetics (apparently, it requires geological times to precipitate this solid). Dolomite is present in many ancient sediments, while it does not appear in modern marine sediments (Kazakov et al., 1959). The only way to overcome this problem is to increase the velocity of the reaction enormously. This objective can be attained by increasing the concentration of CO_2 in the solution by increasing the pressure. In fact, dolomite has been successfully crystallized under hydrothermal conditions in different solutions (Graf and Goldsmith, 1955, Rosenberg and Holland, 1964, Rosenberg et al., 1967, Sureau, 1974). Due to the impossibility to precipitate dolomite, the equilibrium at atmospheric conditions cannot be checked from supersaturation, and only undersaturation experiments have been carried out. All data thus contain the uncertainty whether or not equilibrium has been reached during the experiments. According to Hsu (1963), published values for the activity product of dolomite at 25°C and 1 atm vary from 10^{-17} to 10^{-20}. Such disagreement may be caused by

different reasons. In the first place, as mentioned before, true thermodynamic equilibrium may not have been established for most of the available data. The use of natural dolomite in many of the experiments will also introduce an additional source of diversity in the results, as a consequence of the influence of the different impurities found together with $CaCO_3 \cdot MgCO_3$. The use of pure commercial solid is therefore encouraged, although the synthesis of dolomite in laboratory is not easy.

One of the consequences of the disagreement found in literature for the systems $MgCO_3$-CO_2-H_2O and $CaCO_3$-$MgCO_3$-CO_2-H_2O is reflected in the calculated values for the standard state enthalpy of formation of dolomite. Two different approaches have been used to determine this value: calorimetric studies (Stout and Robie, 1963, Navrotsky and Capobianco, 1987), and determinations from solubility measurements (Yanat'eva, 1955b, Halla, 1958, Kramer, 1959, Garrels et al., 1960, Halla et al., 1962, Stout and Robie, 1963, Langmuir, 1965b, Dandurand and Schott, 1977, Robie and Hemingway, 1995, Königsberger et al., 1999). The values obtained differ from -2144.34 kJ mol^{-1} given by Dandurand and Schott (1977) to -2175.26 kJ mol^{-1} determined by Garrels et al. (1960).

Stout and Robie (1963) determined the standard state heat capacity and entropy of dolomite by calorimetric methods. They also calculated standard state enthalpies and Gibbs free energies from a thermodynamic analysis of dolomite decomposition data by Graf and Goldsmith (1955), and from solubility data of dolomite, magnesite and calcite in aqueous solutions saturated with CO_2 at 1 atm pressure (Yanat'eva, 1954). The values obtained for the enthalpy change for the reaction

$$CaCO_3 + MgCO_3 \Leftrightarrow CaCO_3 \cdot MgCO_3 \qquad\qquad (5\text{-}2)$$
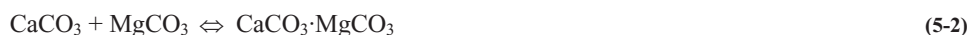
at 25°C by the two analysis methods employed are very similar (-12.30 and -12.84 kJ mol^{-1}, respectively). These values compare relatively well with the one given by Navrotsky and Capobianco (1987). They determined the enthalpy of formation of dolomite by solution calorimetry at 85°C, obtaining an enthalpy change for reaction 5-2 of -11.48 kJ mol^{-1}. However, when they calculated the enthalpy of formation from data given by Robie et al. (1978), they obtained a rather different value (-3.76 kJ mol^{-1}). Such value is closer to the calculations performed by Halla (1958) from solubility measurements at the two triple points (dolomite and calcite/magnesite in equilibrium with the saturated solution). Halla (1958) obtained a value of -3.97 kJ mol^{-1} when using the data reported by him (Halla, 1936), while this value changed to -5.27 kJ mol^{-1} for the data reported by Yanat'eva (1955b).

Königsberger et al. (1999) calculated the Gibbs free energy of formation (-2172 kJ mol^{-1}) and the enthalpy of formation (-2334.8 kJ mol^{-1}) of dolomite from the solubility data of dolomite

in 3 m $NaClO_4$ solutions at 25°C given by Riesen (1969). These values are consistent with those calculated by Stout and Robie (1963), resulting in enthalpy and Gibbs free energy changes for reaction 5-2 of -12.9 and -11.3 kJ mol^{-1}, respectively.

Robie and Hemingway (1995) used considerably more positive values for the enthalpy and Gibbs free energy of formation of dolomite (-2324.5 and -2161.3 kJ mol^{-1}, respectively). These values agree with the ones published in NIST Chemical Thermodynamics Database (1990): -2326.3 and -2163.4 kJ mol^{-1}, respectively. Also, Langmuir (1965b) suggested the use of -2160 kJ mol^{-1} as the value for the Gibbs free energy of dolomite.

Dandurand and Schott (1977) reported very positive values for both the standard state Gibbs free energy and enthalpy of dolomite. They determined the former value (-2144.34 kJ mol^{-1}) from Baron's (1960) experiments on dolomite synthesis. If experimental data by Graf and Goldsmith (1956) are used instead, the value is -2147.06 kJ mol^{-1}.

Tables 5-12 and 5-13 show a summary of the different Gibbs free energies and enthalpies of formation of dolomite found in literature.

Table 5-12

Values for enthalpy and Gibbs free energy of formation of dolomite found in literature.

Reference	Solubility Data	$\Delta_f H^0$ (kJ mol^{-1})	$\Delta_f G^0$ (kJ mol^{-1})
Dandurand and Schott (1977)	Baron (1960)		-2144.3
Dandurand and Schott (1977)	Graf and Goldsmith (1956)		-2147.1
Langmuir (1965b)			-2160.0
Kramer (1959)	Kramer (1959)		-2161.0
Robie and Hemingway (1995)		-2324.5	-2161.3
NIST (1990)		-2326.3	-2163.4
Königsberger et al. (1999)	Riesen (1969)	-2334.8	-2172.0
Garrels et al. (1960)			-2175.3

Table 5-13

Values for the change of standard state enthalpy and Gibbs free energy of reaction 5-2 found in literature.

Reference	Data	$\Delta_r H^0$ (kJ mol^{-1})	$\Delta_r G^0$ (kJ mol^{-1})
Stout and Robie (1963)	Graf and Goldsmith (1955)	-12.30	-11.30
Stout and Robie (1963)	Yanat'eva (1954)	-12.84	
Halla (1959)	Halla (1936)	-3.97	-2.97
Halla (1959)	Yanat'eva (1955)	-5.27	-4.26
Navrotsky (1987)	calorimetry	-11.48	
Navrotsky (1987)	Robie et al. (1978)	-3.76	

The diversity of standard state Gibbs free energy and enthalpy values shown in table 5-12, together with the diversity also found for the system $MgCO_3$-CO_2-H_2O, results in completely

different solubility diagrams for the system $CaCO_3$-$MgCO_3$-CO_2-H_2O (Bär, 1932, Halla and Ritter, 1935, Yanat'eva, 1949, 1952, 1955b, 1957a, Baron and Favre, 1958, Kazakov et al., 1959, Berg and Borisova, 1960a, Garrels et al., 1960, Yanat'eva and Rassonskaya, 1961, Yanat'eva et al., 1961, Lippmann, 1980). Little knowledge is available about the dolomitization process and the intermediate phases presented in it. Many authors (Rosenberg and Holland, 1964, Berner, 1967, Bischoff, 1968, Katz, 1971, Plummer and Mackenzie, 1974) support that the solid phase precipitating in the $CaCO_3$-$MgCO_3$-CO_2-H_2O system and the time required to achieve equilibrium is determined by the activity ratio between calcium and magnesium in the solution.

Yanat'eva (1949, 1952, 1955b, 1957a) obtained calcite, dolomite and magnesite as the solid phases in equilibrium with the solution at 0, 25, 55 and 70°C, and CO_2 pressures of 0.0012 and 1 atm. The appearance of one or another salt (or the triple points) depends on the amounts of Mg^{2+} and Ca^{2+} in the solution. This approach is also followed by Bär (1932) at 17°C, by Halla and Ritter (1935) at 25-40°C, by Lippmann (1980) at 25°C, and by Garrels et al. (1960) at 25°C, all the studies at 1 atm of CO_2 pressure. For the latter investigators, hydromagnesite becomes a stable phase with respect to magnesite and dolomite only at very low carbon dioxide pressures, much lower than the earth surface conditions. Kramer (1959) and Garrels et al. (1960) claim that dolomite is stable in sea water at 25°C. Dolomite even forms when calcite is present in sea water since a smaller carbonate ion concentration is required for dolomite saturation, when comparing to calcite. The reason why calcite is observed instead of dolomite in recent marine sediments is due to the slow rate at which dolomite is formed.

On the other hand, Yanat'eva and Rassonskaya (1961) and Yanat'eva et al. (1961) obtained as solid phases calcium carbonate and the hydrated magnesium carbonates $4MgCO_3 \cdot Mg(OH)_2 \cdot 4H_2O$, $MgCO_3 \cdot 3H_2O$ and $MgCO_3 \cdot 5H_2O$, depending on the temperature. A very similar result is obtained by Baron and Favre (1958) at a partial CO_2 pressure of 0.001 atm. The solid phases in equilibrium with the solution are calcite and nesquehonite at 25 and 40°C, aragonite, nesquehonite and hydromagnesite at 70°C, and aragonite and hydromagnesite at 100°C.

Yanat'eva and Rassonskaya (1961) used a mixture of aragonite and nesquehonite as starting solids for the study of the quaternary system $CaCO_3$-$MgCO_3$-CO_2-H_2O. They obtained isotherms with two branches, corresponding to the crystallization of the pure salts ($CaCO_3$ and $MgCO_3 \cdot 5H_2O$ at 0°C, $CaCO_3$ and $MgCO_3 \cdot 3H_2O$ at 20 and 40°C, and $CaCO_3$ and $4MgCO_3 \cdot Mg(OH)_2 \cdot 4H_2O$ at 55, 70 and 90°C). Nevertheless, the isotherms obtained at 0°C

were depending on the order of mixing of the initial salts. When nesquehonite was introduced all at once, the eutectic solutions contained 330.4 mmoles $Mg(HCO_3)_2$ and 0.55 mmoles $Ca(HCO_3)_2$ per kg of solution. Those quantities increased to 396 mmoles of $Mg(HCO_3)_2$ and 2.76 mmoles of $Ca(HCO_3)_2$ per kg of solution when nesquehonite was introduced in two or three portions at 4-5 minutes intervals. The solid phases obtained in both cases were also different. In the first case aragonite and nesquehonite were found, while in the second case the trihydrate was substituted by lansfordite. The explanation of the different solubility behaviour under equal temperature and CO_2 pressure conditions must be explained as metastable equilibrium, at least for one of the two solutions.

Berg and Borisova (1960a, 1960b) tried to avoid the problem reported by Yanat'eva and Rassonskaya (1961) and placed the initial solid phases (calcite and magnesite) simultaneously in the reaction vessel. After equilibrium, the common crystallization point was obtained. They also performed one experiment where magnesite was substituted by nesquehonite, obtaining rather different amounts of calcium and magnesium carbonates in the solution, and obtaining in that case calcite and nesquehonite as solid phases. Such behaviour manifests, again, that equilibrium was not attained.

According to Bär (1932), Halla and Ritter (1935) and Yanat'eva (1949, 1952, 1955b, 1957a), the points obtained by Berg and Borisova (1960a, 1960b), Yanat'eva and Rassonskaya (1961) and Yanat'eva et al. (1961) fall within the region representing supersaturation with respect to dolomite. Therefore, the absence of dolomite indicates a condition of metastable equilibrium. Such condition, however, proved very persistent and no notable changes were observed during a year, even when some dolomite was introduced in the reaction vessel.

Kazakov et al. (1959) slowly mixed solutions of calcium and magnesium bicarbonate while aerating with atmospheric air. In all the experiments performed covering temperatures from 20 to 60°C, the bottom phases were either calcite and nesquehonite or calcite and hydromagnesite, depending on the CO_2 concentration in the solution. However, at 150°C, and using a much higher CO_2 pressure than in the previous measurements, the phase precipitating from solution was dolomite. Kazakov et al. (1959) concluded dolomite is not formed in open systems where the partial pressure of carbon dioxide is similar to that of normal atmospheric air, but it is easily developed in a closed system at an elevated partial pressure of CO_2. Unfortunately, Kazakov et al. (1959) did not report either the total pressure or the partial pressure of carbon dioxide for their experiments in closed systems.

Other investigators support the coexistence of dolomite and magnesium calcites ($Ca_xMg_{(1-x)}CO_3$) as stable solid phases for the system $CaCO_3$-$MgCO_3$-CO_2-H_2O. Graf and Goldsmith (1955) investigated the transformation of metastable magnesian calcites into dolomite at

temperatures above 500°C. Lower temperatures were not included in the study due to the extremely slow process. They concluded that magnesium calcite of 15 mol% $MgCO_3$ and dolomite are the stable phases in the $MgCO_3$-$CaCO_3$-CO_2-H_2O system at 700°C. Bertram et al. (1991) focused on the solubility of magnesian calcites at low temperatures. They concluded at 50°C dolomite and calcite low in magnesium are the stable phases, a fact that is also observed petrographically. The higher the temperature, the more enriched in magnesium the calcite stable phase. Due to the lack of experimental data the composition of stable magnesian calcites is not known.

In order to be consistent with the approach chosen to explain the stability relations in the $MgCO_3$-CO_2-H_2O system, the values given by the NIST Chemical Thermodynamics Database (1990) for both the Gibbs free energy and enthalpy of formation of dolomite are chosen in the present work. Also, the standard state heat capacity is reported by the NIST Chemical Thermodynamics Database (1990). These values agree with Langmuir (1965b), whose phase diagrams for the magnesium and calcium carbonate are followed in this work.

Table 5-14 shows all the publications found for the system $CaCO_3$-$MgCO_3$-CO_2-H_2O, the ranges of temperature and pressure covered by them and the number of data points reported by each publication. Only a few sources (some of the measurements by Leather and Sen, 1914, Mitchell, 1923 and Kazakov et al., 1959) reported the amount of CO_2 contained in the $CaCO_3$-$MgCO_3$ solution.

Table 5-14
Experimental $MgCO_3$-$CaCO_3$-CO_2-H_2O SLE experimental data sets.

T(°C)	P(atm)	Number of data	Reference
0/55	1	6	Yanat'eva (1955b)
0/90	1	41	Yanat'eva and Rassonskaya (1961)
17	1	2	Bär (1932)
20/150	1/15	12	Kazakov et al. (1959)
22	1	2	Dandurand and Schott (1977)
22/31	1	141	Hsu (1963)
25	1	3	Yanat'eva (1957a)
25	1/16	7	Mitchell (1923)
25	1	4	Yanat'eva (1952)
25	1	2	Berg and Borisova (1960a)
25	1	2	Berg and Borisova (1960b)
25/38.8	1	13	Halla and Ritter (1935)
25/340	200	11	Morey (1962)
30/33	1	40	Leather and Sen (1914)
70	1	3	Yanat'eva (1960)
100	1	4	Leick (1932)

Additional sources dealing with the system $CaCO_3$-$MgCO_3$-CO_2-H_2O but not reported in table 5-14 are Yanat'eva 1955a, 1957b, Yanat'eva and Danilova, 1956, Yanat'eva et al., 1961. They are not included in table 5-14 as the data presented in those papers refer to data that were published previously by the same authors.

Most of the references used CO_2 saturated with water vapour in the gas phase (Mitchell, 1923, Bär, 1932, Halla and Ritter, 1935, Yanat'eva, 1952, 1955b, 1960, Berg and Borisova 1960a, 1960b, Yanat'eva and Rassonskaya, 1961). Some investigators employed air instead (Kazakov et al., 1959, Dandurand and Schott, 1977) or mixtures of CO_2 and air in different proportions (Leather and Sen, 1914, Mitchell, 1923). Finally, some of the experiments are performed using water freed of CO_2 and with no gas phase over the solution (Leick, 1932, Morey, 1962).

A deep analysis to the data presented in table 5-14 will be done in the next paragraphs, as many of the sources are considered unreliable.

Mitchell (1923) performed three measurements in solutions containing both calcite and nesquehonite, using pure CO_2 in the gas phase. For the lowest pressure, the solid phase could not be successfully determined, while dolomite was obtained in the other two measurements. He also performed three additional measurements using natural calcite from Algeria, and mixtures of air and CO_2 in the gas phase covering partial pressures of carbon dioxide from 0.25 to 1 atm. He concluded the solutions were supersaturated with respect to dolomite due to an extremely low rate of precipitation.

Leather and Sen (1914) tried to attain equilibrium in the $CaCO_3$-$MgCO_3$-CO_2-H_2O system following two different directions: By precipitation of dolomite from supersaturated solutions of calcium and magnesium bicarbonate, and by dissolution of natural dolomite. For the first data set, the authors claim that the amount of magnesium carbonate in solution is much larger than expected. This fact could be explained as a supersaturated solution due to the low time allowed for equilibration (seven days). Due to this short time, Leather and Sen (1914) state "it is improbable that in any of the experiments a state of equilibrium had set in". In the second data set, a larger time of contact between the different phases was allowed (up to 250 days) for three of the experiments, although the rest of the measurements were performed after 8 to 13 days. This time is too short for equilibrium to be attained. In addition to that, the dolomite employed contained some impurities as iron oxide, insoluble silicates and sand, and Leather and Sen (1914) did not use any device to keep a constant temperature during the experiments. They confined the experimental setup in a room whose temperature was constant within ± 1°C. Nevertheless, a more precise control of temperature is recommended. Some of the experiments were carried out adding a second solid phase (nesquehonite or

calcite) to the solution to analyze its influence on the solubility behaviour. After plotting the data it can be clearly concluded that true equilibrium was not attained.

Morey (1962) used natural dolomite from Maryland. From 25 to 209°C the X-ray analysis of the solid phase shows it to be dolomite, while from 209 to 304°C the solid phase changes to calcite and brucite. As the water employed in the experiments was previously freed of CO_2, and there was no gas phase over the solution, brucite should be the solid phase encountered in all the experiments according to Langmuir (1965a).

Hsu (1963) determined the solubility and solubility product of dolomite based on shallow ground-water samples from an aquifer in central Florida formed by dolomitic limestone. The main constituents of these waters are calcium, magnesium and bicarbonate, although different amounts of additional constituents are also present. The author assumed the waters had reached equilibrium with respect to dolomite as a consequence of the large contact period between the waters and the rocks (the rate of ground water flow is very slow). Moreover, the ratio between magnesium and calcium concentrations was kept rather constant, suggesting the attainment of calcite-dolomite-solution equilibrium. Nevertheless, the solubility may be influenced by the rest of the species in solution. The amount of total dissolved solids in some cases cannot be neglected (values up to 3560 ppm). Another source of error is the inconstancy of temperature, which varies from 22 to 31°C during the measurements. The author reports the amount of bicarbonate in solution and the pH, but he claims those values "are usually quite inaccurate because of the tendency of bicarbonate in solution to equilibrate with the atmospheric CO_2".

Many of the sources reported in table 5-14 follow stability relations that are in disagreement with the approach followed in the present paper. This is the case of Bär (1932), Halla and Ritter (1935) and Yanat'eva (1952, 1955b, 1957a, 1960).

5.7 Parameters

Table 5-15
Extended UNIQUAC r and q parameters, fitted to experimental data

	r	q
H_2O	0.92	1.40
CO_2 (aq)	**0.75**	**2.45**
Na^+	1.40	1.20
H^+	0.14	$0.1 \cdot 10^{-15}$
Ba^{2+}	**15.67**	**14.48**
Ca^{2+}	3.87	1.48
Sr^{2+}	**7.14**	**12.89**
Mg^{2+}	5.41	2.54
OH^-	9.40	8.88
Cl^-	10.39	10.20
SO_4^{2-}	12.79	12.44
CO_3^{2-}	10.83	10.77
HCO_3^-	8.08	8.68

Table 5-16
$u_{ik}^0 = u_{ki}^0$ parameters for calculating extended UNIQUAC interaction energy parameters
$\left(u_{ik} = u_{ik}^0 + u_{ik}^t (T - 298.15) \right)$

	H_2O	CO_2 (aq)	H^+	Na^+	Ca^{2+}	Ba^{2+}	Sr^{2+}	Mg^{2+}	OH^-	Cl^-	SO_4^{2-}	CO_3^{2-}	HCO_3^-
H_2O	0												
CO_2 (aq)	8.838254	302.248											
H^+	1×10^4	**10^{10}**	0										
Na^+	733.2863	**172.392**	10^{10}	0									
Ca^{2+}	496.3523	**2839.83**	10^{10}	**-100**	0								
Ba^{2+}	**-0.37858**	2500	10^{10}	779.06	2989.759	0							
Sr^{2+}	543.1096	-100.74	10^{10}	-103.9	-402.783	2500	0						
Mg^{2+}	-2.04282	**-581.18**	10^{10}	-70.96	155.2324	**628.5288**	-400.581	0					
OH^-	600.4952	2500	10^{10}	1398.1	164.6378	2500	2500	736.423	1562.9				
Cl^-	1523.393	**1613.01**	10^{10}	1443.2	1805.59	**1403.17**	**1895.877**	2049	1895.5	2214.8			
SO_4^{2-}	752.8792	**1942.4**	10^{10}	845.14	1258.103	2500	2500	1407.21	1225.7	2036.1	1265.83		
CO_3^{2-}	361.3877	2500	10^{10}	547.95	**-769.706**	2500	2500	100	1588	2724.9	1216.76	1458.344	
HCO_3^-	577.0502	**526.305**	10^{10}	1101.9	**2881.408**	2500	2500	100	2500	1736.6	990.48	800.0081	771.038

Table 5-17

$u_{ik}^t = u_{ki}^t$ parameters for calculating extended UNIQUAC interaction energy parameters
($u_{ik} = u_{ik}^0 + u_{ik}^t (T - 298.15)$)

	H_2O	CO_2 (aq)	H^+	Na^+	Ca^{2+}	Ba^{2+}	Sr^{2+}	Mg^{2+}	OH^-	Cl^-	SO_4^{2-}	CO_3^{2-}	HCO_3^-
H_2O	0												
CO_2 (aq)	0.86293	0.35871											
H^+	0	0	0										
Na^+	0.48719	-0.4363	0	0									
Ca^{2+}	-8.0654	10.876	0	-4.656	0								
Ba^{2+}	0.58244	0	0	2.338	72.084	0							
Sr^{2+}	1.2742	0	0	-0.62	-4.2533	0	0						
Mg^{2+}	-3.5542	-2.855	0	1.3394	5.1921	0	-1.437	0					
OH^-	8.5455	0	0	20.278	3.6084	0	0	0	5.6169				
Cl^-	14.631	15.015	0	15.635	11.14	14.89	15.689	12.132	13.628	14.436			
SO_4^{2-}	9.4905	4.7896	0	11.681	50.446	0	10	2.2791	8.5902	12.407	8.3194		
CO_3^{2-}	3.3516	0	0	3.782	-22.727	0	0	1	2.7496	5.7267	7.0067	-1.3448	
HCO_3^-	-0.38795	-3.7342	0	1.829	35.213	0	0	1	0	14.035	6.9646	1.7241	-0.0198

Table 5-18

α and β parameters for calculating the solubility product pressure dependency

	α	β
$BaSO_4$	1.636629×10^{-3}	3.333826×10^{-7}
$SrSO_4$	1.035686×10^{-3}	7.153236×10^{-7}
$CaSO_4$	2.328718×10^{-3}	-8.421355×10^{-7}
$CaSO_4 \times 2H_2O$	1.078224×10^{-3}	3.078141×10^{-7}
$NaCl$	9.927134×10^{-5}	-1.358719×10^{-8}
$CaCO_3$	-3.916945×10^{-3}	-2.092925×10^{-5}

Table 5-19

Thermodynamic properties and related parameters. Bold numbers are taken from the NIST Chemical Thermodynamics Database (1990). The rest of the values were fitted to experimental data.

	$\Delta_r G_f^0$ (kJ mol^{-1})	$\Delta_r H_f^0$ (kJ mol^{-1})	C_{p1} (J mol^{-1}K^{-1})	C_{p2} (J mol^{-1}K^{-2})	C_{p3} (J mol^{-1}K^{-2})
CO_2 (aq)	**-385.98**	**-413.8**	**243**	**0**	**0**
$CaCO_3$	-1129.057	-1208.726	**81.88**	**0**	**0**
$Mg(OH)_2$	-833.51	-921.1407	**77.03**	**0**	**0**
Na_2SO_4	**-1270.16**	**-1387.08**	**128.2**	**0**	**0**
$NaCl$	-384.1258	-411.9584	45.13074	0	0
$MgCO_3$	**-1012.1**	**-1095.8**	**75.52**	**0**	**0**
$MgCO_3 \cdot 3H_2O$	-1723.487	-1953.29	301.4968	0	0
$MgCO_3 \cdot 5H_2O$	-2197.745	-2524.95	367.367	0	0
$3MgCO_3 \cdot Mg(OH)_2 \cdot 3H_2O$	-4602.818	-5069.43	478.6986	0	0
$BaCO_3$	-1136.054	-1222.907	85.5	0	0
$SrCO_3$	-1139.745	-1227.633	1259.146863	-2.827237	-21149.44
$CaCO_3 \cdot MgCO_3$	**-2140.89**	**-2302.72**	**157.4**	**0**	**0**

5.8 References in Chapter 5

Alderman, A.R., Von der Borch, C.C., 1961. Occurrence of magnesite-dolomite sediments in South Australia. Nature 192, 861.

Anderson, G.K., 2002. Solubility of carbon dioxide in water under incipient clathrate formation conditions. J. Chem. Eng. Data 47, 219-222.

Arnorsson, E., 1989. Deposition of calcium carbonate minerals from geothermal waters. Theoretical considerations. Geothermics 18, 33-39.

Bamberger, A., Sieder, G., Maurer, G., 2000. High pressure (vapor-liquid) equilibrium in binary mixtures of (carbon dioxide + water or acetic acid) at temperatures from 313 to 353 K. Journal of Supercritical Fluids 17 (2), 97-110.

Baron, G., Favre, J., 1958. The present state of research directed to the synthesis of dolomite. Inst. Français Pétrole Rev. et Ann. Combustible Liquides 13, 1067-1085.

Baron, G., Wyart, J., 1958. Sur le role des facteurs physicochimiques dans la synthese hydrothermale de la giobertite CO_3Mg a partir des solutions de bicarbonate de magnésium. Acad. Sci. Comptes Rendís 247, 485-487.

Baron, G., 1960. Sur la synthese de la dolomite application au phenomene de dolomitisation. Revue de L' Institut Français du Pétrole 15, 3-68.

Bartholome, E., Friz, H., 1956. Solubility of carbon dioxide in water at high pressures. Chem. Ing. Tech. 28, 706-708.

Beckurts, H., 1881. Beiträge zur kenntniss der carbonate des magnesiums. Arch. Pharm. 18, 429-443.

Benes, P., Selecká, H., 1973. Ion pair formation and solubility of barium carbonate in aqueous solutions. Radiochem. Radioanal. Lett. 13, 339-348.

Berg, L.G., Borisova, L.A., 1960a. Solubility isotherms of the ternary systems Mg^{2+}, $Ca^{2+}//CO_3^{2-}$, H_2O, Na^+, $Ca^{2+}//CO_3^{2-}$, H_2O and Na^+, $Mg^{2+}//CO_3^{2-}$, H_2O at 25°C and PCO_2 = 1 atmosphere. Russian Journal of Inorganic Chemistry 5, 618-620.

Berg L.G., Borisova L.A., 1960b. Metastable equilibria in the quaternary reciprocal system Mg^{2+}, $Ca^{2+}// CO_3^{2-}$, SO_4^{2-}, H_2O at 25°C and PCO_2=1 atmosphere. Russian Journal of Inorganic Chemistry 5, 620-622.

Berner, R.A., 1967. Comparative dissolution characteristics of carbonate minerals in the presence and absence of aqueous magnesium ion. American Journal of Science 265, 45-70.

Bertram, M.A., Mackenzie, F.T., Bishop, F.C., Bischoff, W., 1991. Influence of temperature on the stability of magnesian calcite. American Mineralogist 76, 1889-1896.

Bischoff, J.L., 1968. Kinetics of calcite nucleation: magnesium ion inhibition and ionic strength catalysis. J. Geophys. Res. 73, 3315-3322.

Busenberg, E., Plummer, L.N., Parker, V.B., 1984. The solubility of strontianite ($SrCO_3$) in CO_2-H_2O solutions between 2 and 91°C, the association constants of $SrHCO_3^+$(aq) and $SrCO_3^0$(aq) between 5 and 80°C, and an evaluation of the thermodynamic properties of Sr^{2+}(aq) and $SrCO_3$(cr) at 25°C and 1 atm total pressure. Geochimica et Cosmochimica Acta 48, 2021-2035.

Busenberg, E., Plummer, L.N., 1986. The solubility of $BaCO_3$(cr) (witherite) in CO_2-H_2O solutions between 0 and 90°C, evaluation of the association constants of $BaHCO_3^+$(aq) and $BaCO_3^0$(aq) between 5 and 80°C, and a preliminary evaluation of the thermodynamic properties of Ba^{++}(aq). Geochimica et Cosmochimica Acta 50, 2225-2233.

Bär, O., 1932. Beitrag zum thema dolomitentstehung. Zentralblatt für mineralogie und paläontologie, 46-62.

Cameron, F.K., Briggs, L.J., 1901. Equilibrium between carbonates and bicarbonates in aqueous solution. The Journal of Physical Chemistry 5, 537-555.

Carpenter, A.B., 1963. Mineralogy of the system CaO-MgO-CO_2-H_2O at Crestmore, California. PhD Dissertation, Harvard University, USA.

Cesaro, G., 1910. Crystalline form and composition of hydrated carbonate magnesite. Bull. Cl. Acad. R. Belg. 4, 234-235.

Chase, M.W., 1998. NIST-JANAF Thermochemical Tables, 4th edition, J. Phys. Chem. Ref. Data, Monograph 9, 1-1951.

Christ C.L., Hostetler P.B., 1970. Studies in the system MgO-SiO_2-CO_2-H_2O (II): The activity product constant of magnesite. American Journal of Science 268, 439-453.

Corti, H.R., de Pablo, J.J., Prausnitz, J.M., 1990a. Phase equilibria for aqueous systems containing salts and carbon dioxide. Application of Pitzer's theory for electrolyte solutions. J. Phys. Chem. 94, 7876-7880.

Corti, H.R., Krenzer, M.E., de Pablo, J.J., Prausnitz, J.M., 1990b. Effect of a dissolved gas on the solubility of an electrolyte in aqueous solution. Ind. Eng. Chem. Res. 29, 1043-1050.

Cramer, S.D., 1982. The solubility of methane, carbon dioxide, and oxygen in brines from 0° to 300°C. US Bureau of Mines Report of Investigations, vol. 8706, pp.1-17.

Curry, J., Hazelton, C.L., 1938. The solubility of carbon dioxide in deuterium oxide at 25°C. J. Am. Chem. Soc. 60, 2771-2773.

Dandurand J.L., Schott J., 1977. Stabilite de la magnesite et de la dolomite; interpretation des resultats de mise en solution et de synthese par thermodiffusion. Bull. Soc. Fr. Mineral. Cristallogr. 100, 94-99.

D'Ans, J., Gloss, G., 1938. Über das $MgCO_3 \cdot 3H_2O$, neue basische Carbonate, über basische Carbonate des Magnesiumcarbonats und über basische Magnesiumsulfate. Kali 32, 155-158.

Davies, P.J., Bubela, R., 1973. The transformation of nesquehonite into hydromagnesite. Chem. Geol. 12, 289-300.

Dell, R.M., Weller, S.W., 1959. The thermal decomposition of nesquehonite, $MgCO_3 \cdot 3H_2O$, and magnesium ammonium carbonate $MgCO_3(NH_4)_2CO_3 \cdot 4H_2O$. Trans. Faraday Soc. 55, 2203-2220.

Diamond, L.W., Akinfiev, N.N., 2003. Solubility of CO_2 in water from -1.5 to 100°C and from 0.1 to 100 MPa: evaluation of literature data and thermodynamic modeling. Fluid Phase Equilibria 208 (1-2), 265-290.

Dyer, S.J., Graham, G.M., 2002. The effect of temperature and pressure on oilfield scale formation. Journal of Petroleum Science and Engineering 35, 95-107.

Ellis, A.J., 1959a. The solubility of calcite in carbon dioxide solutions. American Journal of Science 257, 354-365.

Ellis, A.J., 1959b. The solubility of carbon dioxide in water at high temperatures. American Journal of Science 257, 217-234.

Ellis, A.J., 1963. The solubility of calcite in sodium chloride solutions at high temperatures. American Journal of Science 261, 259-267.

Ellis A.J., Golding R.M., 1963. The solubility of CO_2 above 100°C in water and in NaCl solutions. American Journal of Science 261, 47-60.

Engel, M., 1889. Sur la solubilité des sels en présence des acides, des bases et de sels. Ann. Chim. Phys. 17, 349-369.

Fenoglio, M.1930. The presence of nesquehonite in the Viu serpentine of the Lanzo Valley. Atti R. Accad. Lincei, Cl. Sci. Fis. Mat. Nat., Rend. 11, 310-316.

Fenoglio, M., 1933. Lansfordite from the mine at Cogne in the Aosta Valley. Period. Mineral. 4, 433-462.

Fenoglio, M., 1935. Research on nesquehonite from the mine at Cogne in the Aosta Valley. Period. Mineral. 6, 1-17.

Fenoglio, M., 1936. Natural hydrated neutral and basic magnesium carbonates. Atti R. Accad. Lincei, Cl. Sci. Fis. Mat. Nat., Rend. 24, 219-222.

Frear, G.L., Johnston, J., 1929. Solubility of calcium carbonate in certain aqueous solutions. Journal of American Chem. Society 51, 2082-2093.

Garrels, R.M., Thompson, M.E., Siever, R., 1960. Stability of some carbonates at 25°C and one atmosphere total pressure. American Journal of Science 258, 402-418.

Garrels, R.M., Thompson, M.E., 1962. A chemical model for sea water at 25°C and one atmosphere total pressure. American Journal of Science 260, 57-66.

Geffcken, G., 1904. Beiträge zur Kenntnis der Löslichkeitsbeeinflussung. Z. Physik. Chem. 49, 257-302.

Genth, F.A., 1888. Lansfordite, a new mineral. Z. Krystallogr. Mineral. 14, 255-256.

Genth, F.A., Penfield, S.L., 1890. On lansfordite, nesquehonite, and a phseudomorph by nesquehonite on lansfordite. Z. Krytallogr. Mineral. 17, 561.

Giester, G., Lengauer, C.L., Rieck, B., 2000. The crystal structure of nesquehonite, $MgCO_3 \cdot 3H_2O$, from Lavrion, Greece. Mineral and Petrology 70, 153-163.

Giles, M., 2001. Carbonates mineral solubility at low temperatures in the Na-K-Mg-Ca-H-Cl-SO$_4$-OH-HCO$_3$-CO$_3$-CO$_2$-H$_2$O system. Geochimica et Cosmochimica Acta 65(12), 1883-1896.

Gill, J.S., 1998. Silica scale control. Chemical Treatment, 41-45.

Gillespie, P.C., Wilson, G.M., 1982. Gas Processor Association, Tulsa, Research Report RR48 (cited in Diamond and Akinfiev (2003)).

Gothe, E., 1915. Solubility of calcium carbonate and magnesium carbonate in water free from carbon dioxide, with a consideration of the s2. Chem. Ztg. 39, 305-307.

Graf, D.L., Goldsmith, J.R., 1955. Dolomite-magnesian calcite relations at elevated temperatures and CO_2 pressures. Geochimica et Cosmochimica Acta 7, 109-128.

Graf, D.L., Goldsmith, J.R., 1956. Some hydrothermal syntheses of dolomite and protodolomite. J. Geol. 64, 173-186.

Graf, D.L., Eardley, A.J., Shimp, N.F., 1961. A preliminary report on magnesium carbonate formation in Glacial Lake Bonneville. Jour. Geology 69, 219-223.

Graham, G.M., Mackay, E.J., 2003. A background to inorganic scaling-mechanisms, formation and control. 5th Intl. SPE Oilfield Scale Symposium. Aberdeen, UK.

Gurevich, V.M., Gavrichev, K.S., Gorbunov, V.E., Danilova, T.V., Golushina, L.N., Khodakovskii, I.L., 1999. Low-temperature heat capacity of witherite $BaCO_3$(c). Geochemistry International 39(10), 1007-1014.

Haehnel, O., 1924. Über die Löslichkeit det Carbonate des Strontiums, des Bariums und der Schwermetalle in Wasser unter hohen Kohlendioxyddrucken sowie über die Eigenschaften solcher Lösungen. J. Prakt. Chem. 108, 187-193.

Halla, F., Ritter, F., 1935. Eine Methode zur Bestimmung der Änderung der freien Energie bei Reaktionen des Typus A(s) + B(s) = AB(s) und ihre Anwendung auf das Dolomitproblem. Zeitschr. Phys. Chem. 175A, 63-82.

Halla, F., 1936. Mitteilungen der Wiener mineralogischen Gesellschaft. Tschermaks Mineral. Petrog. Mitt. 101, 275-278.

Halla, F., 1958. Thermodynamics of dolomite formation. I. A revision. Zeitschrift fuer Physikalische Chemie 17, 368-374.

Halla, F., Chilingar, G.V., Bissel, H.J., 1962. Thermodynamic studies on dolomite formation and their geologic implications: An interim report. Sedimentology 1, 296-303.

Halla, F., Van Tassel, R. 1964. Löslichkeitsanomalien beim Magnesit. Redes Rundschau 1, 42-43.

Harker, R.I., Tuttle, O.F., 1955. Studies in the system CaO-MgO-CO_2. Part 1. The thermal dissociation of calcite, dolomite and magnesite. American Journal of Science 235, 209-224.

Harned, H.S., Davis, R., 1943. The ionization constant of carbonic acid in water and the solubility of CO_2. J. Am. Chem. Soc. 65, 2030-2037.

Harned H.S., Bonner F.T., 1945. The first ionization of carbonic acid in aqueous solutions of sodium chloride. J. Am. Chem. Soc. 67, 1026-1031.

He S., Morse J.W., 1993. The carbonic acid system and calcite solubility in aqueous Na-K-Ca-Mg-Cl-SO_4 solutions from 0 to 90°C. Geochimica et Cosmochimica Acta 57, 3533-3554.

Harvie C.E., Möller N., Weare J.H., 1984. The prediction of mineral solubilities in natural waters: The Na-K-Mg-Ca-H-Cl-SO_4-OH-HCO_3-CO_3-CO_2-H_2O system to high temperatures and pressures. Geochimica et Cosmochimica Acta 48, 723-751.

Helz, G.R., Holland, H.D., 1965. The solubility and geologic occurrence of strontianite. Geochimica et Cosmochimica Acta 20, 1303-1315.

Holleman, A.F., 1893. Bestimmungen der Löslichkeit sogenannter Unlöslicher salze. Z. Phys. Chem. 12, 125-139.

Hostetler, P.B., 1964. The degree of saturation of magnesium and calcium carbonate minerals in natural waters. I.A.S.H. Comm. Subterranean Waters 64, 34-39.

Hsu, K.J., 1963. Solubility of dolomite and composition of Florida ground waters. Journal of Hydrology 1, 288-310.

Hähnel, O., 1920. Centr. Min. Geol. 25, 25-32 (cited in Diamond and Akinfiev (2003)).

Johnston, J., 1915. The solubility-product constant of calcium and magnesium carbonates. Jour. Am. Chem. Soc. 37, 2001-2020.

Juranek, J., Skollova, Z., Harnova, J., 1987. MINEQUA-Part I. A program for computing the chemistry of calcium carbonate in mineralized and thermal waters. Geothermics 16, 263-270.

Kapustinsky, A.F., Dezideryeva, L.P., 1946. The thermodynamics of strontium. Trans. Faraday Soc. 42, 69-77.

Katz, A., 1971. Zoned dolomite crystals. J. Geol. 79, 38-51.

Kazakov, A.V., Tikhomirova, M.M., Plotnikova, V.I., 1959. The system of carbonate equilibria. Internat. Geol. Rev. 1(10), 1-39.

Kelley and Anderson, 1935. U.S. Bureau of Mines. Bull. 384 (cited in Kapustinsky and Dezideryeva, 1946).

Kendall, J., 1912. The solubility of calcium carbonate in water. Philos. Mag. Ser. 23(6), 958-976.

Kiepe, J., Horstmann, S., Fischer, K., Gmehling, J., 2002. Experimental determination and prediction of gas solubility data for CO_2 + H_2O mixtures containing NaCl or KCl at temperatures between 313 and 393 K and pressures up to 10 MPa. Industrial & Engineering Chemistry Research 41(17), 4393-4398.

Kindyakov, P.S., Khokhlova, A.V., Lapchinskaya, L.L., 1958. Solubility in the reciprocal system lithium carbonate-calcium hydrate-water. Tr. Mosk. Inst. Tonkoi Khim. Tekhnol. 7, 32-44.

Kinsman, D.J.J., 1964. Recent carbonate sedimentation near Abu Dhabi, Trucial Coast, Persian Gulf. PhD dissertation, Imperial College, London.

Kiss, A.V., Lajtai, I., Thury, G., 1937. Über die Löslichkeit von Gasen in Wasser-Nichtelektrolytgemischen. Z. anorg. allg. Chemie 233, 346-352.

Kittrick, J.A., Peyrea, F.J., 1986. Determination of the gibbs free energy of formation of magnesite by solubility methods. Soil Sci. Soc. Am. J. 50, 243-247.

Kline, W.D., 1929. Solubility of magnesium carbonate in water and CO_2. J. Am. Chem. Soc. 51, 2093-2097.

Kohlrausch, F., Rose, F.F., 1893. Die Löslichkeit einiger schwer Löslicher Körper im Wasser, beurteilt aus der elektrischen Leitungsfähigkeit der Lösungen. Z. Physik. Chemie 12, 234-243.

Kritschewsky, I.R., Shaworonkoff, N.M., Aepelbaum, V.A., 1935. Gemeinsame Löslichkeit der Gase in Flüssigkeiten unter Druck. Zeit. Phys. Chem. A 175, 232-238.

Kunerth, W., 1992. Solubility of CO_2 and N_2O in certain solvents. Phys. Rev. 2, 512-524.

Königsberger, E., Königsberger, L-C., Gamsjäger, H., 1999. Low-temperature thermodynamic model for the system Na_2CO_3-$MgCO_3$-$CaCO_3$-H_2O. Geochimica et Cosmochimica Acta 63(19/20), 3105-3119.

Langmuir, D., 1964. Stability of carbonates in the system CaO-MgO-CO_2-H_2O. PhD dissertation, Harvard University.

Langmuir, D., 1965a. Stability of carbonates in the system MgO-CO_2-H_2O. Journal of Geology 73, 730-750.

Langmuir, D., 1965b.Stability of carbonates in the system CaO-MgO-CO_2-H_2O. Journal of Geology 73(5), 730-754.

Latimer, W.M., 1952. The oxidation states of the elements and their potentials in aqueous solutions. 2nd ed. Englewood Cliffs. N.J., Prentice Hall.

Leather, J.W., Sen, J.N., 1910. The system water, calcium carbonate, carbonic acid. Memoirs of the Department of Agriculture in India 1, 117-131.

Leather, J.W., Sen, J.N., 1914. The systems: (a) water, magnesium carbonate and carbonic acid, (b) water, calcium carbonate, magnesium carbonate and carbonic acid. Memoirs Dept. Agric. India Chem. Series 3(8), 205-221.

Leick, J., 1932. The solubilities of calcium carbonate and of magnesium carbonate in water that is free from carbonic acid. Zeitschrift für Analytische Chemie 87, 415-422.

Leitmeier, H., 1915. Zur kenntnis der carbonate II. Neues Jahrb. Mineralog., Abt. B, 655-700.

Levchenko,V.M., Minkin, M.B., Dukhina, T.P., 1970. Magnesium carbonate solubility. Pochvovedenie 8, 144-148.

Li, Y.H., Crane, S.D., Coleman, J. R., 1995. Novel approach to predict the co-precipitation of $BaSO_4$ and $SrSO_4$. SPE 29489, 447-461.

Lippmann, F., 1980. Phase diagrams depicting aqueous solubility of binary mineral systems. Neues Jahrb. Mineralog. Abh. 139, 1-25.

López Gómez, P., 1975. El sistema ternario MgO-CO_2-H_2O. Ion Revista Española de Química Aplicada 35, 417-430.

Lyashchenko, A. K., Churagulov, B. R., 1981. Influence of pressure on the temperature coefficients of the solubility of electrolytes in water. Russ. J. Inorg. Chem. 26, 642-644.

MacDonald, R.W., North, N.A., 1974. The effect of pressure on the solubility of $CaCO_3$, CaF_2 and $SrSO_4$ in water. Can. J. Chem. 52, 3181-3186.

Malegaonkar, M.B., Dholabhai, P.D., Bishnoi, P.R., 1997. Kinetics of carbon dioxide and methane hydrate formation. The Canadian Journal of Chemical Engineering 75, 1090-1099.

Malinin, S.D., 1963. An experimental investigation of the solubility of calcite and witherite under hydrothermal conditions. Geokhimiia 650-667, 631-645.

Malinin, S. D., Savel'eva, N. I., 1972. Carbon dioxide solubility in sodium chloride and calcium chloride solutions at temperatures of 25, 50, and 75.deg. and elevated carbon dioxide pressure. Geokhimiya, 643-653.

Malinin, S. D., Kurovskaya, N. A., 1975. Carbon dioxide solubility in solutions of chlorides at elevated temperatures and carbon dioxide pressure. Geokhimiya, 547-550.

Marck, R., Simek, A., 1913. Über die thermische dissoziation des magnesiumkarbonats. Zeitschr. Anorg. Chem 82, 17-49.

Markham, A.E., Kobe, K.A., 1941a. The solubility of carbon dioxide and nitrous oxide in aqueous salt solutions. J. Am. Chem. Soc. 63, 449-454.

Markham, A.E., Kobe, K.A., 1941b. The solubility of carbon dioxide in aqueous H_2SO_4, $HClO_4$. J. Am. Chem. Soc. 63, 1165-1166.

Matous, J., Sobr, J., Novak, J.P., Pick J., 1969. Solubility of carbon dioxide in water at pressures up to 40 atm. Collection Czechoslav. Chem. Commun. 34, 3982-3985.

McCoy, H.N., Smith, H.J., 1911. Equilibrium between alkali-earth carbonates, carbon dioxide and water. J. Am. Chem. Soc. 33, 468-476.

Merkel, 1924. Wagners Jahresbericht der Chemie 13, 213.

Miles, D.L., Burton, J.D., 1972. The solubility of strontium carbonate in water. Journal of the Chemical Society, Dalton Transactions, 1691-1692.

Miller, J.P., 1952. A Portion of the system calcium carbonate-carbon dioxide-water, with geological implications. Am. J. of Science 250, 161-203.

Millero, F.J., Milne, P.J., Thurmond, V.L., 1984. The solubility of calcite, strontianite, and witherite in NaCl solutions at 25°C. Geochimica et Cosmochimica Acta 48, 1141-1143.

Ming, D.W., Franklin, W.T., 1985. Synthesis and characterization of lansfordite and nesquehonite. Soil Science Society of American Journal 49, 1303-1308.

Mitchell, A.E., 1923. Studies on the dolomite system. Part II. J. Chem. Soc. 123, 1887-1904.

Morandi, M., 1969. La dissociazione termica dell'Idromagnesite e della Nesquehonite. Mineral. Petrogr. Acta 15, 93-108.

Moressée, M., Cesaro, G., 1910. Forme cristalline et composition du carbonate magnésique hydraté préparé par M. Moressée. Sa relation avec la Lansfordite. Bull. Acad. Roy. Belg., 234-265.

Morey, G.W., 1962. The action of water on calcite, magnesite, and dolomite. American Mineralogist 47, 1456-1460.

Morgan, O.M., Maass, O., 1931. An investigation of the equilibria existing in gas-water systems forming electrolytes. Canadian journal of research 5, 162-199.

Morrison, T.J., Billett, F., 1952. The salting-out of non-electrolytes. Part I. The effect of ionic size, ionic charge, and temperature. Journal of Chemical Society, 3814-3822.

Murray, C.N., Riley, J.P., 1971. The solubility of gases in distilled water and sea water IV. Carbon dioxide. Deep-Sea Research 18, 533-541.

Müller, G., Bender, E., Maurer,G., 1988. The vapor-liquid equilibrium of the ternary system ammonia-carbon dioxide-water for high water concentrations at 373-473 K. Ber. Bunsenges. Phys. Chem. 92, 148-160.

Naumov, V.B., Khakimov, A.K., Khodakovskii, I.L., 1974. Solubility of carbon dioxide in concentrated chloride solutions at high temperatures and pressures. Geokhimiya 1, 45-55.

Navrotsky, A., Capobianco, C., 1987. Enthalpies of formation of dolomite and of magnesian calcites. American Mineralogist 27, 782-787.

Nighswander, J.A., Kalogerakis, N., Mehrota, A.K., 1989. Solubilities of carbon dioxide in water and 1 wt% NaCl. J. Chem. Eng. Data 34, 355-360.

NIST Chemical Thermodynamics Database Version 1.1, 1990. U.S. Department of Commerce, National Institute of Standards and Technology, Gaithesburg MD 20899.

NIST Standard Reference Database Number 69, 2003. NIST Chemistry Book (http://webbook.nist.gov/chemistry/).

Novak, J., Fried, V., Pick, J., 1961. Löslichkeit des Kohlendioyds in Wasser bei verschiedenen Drücken und Temperaturen. Collect. Czech. Chem. Commun. 26, 2266-2270.

Oleinik, P.M. Neftepromyslovoe Delo 8, p.7 (cited in Diamond and Akinfiev (2003)).

Onda K., Sada E., Kobayashi T., Kito S., Ito K., 1970. Salting out-parameters of gas solubility in aqueous salt solutions. Journal of Chemical Engineering of Japan 3, 18-24.

Palache, C., Berman, H., Frondel, C., 1951. The system of mineralogy, vol. 2, 7th edition, New York, John Wiley and Sons.

Patterson, C.S., Slocum, G.H., Busey, R.H., Mesmer, R.E., 1982. Carbonate equilibria in hydrothermal systems: First ionization of carbonic acid in NaCl media to 300°C. Geochimica et Cosmochimica Acta 46, 1653-1663.

Patterson C.S., Busey R.H., Mesmer R.E., 1984. Second ionization of carbonic acid in NaCl media to 250°C. J. Solution Chemistry 13, 647-661.

Pfaff, F.W., 1894. Beiträge zur Erklärung über die Entstehung des Magnesits und Dolomits. Neues Jahrb. Mineralog, 485-507.

Pitzer, K.S., 1973. Thermodynamics of electrolytes I. Theoretical basis and general equations. J. Phys. Chem. 77, 268-277.

Plummer, L.N., Busenberg, E., 1982. The solubilities of calcite, aragonite and varetite in CO_2-H_2O solutions between 0 and 90°C, and an evaluation of the aqueous model for the system $CaCO_3$-CO_2-H_2O. Geochimica et Cosmochimica Acta 46, 1011-1040.

Plummer, L.N., Mackenzie, F.T., 1974. Predicting mineral solubility from rate data: application to the dissolution of magnesian calcites. American Journal of Science 274, 61-83.

Poitevin, E., 1924. A new occurrence of landsfordite from Atlin, BC. Am. Mineral. 9, 225-228.

Ponizovskii, A.M., Vladimirova, N.M., 1959. Solubility of the system Na, Mg, Cl, HCO_3 - H_2O. Dokl. Akad. Nauk. SSSR 126(1), 345-346.

Ponizovskii, A.M., Vladimirova, N.M., Gordon-Yanovskii, F.A., 1960. The solubility relation in the system Na, Mg-Cl, HCO_3-H_2O at 0°C with carbon dioxide at 4 and 10 kg/cm^2. Russ. J. Inorg. Chem. 5, 1250-1252.

Postigo, M.A., Pedrosa, G., Katz, M., 1978. Nuevo método experimental para la determinación de solubilidad de gases en líquidos. Anales Asoc. Quim. Argentina 66, 25-30.

Potatov, V.V., Kashpura, V.N., Alekseev, V.I., 2001. A study of the growth of deposits in geothermal power systems. Thermal Engineering 48 (5), 395-400.

Prutton, C.F., Savage, R.L., 1945. The solubility of carbon dioxide in calcium chloride-water solutions at 75, 100, 120°C and high pressures. J. Am. Chem. Soc. 67, 1550-1154.

Raade, G., 1970. Dypingite, a new hydrous basic carbonate of magnesium from Norway. Am. Min. 55, 1457-1465.

Riesen, W.F., 1969. Thermodynamische Untersuchungen am quaternären System Ca^{2+}-Mg^{2+}-CO_2-H_2O. PhD thesis. Universität Bern.

Robie, R.A., 1965. Heat and free energy of formation of herzenbergite, troilite, magnesite, and rhodochrosite calculated from equilibrium data. U.S. Geol. Survey 525, 65-72.

Robie, R.A., Hemingway, B.S., 1972. The heat capacities at low-temperatures and entropies at 298.15 K of nesquehonite, $MgCO_3 \cdot 3H_2O$, and hydromagnesite, $5MgO \cdot 4CO_2 \cdot 5H_2O$. Am. Mineral. 57, 1768-1781.

Robie, R.A., Hemingway, B.S., 1973. The enthalpies of formation of nesquehonite, $MgCO_3 \cdot 3H_2O$, and hydromagnesite, $5MgO \cdot 4CO_2 \cdot 5H_2O$. J. Res. U.S. Geol. Survey 1, 543-547.

Robie, R.A., Hemingway, B.S., Fisher, J.R., 1978. Thermodynamic properties of minerals and related substances at 298.15 K and 1 bar (10^5 Pascals) pressure and at higher temperatures. USGS Bull. 1452, U.S. Government Printing Office, Washington, D.C., pp. 456.

Robie, R.A., Hemingway, B.S., 1995. Thermodynamic properties of minerals and related substances at 298.15K and 1 Bar (10^5 Pascals) pressure and at higher temperatures. U.S. Geol. Survey Bull. 2131.

Robie, R.A., Waldbaum, D.R., 1965. Thermodynamic properties of minerals at high temperature and one atmosphere pressure. U.S. Geol. Survey Bull., 1-256.

Rossini and Bichowsky, 1936. Thermochemistry (cited in Kapustinsky and Dezideryeva, 1946).

Rossini, F.D., Wagman, D.D., Evans, W.H., Levine, S., Jaffe, I., 1961. Selected values of chemical thermodynamic properties. Part I. Tables: U.S. Natl. Bur. Standard Circ. 500.

Rosenberg, P.E., Holland, H.D., 1964. Calcite-Dolomite-Magnesite stability relations in solutions at elevated temperatures. Science 145(1), 700-701.

Rosenberg, P.E., Burt, D.M., Holland, H.D., 1967. Calcite-dolomite-magnesite stability relations in solutions: the effect of ion strength. Geochimica et Cosmochimica Acta 31, 391-396.

Rumpf B., Maurer G., 1993. An experimental and theoretical investigation on the solubility of carbon dioxide in aqueous solutions of strong electrolytes. Ber. Bunsenges. Phys. Chem. 97(1), 85-97.

Rumpf, B., Nicolaisen, H., Öcal, C., Maurer, G., 1994. Solubility of carbon dioxide in aqueous solutions of sodium chloride: experimental results and correlation. J. Solution Chemistry 23, 431-448.

Sander, W., 1912. Über die Löslichkeit der Kohlensäure in Wasser und einigen andern Lösungsmitteln unter höhern Drüken. Z. physik. Chem. 78, 513-549.

Sayles, F.L., Fyfe, W.S., 1973. The crystallization of magnesite from aqueous solution. Geochimica et Cosmochimica Acta 37, 87-99.

Schaller, W.T., Henderson, E.P., 1932. Mineralogy and drill cores from the potash field of New Mexico and Texas. U.S. Geol. Survey Bull. 833, pp. 124.

Schloemer, H., 1952. Hydrothermal studies in the system CaO-MgO-CO_2-H_2O. Neues Jahrb. Mineral. Monatshefte, 129-135.

Schloesing. 1872. Compt. Rend. 74, 1552-1556.

Schott, J., Dandurand, J.L., 1975. Stability of natural carbonates. New values for the free energies of formation of phases in the MgO-CO_2-H_2O and CaO-MgO-CO_2-H_2O systems. C.R. Hebd. Seances Acad. Sci., Ser. C 280 (1). 1247-1250.

Segnit, E.R., Holland, H.D., Biscardi, C. J., 1962. The solubility of calcite in aqueous solutions - I. Geochimica et Cosmochimica Acta 26, 1301-1331.

Servio, P., Englezos, P., 2001. Effect of temperature and pressure on the solubility of carbon dioxide in water in the presence of gas hydrate. Fluid Phase Equilibria 190, 127-134.

Seyler, C.A., Lloyd, P.V., 1917. Studies of the carbonates. Part III. Lithium, calcium, and magnesium carbonates. Journal of Chemical Society 111, 994-1001.

Shagiakhmetov, R.A., Tarzimanov, A.A., 1981.Deposited document SPSTL200khp-D81-1982 (cited in Diamond and Akinfiev (2003)).

Shams El Din, A.M., Mohammed, R.A., 1989. The problem of alkaline scale formation from a study on Arabian Gulf water. Desalination 71, 313-324.

Sharp, W.E., Kennedy, G.C., 1965. The system CaO-CO_2-H_2O in the two phase region calcite + aqueous solution. J. Geol. 60, 391-403.

Sippel, R.F., Glover, E.D., 1964. The solution alteration of carbonate rocks. The effects of temperature and pressure. Geochimica et Cosmochimica Acta 28, 1401-1417.

Soave, G., 1972. Equilibrium constants from a modified Redlich-Kwong equation of state. Chem. Eng. Sci. 27, 1197-1203.

Sonderegger, J.L., Brower, K.R., LeFebre, V.G.A., 1976. A preliminary investigation of strontianite dissolution kinetics. Amer. J. Sci. 276, 997-1022.

Sorbie, K.S., Mackay, E.J., 2000. Mixing of injected, connate and aquifer brines in waterflooding and its relevance to oilfield scaling. Journal of Petroleum Science and Engineering 27, 85-106.

Stewart, F.H., 1949. The petrology of the evaporates of the Eskdale No. 2 boring east Yorkshire, pt. I. The lower evaporate bed. Mineralog. Mag. (London) 28 (206), 621-675.

Stewart, P.B., Munjal, P., 1970. Solubility of carbon dioxide in pure water, synthetic sea water, and synthetic sea water concentrates at -5° to 25°C and 10 to 45 atm pressure. Journal of Chemical and Engineering Data 15, 67-71.

Sureau, J.F., 1974. Étude expérimentale de la dolomitisation de la calcite. Bull. Soc. Fr. Minéral. Cristallogr. 97, 300-312.

Takahashi, G., 1927. Investigation on the synthesis of potassium carbonate by Mr. Engel. Bull. Imp. Hyg. Lab. (Tokyo) 29, 165-262.

Takenouchi, S., Kennedy, G.C., 1964. The binary system H_2O-CO_2 at high temperatures and pressures. American Journal of Science 262, 1055-1074.

Takenouchi, S., Kennedy, G.C., 1965. The solubility of carbon dioxide in NaCl solutions at high temperatures and pressures. American Journal of Science 263, 445-454.

Teng, H., Yamasaki, M., Chun, K., Lee, H., 1997. Solubility of liquid CO_2 in water at 2 temperatures from 278K to 293K and pressures from 6.44 Pa to 29.49 MPa and densities of the corresponding aqueous solutions. J. Chem. Thermodyn. 29, 1301-1310.

Thomsen, K., Rasmussen, P., 1999. Modeling of vapor-liquid-solid equilibrium in gas-aqueous electrolyte systems. Chemical Engineering Science 54, 1787-1802.

Thurmond, V.L., Millero, J.F., 1982. Ionization of carbonic acid in sodium chloride solutions at 25°C. J. Soln. Chem. 11, 447-456.

Townley, R.W., Whitney, W.B., Felsing, W.A., 1937. The solubilities of barium and strontium carbonates in aqueous solutions of some alkali chlorides. J. Amer. Chem. Soc. 59, 631-633.

Travers, A., Nouvel, 1929. Sur la solubilité de $Mg(OH)_2$ aux temperatures élevés. Compt. Rend. Hebd. 188, 499-501.

Treadwell, F.P., Reuter, M., 1898. Über die Löslichkeit der Bikarbonate des Calciums und Magnesiums. Zeitschrift fur Anorganische Chemie 17, 171-204.

Trendafelov, D., Balarew, C., Zlateva, I., Keremidtchieva, B., Gradinarov, S., 1994. Investigations of the $BaSO_4$ conversion to $BaCO_3$ in the quaternary reciprocal water-salt system $BaSO_4 + K_2CO_3 = BaCO_3 + K_2SO_4$. Comptes Rendus de l'Academie Bulgare des Sciences 47 (1), 47-50.

Tödheide, K., Franck, E.U., 1963. Das Zweiphasengebiet und die kritische Kurve im System Kohlendioxid-Wasser bis zu drucken von 3500 bar. Z. Phys. Chem. 37, 387-401.

Van Slyke, D.D., 1939. Determination of solubilities of gases in liquids with use of the Van Slyke-Neill manometric apparatus for both saturation and analysis. J. Biol. Chem. 130, 545-554.

Vazquez, G., Chenlo, F., Pereira, G., Peaguda, J., 1994. Carbon dioxide solubility in aqueous solutions of sodium chloride, copper (II) sulfate, potassium iodide and sodium bromide. Anales de Química 90(5-6), 324-328.

Vilcu, R., Gainar, I., 1967. Löslichkeit der gase unter druck in flüssigkeiten. I. Das system kohlendioxid-wasser. Rev. Roum. Chim. 12(2), 181-189.

Wat, R.M.S., Sorbie, K.S., Todd, A.C., Chen, P., Jiang, P., 1992. Kinetics of $BaSO_4$ crystal growth and effect in formation damage. SPE 23814, 429-437.

Wasmund, R., Bultmann, H., 1980. Einfluss des Saccharosegehalts auf die CO_2-Absorption wässriger Lösungen. Zuckerind. 105, 1085-1087.

Wattenberg, V.H., Timmermann, E., 1937. Die Löslichkeit von Magnesiumkarbonat und Strontiumkarbonat in Seewasser. Kieler Meeresforschungen 2(1), 81-94.

Wells, R.C., 1915a. The solubility of calcite in water in contact with the atmosphere, and its variation with temperature. J. Washington Academy of Sciences 5, 617-622.

Wells, R.C., 1915b. Solubility of magnesium carbonate in natural water. Journal of American Chemical Society 37, 1704-1707.

Weyl, P.K., 1959. The change in solubility of calcium carbonate with temperature and carbon dioxide content. Geochimica et Cosmochimica Acta 17, 214-225.

Wiebe, R., Gaddy, V.L., 1939. The solubility in water of carbon dioxide at 50, 75 and 100°C, at pressures to 700 atmosferes. J. Am. Chem. Soc. 61, 313-318.

Wiebe, R., Gaddy, V.L., 1940. The solubility of carbon dioxide in water at various temperatures from 12 to 40°C and at pressures to 500 atm. J. Am. Chem. Soc. 62, 815-817.

Wolf, M., Breitkopf, O., Puk, R., 1989. Solubility of calcite in different electrolytes at temperatures between 10 and 60°C and at CO_2 partial pressures of about 1kPa. Chemical Geology 76, 291-301.

Wroblewski, S.V., 1883. Ann. Phys. Chem.18, 290-308 (cited in Diamond and Akinfiev (2003)).

Yanat'eva O.K., 1949. Solubility in the system Ca, Mg / CO_3, SO_4-H_2O. Doklady Akademiia Nauk SSSR, 479-481.

Yanat'eva O.K., 1952. Solubility of dolomite in water salt solutions. Akad. Nauk SSSR 20, 252-286.

Yanat'eva, O.K., 1954. Solubility in the system $CaCO_3$-$MgCO_3$-H_2O at different temperatures and pressures of CO_2. Doklady Akad. Nauk. SSSR 96, 777-779.

Yanat'eva, O.K., 1955a. Solubility isotherms at 0 and 55°C for the system Ca, Mg$\|CO_3$, SO_4-H_2O. Akad.Nauk SSSR 26, 266-269.

Yanat'eva, O.K., 1955b. Solubility in the system $CaCO_3$-$MgCO_3$-H_2O at different temperatures. Zhurnal Neorganicheskoi Khimii 1, 1473-1476.

Yanat'eva O.K., Danilova E.P., 1956. Application of the solubility diagram of the system $CaCO_3$-$MgCO_3$-H_2O for the characterization of certain carbonate rocks. Zhurnal Prikladnoi Khimii 29, 1152-1159.

Yanat'eva, O.K., 1957a. Solubility polytherms of the system $(CaCO_3 + MgSO_4 \| CaSO_4 + MgCO_3)$-$H_2O$. Doklady-Akademii Nauk SSSR 112, 1056-1058.

Yanat'eva, O.K., 1957b. Solubility of the System Ca,Mg-CO_3, SO_4-H_2O at 25°C and PCO_2 of 0.0012atm. Zh. Neorgan. Khim. 2(9), 2183-2187.

Yanat'eva, O.K., 1960. The 70°C solubility isotherm of the Ca-Mg-CO_3-SO_4-H_2O system. Russian Journal of Inorganic Chemistry 5, 1247-1250.

Yanat'eva, O.K., Rassonskaya, I.S., 1961. Metastable equilibria and solid phases in the $CaCO_3$-$MgCO_3$-H_2O system. Russian Journal of Inorganic Chemistry 6, 730-733.

Yanat'eva, O.K., Rapoport, G.S., Rassonskaya, I.S., Ustinova, M.B., 1961. Physicochemical studies of calcium and magnesium carbonates applicable to the production of Sovelite. Zhurnal Prikladnoi Khimii 34, 2347-2350.

Yang, S.O., Yang, I.M., Kim, Y.S., Lee, C.S., 2000. Measurement and prediction of phase equilibria for water + CO_2 in hydrate forming conditions. Fluid Phase Equilibria 175, 75-89.

Yasunishi A., Tsuji M., Sada E., 1979. Solubility of CO_2 in aqueous mixed salt solutions. Advances in Chemistry Series 177, 189-203.

Yasunishi A., Yoshida F., 1979. Solubility of carbon dioxide in aqueous electrolyte solutions. Journal of Chemical and Engineering Data 24, 11-14.

Yeh, S.-Y., Peterson R.E., 1964. Solubility of carbon dioxide, krypton, and xenon in aqueous solutions. Journal of Pharmaceutical Sciences 53, 822-824.

Yuan, M., Todd, A.C., Sorbie, K.S., 1994. Sulfate scale precipitation arising from seawater injection: a prediction study. Marine and Petroleum Geology 11(1), 24-30.

Yuan, M.D., Anderson, M., Jamieson, E., 1997. Investigation and improvement of $BaSO_4$ scale inhibition tests. Society of Petroleum Engineers 37304, 765-768.

Zawisza, A., Malesinska, B., 1981. Solubility of carbon dioxide in liquid water. J. Chem. Eng. Data 26, 388-391.

Zelvenskii, Y.D., 1937. The solubility of carbon dioxide under pressure. Jour. Chem. Industry 14, 1250-1257.

Zheng, D-Q., Tain-Min, G., Knapp, H., 1997. Experimental and modeling studies on the solubility of CO_2, $CHClF_2$, CHF_3, $C_2H_2F_4$ and $C_2H_4F_2$ in water and aqueous NaCl solutions under low pressures. Fluid Phase Equilibria 129, 197-209.

6. Sodium Chloride

This chapter will analyze the performance of extended UNIQUAC for the system NaCl-H_2O at high pressure. This work has been submitted for publication as part of the paper titled "Prediction of mineral scale formation in geothermal and oilfield operations using the extended UNIQUAC model. Part II. Carbonate scaling minerals" in Geothermics (authors: Ada Villafáfila García, Kaj Thomsen and Erling H. Stenby).

6.1 NaCl-H_2O System

The volume and surface area parameters for Na^+ and Cl^-, together with all the binary interaction parameters required for the binary system NaCl-H_2O were reported in a previous paper (Thomsen and Rasmussen, 1999). Only the pressure parameters α and β for NaCl need therefore to be estimated on the basis of SLE data at high pressures. Values for these parameters are given in tables 5-15 to 5-18 in Chapter 5. The values for the standard state Gibbs free energy, enthalpy, and heat capacity for NaCl are reported in table 5-19.

The few studies found on the solubility of sodium chloride in pure water at pressures larger than the atmospheric pressure are reported in table 6-1. The experimental conditions and the number of measurements carried out and used in the present work (in brackets) are also given.

Table 6-1
Experimental NaCl-H_2O SLE data sets used for parameter estimation.

T (°C)	P (bar)	Number of data	AAD (m)	Reference
0/30	1/40	14 (14)	2.2E-02	Moeller (1862)
24	1/1500	10 (8)	6.6E-03	Cohen et al. (1911)
25	1/735.5	7 (7)	1.3E-02	Sill (1916)
30	1/1911	14 (6)	7.2E-03	Adams and Hall (1931)
75/300	1/57.5	9 (9)	5.1E-01	Liu and Lindsay (1972)
101.9/168.3	1/5.3	2 (2)	1.1E-01	Eddy and Menzies (1940)
150/350	3.5/137.7	8 (7)	4.4E-01	Schroeder et al.(1935)
183/646.2	7.3/405.8	18 (0)		Keevil (1942)
			$MAAD$ (m):	1.6E-01

Cohen et al. (1911) withdrew samples for analysis after reducing the experimental pressure, a procedure which can lead to solid deposition and can cause erroneous measurements. Sill (1916) realized this problem and developed a new pressure bomb to avoid it. The agreement

between both sources is very good, which seems to prove the results from Cohen et al. (1911) were not affected by solid deposition prior to solubility analysis.

Liu and Lindsay (1972) compared their results with those by Keevil (1942) and Seidell[1] (1965), and assured the agreement among the different sources is very good. They chose for comparison a plot of the solubility expressed as log(molality) versus temperature. When the plot units are changed to molality instead, it can be clearly observed that there is a large disagreement between Keevil (1942) and Liu and Lindsay (1972), with solubility differences as large as 1.75 m NaCl around 250°C. Keevil (1942) also disagrees with the data by Schroeder et al. (1935), and it can be concluded that Keevil's (1942) solubility measurements are considerably lower than the main tendency followed by the other sources reported in table 6-1. Keevil (1942) determined the vapour pressure of sodium chloride solutions at high temperatures. According to him, the experimental method used afforded an approximate measure of the solubility, useful in confirming the solubility curves at high temperatures. But it may be possible that the accuracy is not high enough to use those solubility data for parameter estimation.

Schroeder et al. (1935) reported both experimental temperature and NaCl solubility, but they did not mention the experimental pressure (which was the saturation pressure of the solution). In order to use these data, the total pressure was calculated from:

$$P = a_w P_w^{sat}$$
(6-1)

where P_w^{sat} is the saturation pressure for pure water at temperature T. The water activity was calculated according to the NaCl model presented by Archer (1992). The saturation pressure of water was calculated by the NIST/ASME steam properties formulation for general and scientific use (Harvey et al., 1996).

Some sources (Cohen et al., 1911, Adams and Hall, 1931 and Schroeder et al., 1935) determined sodium chloride solubility in pure water at temperatures or pressures above the range of interest in the present paper. That explains why the number of points used for parameter estimation is in many cases lower than the number of points reported.

The results obtained for the system NaCl-H_2O at high pressure can be divided into two different groups: up to 150°C, and from 150 to 300°C. For the first data set, the results obtained are very satisfactory, with a mean average absolute deviation between extended UNIQUAC calculations and the experimental data ($1.5 \cdot 10^{-3}$ m) lower than the average

---

[1] Seidell (1965) did not perform any experiment himself, but compiled data from Cohen et al. (1911), Sill (1916), and Adams and Hall (1931).

experimental standard deviation ($7.6 \cdot 10^{-3}$ m). Therefore, we can conclude that the calculations for the temperature range 0-150°C are within experimental accuracy.

Figure 6-1, the solubility diagram for the binary NaCl-H_2O system at 30°C, shows such good accuracy. Even though only experimental data up to 1000 bar were used for parameter estimation (higher pressures are difficult to find in geothermal and oil wells), figure 6-1 shows data up to 2000 bar. The prediction done by the extended UNIQUAC model for so large pressures is very good. Therefore, it can be concluded that although the parameters are estimated from data up to 1000 bar, the range of applicability is not limited to that pressure. The predictions performed by the extended UNIQUAC model in the pressure range from 1000 to around 2000 bar are within the experimental accuracy. The mean average absolute deviation between our calculations and the experimental data (8 points reported by Adams and Hall, 1931; and 2 points reported by Cohen et al., 1911) is $2.2 \cdot 10^{-3}$ m NaCl, well below the *ASD* of $7.6 \cdot 10^{-3}$ m.

Figure 6-1 also shows that the influence of pressure on sodium chloride solubility is not strong, as it only increases from 6.17 m NaCl at 1 bar to 6.45 m NaCl at 2000 bar. About 16 gram of salt will therefore precipitate from each kilo of water saturated with NaCl at 2000 bar if the pressure is reduced to atmospheric pressure.
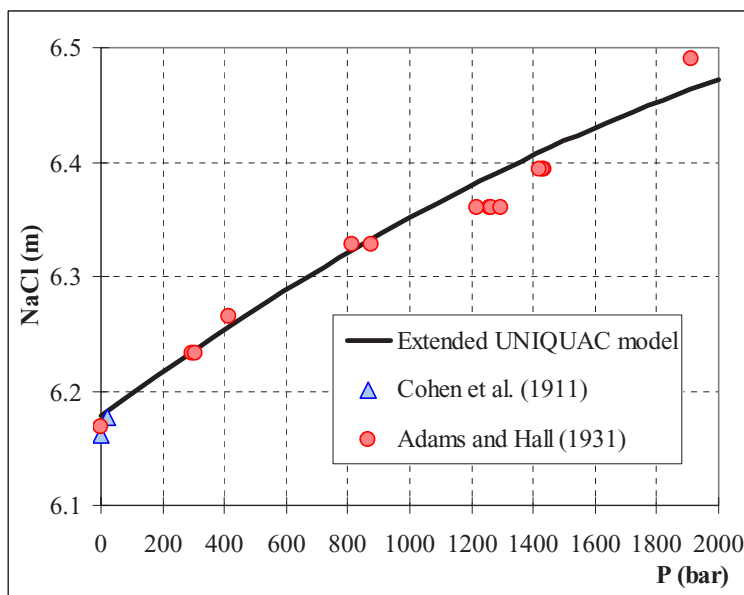

Figure 6-1. Experimental and calculated solid-liquid phase diagram for the NaCl-H_2O system at 30°C

The good agreement between the model and the experimental data from the first data set is not found for the second data set, which covers the temperature range from 150 to 300°C. The *MAAD* between the extended UNIQUAC calculations and the experimental data at high temperatures is $5.3 \cdot 10^{-1}$ m, which is larger than the *ASD*. There are only three sources covering that range of temperatures (Schroeder et al., 1935, Eddy and Menzies, 1940 and Liu and Lindsay, 1972). Schroeder et al. (1935) and Liu and Lindsay (1972) report solubility values quite close at similar *T* and *P* conditions. The latter investigators did not measure the solubility experimentally. Instead, they used an indirect method to obtain, from vapour pressure data, values for both the osmotic coefficient and concentration of saturated solutions. Liu and Lindsay (1972) claim that their method gives considerable precision. The lack of additional information on the system at high temperatures makes it difficult to determine the reliability of both datasets.

The *AAD* for each one of the sources used for the NaCl-H_2O system is shown in table 6-1. The *ASD* found for the experimental data at pressures higher than 1 atm is $7.6 \cdot 10^{-2}$ m NaCl, while the *ASD* for data at atmospheric pressure was calculated to be $5.3 \cdot 10^{-2}$ m. According to the International Critical Tables (1928), the solubility of sodium chloride in water is estimated experimentally with an accuracy of 0.2% ($3.4 \cdot 10^{-2}$ m) below 55°C and 1 atm, and of 0.5% ($8.6 \cdot 10^{-2}$ m) in the range 60 to 110°C. Above this temperature the accuracy is unknown (Eddy and Menzies, 1940). It is likely that the standard deviation at pressures higher than 1 atm is larger than those values, as the experimental conditions imply a higher difficulty. For all the sources in table 6-1 the *AAD* is lower than the *ASD*, except for Schroeder et al. (1935), Eddy and Menzies (1940) and Liu and Lindsay (1972), which happen to be the sources reporting experimental data at the highest temperatures.

The results obtained by the extended UNIQUAC model at atmospheric pressure and temperatures up to 110°C, and the sources at those conditions, are not mentioned here due to space considerations. Nevertheless, all the calculations performed at atmospheric pressure are within experimental accuracy. The mean average absolute deviation between extended UNIQUAC calculations and the experimental data for all the sources employing atmospheric pressures is $4.6 \cdot 10^{-2}$ m NaCl, while the average standard deviation for those experimental data is higher ($5.3 \cdot 10^{-2}$ m).

6.2 References in Chapter 6

Adams, L.H., Hall, R.E., 1931. The influence of pressure on the solubility of sodium chloride in water. A new method for the measurement of the solubilities of electrolytes under pressure. Journal of the Washington Academy of Sciences 21(9), 183-194.

Archer, D.G., 1992. Thermodynamic properties of NaCl+H_2O system II. Thermodynamic properties of NaCl (aq), NaCl·$2H_2O$ (c), and phase equilibria. J. Phys. Chem. Ref. Data 21, 793-829.

Cohen, E., Inouye, K., Euwem, C., 1911. Piezochemische studien VII. Z. Physik. Chem. 75, 257-304.

Eddy, R.D., Menzies, A.W.C., 1940. The solubilities of certain inorganic compounds in ordinary water and in deuterium water. J. Phys. Chem. 44, 207-235.

Harvey, A.H., Perskin, A.P., Klein, S.A., 1996. NIST/ASME steam properties formulation for general and scientific use.

International Critical Tables, 1928. Vol. 3. McGraw-Hill Book Co., New York, pp.369.

Keevil, N.B., 1942. Vapor pressures of aqueous solutions at high-temperatures. J. Am. Chem. Soc. 64, 841-850.

Liu, C-T., Lindsay, W.T., 1972. Thermodynamics of sodium chloride solutions at high temperatures. Journal of Solution Chemistry 1(1), 45-69.

Moeller, 1862. Ueber den Einflufs der Drucke auf die Löslichkeit einiger Salze. Annals of Physics 117, 386-416.

Schroeder, W.C., Gabriel, A., Partridge, E.P., 1935. Solubility equilibria of sodium sulfate at temperatures of 150 to 350°C. I. Effect of sodium hydroxide and sodium chloride. Journal of the American Chemical Society 57, 1539-1546.

Seidell, A., 1965. Solubilities of inorganic and metal-organic compounds. Am. Chem. Soc., 4th ed., vol. 2, pp. 959.

Sill, H., 1916. The influence of pressure on solubility. Journ. Am. Chem. Soc. 38, 2632-2643.

Thomsen, K., Rasmussen, P., 1999. Modeling of vapor-liquid-solid equilibrium in gas-aqueous electrolyte systems. Chemical Engineering Science 54, 1787-1802.

7. Prediction of Scaling Minerals Solubilities in Natural Waters: Validation of the Model

The ability of the model to simulate within experimental accuracy the solubility behaviour of scaling minerals in binary, ternary and quaternary systems, from -20 to 300ºC, and up to 1000 bar, has been demonstrated in Chapters 4 to 6. In this chapter, the model will be validated by comparing our predictions to independent real natural waters data that were not used during the parameterization process. The brine compositions and observed scale occurrences were collected from published data (Mitchell et al., 1980, Jacques and Bourland, 1983, Yuan and Todd, 1991, Yuan et al., 1993).

The solid-liquid, vapour-liquid and speciation equilibria calculations explained in Chapter 3 have been implemented into SPECS (Separation and Phase Equilibrium Calculations). The program has been developed at IVC-SEP and is provided with a friendly user interface which allows the user to perform a great variety of tasks, including several equations of states and excess models, and a wide database of 100 components (http://www.ivc-sep.kt.dtu.dk/research/specs.htm). For electrolyte systems, the user can select up to 8 different ions among the species H_2O, $CO_2(aq)$, Na^+, K^+, Mg^{2+}, Ca^{2+}, NH_4^+, Ba^{2+}, H^+, Cu^{2+}, Ni^{2+}, Sr^{2+}, Fe^{2+}, Zn^{2+}, Mn^{2+}, Co^{2+}, Cl^-, SO_4^{2-}, NO_3^-, OH^-, CO_3^{2-}, HCO_3^-, SO_3^-, HSO_3^-, and $S_2O_5^{2-}$. Two different tasks are available: Calculation of binary, ternary and quaternary phase diagrams at constant pressure, and scale predictions for a given composition, temperature and pressure. In the latter case, the output file reports the solubility indices of the different salts forming the feed stream, and the precipitating minerals at equilibrium. The maximum amount of solid phase(s) precipitating is also reported. As a scaling prediction model, SPECS is useful to determine whether scale may occur at certain locations within the reservoir, and the maximum amount of precipitation to be expected. The model cannot directly predict the scaling rate, but it may be also useful in that sense as it determines the degree of supersaturation. SPECS determines the solid phase(s) precipitating at thermodynamic equilibrium. Whether that(those) phase(s) precipitate in reality or not is also determined by many other factors as kinetics. Therefore, it may be possible that any other salts which is supersaturated in the feed stream precipitates instead of that found at thermodynamic equilibrium.

7.1 Validation of the Model

Jacques and Bourland (1983) predicted celestite scaling tendency in three brines from the same field using an empirical equation developed from their own solubility measurements. Yuan and Todd (1991) also tested the scaling tendency in those waters using the model they developed for barium, strontium, and calcium sulphates based on Pitzer's framework. The results obtained by Jacques and Bourland (1983) and Yuan and Todd (1991), together with the results obtained by us, are reported in table 7-1. The chemical analyses of the waters and field observations regarding scale are also reported in table 7-1. In order to keep electrical neutrality in the solution, the amounts of Cl^- reported by Jacques and Bourland (1983) were slightly increased to 85910.7, 76517.9 and 84308.4 $mg \cdot L^{-1}$ for brines A, B and C, respectively. It was assumed that the density of the brines was comparable to that of water at the same temperature and pressure. Brine A corresponds to a well that had borderline $SrSO_4$ scaling tendency. Brine B was from a well that had $SrSO_4$ scale when untreated with scale inhibitor. Brine C came from a well without scaling problems. SI stands for solubility index, which is the activity product divided by the solubility product.

Table 7-1
$SrSO_4$ scale formation prediction

$(mg \cdot L^{-1})$	A[1]	B[2]	C[3]
Sr	560	565	550
Na	43817	39292	44275
Ca	7930	6977	6967
Mg	1422	1270	1215
Cl	85555	76148	83957
SO_4	210	540	100
HCO_3	232	311	360
T (°F)	230	230	230
P (psig)	2500	2500	2500
SI ($SrSO_4$)			
Jacques and Bourland (1983)	1.01	2.38	0.43
Yuan and Todd (1991)	1.04	1.70	0.72
SPECS	1.39	3.72	0.68
Field Observation			
	Borderline	Scale	No scale

1 A corresponds to a well that had borderline SrSO4 scaling tendency.

2 Brine B was from a well that had SrSO4 scale when untreated with scale inhibitor.

3 Brine C came from a well without scaling problems.

The agreement between our results and those reported by Jacques and Bourland (1983), and Yuan and Todd (1991), is good. In the three cases, the solubility index for celestite is above one for brines A and B, and below one for brine C, predicting scaling problems in wells A and B, but not in C. Our predicted solubility indices are the largest ones for brines A and B. Neither Jacques and Bourland (1983) nor Yuan and Todd (1991) included in their models the possibility of precipitation of any other mineral but $CaSO_4$, $SrSO_4$ and $BaSO_4$ (Jacques and Bourland (1983) did not even consider the possibility of co-precipitation of different sulphate minerals, but focused only on $SrSO_4$). This fact may explain the different solubility indices obtained in table 7-1. SPECS also predicts precipitation of $CaCO_3$ for the three brines.

The composition of the formation water of one of the major oilfields in the North Sea (Forties oilfield) and of the North sea injection water is reported in table 7-2. The sulphate scaling tendency in the mixed injection and formation water was predicted by SPECS at different temperatures and pressures, and the results obtained by our model have been compared to predictions performed by Mitchell et al. (1980), Yuan and Todd (1991), and Yuan et al. (1993) for the same waters. Figures 7-1 to 7-4 illustrate the predicted results by SPECS. In all the cases, the largest saturation index is obtained for barite, and the lowest one for gypsum or anhydrite. Thus, barite is the most likely mineral to precipitate, unless kinetic impediments avoid it. At all temperature and pressure conditions, mixtures of injection and formation water containing from 0 to 100% seawater were undersaturated with respect to both anhydrite and gypsum. For mixtures ranging from 20 to 80% seawater, the model predicts barite and celestite precipitation, but for 20% seawater at 25ºC and 300 bar, where the saturation index for $SrSO_4$ is 0.9873. The amounts of solid precipitating are also indicated in figures 7-1 to 7-4. Note that the mixing ration at which maximum mineral precipitation is obtained does not correspond to the maximum supersaturation. For example, at 25ºC and 1 bar, the largest predicted amount of $BaSO_4$ precipitation (350 mg·L^{-1}) is obtained at 20% seawater, while the largest supersaturation (SI equal to 1200) corresponds to 60% seawater.

The agreement between our results and those reported by Mitchell et al. (1980), Yuan and Todd (1991), and Yuan et al. (1993) is very good. The same minerals are predicted to precipitate, and the maximum calculated amounts of precipitated $SrSO_4$ and $BaSO_4$ are very close. Yuan and Todd's (1991) results are presented in figures 4A to 5D in their paper, and in figures 1 and 2 in Yuan el al's. (1993) paper. According to Yuan and Todd (1991), these predictions are confirmed by field observation and have been reported by Mitchell et al. (1980), Hughes and Whittingham (1982), and Tanner and Whittingham (1986).

It can be observed in figures 7-1 to 7-4 that barite is more likely to form at 25ºC than at 100ºC, and its precipitation is also favoured at low pressures. On the other hand, celestite is more likely to precipitate at 100ºC than at 25ºC, and its precipitation is also favoured at low pressures. Regarding the ratio between injected and seawater, the largest solubility indices for both salts are found around 60% seawater, while the maximum amount of precipitation is found at different mixture ratios depending on temperature and pressure.

Table 7-2
Composition of Forties and North Sea water

Ions (mg·L^{-1})	Forties water	North Sea water
Na	30200	11000
K	430	340
Mg	480	1320
Ca	3110	403
Ba	250	0
Sr	660	0
Cl	53000	19800
SO$_4$	0	2480
HCO$_3$	360	135
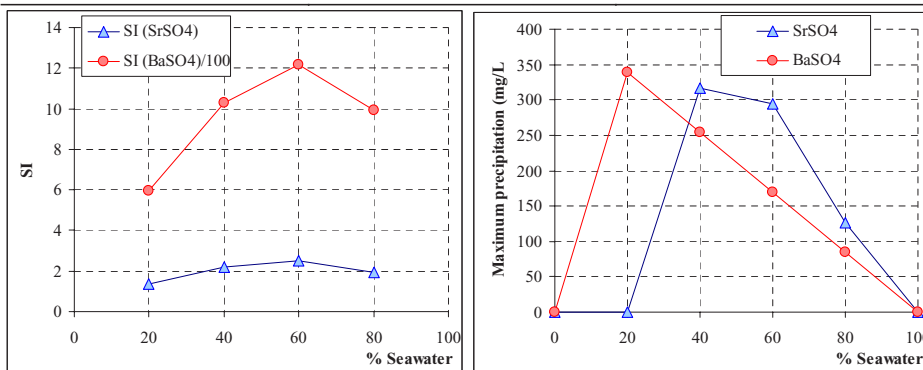
Figure 7-1. SPECS predictions for mixtures of North Sea and Forties water at 25ºC and 1 bar
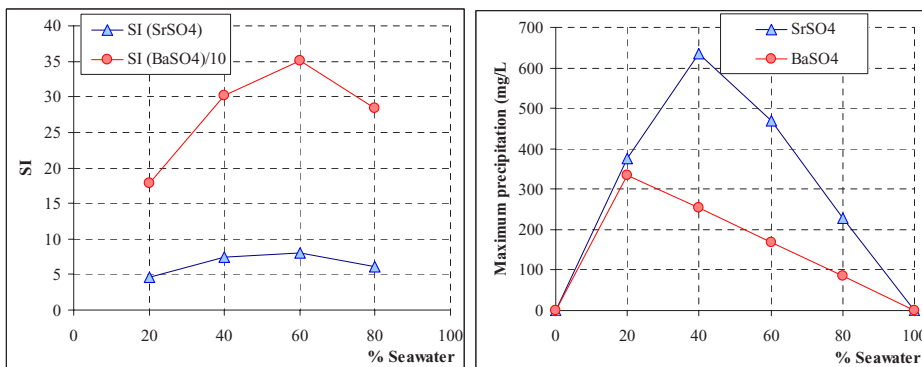
Figure 7-2. SPECS predictions for mixtures of North Sea and Forties water at 100°C and 1 bar
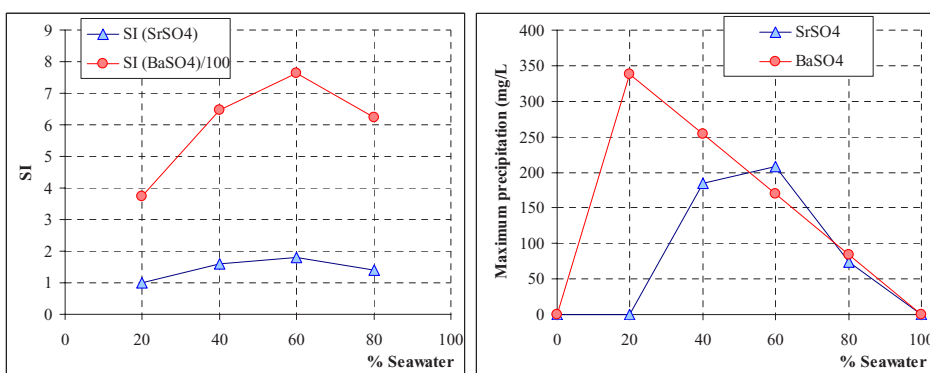
Figure 7-3. SPECS predictions for mixtures of North Sea and Forties water at 25°C and 300 bar

Figure 7-4. SPECS predictions for mixtures of North Sea and Forties water at 100°C and 300 bar

Graham et al. (2003) studied scaling problems in the Kittiwake field, located in the central North Sea. The reservoir is characterized by high salinities and calcium concentrations, and relatively large temperatures (around 130°C) downhole. The composition of the field and the sea water is reported in table 7-3.

As the field matured, the water cut increased over 80% and scaling problems started to be severe. The formation of anhydrite scale downhole has been reported by Graham et al. (2003). Predictions were performed by SPECS, obtaining saturation indices above 1 for anhydrite when the seawater to formation water ratio was over 70%, while the solution was found to be undersaturated for lower ratios. Thus, our predictions are in agreement with field observations. Celestite and barite precipitation is also predicted, agreeing with Graham et al's. (2003) calculations. The maximum amount of precipitation for the different sulphates against the seawater-formation water ratio is given in figure 7-5. The amounts of maximum precipitation for both $BaSO_4$ and $SrSO_4$ predicted by SPECS are in remarkably good agreement with Graham et al.'s (2003) predictions. Regarding anhydrite, the latter investigators report higher amounts of mineral precipitating, and predict $CaSO_4$ scale formation for lower ratios than 70% seawater. Nonetheless, Kittiwake field has been in production since the 1980s, and severe anhydrite scale formation has only become important for the mature field, when the water cut increased over 80%.

Table 7-3
Composition of Kittiwake formation water and central North Sea water

Ions (mg·L^{-1})	Kittiwake formation water	Sea water
Na	56000	10890
Ca	14500	428
K	4350	460
Mg	10600	1368
Ba	24	0
Sr	265	0
SO4	0	2960
Cl	147097	19773

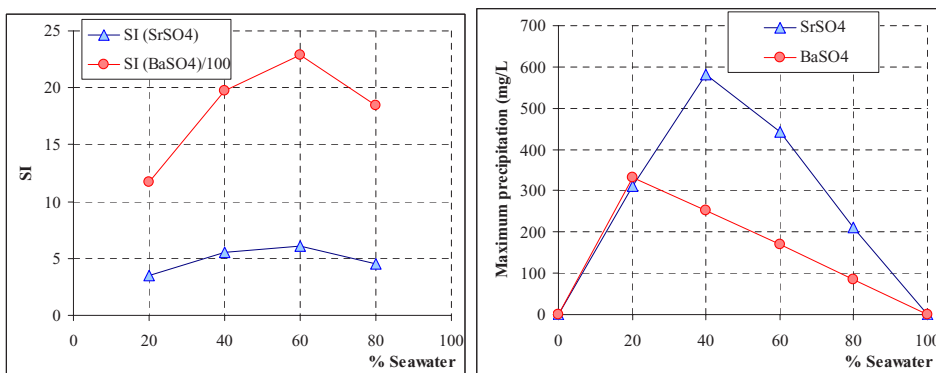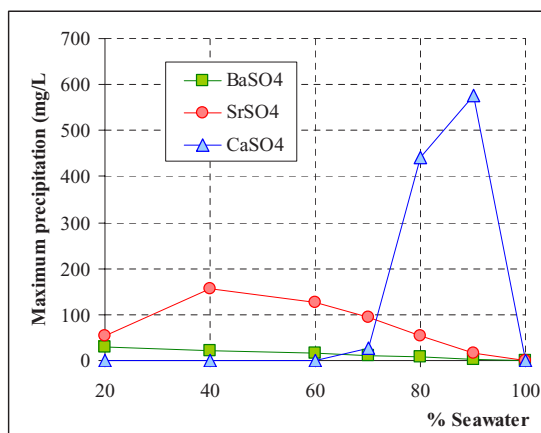**Figure 7-5.** SPECS predictions for mixtures of North Sea and Kittiwake formation water at 130°C and 68 bar

7.2 References in Chapter 7

Graham, G.M., Frigo, D.M., Poynton, N., 2003. Calcium sulphate (anhydrite) scale control in a mature asset-the Kittiwake and Fulmar reservoirs. SPE 80386, 1-11.

Hughes, C.T., Whittingham, K.P., 1982. The selection of scale inhibitors for Forties field. SPE European Petroleum Conference, London.

Jacques, D.C., Bourland, B.I., 1983. A study of solubility of strontium sulphate. SPEJ, 292-300.

Mitchell, R.W., Grist, D.M., Boyle, M.J., 1980. Chemical treatments associated with North Sea projects. JPT, 904-912.

Tanner, R.N., Whittingham, K.P., 1986. Scale control during waterflooding operations: A field appraisal of inhibitor requirement and performance. SPE 14127.

Yuan, M.D., Todd, A.C., 1991. Prediction of sulfate scaling tendency in oilfield operations. Society of Petroleum Engineers, 237-250.

Yuan, M.D., Todd, A.C., Sorbie, K.S., 1993. Sulphate scale precipitation arising from seawater injection: a prediction study. Marine and Petroleum Geology 11 (1), 24-30.

8. Experimental Determination of Solubilities

In the process of designing and selecting the most appropriate setup and/or analytical technique to determine experimentally the solubility of sparingly soluble salts ($BaSO_4$ and $SrSO_4$ in particular) in water and NaCl solutions at high temperature and pressure, different alternatives were studied. All those alternatives (synthetic fluid inclusions technique, electrochemical technique, quartz crystal microbalances, and conductivity measurements), together with their physical base, potentials, advantages and disadvantages for the present purpose, will be presented in this chapter.

Results for conductivity measurements can be found in Appendix II.

8.1 General Overview

There is a large variety of methods to determine the solubility of solids in liquids, depending on the characteristics of the system analyzed and the range of temperature, pressure and concentration to be covered. According to Hefter and Tomkins (2003), they can be divided into direct or indirect methods. In the latter case, the solubility product is the quantity determined experimentally instead of the solid solubility, which can be calculated afterwards from the previous value.

Direct methods can also be divided in two subgroups (Hefter and Tomkins, 2003): Analytical methods (the solubility is determined by chemical analysis of the liquid and solids in equilibrium) and synthetic methods (the solubility is determined via the variation of a property of a solution of known initial concentration when changing temperature, pressure or composition).

The experimental procedure followed in analytical methods consists of preparing the sample and agitating it at constant temperature and pressure until equilibrium is reached. At this point the solid is separated from the liquid and the latter is analyzed in order to determine the solubility. It is important to keep a constant temperature and pressure during the separation process, otherwise some precipitation or dilution may take place and contaminate the results. The solid phase should also be analyzed (chemical analysis, X-ray, infrared spectra) after proper drying, to assure it did not undergo any modification during the experiment. Many different devices can be used to follow this procedure, but they are all formed by three main parts:

- o   Vessel containing the test solution placed inside a device to keep constant temperature (oven, jacket, thermostatic bath, etc.) and a constant pressure.

- o Agitation device (magnetic stirrer, rotator, vibrator, oscillator, etc.).
- o Sampling device connected to a separation device (a filter generally, although centrifugation or decantation can also be employed).

An alternative to the agitation device to provide a good contact between the liquid and solid phases is the use of a column containing the solid phase, through which the liquid is percolated.

In order to obtain reliable data the experimental difficulties of the particular system to study must be carefully reviewed and solved. In general, the following points must be taken into account before starting any solubility measurement:

- o The starting solid material should not contain any impurities, to avoid contamination of the results, especially for sparingly soluble salts.
- o The solid should be characterized with respect to its composition and structure. It is also convenient to reanalyze the solid after the experiment in order to check it did not undergo any modification.
- o Special care must be taken when using reagents that can experience denaturalization due to hygroscopocity, oxidation, etc.
- o The time required to achieve equilibrium must be determined prior to the measurements to make sure supersaturation or undersaturation is avoided, and that no metastable phases are present. Whenever possible, the equilibrium should be approached from different directions. If this is not an option, the solubility constant calculated from different initial conditions can be used to test the equilibrium.
- o It is also important to take into account possible interactions between the test solution and the recipients used for storage or the atmosphere.
- o If separation of the solid and liquid phases is required, it must be performed under the experimental temperature and pressure.

There is no general method or equipment to determine solubilities of water-salt systems at high temperatures and pressures. For each system the setup has to be designed according to the temperature and pressure ranges covered, and the characteristics of the particular system. The systems of interest in the present work are sparingly soluble compounds, which are generally characterized by a slow kinetics. Therefore, analytical methods are preferred against synthetic methods. Due to the large temperatures, pressures and salt concentrations to be covered, an adequate material standing those conditions and resistant to corrosion must be employed. A ceramic material avoids corrosion problems, but introduces experimental error to the measurements due to its porosity. Nevertheless, Plevachuk and Sklyarchuk (2000) used a ceramic cell with a special design to minimize loss of solution

through the pores in the experimental determination of solubilities. Some authors (Jacques, D.C., Bourland, 1983, Howell et al., 1992) performing experiments at high temperature, pressure and salt concentration report corrosion of 316 stainless steel after short periods of use. Alternative materials found in the literature are Boron nitride (Sokolovskii et al., 1995), 316 stainless steel covered with a silver layer (Strübel, 1966), Teflon-lined 318 stainless steel (Schulien, 1987), Hastelloy C (Jacques and Bourland, 1983), Titanium alloy (Howell et al., 1992), platinum liner in a stainless steel vessel (Jensen, 1996), Haynes satellite number 25 (Sharp and Kennedy, 1965). Working under nitrogen atmosphere also helps to reduce corrosion problems.

The low solubility of both $BaSO_4$ and $SrSO_4$ in pure water and in NaCl solutions requires an analytical technique with very low detection limits. Different analytical procedures have been employed to analyze both barium and strontium contents: chemical, colorimetric, atomic absorption spectrometry, radioactive tracer methods, atomic emission, liquid scintillation counting, X-ray fluorescence, isotope dilution mass spectrometry (Bender et al., 1972). In some cases, gravimetric methods are also employed, although they are not recommended for so low solubility values.

8.2 Synthetic Fluid Inclusion Technique

The synthetic fluid inclusion technique (SFIT) is a relatively new experimental procedure which allows the measurement of pressure-volume-temperature-composition (PVTX) properties of aqueous solutions in a wide range of temperature, pressure, and composition. The SFIT is based on the analysis of lab-generated fluid inclusions (microsamples of fluid entrapped as imperfections within crystals (Sterner and Bodnar, 1984)). This method is especially useful to study high salinity fluids at elevated temperature and pressure, because it avoids the problems of corrosion and sampling which appear in conventional techniques (Schmidt and Bodnar, 2000).

The SFIT has been established as a proven method for the determination of phase equilibria and volumetric properties in aqueous fluid systems containing salt and volatiles. PVTX properties in the system $NaCl-CO_2-H_2O$ at elevated temperatures and pressures were determined by Schmidt et al. (1995), and Schmidt and Bodnar (2000). Synthetic fluid inclusions have also been used with success to determine solid-liquid equilibrium and volumetric and critical properties in the $NaCl-H_2O$ system by Sourirajan and Kennedy (1962), Sterner and Bodnar (1984), and Bodnar (1995); and in the $KCl-H_2O$ system by Bodnar and Sterner (1985).

8.2.1 Experimental Procedure

The SFIT is based on the isolation of samples in quartz (SiO_2) at the desired experimental *T* and *P*, for a posterior study under a microscope. The first step is the preparation of the quartz cylinders (around 2-3 cm long and 4 mm diameter) used to isolate the sample. The cylinders are heated to around 350°C. Then, they are removed from the oven and immersed in cold, distilled water, causing the cracking of the quartz due to the instantaneous temperature drop. The water remaining in the fractures is dried using a vacuum oven at 110°C. After this, the cores can be stored in vacuum desiccators until the experiments are carried out (Bodnar, 1995). This procedure has proven to create a large number of closely spaced fractures without leading to the core disintegration (Sterner and Bodnar, 1984).

The second step is to trap part of the solution of known composition in the fissures of the quartz core. To do so, one quartz cylinder is introduced into a platinum capsule together with the solution of interest. The system is heated and pressurized to experimental conditions using an oven and a high pressure autoclave. Part of the solution will enter the fractures in the quartz. Due to dissolution and reprecipitation processes, the fractures will partially heal, and small amounts of solution become isolated (fluid inclusions). According to Bodnar and Sterner (1985), the density and composition of the fluid trapped is representative of the bulk fluid present in the capsule, and no change is experienced during quenching to ambient conditions.

The third step is to analyze the fluid inclusions to determine the PVTX properties of interest once the sample is cooled to room conditions. The quartz cores are cut into disks 0.25-0.5 mm thick, and polished on both sizes before being examined under a microscope provided with a heating/cooling stage (Bodnar, 1995). At room temperature, the inclusions generally contain two or more phases, although they are originally trapped in a single, homogeneous fluid phase at the *T/P* formation conditions. These multiple phases appear as a consequence of phase changes during cooling. A heating/cooling stage coupled to the microscope is used to determine the temperatures at which the different phases disappear, providing the information needed to determine PVTX properties of aqueous solutions.

8.2.2 Application of SFIT to Solubility Measurements

To determine solubility values, synthetic fluid inclusions of different known concentrations are trapped following the procedure explained before. If the solution is supersaturated at room conditions, the inclusion will contain an additional solid phase. The temperature of

dissolution of such a phase is measured, and a relationship between solubility and temperature, at a given pressure, can be obtained.

8.2.3 Drawbacks of the SFIT

The use of SFIT implies certain assumptions (Vityk and Bodnar, 1998):

- o   The inclusion traps a single, homogeneous phase.
- o   Nothing is added or lost from the inclusion after it is trapped.
- o   No reactions take place within the fluid inclusion between the time of trapping it and analyzing it.
- o   The inclusion volume remains constant.

According to Vityk and Bodnar (1998), not all these assumptions are always certain. Even though Sterner and Bodnar (1984) performed a great variety of experiments concluding that inclusions trap representative samples of the parent solutions, other workers (Barnes et al., 1969) have reported that they may not.

Another disadvantage of SFIT is the slow fracture healing rates. Schmidt and Bodnar (2000) run experiments during about eight weeks for temperatures of $300^{\circ}C$.

Special care must also be taken regarding the inclusion's size. If the fluid inclusions are too small (2 to 3 µm) the phase changes are often very difficult to observe. On the other hand, for large inclusions (larger than about 10 µm) high internal pressures during heating for homogenization are generated. Such pressures result in a stretch or decrepitate of the quartz core. The maximum internal pressure an inclusion in quartz can stand without stretching or crackling decreases for increasing inclusion size.

The main disadvantage of this technique for the present purpose is the saturation of the solutions with silica. Therefore, the experiments would determine barite solubility in the $BaSO_4$-SiO_2-$NaCl$-H_2O system, which is not the aim of the present work. Maybe, this problem could be solved trying to find a material which allows the formation of fluid inclusions but does not interfere with the system being investigated.

8.3 Electrochemical Technique

An electrochemical-based technique to investigate deposition of different scaling minerals on metallic surfaces has been presented by Morizot et al. (1999), Neville et al. (1999), Neville and Morizot (2000), and Morizot and Neville (2001). The results obtained (for $CaCO_3$ by Neville et al., 1998 and Morizot et al., 1999; for both $CaCO_3$ and $BaSO_4$ by Morizot and Neville, 2001 and Morizot et al., 2002; and for $CaCO_3$, $MgCO_3$ and $Mg(OH)_2$

by Neville and Morizot, 2002) show this method to be a promising tool for studying nucleation and growth of mineral scale at solid surface, as well as inhibitor performance. It could also be used as a method for online monitoring of scale formation down the well. The technique is also a good tool to find out the relationship between the scale formation precipitated from the bulk solution and the one formed at a solid surface. According to Hasson (1996), field experience shows that inhibition does not follow the same behaviour as predicted in the laboratory test from bulk solution precipitation rates.

The oxygen reduction reaction (reaction 8-1) on a rotating disk electrode (RDE) surface can be followed and related to the extent of surface scale.

$$O_2 + 2H_2O + 4e^- \rightarrow 4(OH)^-$$ (8-1)

We believe the same principle could also be used to measure solubility of sparingly soluble minerals at different temperatures and pressures.

8.3.1 Background

The technique is based on the change observed in the rate of reaction 8-1 at a RDE surface under potentiostatic control when scale starts forming on it. The schematic of the technique is presented in figure 8-1. At the beginning, the diffusing oxygen reaches the whole electrode surface area (A_i). Once scale has deposited, the surface available to the oxygen is reduced (A_f), and thus the extent of reaction 8-1.

The mass transport of oxygen by diffusion under varying hydrodynamic conditions to the surface of the electrode is analyzed by using the transport equations developed by Levich (1942), Adams (1969), and Filinovsky and Pleskov (1976). A rotating disk electrode is chosen because the mass transport to its surface is well defined and uniformly distributed along the whole surface, and can be varied by changing the rotational speed.

For a reaction under mass control (as it is the case for equation 8-1) at a constant potential, the limiting current (i_L, mA) can be related to the RDE rotational speed (ω, rad·s^{-1}) via equation 8-2

$$i_L = 0.62nFAC^b D^{2/3} v^{-1/6} \omega^{1/2}$$ (8-2)

where n is the number of electrons involved in electrode reaction, F is the Faraday's constant (96487 C equiv^{-1}), A is the electrode area in cm^2, C^b is the bulk concentration of electroactive species in mol dm^{-3}, D is the diffusion coefficient of the electroactive species in cm^2 s^{-1}, and v is the kinematic viscosity in cm^2 s^{-1}. For reaction 8-1, the electroactive species is oxygen.
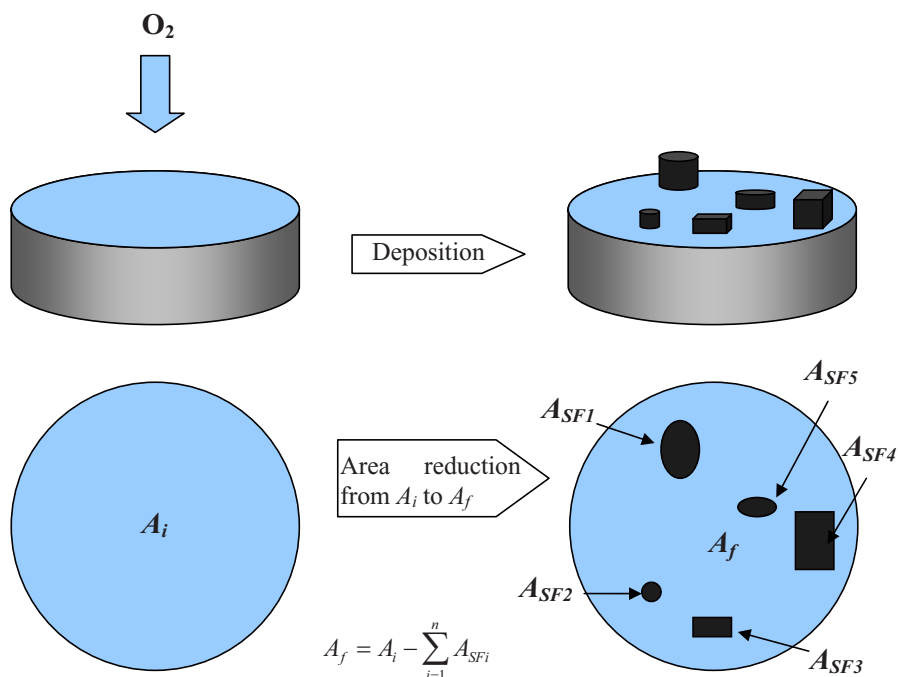
Figure 8-1. Schematic representation of active surface area before and after scale deposition (A_{SF} stands for area of solid formation).

For a constant rotation speed, equation 8-2 shows that the limiting current remains constant unless there is a change in the electrode surface area. Therefore, a decrease in i_L will correspond to scale formation on the surface. Equation 8-2 is used to calculate the difference in active surface area before and after scale formation has taken place.

This method has been validated by using image analysis. The surface coverage determined by this technique and that determined by image analysis are in good agreement, increasing the accuracy for highly covered surfaces (Neville et al., 1998).

8.3.2 Experimental Procedure

The experimental procedure consists of three main steps:

- ○ Analysis of the i_L vs. $\omega^{1/2}$ behaviour for a clean electrode to determine the initial active surface area.
- ○ Immersion of the electrode in a supersaturated solution of the species of interest and waiting for the scale to form on the surface.
- ○ Final analysis to determine the extent of scale formation on the surface.

The different slope of the plots i_L vs. $\omega^{1/2}$ during the initial and final analysis is a consequence of the decrease in the active surface area as a result of solid deposition, as all the other variables in equation 8-2 are kept constant. Comparison of the two data sets will indicate the percentage of electrode surface covered by solid:

$$\% \text{ covered} = \frac{m_1 - m_2}{m_1} \cdot 100 \tag{8-3}$$

where m_1 is the gradient i_L vs. $\omega^{1/2}$ for the clean electrolyte, and m_2 is the same gradient for the scaled electrolyte.

Two separate apparatus are required to carry out the three steps. The setup to generate scale formation on the electrode surface is shown in figure 8-2 (a), while the experimental setup for the electrochemical analysis is shown in figure 8-2 (b). The latter is a three-electrode electrochemical cell. The working electrode is the RDE, while the reference electrode is a saturated calomel electrode (SCE). A platinum electrode is used as the inert auxiliary electrode (Neville et al., 1999). The RDE speed is measured via a tachometer.

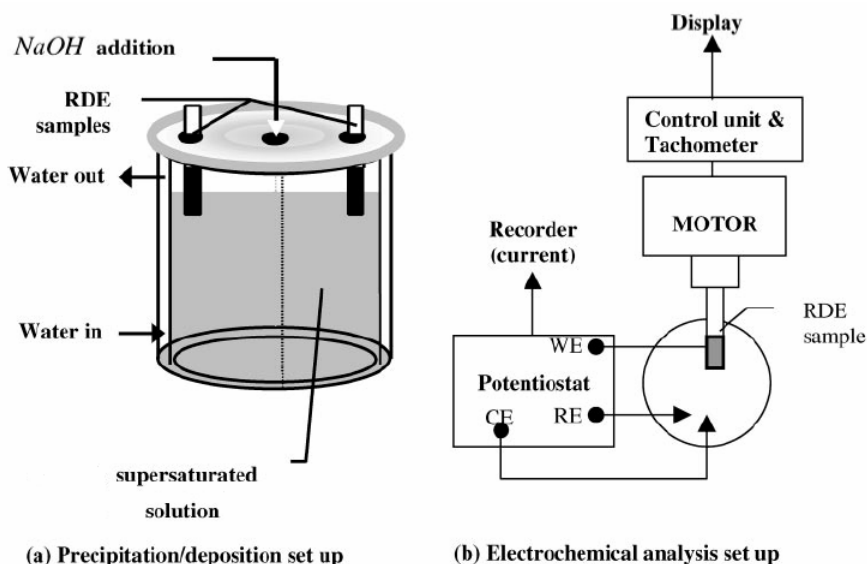**Figure 8-2.** Experimental setup for (a) precipitation and deposition of salt and (b) electrochemical analysis (Neville and Morizot, 2000).

The performance of different inhibitors can be easily studied using this new technique. The response to the addition of a given quantity of inhibitor to the supersaturated solution in contrast to the inhibited solution can be analyzed in the same way as explained previously.

8.3.3 Application to Solubility Measurements

The principle used to develop the new technique presented above could be used to perform solubility measurements. The appearance of the first particle of solid on the electrode can be followed by measuring the current i_L. According to equation 8-2, for a constant temperature, pressure and angular velocity, the limiting current has a constant value unless the electrode area changes as a consequence of solid formation. Such change in the current value can be used to determine the solubility.

The kinematic viscosity and the diffusion coefficient depend on both temperature and pressure. Therefore, both the electrochemical cell and the precipitation/deposition setup should be maintained at the same T and P conditions. In order to avoid dissolution of the scale when analyzing the current, a solution at equilibrium with respect to the precipitating solid, and with the same NaCl concentration as the precipitation setup, should be used as analysis solution.

An alternative procedure could be based on using the same device both for the electrochemical analysis and the precipitation process. A solution of known composition of the species of interest in a known concentration of NaCl is employed as analysis solution. The temperature is increased to the desired value, and pressure is increased to a value higher to the pressure corresponding to the solubility point. In that way, an undersaturated solution is the starting point for the experiment. Pressure is decreased slowly and the current is recorded, until a decrease in the current is observed. That point corresponds to the first solid deposited on the electrode, and indicates the pressure at which the original solution reaches solid-liquid equilibrium. The same procedure can be followed for different temperatures and NaCl concentrations covering the required ranges of temperature and composition. If we want to attain equilibrium from a supersaturated solution, the pressure will be slowly increased instead of decreased, until a current change is observed. However, if the attainment of equilibrium is slow, this procedure can be time consuming.

8.3.4 Drawbacks of the Electrochemical Method

The development of the electrochemical approach follows some assumptions that may not always be true, and therefore, could affect the final results:

- ○   The solid deposited on the electrode surface does not allow oxygen transport through the crystal lattice, and therefore the electrochemical reaction only takes place on the free surface.

- o The corrosion reaction of the substrate with the electrolyte does not influence the results.

- o Deposits do not re-dissolve once they have been formed.

- o The rate of oxygen reduction is constant, and the diffusion coefficient of oxygen to the active sites is constant for bare and scaled electrolytes.

The deposited solid may have a complex shape, with parts not completely in contact with the surface (i.e., ellipsoidal). The oxygen reduction reaction could take place on those "cavities" formed by the solid, at a lower rate than on the free surface, but this possibility has not been accounted for by this technique.

The method assumes the surface is equally accessible for oxygen reduction. Nevertheless, the deposition of crystals will induce local turbulence effect, which will enhance the supply of oxygen near the solids.

Neville et al. (1999) noticed that the relationship i_L vs. $\omega^{1/2}$ showed a small degree of non linearity when scale had deposited on the electrode's surface. Even though a good linear correlation coefficient was obtained (0.99), this behaviour indicates that the non uniform layer created on the electrode is generating some instability. The problem may be important when having many scale layers.

When studying the applicability of the electrochemical technique to solubility measurements, several inconvenient points were found:

- o All the studies performed using the electrochemical technique were performed at room temperature and atmospheric pressure (Neville and Morizot (2000) performed some measurements at 80°C and 1 atm). Accuracy and feasibility of the technique at high temperature and pressure has not been addressed.

- o The kinematic viscosity and the diffusion coefficient depend on pressure, and even though the dependence is not very strong, changing its value may lead to different limiting currents for the same surface area.

- o After every change in the pressure conditions, it is required to wait the time needed to attain equilibrium for the particular system being analyzed. Therefore, for slow reactions, this procedure is not appropriate.

- o If two different devices are employed (one for the electrochemical analysis and another one for the precipitation process), the electrode should be transferred from one to another at a constant temperature and pressure to avoid experimental errors.

8.4 Quartz Crystal Microbalances

Quartz crystal resonators are widely used nowadays for physical, chemical and biochemical sensing. This device is sensitive to mass changes at its surface, being called quartz crystal microbalance (QCM). It is a microgravimetric technique capable of measuring as small as ng order of mass changes on the surface of the crystal (Iitaka et al., 1997). This accuracy is reduced when the fluid in contact with the quartz is a liquid.

8.4.1 Background

8.4.1.1 Piezoelectricity

Quartz crystal microbalances are based on the phenomenon of piezoelectricity, which is a coupling between a material's mechanical and electrical behaviours. When a mechanical stress is applied on a piezoelectric material, an electrical charge appears on its surface. This phenomenon is called piezoelectricity. Piezoelectric materials also display a converse piezoelectric effect: When an electrical charge is applied, the material deforms mechanically.

Many crystalline materials exhibit piezoelectric behaviour, but only a few materials exhibit the phenomenon strongly enough to use them in applications taking advantage of piezoelectricity. Quartz, Rochelle salt, lead titanate zirconate ceramics, barium titanate and polyvinylidene fluoride are found among these materials.

A quartz crystal sensor will be formed by the quartz disc with electrodes on both sides. The thickness of the disk has to be very small in order to have a high sensitivity (Ferrari et al., 2000). The quartz crystal resonator is sensitive to mass changes at its surface. Therefore, it can be used as a quartz crystal microbalance to measure changes of a known mass of salt placed on the crystal, due to dissolution in a liquid media. Salt precipitation on the crystal surface from a supersaturated solution can also be studied by means of the QCM.

8.4.1.2 Frequency Response

There are different factors affecting the frequency response of a piezoelectric quartz crystal (Guigard et al., 2001):

- o   Mass located on the crystal surface
- o   Pressure
- o   Temperature
- o   Properties of the fluid surrounding the crystal (density and viscosity)

- ○   Mounting effects

Considering all the effects mentioned above, the measured frequency (F) of a quartz crystal can be expressed as:

$$F = F_0 + \Delta F_m + \Delta F_P + \Delta F_T + \Delta F_f \tag{8-4}$$

where F_0 is the crystal's inherent frequency, ΔF_m is the frequency change due to mass placed on the crystal, ΔF_P is the frequency change due to the pressure, ΔF_T is the frequency change due to the temperature, and ΔF_f is the frequency change due to changes in the density and viscosity of the surrounding fluid. The mounting effects, or external stresses, are kept constant if handling of the crystal is avoided through the experiment (Guigard et al., 2001).

8.4.1.2.1 Mass Effects

Several equations can be found in the literature relating the frequency change of a crystal immersed in a gaseous phase as a consequence of the mass placed on its surface (ΔF_m). The first relationship was proposed by Sauerbrey (1959):

$$\Delta F_m = -\frac{2F_0^2}{N \cdot A\sqrt{\rho_q c_q}} \Delta m \tag{8-5}$$

where ρ_q is the crystal density, c_q the crystal stiffness, Δm the change of mass located on the crystal, N the harmonic and A the crystal area.

According to equation 8-5, the mass sensitivity of the crystal is not dependent on the kind of deposited material. It only depends on crystal's properties (density, stiffness, area and inherent frequency). Therefore, calibration is not required. Nevertheless, Sauerbrey (1959) assumed the mass placed on the quartz could be assimilated to an increase in the effective thickness of the quartz resonator. The film added was assumed to have the same density and acoustic properties as quartz. Those assumptions reduce the range of applicability of equation 8-5 to small mass loads and ratios of $\Delta F/F_0$ lower than 2% (Hayward et al., 1998).

The use of quartz crystal microbalances in liquids is more complicated than in gaseous media. In this case the frequency shift is due to two contributions: The mass load and the effect caused by changes in the liquid properties. Kanazawa and Gordon (1985) studied the changes in the quartz crystal frequency when it was immersed in a viscous medium, and developed an equation accounting for such changes.

$$\Delta F = \frac{-F_0^{3/2}}{N}\sqrt{\frac{\rho\mu}{\rho_q c_q \pi}}$$

(8-6)

where ρ and μ are the density and viscosity of the bulk fluid, respectively.

Combining equations 8-5 and 8-6:

$$\Delta F_{Total} = -\frac{2F_0^2}{N\sqrt{\rho_q c_q}}\left(\frac{\Delta m}{A}+\sqrt{\frac{\rho\mu}{4\pi F_0}}\right)$$

(8-7)

8.4.1.2.2 Temperature and Pressure Effects

In order to quantify the pressure and temperature effect on the frequency shift of the quartz crystal, initial experiments could be performed using a clean crystal. When the frequency has stabilized for the unload crystal, the pressure can be increased keeping a constant temperature. The frequency shift measured is a consequence of the pressure effect exerted on the crystal and the changes in density and viscosity of the liquid, and thus the frequency measured is

$$F = F_0 + \Delta F_P + \Delta F_f$$

(8-8)

ΔF_f can be quantified using equation 8-6 once the viscosity and density of the liquid are known. The process can be repeated until all the pressures of interest have been covered, and all the values for ΔF_P have been calculated. The same procedure can be followed to study the frequency shift due to temperature. In this case the frequency is given by

$$F = F_0 + \Delta F_T + \Delta F_f$$

(8-9)

Again, the different values of ΔF_f for the range of temperatures of interest can be calculated from equation 8-6.

In case the term ΔF_f cannot be calculated accurately at the large temperatures and pressures of interest (up to $300^\circ C$ and 700 bar) a different approach can be followed. The effects of pressure, temperature and changes in liquid density and viscosity can be grouped in a single term ΔF_{TPf}, so that the measured frequency at each temperature and pressure pair is

$$F = F_0 + \Delta F_{TPf}$$

(8-10)

The advantage of such procedure is a lower experimental error:

o   The experimental errors introduced by the density and viscosity calculations and/or measurements are avoided.

    o   The addition of the experimental errors implied in the separate measurements of the temperature and pressure effects is avoided. Instead, a lonely measurement is done reducing the total error.

Another advantage of using the term ΔF_{TPf} is that it would include any other possible effect taking place in the system and not accounted for in a proper way when using equations 8-8 and 8-9 (e.g., the effect of the mass of water adsorbed to the crystal surface).

The disadvantage of the procedure is the need to perform experiments for each temperature and pressure pair of interest. In this case, for each temperature the whole range of pressures has to be covered, and vice versa, increasing considerably the number of experiments to perform.

Both procedures could be followed for a set of T and P points in order to know if the experimental error for the first approach is considerably larger that when using the second approach. Depending on the results, the most appropriate procedure can be chosen.

A very tight control of the temperature is needed through the experiment to obtain reliable results and a stable frequency. The resonant frequency is a sensitive function of temperature, and small temperature fluctuations can swamp the typical frequency shifts involved with the mass variations. When working with gases, the intrinsic temperature dependence of the QCM is negligible near room temperature (around 1-3 Hz $^{o}C^{-1}$). When the crystals are immersed in liquid, much larger changes in frequency with temperature are observed. Ferrari et al. (2000) carried out experiments on several uncoated sensors having a value for F of 7 MHz, and obtained a thermal sensitivity (dF/dT) around -470 Hz $^{o}C^{-1}$, which corresponded to -67 ppm $^{o}C^{-1}$. Another effect which needs to be accounted for is the importance of the temperature history of the crystal. It is often observed that the frequency versus temperature curve obtained going from T_1 to T_2 does not coincide with the curve obtained going from T_2 to T_1.

8.4.2 Experimental Procedure

Preliminary studies to the solubility experiments are required in order to characterize the frequency response of the clean quartz crystal against changes in both temperature and pressure (and the consequent changes in fluid properties). The quartz crystal will be placed inside the pressure vessel in contact with the liquid medium. Temperature and pressure will be then increased to the desired values. When the frequency has stabilized, the value of ΔF_{PTf} will be calculated according to equation 8-10. The procedure will be repeated for the whole range of temperatures and pressures of interest. When the liquid is different from

distilled water, all the range of concentrations to be used in the solubility experiments has to be analyzed. It would be convenient to use an equal volume of water or solution to determine ΔF_{PTf}, in case this factor could influence the results. Nevertheless, this influence could also be studied by performing experiments using different volumes of water/solution under the same temperature and pressure conditions.

Once the value of ΔF_{PTf} is known for all the conditions to be studied, the solubility measurements can start. Two different approaches could be used:

- Precipitation of salt on the QCM from a supersaturated solution
- Dissolution of the solid salt deposited on the QCM

The first approach was used by Abdel-Aal et al. (2001) to study the adhesion mechanism of CaCO$_3$ scale at 25°C. Eun. et al. (1999) studied the growth of cadmium selenite and barium sulphate crystals on a QCM from supersaturated solutions. Guigard et al. (2001) measured the solubility of two copper salts in supercritical CO$_2$ using the dissolution approach.

The disadvantage of the precipitation approach is the possibility of solid formation on the vessel walls, which will not be accounted for by the QCM. Anyhow, this problem could also appear when following the dissolution method, due to a continuous process of dissolution and reprecipitation, although it is thought to happen in a lower extent.

The main drawback of the dissolution approach is the necessity of placing the solid salt on the crystal surface. The equations developed to relate frequency shifts and mass changes assumed the mass on the crystal to be a thin layer with constant properties. Bond et al. (1997) solved this problem by adhering the microcrystals ([(C$_4$H$_9$)$_4$N][Ce(CO)$_5$I]) to the electrode by smearing the electrode surface with a cotton swab containing the powdered material. They transferred masses between 3 and 6 μg by this procedure. Nonetheless, those values are too low even for the lowest soluble salts of our interest. Guigard (2001) generated a layer on the crystal by allowing the solvent to evaporate. They dissolved the salt in water and placed a known volume of that solution on the crystal using a syringe. Afterwards, the solvent is allowed to evaporate. The mass of salt placed on the crystal can be calculated using two different methods. The first one implies the knowledge of the volume and concentration of the solution placed on the crystal. The second method is based on the frequencies measured before and after the crystal loading, and on the use of equation 8-5. Guigard et al. (2001) reported an average deviation of 28% for the masses of bis(thenoyltrifluoroacetonato)copper(II) measured using these two methods. They explain the difference as experimental errors introduced due to remaining mass on the syringe tip, volume delivered, concentration and solvent residue on the crystal. They believe the mass

calculated from Sauerbrey's (1959) equation is more accurate than that from volume and density.

For slightly soluble salts (as $BaSO_4$ and $SrSO_4$), the homogeneous deposition of powdered solid salt directly on the crystal surface would be the easiest way to proceed. In order to assure the method is reliable, the equations presented before could be tested by performing different experiments where the mass loaded is known. If the equations are found to give inaccurate results, a calibration could solve the problem.

Once the salt is deposited on the crystal, the temperature and pressure conditions are increased to the desired value. To do so, an oven and a pressure vessel connected to a pump can be used. When the equilibrium has been reached and the frequency has stabilized, F is measured. This procedure is repeated for the different T and P conditions to be analyzed.

The setup to determine solubility of sparingly soluble salts in a liquid phase at high temperature and pressure, by means of the QCM technique, is represented in figure 8-3. To avoid breakage of the QCM, a very tight and fast-acting pressure control system is required. Otherwise, the differential pressure between the liquid and gaseous phases could easily cause the crystal breakage. To get good sensitivity, the crystal's thickness is less than 1 mm, and therefore the differential pressure it can stand is very low. The same setup could also be used replacing the air by a liquid phase, but it would imply a considerable decrease in the sensitivity of the QCM.

Apart from the assumptions done in the development of equations 8-4 to 8-10 and the difficulties to place the solid salt homogeneously on the crystal surface, the main disadvantage of this method is the large cost and complexity of the design. For these reasons, it was discharged for the present purpose, although it is believed to have a high potential for the determination of solubility of sparingly soluble salts, avoiding at the same time the problems found in such cases to come across a reliable analytical technique.
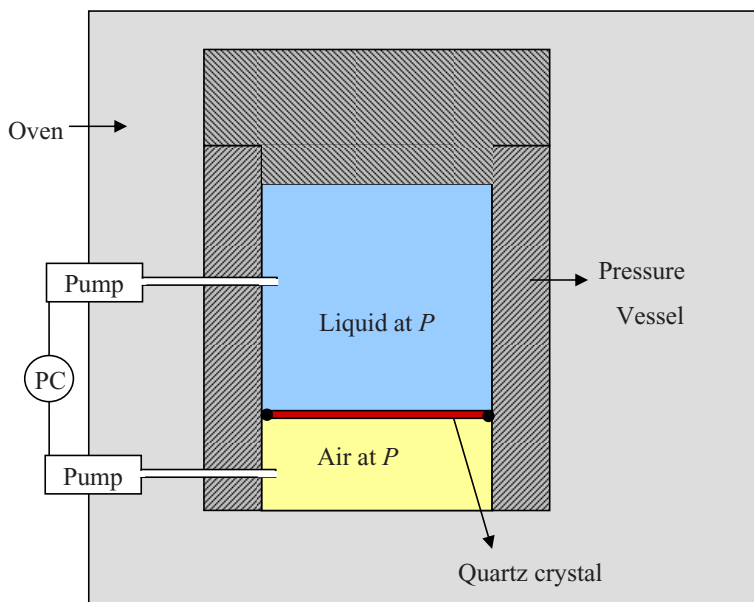
Figure 8-3 Experimental QCM setup

8.5 Conductivity Measurements

Conductivity of a solution is a measurement of its ability to carry an electrical current. The electrical conductivity increases with the amount of solids dissolved, and therefore, it has been widely used to determine salt concentrations in water. To measure conductivity, a constant voltage is applied across two electrodes separated by a constant distance. The electrical current transported through the solution depends on the number and type of ions dissolved in it.

The conductivity technique has previously been used at high pressures and temperatures to study asphaltenes precipitation (Fotland, 1996). The liquid-liquid coexistence curve on the phase diagram of the Pb-Ga system was determined on the basis of electroconductivity measurements by Sokolovskii et al. (1995). Plevachuk and Sklyarchuk (2000) developed an experimental technique for electrical conductivity measurements in a wide temperature range (up to 1730°C) under high pressures (up to 500 bar).

8.5.1 Background

There are many different methods to determine solubility of solids in liquids. One way to perform such measurement is by the so-called synthetic methods, where no chemical

analysis is required. A sample of known initial composition is prepared. One of the equilibrium parameters (E, being temperature, pressure or composition; or any function of E) is then modified and one of the system properties (P) is followed. When there is a phase change, a break will appear in the plot P vs. E (or $f(E)$). This principle may be used to measure the solubility of salts in water.

8.5.2 Experimental Procedure

Even though synthetic methods are not recommended for sparingly soluble salts, as they are usually characterized by slow kinetics, conductivity experiments were performed for SrSO$_4$-H$_2$O systems in order to study the real feasibility of this technique for our purposes. Celestite (SrSO$_4$) was chosen over barite due to the extremely low conductivity values for the latter salt. In order to simplify the experimental setup, and as the main purpose was to verify the validity of the method for our needs, the experiments were performed at room temperature and pressure. The electrical conductivity of celestite-water solutions was followed (P) when changing the composition (E). The concentration of salt in the solvent was continuously decreased by adding a constant flow rate of distilled water, by means of an ISCO pump. The conductivity was measured by a conductivity meter (Lutron CD-4303). If experiments had to be carried out at high constant pressures, a bellow connected to a pump could be located inside a pressure vessel containing the solution. The pump introducing water to the system would work in a constant flow mode, while the pump connected to the bellow would supply a constant pressure. Operating in this way, water is constantly introduced into the vessel, which will maintain a constant pressure due to the volume compensation of the bellow.

A supersaturated solution at room temperature and pressure was prepared, by adding a known amount of pure commercial powder SrSO$_4$ in a known volume of distilled water. The solution was stirred with a magnetic stirrer, and the conductivity was constantly measured at the same time as a very low water flux is added to the vessel containing the solution. The experimental setup is shown in figure 8-4.

When a new volume of water is added to the solution, part of the excess solid will dissolve, keeping a constant conductivity value. This procedure will go on until the last particles of solid are dissolved. From that moment, a new addition of water to the solution will cause a dilution process, and therefore the conductivity will experience a decrease. Therefore, the break in the plot conductivity vs. solution volume will indicate when dilution starts to take place. The solubility value at the experimental conditions can be calculated from the initial

weight of salt and the initial volume of water, together with the volume of water added until the break point appears.

The results from the different conductivity experiments carried out are presented in Appendix II. The conclusion drawn from those results is the lack of validity of this experimental procedure to determine celestite solubility in pure water. The slow kinetics of the system (equilibrium was attained only after at least 20 hours) makes any synthetic technique inappropriate to obtain reliable solubility measurements in a reasonable time.
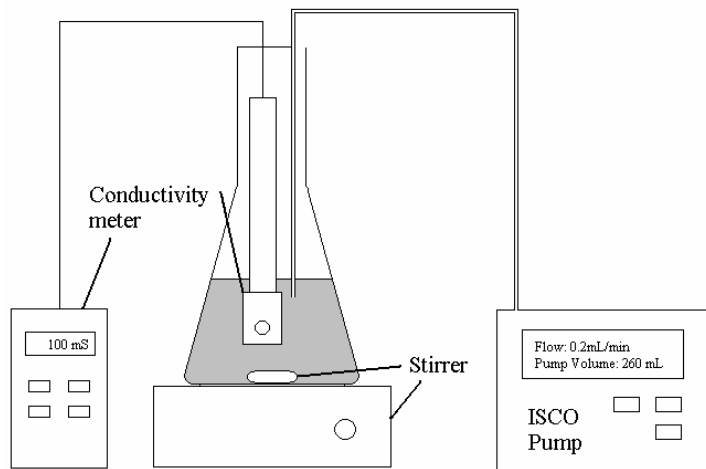

Figure 8-4 Experimental conductivity setup

8. 6 References in Chapter 8

Abdel-Aal, N., Satoh, K., Sawada, K., 2001. Study of adhesion mechanism of calcareous scaling by using quartz crystal microbalance technique. Analytical Sciences 17, 825-828.

Adams, R.N., 1969. Electrochemistry at solid electrodes, Dekker, 1969

Barnes, H.L., Lusk, J., Potter, R.W., 1969. Composition of fluid inclusions. Proceedings of COFFI (ed. E. Roedder) 2, 13.

Bender, M., Snead, T., Chan, L.H., Bacon, M.P., Edmond, M., 1972. Barium intercalibration at Geosecs I and III. Earth and Planetary Science Letters 16, 81-83.

Bodnar, R.J., Sterner, S.M., 1985. Synthetic fluid inclusions in natural quartz. II. Application to PVT studies. Geochimica et Cosmochimica Acta 49, 1855-1859.

Bodnar, R., 1995. Experimental determination of the PVTX properties of aqueous solutions at elevated temperatures and pressures using synthetic fluid inclusions: H_2O-NaCl as an example. Pure & Applied Chemistry 67 (6), 873-880.

Bond, A.M., Colton, R., Mahon, P.J., Tan, W.T., 1997. Tetrabutylammonium cation expulsion versus perchlorate electrolyte anion uptake in the electrochemical oxidation of microcrystal of $[(C_4H_9)_4N][Ce(CO)_5I]$ mechanically attached to a gold electrode: A voltammetric and quartz crystal microbalance study. J. Solid State Electrochem. 1, 53-61.

Borngräber, R., Schröder, J., Lucklum, R., Hauptmann, P., 2002. Is an oscillator-based measurement adequate in a liquid environment?. IEEE Transactions on Ultrasonics, Ferroelectrics, and Frequency Control 49 (9), 1254-1259.

Eun, H., Umezawa, Y., 1999. Quartz crystal microbalance for selenite sensing based on growth of cadmium selenite crystals immobilized on a monolayer of phosporylated 11-mercapo-1-undecanol. Microkim. Acta 131, 177-185.

Ferrari, V., Marioli, D., Taroni, A., Ranucci, E., 2000. Multisensor array of mass microbalances for chemical detection based on resonant piezo-layers of screen-printed PZT. Sensors and Actuators 68, 81-87.

Filinovsky, V., Pleskov, Y., 1976. Rotating disk and ring electrodes in investigations of surface phenomena at the metal-electrode surface. Progress in Surface and Membrane Science, Vol. 10. Cadenhead, D.A., Danielli, J. (Eds.), Academic Press, London.

Fotland, P., 1996. Precipitation of asphaltenes at high pressures; experimental technique and results. Fuel science and technology int'l. 14 (1&2), 313-325.

Guigard, S.E., Hayward, G.L., Zytner, R.G., Stiver, W.H., 2001. Measurement of solubilities in supercritical fluids using a piezoelectric quartz crystal. Fluid Phase Equilibria 187-188, 233-246.

Hasson, D., 1996. Influence of the flow system on the inhibitory action of $CaCO_3$ scale prevention additives. Desalination 108, 67-80.

Hayward, G.L., Thompson, M., 1997. A transverse shear model of a piezoelectric chemical sensor. Journal of Applied Physics 83 (4), 2194-2201.

Hefter, G.T., Tomkins, R.P.T., 2003. The experimental determination of solubilities. John Wiley & Sons, vol. 6, West Sussex, England.

Howell, R.D., Raju, K., Atkinson, G., 1992. Thermodynamics of "Scale" mineral solubilities 4. $SrSO_4$. J. Chem. Eng. Data 37, 464-469.

Iitaka, K., Tani, Y., Umezawa, Y., 1997. Orthophosphonate ion-sensors based on a quartz crystal microbalance coated with insoluble orthophospate salts. Alalytica Chimica Acta 338, 77-87.

Jacques, D.C.; Bourland, B.I., 1983. A study of solubility of strontium sulphate. SPEJ 292-300.

Jensen, J.P., 1996. Phase equilibria for aqueous electrolyte systems at high temperature and pressure. Ph.D. Thesis, Department of Chemical Engineering, Technical University of Denmark.

Kanazawa, K.K., Gordon, J.G., 1985. Anal. Chim. Acta 175, 99.

Levich, B.G., 1942. Acta Physicochimica URSS 17, 257

Morizot, A.P., Neville, A., Hodgkiess, T., 1999. Studies of the deposition of $CaCO_3$ on a stainless steel surface by a novel electrochemical technique. Journal of Crystal Growth 198/199, 738-743.

Morizot, A.P., Neville, A., 2001. Using an electrochemical approach for monitoring kinetics of $CaCO_3$ and $BaSO_4$ scale formation and inhibition on metal surfaces. Society of Petroleum Engineers, 220-223.

Morizot, A.P., Neville, A., Taylor, J.D., 2002. An assessment of the formation of electrodeposited scales using scanning electron and atomic force microscopy. Journal of Crystal Growth 237-239, 2160-2165.

Neville, A., Morizot, A.P., 2002. Calcareous scales formed by cathodic protection – an assessment of characteristics and kinetics. Journal of Crystal Growth 243, 490-502.

Neville, A., Morizot, A.P., 2000. A combined bulk chemistry/electrochemical approach to study the precipitation, deposition and inhibition of $CaCO_3$. Chemical Engineering Science 55, 4737-4743.

Neville, A., Hodgkiess, T., Morizot, A.P., 1999. Electrochemical assessment of calcium carbonate deposition using a rotating disc electrode (RDE). Journal of Applied Electrochemistry 29, 455-462.

Plevachuk, Y.; Sklyarchuk, V., 2000. Electrophysical measurements for strongly aggressive liquid semiconductors. Meas. Sci. Technol. 11, 1-4.

Sauerbrey, G. 1959. Use of quartz vibrator for weighing thin layers and as a micro-balance. Zeitschrift für Physik 155 (2), 206-222.

Schmidt, C., Bodnar, R.J., 2000. Synthetic fluid inclusions: XVI. PVTX properties in the system H_2O-NaCl-CO_2 at elevated temperatures, pressures, and salinities. Geochimica et Cosmochimica Acta 64 (22), 3853-3869.

Schulien, S., 1987. High-temperature/high-pressure solubility measurements in the systems $BaSO_4$-NaCl-H_2O and $SrSO_4$-NaCl-H_2O in connection with scale studies. SPE symposium (SPE 16264), San Antonio, Texas.

Sharp, W.E., Kennedy, G.C., 1965. The system CaO-CO_2-H_2O in the two phase region calcite + aqueous solution. J. Geol. 60, 391-403.

Sokolovskii, B.; Plevachuk, Y.; Didoukh, V., 1995. Electroconductivity and liquid-liquid equilibrium in the Pb-Ga system. Phys. Stat. Sol. (a) 148, 123-128.

Sourirajan, S., Kennedy, G. C., 1962. The system H_2O-NaCl at elevated temperatures and pressures. American J. Sci. 260, 115-141.

Sterner, S.M., Bodnar, R.J., 1984. Synthetic fluid inclusions in natural quartz I. Compositional types synthesized and applications to experimental geochemistry. Geochimica et Cosmochimica Acta 48, 2659-2668.

Strübel, G., 1966. Die hydrothermale Löslichkeit von Cölestin in System $SrSO_4$-NaCl-H_2O. Neues Jahrb. Mineral. Mon., 99-107.

Vityk, M.O., Bodnar, R.J., 1998. Statistical microthermometry of synthetic fluid inclusions in quartz during decompression reequilibration. Contrib Mineral Petrol 132, 149-162.

9. BaSO₄ Solubility in NaCl at High Temperature and Pressure

A study of the solubility of barite ($BaSO_4$) in sodium chloride solutions from very diluted to highly concentrated solutions, under hydrothermal conditions, was undertaken in connection with research on the scale formation problem found in many industrial processes. The deposition of barium sulphate as scale from highly concentrated brines found in oil and geothermal wells is a common problem (Templeton, 1960). The thermodynamic models used to predict mineral solubility in natural waters must be based on a relatively large amount of accurate experimental data of the scale forming phases at the different conditions of temperature, pressure and composition found in real life. Some of the available data on the solubility of barium sulphate in sodium chloride are inconsistent, and most of the published data only cover a narrow range of low temperature (around 25°C) and NaCl concentration, and are measured at atmospheric pressure. The use of such data can lead to weak models and inaccurate predictions. The few sources dealing with high temperature and pressure cannot be cross-checked due to the different experimental conditions. Therefore, a larger databank is necessary to understand and predict the causes of precipitation and dissolution of barite in nature.

An experimental setup has been developed in order to measure the solubility of barite and/or celestite ($SrSO_4$) in aqueous solutions of sodium chloride (NaCl) at high temperatures (up to 250°C), high pressures (up to 700 bar), and high ionic strengths (from very diluted NaCl solutions up to the saturation point). The setup is shown in figures aIII-3 and aIII-4 in Appendix III.

9.1 Previous Studies of BaSO₄ Solubility in NaCl Solutions

The solubility of barium sulphate in sodium chloride solutions has been previously studied by Templeton (1960), Uchameyshvili et al. (1966), Strübel (1967), Davis and Collins (1971), Blount (1977), and Schulien (1987). Nevertheless, published data on the solubility of barite at temperatures above 25°C and pressures larger than 1 atm are scarce. The ranges of temperature, pressure and NaCl concentration covered by the different investigators are given in table 9-1.

The experimental procedure followed by the majority of the sources determining barite solubility in NaCl solutions can be divided into four main steps:

- Preparation of the starting solid by precipitation. In some cases natural barite or commercial crystalline powder is employed, and this step may be avoided.

- o Placement of a solution containing excess of BaSO$_4$ in a device keeping constant temperature and pressure. This step may include agitation of the sample during the equilibration period. In some studies, only one of the variables is kept constant (e.g., pressure), while the other (e.g., temperature) is changed slowly.
- o Sampling of the solution after equilibrium is reached.
- o Analysis of the Ba^{2+} concentration.

The main differences among the procedures used by the different investigators are found in the choice of analytical technique, device to heat, pressurize and agitate the samples, etc. A summary of the experimental procedure followed by each investigator is reported in table 9-2.

Table 9.1
Experimental measurements of BaSO$_4$ solubility in NaCl solutions

T (^{o}C)	P(bar)	NaCl (m)	Number of data	Reference
20/350	1/165	0.1-2	41	Strübel (1967)
25/95	1	0.1-5	108	Templeton (1960)
25	1	0.01-2	8	Davis and Collins (1971)
80/120	1/414	0.1-2	34	Schulien (1987)
94/253	5/560	0.2-4	35	Blount (1977)
95/340	1/165.4	0.25-2	84	Uchameyshvili et al. (1966)

Table 9-2
Experimental procedures used to determine BaSO$_4$ solubility in NaCl solutions

Reference	Agitation	Initial solid	Pressurizing	Filter	Dilution
Templeton (1960)	Stirrer	Precipitated BaSO$_4$	No	Millipore hypodermic syringe filter	Yes
Uchameyshvili et al. (1966)	Rocking	Natural barite	No	No	No
Strübel (1967)		Natural barite		No	No
Davis and Collins (1971)	Shaking	Precipitated BaSO$_4$	No	Double Watman no. 42 filter paper	No
Blount (1977)	Rocking	Precipitated BaSO$_4$	Pressure vessel (±3 bar)		Some
Schulien (1987)	No	Commercial powder BaSO$_4$	2 pressure vessels	0.5 µm Millipore filter	Yes

Reference	Time (h)	Heating	Analysis	P medium
Templeton (1960)	24-48	Water bath (± 0.05^{o}C)	Ba: spectrographic method (±5%)	
			S: microreduction-colorimetric method (±0.3 mgL^{-1})	
Uchameyshvili et al. (1966)	48-72	Electrical resistance furnace	Syngle crystal weight-loss method	
Strübel (1967)	10-2500[a]		Single crystal weight-loss method	
			X-ray fluorescence	
Davis and Collins (1971)	72	Heat lamp (±1°C)	Liquid scintillation counting (±20%)	
Blount (1977)	48-288	Muffle furnace (±1.5%)	Ion exchange resin + X-ray fluorescence (±5%[b])	Water
Schulien (1987)	4-48	Environmental chamber	Atomic absorption spectrometry (±3%)	Nitrogen (g)

[a] 10 h were waited for the experiments at 600°C, while 2500 h were waited when the experimental temperature was 150°C.
[b] for high NaCl concentrations (4 m) the uncertainty is larger (around 7%)

9.1.1 Starting Material

In the majority of studies the solid employed was either natural barite (Uchameyshvili et al., 1966, Strübel, 1967) or precipitated barium sulphate (Templeton, 1960, Davis and Collins, 1971, Blount, 1977), which may lead in both cases to experimental errors. Only Schulien (1987) used commercial crystalline $BaSO_4$ powder.

Natural barite contains different amounts of other species which will affect the barium concentration in the solution. According to Blount (1977), natural barites may contain mineral inclusions which will dissolve increasing the ionic strength and modifying barite solubility.

Precipitated $BaSO_4$ can also lead to erroneous solubility measurements resulting from poor solid crystallinity or occluded reactants. According to Balarew (1925), $BaSO_4$ precipitates contain up to as much as 1% of occluded $BaCl_2$. Templeton (1960) used commercial $BaCl_2$ and Na_2SO_4 to obtain barite with a 0.026% excess of soluble sulphate.

9.1.2 Analytical Techniques

A wide variety of analytical procedures were used by different investigators to determine the solubility of barium sulphate. Templeton (1960) analyzed the barium content by a spectrographic method (Grabowski and Unice, 1958) resulting in a precision of 5% for barium concentrations larger than 3 mg L^{-1}. Total sulphur was determined by a microreduction-colorimetric method (Johnson and Nishita, 1952), allowing a precision of 0.3 mg L^{-1} in the concentration range from 1 to 45 mg L^{-1}. All the measurements were carried out both from supersaturation and undersaturation, to assure equilibrium was attained.

The single-crystal weight-loss method was employed by Uchameyshvili et al. (1966) and Strübel (1967). The latter also analyzed the total barium content by X-ray fluorescence. Due to the low solubility of $BaSO_4$ in water (of the order of 10^{-5} m) and in NaCl solutions (of the order of 10^{-4} m) the weight-loss method is not recommended. Uchameyshvili et al. (1966) used a very accurate (0.01 mg) microanalytical balance, but they also employed considerably large quantities of natural barite crystals (from 2 to 7 g) and low volumes of solution (40 mL), which may lead to large errors by the weight-loss method.

Davis and Collins (1971) measured the sulphate concentration of a radioisotope-tagged (^{35}S) solution of precipitated $BaSO_4$ by liquid scintillation counting, resulting in efficiency around 20%. Total barium was also analyzed by emission spectroscopy, but the precision obtained for concentrations of 1 mg L^{-1} and lower was not satisfying. When the data of the

barium ion and the sulphate ion are given separately, it can be clearly observed the disagreement between both experimental techniques is very high.

Blount (1977) determined the amount of barium by X-ray fluorescence after taking up the barium contained in the experimental solution by means of a chelating ion-exchange resin. To avoid interferences, high ionic strength solutions were diluted 1:10. The accuracy of the method is reported to be better than $\pm$ 5%. Nevertheless, the uncertainty of barium analysis for 4 m NaCl solutions is quite large (around $\pm$ 7%). When having high ionic strength media the recovery of barium by the resin may be interfered by other cations, sodium in this case. Finally, Schulien (1987) analyzed the barium content in the sample by atomic absorption spectroscopy, reporting an accuracy of $\pm$ 3%.

9.1.3 Dilution

Some of the previous analyses (at atmospheric pressure and room temperature) are performed directly on the experimental samples, without previous dilution. The solubility of barite decreases with decreasing pressure and may also decrease with decreasing temperature. Therefore, dilution is a requirement in most of the cases to avoid precipitation when both temperature and pressure are decreased from the experimental values to room conditions. Otherwise, erroneous low solubility values are very likely to be measured as a result of precipitation.

From the sources shown in table 9-1, only Templeton (1960) and Schulien (1987) diluted their samples with barium free-NaCl solution of the same concentration as in the experiment, prior to the change of the experimental conditions and the analysis. Templeton (1960) only diluted the samples for the determination of barium, while sulphate determinations were made on the undiluted samples.

Blount (1977) only diluted high ionic strength samples to avoid interferences during the ion exchange process to recover barium. The limit value chosen by Blount (1977) to decide whether dilution was required or not is not mentioned in his publication. Therefore, it is not possible to determine the data that may be affected by precipitation before analysis.

It is unlikely that Uchameyshvili et al. (1966) and Strübel (1967) data are affected by this experimental error as the weight-loss method is employed.

Davis and Collins (1971) only performed measurements at 25°C and 1 atm, thus their data are also safe from this experimental error.

9.1.4 Agitation

Agitation of the sample is provided by means of a stirrer (Templeton, 1960), a shaker (Davis and Collins, 1971), or by rocking the setup (Uchameyshvili et al., 1966, Blount, 1977). Schulien (1987) did not use any kind of mixing mechanism in the sample solution.

9.1.5 Time Required to Attain Equilibrium

The time waited for the different investigators before performing the analysis varies from 4 hours (Schulien, 1987) to 2500 hours (Strübel, 1967). Even though Schulien (1987) usually waited 24 hours prior analysis, he assures the results did not vary after 4 hours.

9.1.6 Temperature

Different devices were employed to increase and keep a constant temperature. Templeton (1960) used a water bath thermostat controlled to within $\pm 0.05^{o}$C. Uchameyshvili et al. (1966) introduced the vessel containing the solution into and electrical resistance furnace and measured the temperature by means of a Chromel-Kopel thermocouple accurate to ± 1-3°C. Similar ovens to heat up the solution were also used by Blount (1977) and Schulien (1987). A heat lamp was employed to slightly increase the temperature above the stabilized room temperature (25 ± 1°C) for Davis and Collins (1971) measurements.

9.1.7 Pressure

There are only two sources in table 9-1 performing experiments at pressures larger than 1 atm or the saturation pressure of the solution (Blount, 1977 and Schulien, 1987). Blount (1977) uses a pressure vessel formed by an inner cell containing the sample and surrounded by an outer space. Water is pumped to or out from the space in order to control the pressure. Schulien (1987) employed a high pressure autoclave vessel and nitrogen gas as pressure medium.

9.1.8 Filtration

The filtration procedure followed by some of the sources shown in table 9-1 (Templeton, 1960, Blount, 1977) is inaccurate, as the samples were filtered at atmospheric conditions. Large changes in temperature and pressure will then be experienced by the solution while it is being filtered, which could lead to solid deposition in the sampling tube or in the filter. Part of those deposits could also be re-dissolved when taking out new samples.

Templeton (1960) withdrew the samples through a Millipore hypodermic syringe filter. Davis and Collins (1971) used a double Watman number 42 filter paper. Blount (1977) withdrew samples by opening a valve located at the other end of a pipe connected to the sample cell. Schulien (1987) filtrated at the experimental conditions by using a 0.5 µm Millipore filter connecting two pressure vessels.

As mentioned in Chapter 4, many of the data are shown to be inaccurate and most of them could not be tested for their reliability. It is clear, at certain conditions, the existence of erroneous measurements, as two sources report rather different values. Nevertheless, due to the lack of data at the same conditions it is not possible to conclude which sources are reliable.

Even though the procedure followed by Schulien (1987) seems to be the most reliable experimentally (commercial powder $BaSO_4$ used as starting solid, filtration under experimental conditions, dilution prior analysis to avoid precipitation), his results strongly disagree with the other sources shown in table 9-1. The main shortcoming of Schulien's (1987) work is the short time awaited to assure equilibrium (he assures 4 hours were enough). Moreover, no agitation device is employed, and thus, it is very unlikely that his solutions were at equilibrium. This fact could explain the much lower values reported by Schulien (1987) when compared to other sources in table 9-1.

Some of the measurements performed by Blount (1977) may be affected by precipitation of $BaSO_4$ during filtration or prior analysis, which could explain the low values obtained.

Uchameyshvili et al. (1966) and Strübel (1967) data may contain some inaccuracies as a consequence of the use of natural barite and the single crystal weight-loss method to analyze the solubility.

9.2 Previous Studies of SrSO₄ Solubility in NaCl Solutions

As mentioned in a previous chapter, there is a large disparity in the reported solubility values for celestite in sodium chloride solutions. This inconsistency is aggravated at high temperature and pressure conditions. Table 9-3 shows the ranges of temperature, pressure and NaCl concentration covered by different investigators reporting $SrSO_4$ solubility in $NaCl-H_2O$.

The experimental procedure followed by the majority of the sources determining celestite solubility in NaCl solutions can be divided in the same four main steps reported previously for barite. Culberson et al. (1978) employed a different approach using a 1 cm internal diameter column packed with solid $SrSO_4$ through which the NaCl solution is passed

various times. To prevent channelling, the solid was inverted several times and allowed to resettle before each measurement.

A summary of the experimental procedure followed by each investigator is reported in table 9-4.

Table 9-3
Experimental measurements of SrSO$_4$ solubility in NaCl solutions

T (^{o}C)	P (bar)	NaCl (m)	Number of data	Reference
-0.05/25	1	0.004-0.05	10	Lucchesi and Whitney (1962)
10.3/40	1	0.05-5.6	36	Reardon and Armstrong (1987)
20/90	1	0.1-2.6	32	Strübel (1966)
25	1	0.01-2	10	Davis and Collins (1971)
25	1	0.5	5	Brower and Renault (1971)
25	1	0.73	1	Culberson et al. (1978)
25	1	0.4-5.1	8	Müller (1960)
25/253.5	1/600	0.5-5	436	Howell et al. (1992)
25/125	1/2.3	0.2-5.7	24	Vetter et al. (1983)
80/120	1/414	0.1-2	49	Schulien (1987)
100/305	0.2/165	0.2-3.7	41	Jacques and Bourland (1983)

Table 9-4
Experimental procedures used to determine SrSO$_4$ solubility in NaCl solutions

Reference	Agitation	Initial solid	Pressurizing	Filter	Dilution
Lucchesi and Whitney (1962)	Rods	Precipitated SrSO$_4$	No	No	No
Reardon and Armstrong (1987)	Rods	Precipitated SrSO$_4$	No	No	No
Strübel (1966)		Natural celestite	No		?
Davis and Collins (1971)	Shaking	Precipitated SrSO$_4$	No	Double Whatman no. 42 filter paper	No
Brower and Renault (1971)	Rods	Precipitated SrSO$_4$	No	No	No
Culberson et al. (1978)	No	Precipitated SrSO$_4$	No	No	No
Müller (1960)		Precipitated SrSO$_4$			
Howell et al. (1992)	No	Precipitated SrSO$_4$	High pressure pump	Coarse (40-60µm) fritted glass filter	Yes
Vetter et al. (1983)	Shaking	Precipitated SrSO$_4$	No	No	No
Schulien (1987)	No	Commercial powder SrSO$_4$	2 pressure vessels	0.5 µm Millipore filter	Yes
Jacques and Bourland (1983)	Rods	Precipitated SrSO$_4$	2 pressure vessels	Yes	Yes

Reference	Time (h)	Heating	Analysis	P medium
Lucchesi and Whitney (1962)		Thermostat (±0.005°C)/Ice-water bath	Liquid scintillation counting (±1%)	
Reardon and Armstrong (1987)		Water bath	Atomic absorption spectrometry (±1%) Ion chromatography for sulphates (±5%)	
Strübel (1966)	35-340	Oven		
Davis and Collins (1971)	72	Heat lamp (±1°C)	Liquid scintillation counting (±20%)	
Brower and Renault (1971)			Atomic absorption spectrometry (±10%)	
Culberson et al. (1978)		Water jacket + controller (±0.05°C)	Atomic absorption spectrometry	
Müller (1960)	48		Titration	
Howell et al. (1992)	24	Oven + T controller (±1°C)	Atomic absorption spectrometry	
Vetter et al. (1983)	72-168	Heat box	Liquid scintillation counting (90Sr, 32S)	
Schulien (1987)	4-48	Environmental chamber	Atomic absorption spectrometry (±1%)	Nitrogen (g)
Jacques and Bourland (1983)	72	Oven + T controller (±0.1°C)	Atomic absorption spectrometry	Nitrogen (g)

9.2.1 Starting Material

The majority of the studies of celestite solubility used SrSO$_4$ synthesized by reaction of a sulphate salt, usually Na$_2$SO$_4$, and a strontium salt, usually SrCl$_2$ (Lucchesi and Whitney, 1962, Brower and Renault, 1971, Davis and Collins 1971, Culberson et al., 1978, Jacques and Bourland, 1983, Vetter et al., 1983, Howell et al. 1992). Reardon and Armstrong (1987) obtained celestite by titrating a 0.003 m H$_2$SO$_4$ solution with a Sr(OH)$_2$ solution to a pH of 5.7, which, according to these investigators, ensures a purer solid than the one obtained with SrCl$_2$ and Na$_2$SO$_4$. They also performed tests to assure their starting material was not affected by surface poisoning effects before the solubility experiments were conducted. Müller (1960) precipitated celestite from commercial solutions of SrCl$_2$ and H$_2$SO$_4$. Natural mineral from Girgenti, Bristol and Gembeck containing 0.09% CaO and barium traces was employed by Strübel (1966). The latter investigator also used precipitated SrSO$_4$ in some of his measurements. Only Schulien (1987) used commercial crystalline SrSO$_4$ in his solubility determinations. As mentioned previously for the case of barite, the use of either natural minerals of precipitated strontium sulphate may lead to experimental errors. Therefore, the use of crystalline commercial powder is preferred.

9.2.2 Analytical Techniques

Mainly, two analytical techniques were used to determine strontium concentrations in the samples: Liquid scintillation counting (LSC) and atomic absorption spectrometry (AAS). Lucchesi and Whitney (1962), Davis and Collins (1971) and Vetter et al. (1983) used LSC, resulting in efficiencies between 1% (Lucchesi and Whitney, 1962) and 20% (Davis and Collins, 1971). AAS was used by Brower and Renault (1971), Culberson et al. (1978), Jacques and Bourland (1983), Reardon and Armstrong (1987), Schulien (1987) and Howell et al. (1992), resulting in efficiencies between 1% (Reardon and Armstrong, 1987, Schulien, 1987) and 10% (Brower and Renault, 1971). Müller (1960) determined the Sr^{2+} concentration by titration, a method which is not recommended for the low solubility values being analyzed. Reardon and Armstrong (1987) also determined sulphate concentrations on selected samples by ion chromatography, obtaining larger analytical uncertainties ($\pm$ 5%) than when using AAS. Vetter et al. (1983) used two different tagged isotopes (^{90}Sr and ^{32}S) for cross-checking of the results. In some case, their deviations were as large as 30 %.

Two sources (Lucchesi and Whitney, 1962 and Reardon and Armstrong, 1987) performed analysis on the final solid phase. Lucchesi and Whitney (1962) used X-ray powder diffraction photographs on the solid, concluding it was pure strontium sulphate. Reardon

and Armstrong (1987) analyzed the sodium content of the final solid, in order to prove that substantial substitution of Cl^- for SO_4^{2-} and Na^+ for Sr^{2+} did not occur in the solid phase.

9.2.3 Dilution

To avoid precipitation of strontium sulphate when pressure is decreased from the experimental value to atmospheric pressure, the samples were diluted with water (Howell et al., 1992) or NaCl solution (Schulien, 1987, Jacques and Bourland, 1983). All other sources shown in table 9-3 performed experiments at atmospheric pressure, and therefore dilution is not required (celestite solubility has a maximum around 25ºC).

9.2.4 Agitation

Agitation of the sample is provided by means of a shaker (Davis and Collins, 1971 and Vetter et al., 1983), or a roller/rod (Lucchesi and Whitney, 1962, Brower and Renault, 1971, Jacques and Bourland, 1983, Reardon and Armstrong, 1987). Culberson et al. (1978), Schulien (1987) and Howell et al. (1992) did not use any kind of mixing mechanism in the sample solution.

9.2.5 Time Required to Attain Equilibrium

The equilibration time waited for the different investigators before sampling varies from 4 hours (Schulien, 1987) to 340 hours (Strübel, 1966). As in the case of barite, Schulien (1987) carried out experiments in time intervals from 4 to 72 hours, concluding that the results did not vary after 4 hours, when equilibrium had been attained. Brower and Renault (1971) monitored the conductivity of the $SrSO_4$-H_2O system as a function of time to verify the attainment of equilibrium. According to them, equilibrium is reached in less than one minute by dissolution, but may be much slower by precipitation. Reardon and Armstrong (1987) approached the equilibrium from both super and undersaturation, increasing or decreasing progressively the temperature. This procedure was also followed by Lucchesi and Whitney (1962) for some of their measurements. Davis and Collins (1971) prepared all samples in duplicate to assure equilibrium.

9.2.6 Temperature

Davis and Collins (1971) used a heat lamp to slightly increase the temperature above a stabilized room at $25 \pm 1°C$. An oven was used by Strübel (1966), Jacques and Bourland

(1983), Schulien (1987) and Howell et al. (1992), to increase the temperature up to 90, 305, 120 and 253°C, respectively. Some of the ovens were equipped with temperature controllers to keep the temperature as constant as possible (± 0.1°C for Jacques and Bourland, 1983, and ± 1°C for Howell et al., 1992). Reardon and Armstrong (1987) employed a water bath. Vetter et al. (1983) performed some measurements at room temperature, where no heating device or temperature controller was used. For the high temperature solubility determinations (up to 125°C), the solution was place inside a thermally insulated constant temperature heat box. Culberson et al. (1978) kept a constant temperature throughout the column by means of a water jacket and a proportional temperature controller to within ± 0.05°C. Lucchesi and Whitney (1962) used a thermostat regulated at 25 ± 0.005°C for their solubility determinations at this temperature, while an ice-water bath was used for the measurements at -0.05°C.

9.2.7 Pressure

Only a few sources (Jacques and Bourland, 1983, Schulien, 1987, Howell et al., 1992) performed experiments at pressures larger than 1 atm or the saturation pressure of the solution. Howell et al. (1992) employed a pressure vessel connected to a high pressure pump. Jacques and Bourland (1983), and Schulien (1987) used two pressure vessels (one containing the solution and the other to filtrate under experimental conditions) and employed nitrogen as pressurizing medium. At the high temperature and pressure conditions measured, nitrogen solubility may be relatively high both in water and in NaCl solutions, and may have some influence on the results obtained. According to Sun et al. (2001), the solubility of nitrogen in water at 150°C and 400 bar (conditions measured by Schulien, 1987) is 0.1386 m, while this value decreases to 0.0638 m at the same conditions for a 4 m NaCl solution.

9.2.8 Filtration

After equilibrium is obtained, separation of the liquid and solid phases under conditions as close as possible to those of the test is required. Howell et al. (1992) prevented the pass of solid particles into the sample using a coarse (40-60 μm) fritted glass filter mounted inside the reaction vessel. The size of the filter pore selected by Howell et al. (1992) is 10 times larger than in the rest of the literature on SrSO$_4$ solubility in water and in NaCl solutions. Jacques and Bourland (1983) devised a two pressure vessel system where SrSO$_4$ was dissolved to the saturation point in one vessel and then filtered under experimental

conditions to the second vessel. A very similar procedure formed also by two pressure vessels connected through a filter was used by Schulien (1987). The filter membrane used was a Millipore Fluoropore filter of 0.5 µm pore size. Davis and Collins (1971) used a double Whatman number 42 filter paper. The rest of the sources shown in table 9-3 do not report to have filtrated the samples. Vetter et al. (1983) did not use a filter, but allowed the solution to settle for some time, usually 24 hours.

9.3 Our Experimental Method

An excess of crystalline powder $BaSO_4$ was added to NaCl solutions, and the mixtures were heated up and pressurized. After agitating for the time required to attain equilibrium, the solution was filtrated under the experimental conditions and the samples were stored for analysis by inductively coupled mass spectrometry (ICP-MS).

9.3.1 Materials

Extra pure (97.5-100 %) finely powdered commercial barium sulphate (222515000 from Acros Organics) was used in the experiments. All water used was distilled water. Commercial sodium chloride (207790010 from Acros Organics) of 99.5 % purity was used. Due to the highly hygroscopic characteristics of sodium chloride, the powder was dried at 100°C in an oven during 16 hours prior to its use and always placed inside a desiccator.

9.3.2 Experimental Device

The experimental device designed and built to carry out experimental determinations of $BaSO_4$ and $SrSO_4$ solubility in the systems $NaCl-BaSO_4-H_2O$ and $NaCl-SrSO_4-H_2O$ is shown in Figure 9-1.

The system is mainly formed by two high pressure vessels in series with two pumps, connected through a filter and placed inside an oven.

The pressure vessels (TOC3-20-HC276/Piston from High Pressure Equipment Company (HIP), http://www.highpressure.com) are tubular piston reactors made of Hastelloy C 276. This material is chosen in order to avoid corrosion problems found for 316 stainless steel (Jacques and Bourland, 1983, Howell et al., 1992). Each vessel is formed by a 20" long cylindrical body of ¾" internal diameter (ID) and 1½" outside diameter (OD), and two caps provided with Kelrez o-rings. The volume of the pressure vessels is selected according to DTU's safety regulations (pressure-volume ratio limited to 200 bar L^{-1} for high pressure

equipment). The vessels can stand up to 300°C and 10000 psi. Figure 9-2 shows the cross section of a pressure vessel and a cap.
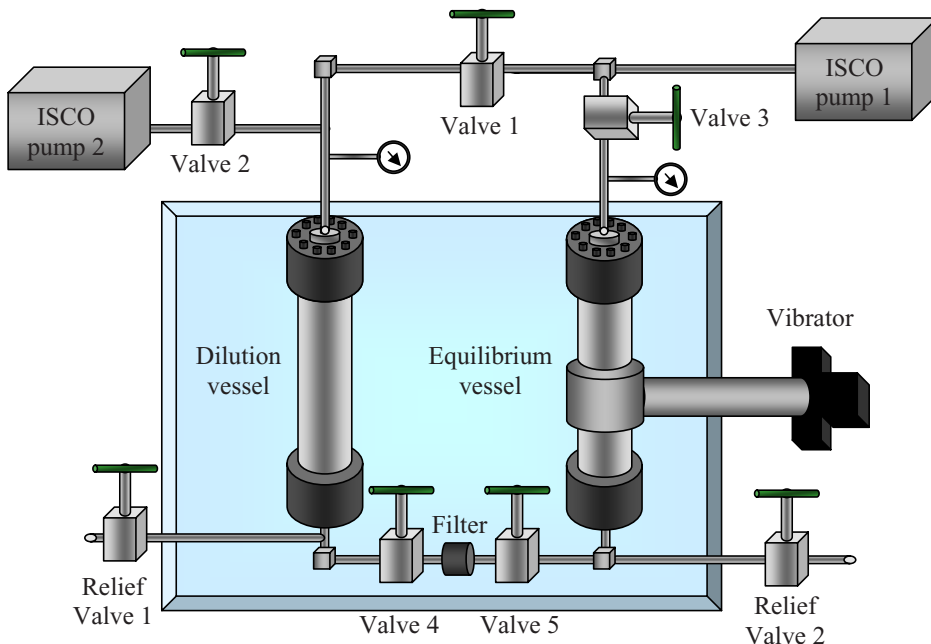

Figure 9-1. Experimental setup for the high pressure/high temperature solubility measurements

The line filter (10-51AF4-5HC276 from HIP) is formed by four sintered stainless steel filter discs of 0.5 μm pore size inserted in a body made of Hastelloy C 276, material also used for the end covers. It can stand up to 10000 psi.

The oven (UT6420 from Heraeus) has a total volume of 375L, whit a chamber size 554 mm width, 1319 mm long and 522 mm depth. The oven is provided with a Digicon electronic temperature controller and digital display of the set point and the real temperature value. It allows excellent temperature uniformity (2%). The uncertainty in the temperature measured by the oven is ± 0.5^{o}C.

The pumping system (ISCO pump 1 and ISCO pump 2 in figure 9-1) consists of a pressure/flow rate controller and a piston-driven pump module (D Series Syringe Pumps 100DX from ISCO). The cylinders, pistons and caps are made of Nitronic 50, and the seals are manufactured of graphite-impregnated Teflon. The ISCO pumps can work in two different modes: constant flow and constant pressure. The pump is also supplied with two valves that can be handled to reverse the flow direction. In that way, each pump can either drive water to the pressure vessel or remove water from the pressure vessel. The uncertainty

in the pressure measured by the ISCO pump is $\pm$ 0.05 bar. The maximum pressure is 10000 psi, while the flow can vary from $1 \cdot 10^{-5}$ mL min^{-1} to 50 mL min^{-1}. The pump capacity is 103 mL. Additional readings (accuracy of 100 psi) of the pressure can be done in the two pressure gauges (4.5PG10 from HIP) placed in the line with each pressure vessel.
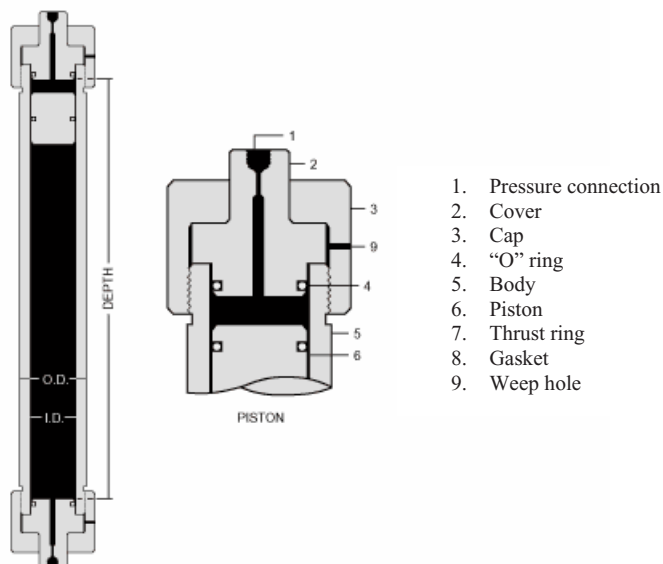

1. Pressure connection
2. Cover
3. Cap
4. "O" ring
5. Body
6. Piston
7. Thrust ring
8. Gasket
9. Weep hole

Figure 9-2. Cross-section of piston high pressure vessel and cap

The two valves located inside the oven (valves 4 and 5 in figure 9-1) are high temperature valves (30-11HF4-HT from HIP), standing up to 538°C and 30000 psi. The body is manufactured from high tensile type 316 stainless steel with grafoil packing. They are provided with an extension to remove the stuffing box away from the hot area of the valve, and allowing placing the handle outside the oven for an easier operation of the equipment.

The valves placed outside the oven (valves 1 and 2 in figure 9-1; 30-11HF4 from HIP) work at room temperature and therefore do not need special features as the previous ones. The valve body is made of high tensile type 316 stainless steel and hardened 17-4PH stainless steel for the lower section stems. The packing includes 90 durometer Buna-nitrile O-ring. They can stand up to 30000 psi.

The safety valves (Safety Head LPSH2-1/4A from BuTech Pressure Systems) are fitted with a rupture disc with a nominal burst pressure of 10000 psi (relief valves 1 and 2 in figure 9-1). Both the safety heads and the rupture discs are manufactured in 316 stainless steel.

All the additional components of the experimental device schematized in figure 9-1 (tubing, adapters, couplings, tees, etc.) were manufactured in 316 stainless steel. The tubing OD is ¼".

To provide agitation a pneumatic turbine-vibrator (NCT 10 from Copenhagen Vibrator Products ApS) is connected to the equilibrium vessel.

9.3.3 Experimental Procedure

Sufficient excess of powder barite was added to a NaCl solution of the desired concentration. After vigorous agitation, this sample was used to fill the equilibrium vessel. The dilution vessel was filled with a known amount of distilled water[1]. The tubing connecting both ISCO pumps with the vessels, and the tubing connecting both vessels and the filter is filled with water by pumping liquid from the ISCO pumps. This operation will assure an exact value of the filtrated volume, which could be erroneous if air is present in any of the mentioned pipes. The vessels are then transferred to the preheated oven chamber and properly screwed in both ends. Placing the vessels and the filtration system inside an oven will keep a constant temperature distribution.

Valves 4 and 5 (see figure 9-1) are closed to assure no sample is passing from one vessel to another. The whole system is pressurized to the desired pressure by using ISCO pump 1 in a constant pressure mode and keeping valves 1 and 3 open. To provide mixing of the solution in the equilibrium vessel a vibrator was used. After allowing the sample to attain equilibrium the solution is filtered at the experimental temperature and pressure by driving liquid from the equilibrium vessel to the dilution vessel through a 0.5 μm pore size filter. This operation requires the use of two ISCO pumps: ISCO pump 1 will work in the constant pressure mode, while ISCO pump 2 will work in the constant flow mode. Operating in this way, ISCO pump 1 will maintain a constant pressure by a positive displacement of the piston in the equilibrium vessel, while ISCO pump 2 will move the piston in the dilution vessel upwards, allowing the filtrated solution to be hold in the dilution vessel. To avoid water to bypass from one pump to the other, valve 1 must be closed during the filtration. A schematic diagram of the filtration procedure is shown in figure 9-3.

Once the desired volume of sample has been filtered, the pressure is decreased to 1 atm and the system cooled down to room temperature before taking the sample out and storing it for a later analysis. Precipitation as a consequence of the changes in both temperature and

---

[1] NaCl solution substitutes distilled water in the filtration reactor when dilution with the available volume of water is not enough to avoid barite precipitation when decreasing the experimental temperature and pressure to room conditions.

pressure is avoided due to the dilution process taking place in the dilution vessel. Previous calculations determine the maximum filtration volume allowed to assure precipitation will not take place when the experimental conditions are changed to atmospheric pressure and room temperature.
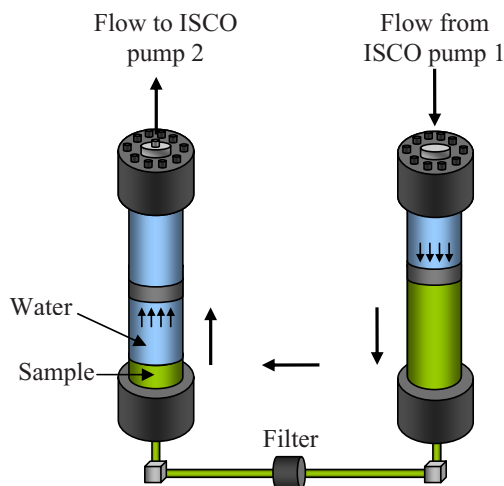

Figure 9-3. Filtration process

9.3.4 Experimental Uncertainties

The temperature was measured within $\pm$ 0.5^{o}C, and the uncertainty of the experimental pressure was $\pm$ 0.05 bar.

The uncertainty associated with weighing starting materials (NaCl) during sample preparation is $\pm$ 0.05 mg. The volume of NaCl sample prepared was always 1 L, and thus the largest error, corresponding to the lowest NaCl concentration employed (0.1 M) is $\pm$ 8.6$\cdot$10^{-4}%.

The uncertainty related to the weight of the distilled water used to fill in the dilution vessel is $\pm$ 0.5 mg. That uncertainty is translated into absolute deviation values for barite concentration within the range 10^{-11} to 10^{-10} m. The highest deviation found for all the measurements performed is 2.72$\cdot$10^{-10} m BaSO$_4$ ($\pm$ 3.1$\cdot$10^{-4}%), a value low enough to be neglected. For NaCl solubility determinations, the absolute deviation is found within the range 4.7$\cdot$10^{-5} to 6.6$\cdot$10^{-5} M (molarity).

The uncertainty associated to the filtration volume is $\pm$ 0.005 mL, which results in absolute deviations for the concentration of BaSO$_4$ of the order of 10^{-8} m. The highest absolute deviation found is 8.54$\cdot$10^{-8} m BaSO$_4$, a value that can be neglected if we take into account

the measured concentrations are of the order of 10^{-5} m. For NaCl solubility determinations, the absolute deviation is found within the range $1 \cdot 10^{-3}$ to $2.3 \cdot 10^{-3}$ M.

The standard deviations and variation coefficients associated to the ICP-MS determinations are given in tables aIII-1 to aIII-3 in Appendix III.

9.4 Analytical Technique: Inductively Coupled Plasma Mass Spectrometry

The determination of barite solubility is a rather complex task due to the difficulty of finding a reliable analytical technique able to measure accurately so low concentrations. Any colorimetric/gravimetric/titration technique, or any technique involving the measurement of masses and/or volumes must be rejected, as it will very likely imply large experimental errors. Barite solubility in water is of the order of 10^{-5} m, while barite solubility in NaCl solutions is of the order of 10^{-4} m. Moreover, in order to avoid precipitation when the experimental temperature and pressure are brought to atmospheric conditions, high dilution rates are required. Thus, the final concentrations to be measured may be well below 1 ppm (and therefore, the detection limit of the analytical technique should be at least 10 times lower).

Vetter et al. (1983) studied the accuracy of atomic absorption (AA), atomic emission (AE) and liquid scintillation counting (LSC) in the determination of SrSO₄ concentrations. They prepared solutions of known amounts of Sr^{2+} in distilled water and in solutions of NaCl, MgCl₂ and CaCl₂, and analyzed them by AA, AE and LSC. They concluded that AE is consistently inaccurate and, thus, unreliable. The same conclusion is supported by Davis and Collins (1971) when studying BaSO₄ solubility.

According to Vetter et al. (1983), the AA method gave systematically low values of strontium concentration, with a relative deviation with respect to their standards as high as 16%. This value is expected to be even larger for barite due to its lower solubility. Rollemberg and Curtius (1982) used flameless atomic absorption to determine barium in natural waters, after separating it from the interfering ions by ion-exchange chromatography. The relative deviation was over 10% for most of the measurements, and reached 20% for 100 ppm samples, even though the detection limit of the device used was 9 ppm. Roe and Froelich (1984) determined barium with a precision about ± 13% by graphite furnace atomic absorption, with a detection limit of 0.6 ppm.

Vetter et al. (1983) state high accuracy can be obtained in SrSO₄ determinations by LSC. Nevertheless, Davis and Collins (1971) measured the sulphate concentration of a

radioisotope-tagged (^{35}S) solution of precipitated $BaSO_4$ by LSC, resulting in a low reproducibility ($\pm$ 20%)

All the problems found in the literature for AA and AE, together with the capabilities found at DTU, made us choose ICP-MS to determine our $BaSO_4$ concentrations.

9.4.1 Introduction

Inductively coupled plasma mass spectrometry (ICP-MS) is widely used for trace (ppb-ppm) and ultra-trace (ppq-ppb) elemental analysis. ICP-MS has become the most prominent MS technique due to its extremely low detection limits (see figure 9-4) for the majority of the elements and its multi-element capability (Stuewer and Jakubowski, 1998). Since 1983, when the technique was made commercially available, ICP-MS devices have been used worldwide in many different application areas such as environmental, geochemical, medical, nutritional, nuclear, chemical, metallurgical, etc. ICP-MS has clear advantages when compared to other spectroscopic techniques (flame atomic absorption, inductively coupled plasma optical emission spectrometry, emission atomic absorption): It can be used for multi elemental analysis of solid, liquid and vapour samples; it is fast (it can determine all the elements in about six minutes); it has lower detection limits (see figure 9-4) and a larger linear interval than any other spectroscopic technique; and it can be used for isotopic analysis.

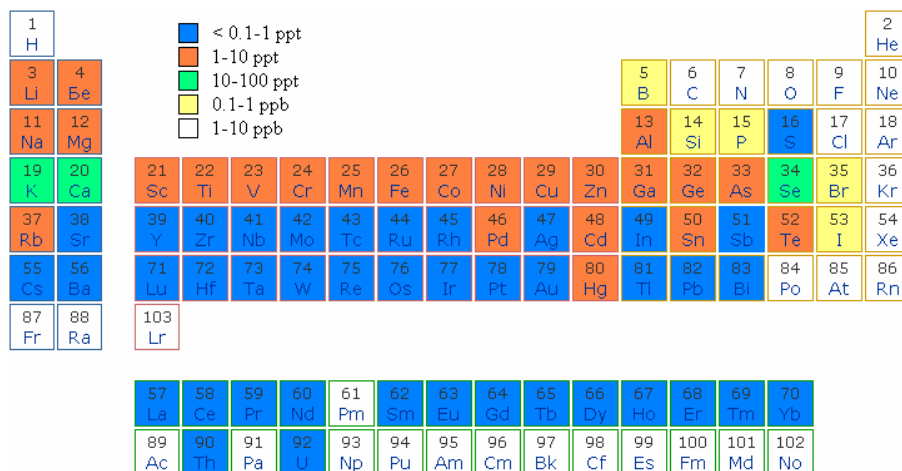Figure 9-4 shows the detection limits achievable by a quadrupole-based ICP-MS device.

Figure 9-4. Approximate detection limits achievable by ICP-MS

9.4.2 Principles of Operation

There is a wide range of commercial ICP-MS systems with different capabilities, strengths and limitations. Nevertheless, most of them are formed by nebulizer, spray chamber, plasma torch, MS interface, ion lenses, mass separation device and ion detector. The schematic diagram of a typical ICP-MS instrument is shown in figure 9-5. The sample, which is generally a liquid, is pumped into a nebulizer where aerosol is generated. The finest droplets are selected by means of a spray chamber, and transported into the plasma, where the sample follows different processes as it travels: vaporization, atomization and ionization. Most of the ions generated are positively charged due to the removal of one electron from the outer shell of the atom by the energy (heat) applied from a plasma discharge. The ions are then transported into the mass separation device passing through an interface which allows a gradual change of pressure from atmospheric conditions to the vacuum required by the mass spectrometer. The current of ions is focused by different ion lenses and transformed into an electrical signal in the ion detector after proper separation in the mass spectrometer.
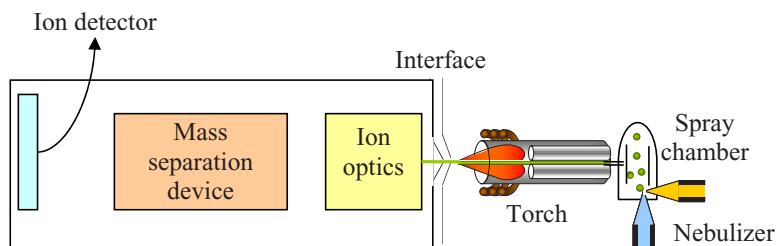

Figure 9-5. Schematic of and ICP-MS system

9.4.2.1. Sample Introduction

The sample containing the analyte of interest may be introduced in the torch as a gas or as aerosol of fine droplets or solid particles. The fine aerosol generation is achieved by a nebulizer followed of a spray chamber for droplet selection. In the nebulizer, the liquid sample is broken up into fine aerosol. Figure 9-6 shows a pneumatic nebulizer, where the mechanical force of a gas flow (generally argon) is used to generate a droplet dispersion of the analyte solution (Thomas, 2001). Alternative pneumatic nebulizer designs are available in the market to fulfil different requirements (e.g., high TDS or small sample volume).
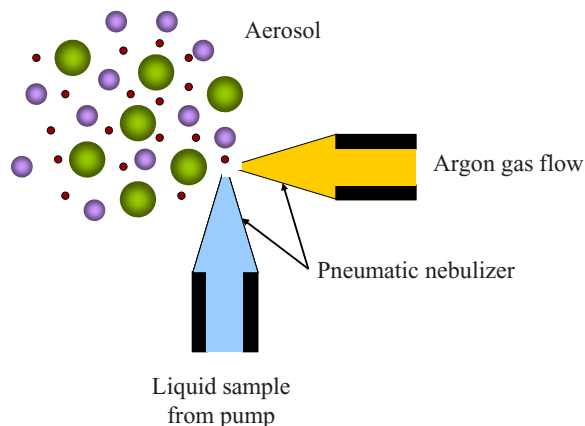
Figure 9-6. Pneumatic cross-flow nebulizer

Once the aerosol is formed in the nebulizer, the finest droplets (smaller than 8 μm in diameter, representing 1-2% of the total aerosol) are selected by a spray chamber. The most common spray chamber is the so-called double-pass or Scott chamber. The aerosol enters through a central tube and runs through the whole length of the chamber. The largest droplets fall due to gravity forces and will be removed through a drain tube, while the finest droplets pass to the space between the central tube and the outer wall and are transported to the torch.

9.4.2.2 Torch and Plasma

The system to generate the plasma is formed by a torch and a copper coil supplied by a radio frequency (RF) power (typically 750-1500 W). The RF passing through the coil will generate an intense electromagnetic field. Then, a high voltage spark from a Tesla coil causes some electrons of the flowing argon to be removed from their atoms. The electrons are accelerated by the magnetic field and crash against new argon atoms stripping off more electrons. The chain reaction will continue and will transform the gas into atoms, ions and electrons forming a high temperature plasma discharge (around 10000 K), which is maintained by the continuous RF supply.

The sample aerosol is driven at a very high velocity to the plasma, creating a hole or channel in the centre of the plasma. Then, the sample undergoes different physical changes as it travels through the different temperature zones of the plasma. These changes can be seen in more detail in figure 9-7. The first step is desolvation of the droplet, which becomes a solid microparticulate. Then the solid is vaporized and passes into a gaseous form, and

afterwards atomization takes place. The ground-state atoms will collide with argon electrons and will be transformed into positive ions.

Argon is the most common gas used to sustain the ICP. It has a high first ionization energy (16 eV), and therefore it is very convenient to ionize most of the elements of the periodic table, with ionization energies in most of the cases below 10 eV (corresponding to > 50 % ionization). At the same time, it also has a very high second ionization energy (27 eV), resulting in a very low population of Ar^{+2} ions. Nevertheless, different gases may be used for plasma generation, and it has been noticed that mixtures of argon and N_2, Xe, or H_2 may substantially reduce certain polyatomic ions (Jarvis et al., 1992).
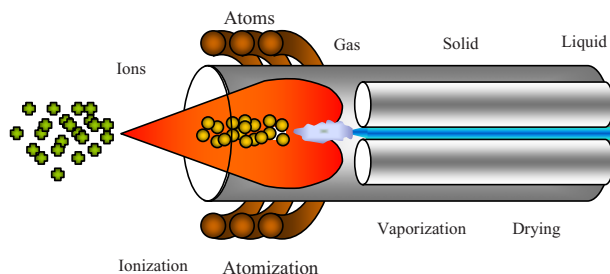

Figure 9-7. Physical changes experienced by the sample through the torch

9.4.2.3 Interface Region

Once the positively charged ions are generated in the plasma, they are conducted to the mass spectrometer, which works at high vacuum (10^{-4}-10^{-6} torr). As the plasma is generated under atmospheric pressure, a middle step is required in order to efficiently transport the ions keeping electrical integrity. This is the purpose of the interface region. It is formed by two metallic cones (sampler cone and skimmer) with very small orifices in the centre, and maintained at a vacuum of about 1 Torr.

9.4.2.4 Ion Focusing System

After the ions leave the skimmer, they must reach the mass separation device. Ion lenses placed between the skimmer cone and the mass spectrometer (ion optics) are used to focus and transmit the ion beam. The ion optics consists of a group of metallic plates, barrels or cylinders associated to different voltages. Their purpose is to focus the ions and to reject particulates, neutral species and photons from reaching the mass analyzer and detector.

In many devices a grounded metal disc is placed right after the skimmer in order to stop particulates, neutral species and photons, while the ions are able to move around it and go

on their way to the mass analyzer. Another option to get rid off undesired species is to place the mass analyzer below or above the central stream axis, so only the desired focused ions are in the same axis as the analyzer (see figure 9-8).
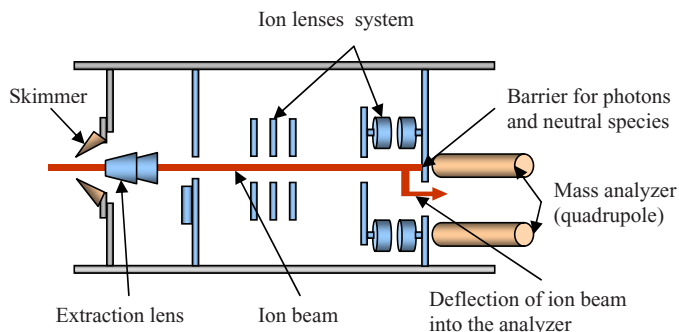

Figure 9-8. Ion lenses diagram

9.4.2.5 The Mass Analyzer

After the ions emerge from the ion optics, they pass to the mass separation device and are separated according to their mass to charge ratio. Its objective is to allow analytes of a given mass to charge ratio to pass through the separation device and enter the detector, while the non-analyte, interfering and matrix ions are filtered.

The most used mass analyzer is the so-called quadrupole. It is formed by four metal rods or metal surfaces forming a squared cross section. A diagram of this configuration is shown in figure 9-9. A direct current (DC) is applied on one pair of opposite rods, while a radio frequency field (RF) is applied to the other pair. If the current values are selected properly, only ions of a given mass to charge ratio will have a stable path through the rods and will emerge at the end of it (red ion in figure 9-9). The rest of the ions will strike the rods and be nebulized, or will pass through the rods space. In any case, those ions will be lost and will not reach the detector. Then, the scanning process is repeated for a different analyte with a different mass to charge ratio, and the process goes on until all the analytes of interest have been scanned.
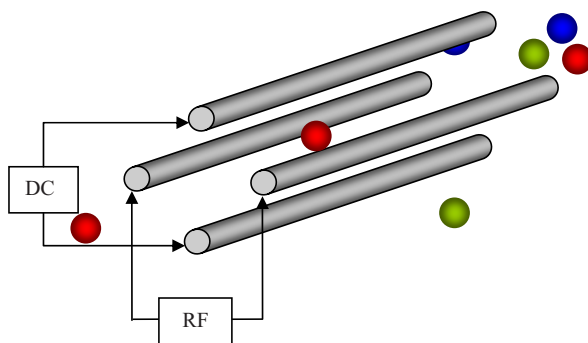
Figure 9-9. Quadrupole mass spectrometer

9.4.2.6. Ion Detector

After the desired mass to charge ratios to analyze have been separated in the previous step, the ions must be counted and transformed into an electrical signal in order to be able to determine the element concentration. The channeltron electron multiplier is an open glass cone coated with a semiconductor material, having the capability of generating electrons from a hitting ion. The upper part of the cone is biased to a negative potential of around -3kV, while the back part of the device near the collector is kept at ground. Therefore, the resistance of the coating varies with the position. When a positive ion leaves the mass analyzer it is attracted to the negative potential at the mouth of the channeltron and hits this surface. As a consequence, one or more secondary electrons form, and they move down the tube due to the potential gradient. In their way down the tube, these secondary electrons strike new areas of the coating surface, and more secondary electrons are emitted. The process is repeated many times and the result is a discrete pulse formed by many millions of electrons (10^8) (Jarvis et al., 1992). This pulse is conducted to a pre-amplifier where it is detected, and to a digital discriminator and counting circuit, where the pulses above a certain amplitude are counted.

9.4.3. Interferences in ICP-MS

The interferences in ICP-MS can be divided into spectroscopic interferences and non-spectroscopic interferences, or matrix effects. The first type of interferences may be also divided in four different subgroups: isobaric overlap, polyatomic ions, refractory oxide ions and doubly charged ions. The matrix effects can also be divided into two subgroups:

Suppression and enhancement effects, and physical effects caused by high total dissolved solids.

9.4.3.1 Isobaric Overlap

The isobaric overlap is found when the sample to analyze contains two elements which have isotopes of the same mass to charge ratio. Actually, the mass to charge ratio of those isotopes may differ, but in a very small quantity which cannot be resolved by the quadrupole mass analyzer. The use of a high resolution mass analyzer may solve this problem and discriminate between very small differences in mass to charge ratios.

This kind of interference is only found for mass to charge ratios above 36, and they increase for low masses, while are not frequent for high masses. There are overlaps with the plasma gas (generally Ar) and the impurities it contains (Xe, Kr). The most abundant isotope of argon is ^{40}Ar (99.6%), making the determination of either ^{40}Ca (96.9%) or ^{40}K (0.01%) impossible.

Isobaric overlaps can be avoided by choosing another isotope of the element free of interferences. If this is not a possibility (there is no isotopes free of interferences or the natural abundance is too low) mathematical corrections using another isotope (free of interferences) of the interfering element may be applied. For example, the determination of ^{204}Pb in the presence of Hg will be interfered by ^{204}Hg. A correction based on the isotope ^{201}Hg, which is free of interferences, may solve the problem:

$$^{204}\text{Pb} = \text{Total signal} - {}^{201}\text{Hg} \cdot (6.7/13.8) \tag{9-1}$$

where 6.7 and 13.8 are the natural abundances in weight percentage of ^{204}Hg and ^{201}Hg, respectively.

9.4.3.2 Polyatomic Ions

Polyatomic ions result from the combination of two or more atomic species (e.g., NOH^+, Ar_2H^+). They are the most important type of interference, although in practical analysis there are relatively few serious interference effects if care is taken in the sample preparation process. They are generally formed by the combination of argon, hydrogen and oxygen (the most abundant species in the plasma) among them or with any other element present in the sample (e.g., ^{40}Ar^{40}Ar, ^{40}Ar^{16}O, ^{40}Ar^{1}H). Polyatomic ion peaks are only significant up to a mass to charge ratio around 82.

The amount of polyatomic ions depends on many factors, being the most important ones the geometry of the extraction system, operating parameters for plasma and nebulizer systems, and the characteristics of the sample.

For this type of interference mathematical corrections are not a reliable solution as polyatomic ion peaks may be relatively large compared to the analyte contribution. Therefore, whenever possible, the selection of another isotope not interfered by polyatomic ions is preferred, even though the natural abundance of such isotope is low.

Many of the polyatomic ion interferences contain oxygen and/or hydrogen originated from the dissociation of vapour water from the solution. To reduce such interferences it is necessary to reduce the population of both oxygen and hydrogen ions. This may be achieved by decreasing the temperature in the spray chamber with a cooling system.

9.4.3.3 Refractory Oxides

Refractory oxides result from the incomplete dissociation of the sample matrix or from a recombination of ions in the plasma tale. The consequence is refractory oxides of the type MO^+, MO_2^+ or MO_3^+, interfering 16, 32 and 48, respectively, mass units above the M^+ peak. For the majority of elements the ratio MO^+/M^+ is lower than 1.5%, while the ratio MO_2^+/M^+ is lower than 0.002%. Generally, the appearance of refractory oxides is determined by the monoxide bond strength of the element, being the formation of MO^+ favoured for the highest oxide bond strength.

The percentage of refractory oxides can be minimized by optimizing the radio frequency power (higher power will break more oxides) and the nebulization flow (determines the location in the axis at which dissociation of the molecules is complete).

9.4.3.4 Doubly Charged Ions

The big majority of ions generated in the plasma are of type M^+, although doubly charged ions may also be formed. The presence of M^{2+} will be determined by the second ionization energy of that element and by the operation conditions of the plasma. Only elements with a second ionization energy lower than the first ionization energy of the plasma gas (16 eV in the case of Ar) will generate M^{2+} ions. These elements are alkaline earths, rare earths, and some transition metals. The nebulizer flow can also influence on the amount of doubly charged ions. If the flow is too low, the plasma temperature will increase resulting in a larger amount of M^{2+}. Generally, the amount of doubly charge ions is lower than 1 %.

The consequence of the appearance of M^{++} ions is the decrease in the M^{+} signal, and the possibility of isobaric overlaps in m/2. When alternative isotopes cannot be used, some corrections will be needed in order to minimize these interferences.

9.4.3.5 Physical Effects Caused by High Dissolved Solids

The use of ICP-MS is limited to samples containing small amounts of dissolved solids. Solutions with a TDS content above 500 mg L^{-1} cause a considerable signal drift over short periods of time. Moreover, the nebulizer and sampling cones are easily blocked by the solids due to their small orifices. For these reasons, samples containing more than 0.2 % of TDS are not recommended for ICP-MS analysis under continuous flow. Working with transient signals the amounts of solids can be increased up to 2-3 %.

The signal drift experienced at the beginning as a consequence of solid deposition on the cones can be reduced if a similar solution is employed for 20 minutes previous to the analysis. Operating in that way the signal will be more stable and some corrections may be applied to reduce this effect. The signal drift can be corrected by using internal standards.

9.4.3.6 Suppression and Enhancement Effects

Suppression and enhancement effects result from a high concentration of easily ionized elements in the sample. The causes generating them are not very clear, although many investigators think they appear due to changes in the flux and composition of the ion beam. Such changes appear as a consequence of space charge effects around the skimmer area. The final result is suppression (generally) or enhancement of the signal, being the effects more pronounced for light elements than for heavy ones.

Non spectroscopic interferences are difficult to quantify and to control. A previous scan of the sample is recommended in order to have a closer knowledge of the sample and to find out possible interferences. Some possibilities to decrease their effects are:

- Dilution of the sample to decrease the TDS below 0.2 % (or 2% when working with transient signal)
- Internal standards with similar mass and ionization energy to that of the analyte in order to control the signal drift
- Instrumental optimization
- Standard addition calibration techniques
- Separation of the analyte from the matrix (ion exchange separation, co-precipitation)

9.5 Results

9.5.1 Time Required to Achieve Equilibrium

The first set of experiments performed was devoted to estimate the time required to achieve equilibrium for the BaSO$_4$-NaCl-H$_2$O system at the slowest conditions (lowest temperature, pressure and NaCl concentration to be measured: 50ºC, 100 bar and 0.1 m). Once this time is determined, experiments covering the temperature range 50-250ºC, the pressure range 100-600 bar, and the concentration range 0.1-6 m NaCl can be carried out.

To determine the equilibrium time, 17 experiments in 0.1 m NaCl solutions were carried out at 50ºC and 100 bar, keeping those conditions constant for different periods of time. In order to check the reproducibility of the results, some of the experiments were repeated up to 3 times. The final samples were analyzed by ICP-MS, and the ICP-MS results were corrected for the dilution process in order to get the real concentration of BaSO$_4$ in the original sample. Eight different standards of 50, 100, 150, 200, 500, 1000, 1500 and 2000 ppb of barium in pure water were used for calibration, together with a blank solution containing no barium. Those standards covered the whole concentration range to be measured. The calibration curves are shown in figure aIII-1 in Appendix III. Four isotopes of barium (^{135}Ba, ^{136}Ba, ^{137}Ba and ^{138}Ba) were followed, the final results being the average of all of them. Each measurement was repeated five times. The results are given in table aIII-1 in Appendix III. In order to cross-check the ICP-MS results, a commercial standard containing 100 ppb of barium along with other components is used.

The results obtained for the first set of experiments are given in figure 9-10. In order to study the influence of the agitation process in the final time required to achieve equilibrium, two different sets of experiments were performed: Using vibration during the whole experimental run (blue triangles), and using a combination of vibration for a time reported in figure 9-10, plus 16 h (red circles) or 44 h (green square) without any kind of agitation. The measurements performed by Templeton (1960) and Strübel (1967) at 50ºC, 0.1 m NaCl and 1 atm are included for comparison.

Figure 9-10 does not show the expected increasing barium concentration with time for low time values, and a plateau from a certain time corresponding to equilibrium. Therefore, it is not possible to determine the equilibrium time from these results. Moreover, the concentration measured for the 100 ppb Ba^{2+} commercial standard is 219.6 ppb, and thus corresponding to a residual deviation of 119.6%. No clear explanation has been found for this extreme inaccuracy, since the device was calibrated for the whole range of concentrations measured, and the calibration curves show a nice linearity with R^2

coefficients above 0.999 in all the cases. The large errors could be related to the different matrix used in our samples (around 0.1 % NaCl) and in the commercial standard. Nevertheless, this is not a very likely explanation, since both matrices are simple, and a tuning of the ICP-MS device is performed prior to the measurements, using a standard containing different elements covering the whole range of masses. Therefore, the setup should be prepared to measure accurately any component, independently of its mass to charge ratio and the matrix (provided that its salinity is below 2-3 %).
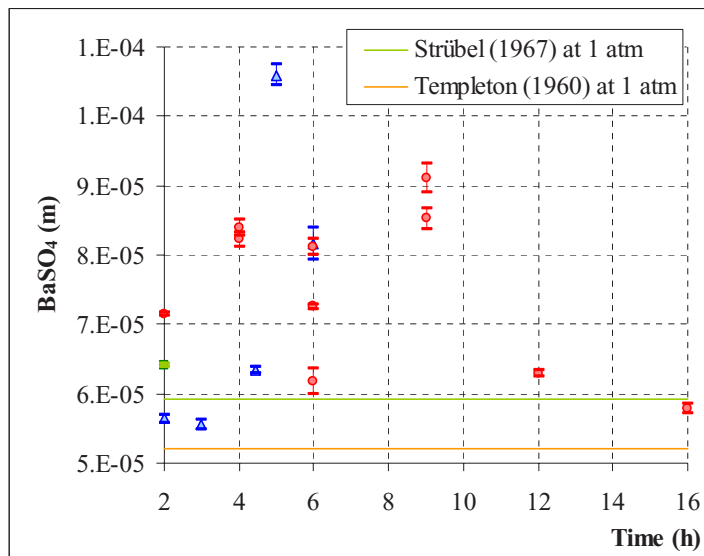

Figure 9-10. Barium concentrations after different running times. Red circles represent experiments where the sample was vibrated for X hours, and kept at constant *T* and *P* for another 16 hours. Blue triangles represent experiments where the sample was vibrated for X hours and filtrated directly afterwards. Green squares represent experiments where the sample was vibrated for X hours, and kept at constant *T* and *P* for another 44 hours.

Due to the unreliable results obtained in figure 9-10, some of the previous ICP-MS measurements were repeated. In order to resemble the experimental samples, the new standards (400, 800 and 1200 ppb of Ba^{2+}) were prepared in 0.1% NaCl instead of pure water, and the blank was a 0.1% NaCl solution. Calibration curves for the different isotopes are shown in figure aIII-2 in appendix III. Three additional standards of 100, 500 and 1000 ppb of Ba^{2+} in 0.1% NaCl were prepared to cross-check the results, together with the commercial standard (100 ppb) used previously. The new measurements are reported in table a3-II in Appendix III. Figure 9-11 compares the new results (DTU_2) with the previous ones (DTU_1).
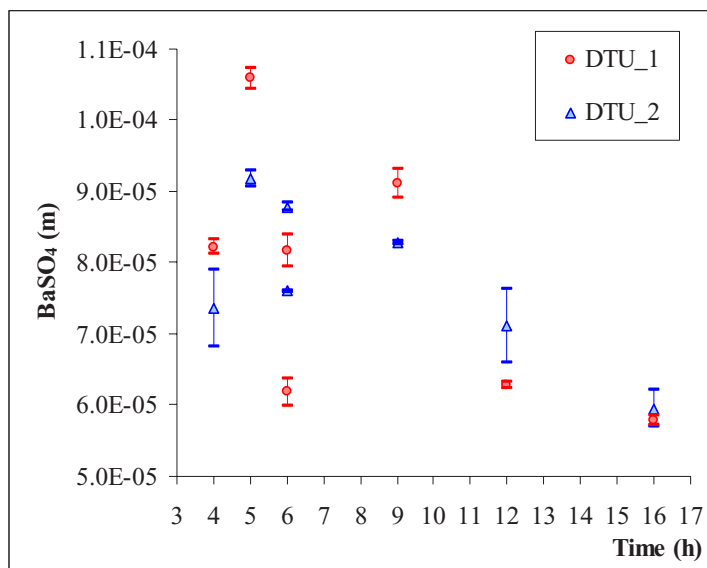
Figure 9-11. Barium concentration from ICP-MS measurements for different running times. DTU_1 refers to the first measurements (reported in table aIII-1 in Appendix III), while DTU_2 refers to the second ICP-MS measurements on the same samples (reported in table aIII-2 in Appendix III).

It is clear from figure 9.11 that the analytical technique used is not reliable, and the results are affected by a random error. Only for one of the samples measured (16 h), the values obtained from both analysis agree. The rest of the points are characterized by extreme deviations. Moreover, the measured values for the 4 different standards used as tests evidence the inaccuracy of the measurements. Table 9-5 shows the real and measured values for those standards, together with the *%RD*, always above 27%, and reaching up to 90%.

Table 9-5
Real and measured standard's concentrations by ICP-MS

Real concentration (ppb)	Measured concentration (ppb)	% RD
100	162.5	**62.5**
500	659.7	**31.9**
1000	1277.8	**27.8**
100	190.3	**90.3**

After measurements failed twice in the ICP-MS device located at the Chemistry department of DTU, and with no clear explanation about the causes of the failure, it was decided to use an alternative ICP-MS device to clarify whether the equipment was the source of the error. All the 17 samples were sent to a certified laboratory (Steins Laboratorium A/S) to be

measured by ICP-MS. Among the samples, 4 standards of 500, 1000, 1500, 2000 and 2500 ppb Ba^{2+} in 0.1 % NaCl were included to cross-check the results. The values reported by the laboratory for the samples and standards are given in table aIII-3 in Appendix III. Figure 9-12 compares the new laboratory results with measurements performed at DTU. Again, the same inaccuracy and extreme deviations between the different data is observed. The highest deviation is found for the measurements after 12 hours, where the concentration ranges from $6.3 \cdot 10^{-5}$ m to $1.5 \cdot 10^{-4}$ m.
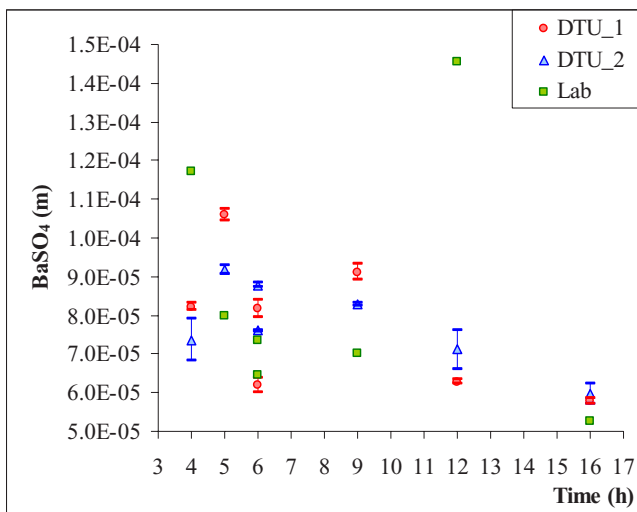

Figure 9-12. Comparison of different ICP-MS measurements

The results reported by the laboratory for the prepared test-standards are given in table 9-6. Those result evidence the lack of reliability of the analytical technique for our particular case, since the lowest residual deviation is around 20%, while the highest *RD* value is above 100%. The laboratory assures to have used two NIST certified reference solutions to check the measurements, obtaining good results (also reported in table 9-6). We cannot find an explanation to this behaviour, unless the different matrix in samples and reference solutions plays an important role in the different values obtained. It is addressed that high salinity solutions involve problems and signal drifts in ICP-MS measurements, but that should not be the case for dilute concentrations (the NaCl content in our samples ranges from 0.05 to 0.1 %).

The experimental conditions, filtration volumes and dilution masses used in experiments 1 to 17, together with the calculated BaSO₄ concentration from the ICP-MS measurements is reported in tables aIII-4 and aIII-5 in Appendix III.

Table 9-6
Real and measured standard's concentrations by ICP-MS by Stein Laboratorium A/S

Real c (ppb)	Measured c (μg L^{-1})	Measured c (ppb)	% RD
500	1100	1097	**119.5**
1000	1600	1596	**59.6**
1500	2000	1995	**33.0**
2000	2400	2394	**19.7**
2500	3700	3691	**47.7**
148.0[a]	144.5	144.5	**-2.4**
544.2[b]	522.4	522.4	**-4.0**

[a] NIST 1640 certified reference solution
[b] NIST 1643 certified reference solution

In a final attempt to obtain reliable results, the technique of inductively coupled plasma optical emission (ICP-OES) was tested. Five different samples (reported in table 9-7) were analyzed. In order to determine the reproducibility of the technique, numbers 1 and 2 correspond to the same sample (experiment 13 in table aIII-1 in Appendix III). Numbers 3 and 4 are standards containing 500 and 1500 ppb Ba^{2+} in 0.1% NaCl. To tackle the possible influence of the NaCl matrix, a standard of the same concentration as number 4 (1500 ppb) but using pure water instead was also examined. Unfortunately, the results show again a large disparity between the measured and actual concentrations. The outcome for standards 4 and 5 is rather close, and evidences that matrix effects are not the explanation to the inaccurate results. Moreover, the concentrations for 1 and 2 should be equal, since both correspond to the same sample, but contrary to that, they differ with almost 200 ppb. Such discrepancy shows that the technique is not reliable for our purpose, regardless of the matrix.

Table 9-7
ICP-OES measurements

Number	Real c (ppb)	Measured c (ppb)
1		1770
2		2010
3	500	1050
4	1500	2040
5	1500	1960

New measurements were not performed due to the lack of time and capabilities. Internal standards could have been used to examine the influence of the matrix on the final results, although this is not believed to be the problem. Matrix effects should affect in the same

manner number 1 and 2 in table 9-7, but this is not the case. Therefore, an alternative source of error must account for such disparity.

After the unfruitful results obtained for barite solutions, our experimental setup was tested with NaCl solutions in order to demonstrate it is capable of determining the solubility of salts at high temperatures and pressures.

9.5.2 Validation of the Setup

The experimental procedure and setup were validated by measuring sodium chloride solubility at high temperature and pressure. A salt with a high solubility in water was chosen in order to avoid the analytical problems found for barite. The NaCl concentration was determined by titration with $AgNO_3$.

The first step in the validation of the setup was determining the time required to reach equilibrium for the binary NaCl-H_2O system. For this purpose, different experiments at 30ºC and 1 atm were performed, for different running times. Figure 9-13 shows the NaCl concentration behaviour against the experimental time, along with some experimental data available in the literature for comparison.

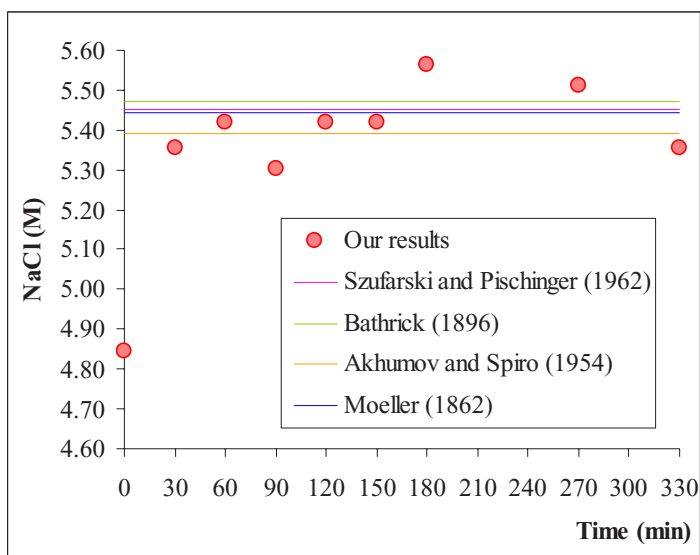**Figure 9-13.** Determination of the equilibrium time for the system NaCl-H_2O at 30ºC and 1 atm with agitation (vibration). M refers to molarity.

Figure 9-13 shows a steep increase in NaCl concentration for the low time values, while it reaches a plateau for times above around 30 minutes. When comparing our results to those published by Moeller (1862), Bathrick (1896), Akhumov and Spiro (1954) and Szufarski

and Pischinger (1962) at the same experimental conditions, a general agreement is observed. Therefore, it can be concluded that the system NaCl-H$_2$O at 30ºC and 1 atm reaches equilibrium after 60 minutes of vibration. This time is expected to be lower when temperature is raised.

If no agitation is used, the NaCl concentration increases much slowly with time, as observed in figure 9-14. In this case, more than seven hours are required to guarantee equilibrium.
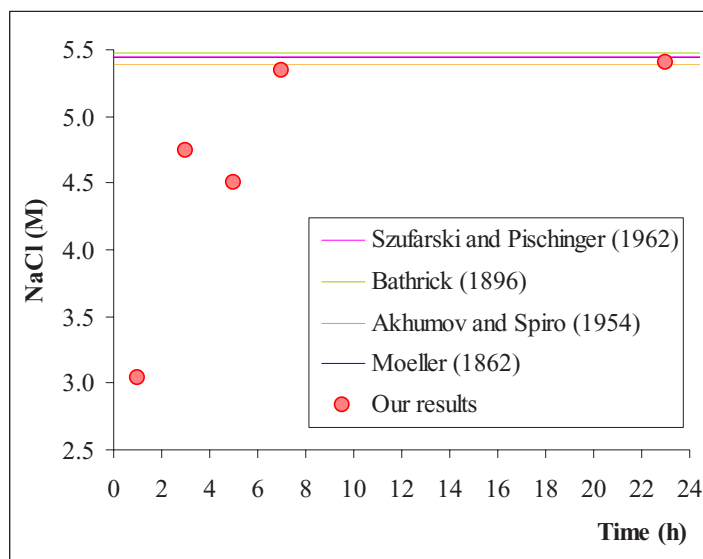

Figure 9-14. Determination of the equilibrium time for the system NaCl-H$_2$O at 30ºC and 1atm when no agitation is used. M refers to molarity.

To make sure all our experimental values correspond to equilibrium conditions, vibration was used for a minimum of two hours for each determination.

The next step in the validation of the setup was comparing our results with available literature data. Measurements of sodium chloride solubility at high pressure are not very abundant. A more detailed explanation about the experimental conditions and number of measurements found in the literature on the solubility of sodium chloride in pure water at pressures larger than the atmospheric pressure is reported in table 6-1 in Chapter 6. Three sources (Cohen et al., 1911, Sill, 1916, and Adams and Hall, 1931) report NaCl solubility data at high pressure and temperatures in the range 24 to 30ºC which are in close agreement with each other. Thus, we performed different experiments at 30ºC and different pressures in order to compare our results to the available data. The experimental conditions and calculated solubilities are reported in table aIII-8 in Appendix III. Figure 9-15 shows the values for the NaCl solubility in pure water at 30ºC and pressures ranging from 1 to 400 atm

obtained from our experimental measurements, along with experimental data available in the literature and calculations by the extended UNIQUAC model. All the sources show a close agreement among them, and also with our new values and the model calculations. Therefore, it is proven our setup is capable of replicating available published data.
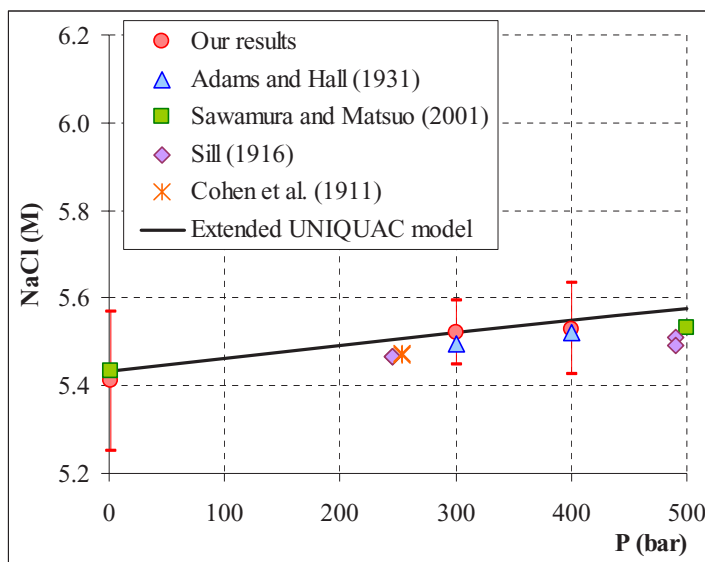

Figure 9-15. NaCl solubility (in molarity) in pure water at 30ºC

The reproducibility of the results was studied at 100ºC and different pressures, especially at 500 bar. The experimental conditions were chosen in order to demonstrate results are reproduced not only at low temperature and pressure, but also at more complex experimental conditions. Figure 9-16 shows the determination of sodium chloride solubility in pure water at 100ºC and different pressures. Extended UNIQUAC calculations are also reported. No data at 100ºC or similar and pressures larger than 1 atm were found in the literature, and therefore only one point at atmospheric pressure is given. The point corresponds to the average solubility value out of 22 sources found in the literature. The experimental conditions used, titration volumes and calculated results are reported in table aIII-9 in Appendix III.

The reproducibility of experiments at 100 and 300 bar is very good, with a variation coefficient (*CV*, equation aIII-1 in Appendix III) as low as 0.21 and 0.83 %, respectively. This accuracy is not so high at 500 bar, where the variation coefficient increases to 4.84 %. Nonetheless, the value is low enough to demonstrate experiments can be reproduced, and the experimental setup can be used to accurately determine salt solubility at high

temperature and pressure. The agreement of our experimental solubilities with extended UNIQUAC calculations is also remarkably good.
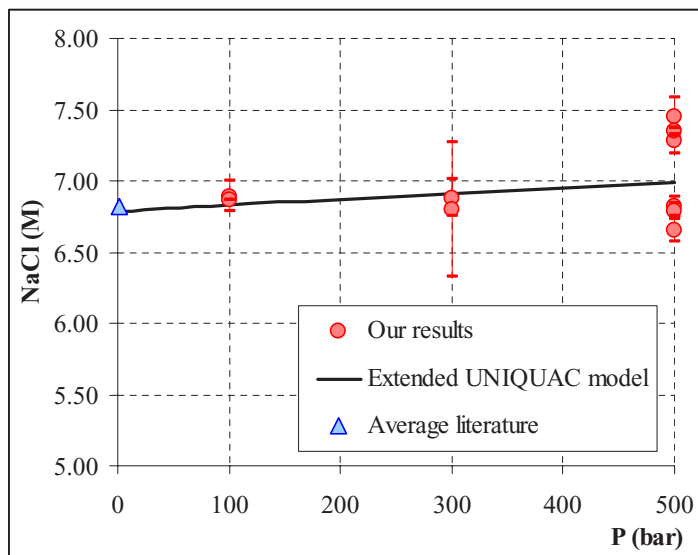

Figure 9-16. NaCl solubility (in molarity) in pure water at 100ºC

After analyzing the results shown in figures 9-15 and 9-16 it seems clear the experimental setup developed is capable of determining salt solubility at high temperature and pressure. The problems encountered when studying barite are therefore related to inaccuracies in the analytical technique.

9.6 References in Chapter 9

Adams, L.H., Hall, R.E., 1931. The influence of pressure on the solubility of sodium chloride in water. A new method for the measurement of the solubilities of electrolytes under pressure. Journal of the Washington Academy of Sciences 21(9), 183-194.

Akhumov, E.I., and Spiro, N.S., 1954. Rastvorimost' khloridov v soljanoj kislote. Zhurnal Prikladnoj Khimii 11 (27), 1163-1169.

Balarew, D. 1925. Löslichkeit und korngrösse. 1. Z. Anorg. Allg. Chem. 145, 122-126.

Bathrick, H. A., 1896. Precipitation of salts. J. Phys. Chem. 1, 157-169.

Blount, C.W., 1977. Barite solubilities and thermodynamic quantities up to 300 ºC and 1400 bars. American Mineralogist 62, 942-957.

Brower, E., Renault, J., 1971. Solubility and enthalpy of the barium strontium sulphate solid solution series. New Mexico State Bureau of Mines and Mineral Resources, Circular 116.

Cohen, E., Inouye, K., Euwem, C., 1911. Piezochemische studien. VII.. Z. Physik. Chem. 75, 257-304.

Culberson, C.H., Lathman, G., Bates, R.G., 1978. Solubilities and activity coefficients of calcium and strontium sulfate in synthetic seawater at 0.5ºC and 25ºC. J. Phys. Chem. 82, 2693-2699.

Davis, J.W., Collins, A.G., 1971. Solubility of barium and strontium sulfates in strong electrolyte solutions. Environmental Science & Technology 5, 1039-1043.

Grabowski, R.J., Unice, R.C., 1958. Quantitative spectrochemical determination of barium and strontium. Analytical Chemistry 30, 1374-1379.

Howell, R.D., Raju, K., Atkinson, G., 1992. Thermodynamics of "Scale" mineral solubilities 4. SrSO$_4$. J. Chem. Eng. Data 37, 464-469.

Jacques, D.C.; Bourland, B.I., 1983. A study of solubility of strontium sulphate. SPEJ 292-300.

Jarvis, K.E., Gray, A.L., Houk, R.S., 1992. Handbook of Inductively Coupled Plasma Mass Spectrometry. Blackie & Sons Ltd., Suffolk, Great Britain.

Johnson, C.M., Nishita, H. 1952. Analytical Chemistry 24, 736.

Lucchesi, P.J., Whitney, E.D., 1962. Solubility of strontium sulphate in water and aqueous solutions of hydrogen chloride, sodium chloride, sulphuric acid and sodium sulphate by the radiotracer method. J. Appl. Chem. 12, 277-279.

Moeller, K., 1862. Ueber den Einflufs des Drucks auf die Löslichkeit einiger Salze. Annals of Physics 117, 386-417.

Müller, G., 1960. Die Löslichkeit von Coelestin (SrSO$_4$) in wässerigen NaCl- und KCl-lösungen. Neues Jahrb. Mineral. Mon., 237-239.

Reardon, E.J., Armstrong, D.K., 1987. Celestite (SrSO$_4$(s)) solubility in water, seawater and NaCl solution. Geochimica et Cosmochimica Acta 51, 63-72.

Roe, K.K., Froelich, P.N., 1984. Determination of barium in seawater by direct injection graphite furnace atomic absorption spectrometry. Anal. Chem. 56, 2724-2726.

Rollemberg, M.C.E., Curtius, A.J., 1982. Flameless atomic absorption determination of barium in natural waters using the technique of standard additions. Mikrochimica Acta 2, 441-447.

Sawamura, S., Matsuo, H., 2001. Solubility of several organic and inorganic compounds at high pressure. Koatsuryoku no Kagaku to Gijutsu 11(2), 129-136.

Schulien, S., 1987. High-temperature/high-pressure solubility measurements in the systems BaSO$_4$-NaCl-H$_2$O and SrSO$_4$-NaCl-H$_2$O in connection with scale studies. SPE symposium (SPE 16264), San Antonio, Texas.

Sill, H., 1916. The influence of pressure on solubility. Journ. Am. Chem. Soc. 38, 2632-2643.

Strübel, G., 1966. Die hydrothermale Löslichkeit von Cölestin in System SrSO$_4$-NaCl-H$_2$O. Neues Jahrb. Mineral. Mon., 99-107.

Strübel, V.G., 1967. Zur Kenntnis und genetischen Bedeutung des Systems BaSO$_4$-NaCl-H$_2$O. Neues Jahr. Miner. Monatsh., 223-234.

Stuewer, D., Jakubowski, N., 1998. Elemental analysis by inductively coupled plasma mass spectrometry with sector field instruments: A progress report. Journal of Mass Spectrometry 33, 579-590.

Sun, R., Hu, W., Duan, Z., 2001. Prediction of nitrogen solubility in pure water and aqueous NaCl solutions up to high temperature, pressure, and ionic strength. Journal of Solution Chemistry 30(6), 561-573.

Szufarski Z., Pischinger E., 1962. Badania rozpuszczalnosci weglanu, siarczanu i chlorku sodowego. Przemysl Chemiczny 41, 695-698.

Templeton, C.C., 1960. Solubility of barium sulfate in sodium chloride solutions from 25° to 95°C. Journal of Chemical and Engineering Data 5 (4), 515-516.

Thomas, R., 2001. A beginner's guide to ICP-MS. Part II. The sample-introduction system. Spectroscopy 16 (5), 56-60.

Uchameyshvili, N.Y., Malinin, S.D., Khitarov, N.I., 1966. Solubility of barite in concentrated chloride solutions of some metals at elevated temperatures in relation to problems of the genesis of barite deposits. Geochem. Int. 10, 951-963.

Vetter, O.J.G., Vandenbroeck, I., Nayberg, J., 1983. SrSO$_4$: the basic solubility data. Society of Petroleum Engineers, 271-281.

10. Conclusions

The solubility of sparingly soluble salts found in natural waters has been studied in connection to the problem of scale formation found in geothermal and oilfield operations.

The extended UNIQUAC model presented by Thomsen and Rasmussen (1999) has been chosen to calculate aqueous phase activity coefficients, while the Soave-Redlich-Kwong equation of state is used to calculate fugacities in the gas phase. The model has been improved by the addition of two parameters in order to account for the pressure dependency of solubility. The extended UNIQUAC model has been chosen over other alternatives due to its excellent relationship between accuracy and simplicity. It only requires two parameters per species, plus two parameters per species pair, while the temperature dependency is accounted for in the model equations. The figures presented through this thesis show that the extended UNIQUAC model is capable of giving accurate results even at very high temperatures and pressures. Most of the data used for the parameter estimation could be reproduced by the model within the experimental accuracy.

More than 7000 SLE measurements have been collected, covering a wide range of temperature (up to $300^{o}C$), pressure (up to 1000 bar) and concentrations up to saturation. All these data have been analyzed prior to their use, and those found to be unreliable have not been used for parameter estimation. Unknown parameters for the species $CO_2(aq)$, H^+, Na^+, Ba^{2+}, Sr^{2+}, Ca^{2+}, Mg^{2+}, Cl^-, OH^-, SO_4^{2-}, CO_3^{2-} and HCO_3^-, and for their interactions, have been estimated on the basis of those SLE data.

The extended UNIQUAC model with the new parameters has been used to calculate vapour-liquid, solid-liquid, and speciation equilibria in systems found to form scale in geothermal and oilfield operations. The scaling minerals $CaSO_4$, $CaSO_4 \cdot 2H_2O$, $SrSO_4$, $BaSO_4$, $CaCO_3$, $BaCO_3$, $SrCO_3$, $MgCO_3$, $MgCO_3 \cdot 3H_2O$, $MgCO_3 \cdot 5H_2O$, $Mg(OH)_2$, and $3MgCO_3 \cdot Mg(OH)_2 \cdot 3H_2O$ have been studied.

The validity of the model has been demonstrated by performing solubility calculations for different scaling minerals in natural waters. The model has been implemented in the computer program SPECS developed at IVC-SEP. This program has been employed to determine solubility indices of complex electrolyte solutions of high ionic strength up to high temperatures and pressures. The match of our results with field observations, and the agreement with other sources, makes us confident about the reliability of the extended UNIQUAC model.

The simplicity of the model, together with the good performance obtained for all the systems investigated, make our model an appropriate choice as a tool to study scale formation. As the model only contains binary interaction parameters, it can be applied to any multicomponent system for which the binary parameters are known.

The experimental part of the Ph.D. project was intended to complete the gaps found in the literature reporting barite solubility in NaCl solutions. In this context, alternative experimental procedures have been addressed and evaluated. An experimental setup to determine salt solubility at high temperature (up to 300ºC) and pressure (up to 10000 psi) has been designed and built. The setup has been validated performing measurements of sodium chloride solubility in pure water at 30 and 100ºC, and different pressures. Experiments have also been carried out for $BaSO_4$-NaCl-H_2O solutions at 50ºC and 100 bar, in order to determine the time required by that system to attain equilibrium. Problems with the analytical techniques employed (ICP-MS and ICP-OES) have resulted in unreliable data and in the impossibility to further study the system $BaSO_4$-NaCl-H_2O.

References in Chapter 10

Thomsen, K., Rasmussen, P., 1999. Modeling of vapor-liquid-solid equilibrium in gas-aqueous electrolyte systems. Chemical Engineering Science 54, 1787-1802.

Appendix I: Helgeson's and Bromley's Models

In this section, I will briefly present the thermodynamic models developed by Helgeson (Helgeson, 1967, 1969, Helgeson and Kirkham, 1974a, b, 1976; Helgeson et al., 1978, 1981, Shock and Helgeson, 1988, Johnson et al., 1992) and Bromley (1973). Both models were studied at the very beginning of this Ph.D. project in order to address their applicability to calculate and predict the solubility behaviour of scaling minerals in multicomponent solutions at high temperature and pressure.

Helgeson Model

Helgeson calculated successfully thermodynamic and transport properties of aqueous species at temperatures up to 1000°C and pressures up to 5 kbar. A detailed description of the equations developed can be found in Shock and Helgeson (1988).

Standard States

- o Minerals and pure liquids: Unit activity of the pure component at all pressures and temperatures.
- o Gases: Unit fugacity of the hypothetical ideal gas at 1 bar and any temperature.
- o Aqueous species other than water: Unit activity of the species in a hypothetical 1 molal solution referenced to infinite dilution at any pressure and temperature.

Gibbs Free Energy

The standard state Gibbs free energy ($\Delta G^0_{P,T}$) of minerals, gases, and aqueous species at T and P can be calculated from the standard state Gibbs free energy of formation ($\Delta_f G^0$) of the species from its elements in their stable phase at the reference pressure (P_0) and temperature (T_0), and a term accounting for the differences in the standard state Gibbs free energy of the species that arise from changes in pressure and temperature ($G^0_{P,T} - G^0_{P_0,T_0}$):

$$\Delta G^0_{P,T} = \Delta_f G^0 + (G^0_{P,T} - G^0_{P_0,T_0}) \tag{aI-1}$$

For the *j-th* aqueous solute species, the second term on the right hand side of equation aI-1 can be calculated as (Tanger and Helgeson, 1988)

$$G_{j,P,T}^0 - G_{j,P_0,T_0}^0 = -S_{j,P_0,T_0}^0(T-T_0) - c_{1,j}\left(T\ln\left(\frac{T}{T_0}\right) - T + T_0\right) + a_{1,j}(P-P_0)$$

$$+ a_{2,j}\ln\left(\frac{\Psi+P}{\Psi+P_0}\right) - c_{2,j}\left(\left(\left(\frac{1}{T-\Theta}\right)-\left(\frac{1}{T_0-\Theta}\right)\right)\left(\frac{\Theta-T}{\Theta}\right)-\left(\frac{T}{\Theta^2}\right)\ln\left(\frac{T_0(T-\Theta)}{T(T_0-\Theta)}\right)\right) \qquad \text{(aI-2)}$$

$$+\left(\frac{1}{T-\Theta}\right)\left(a_{3,j}(P-P_0) + a_{4,j}\ln\left(\frac{\Psi+P}{\Psi+P_0}\right)\right)$$

$$+ w_j(Z+1) + w_{j,P_0,T_0}(Z_{P_0,T_0}+1) + w_{P_0,T_0}Y_{P_0,T_0}(T-T_0)$$

where Ψ and Θ are constants equal to 2600 bar and 228 K, respectively, S^0 is the standard state entropy, Z and Y are solvent Born functions (dependent on both pressure and temperature), $a_{i,j}$ and $c_{i,j}$ are P/T independent adjustable regression parameters unique to the *j-th* aqueous solute species, and w is the Born coefficient.

For a mineral or gas, equation aI-2 is transformed into

$$G_{j,P,T}^0 - G_{j,P_0,T_0}^0 = -S_{j,P_0,T_0}^0(T-T_0) + \sum_{i=1}^{1+\Phi_T} a_i\left[T_{i+1}-T_i-T_{i+1}\ln\left(\frac{T_{i+1}}{T_i}\right)\right] +$$

$$+ \sum_{i=1}^{1+\Phi_T}\left\{\frac{(-c_i - b_i T_{i+1}T_i^2)(T_{i+1}-T_i)^2}{2T_{i+1}T_i^2}\right\} \qquad \text{(aI-3)}$$

$$+ V_{P_0,T}^0(P-P_0) - \sum_{i=1}^{\Phi_P}\int_{P_{ti,T}}^{P}\Delta V_{ti}^0 dP - \sum_{i=1}^{\Phi_T}\frac{\Delta H_{ti}^0}{T_{ti}}(T-T_{ti})$$

where Φ_P (0 for gases) denotes the number of phase transitions from (P_0, T) to (P, T). $P_{ti,T}$ represents the pressure of the *i-th* phase transition at T, where $P_0 < P_{ti,T} < P$. Φ_T (0 for gases) is the number of phase transitions from (P_0, T_0) to (P_0, T), being $T_1 = T_0$ and $T_{i>1} = min(T, T_{ti-1,P0})$. a_i, b_i, and c_i correspond to adjustable regression coefficients that are unique to the specified mineral or gas from T_i to T_{i+1}. V^0 and H^0 are the standard molal volume and standard state enthalpy.

For any reaction among *i'* minerals and gases (excluding water), *j'* aqueous solute species, and water:

$$\Delta_r G_{P,T}^0 = \sum_{i=1}^{i'}\nu_i\Delta G_{i,P,T}^0 + \sum_{j=1}^{j'}\nu_j\Delta G_{j,P,T}^0 + \nu_{H_2O}\Delta G_{H_2O,P,T}^0 \qquad \text{(aI-4)}$$

and

$$\ln K_{P,T} = \frac{-\Delta_r G_{P,T}^0}{RT} \qquad \text{(aI-5)}$$

where ν_i, ν_j, and ν_{H_2O} refer to the stoichiometric reaction coefficients of the subscripted species, R is the universal gas constant, and $K_{T,P}$ the equilibrium constant at T and P.

Activity Coefficients

Activity coefficients for cation i, anion l and neutral species n can be calculated as

$$\log \gamma_i = -\frac{A\, z_i^2 \bar{I}^{1/2}}{\Lambda} + \Gamma_\gamma + w_i^{abs} \sum_k b_k y_k \bar{I} + \sum_l \frac{b_{il} \bar{y}_l \bar{I}}{\psi_l} \tag{aI-6}$$

$$\log \gamma_l = -\frac{A\, z_l^2 \bar{I}^{1/2}}{\Lambda} + \Gamma_\gamma + w_l^{abs} \sum_k b_k y_k \bar{I} + \sum_i \frac{b_{il} \bar{y}_i \bar{I}}{\psi_i} \tag{aI-7}$$

$$\log \gamma_n = \Gamma_\gamma + w_n \sum_k b_k y_k \bar{I} + \sum_i \frac{b_{ni} \bar{y}_i \bar{I}}{\psi_i} + \sum_l \frac{b_{nl} \bar{y}_l \bar{I}}{\psi_l} \tag{aI-8}$$

where A is the Debye-Hückel parameter, z is the ionic charge, $\bar{I}$ is the effective ionic strength, and b_{il}, b_{ni}, and b_{nl} are the short-range interaction parameters. Γ_γ is a mole fraction/molality conversion factor:

$$\Gamma_\gamma = -\log(1 + 0.0180153 m') \tag{aI-9}$$

m' is the sum of molalities of all solute species.

The activity coefficient for the *k-th* component consisting of the *i-th* and *l-th* ions is

$$\log \gamma_{\pm,k} = -\frac{A\, |z_i z_l| \bar{I}^{1/2}}{\Lambda} + \Gamma_\gamma + \frac{w_k}{v_k} \sum_k b_k y_k \bar{I} + \frac{v_{i,k}}{v_k} \sum_l \frac{b_{il} \bar{y}_l \bar{I}}{\psi_l} + \frac{v_{l,k}}{v_k} \sum_i \frac{b_{il} \bar{y}_i \bar{I}}{\psi_i} \tag{aI-10}$$

where

$$\Lambda = 1 + \mathring{a}_k b \bar{I}^{\frac{1}{2}} \tag{aI-11}$$

$$\psi_i = \frac{Z_i^2}{2} \tag{aI-12}$$

$$\psi_k = \frac{\sum_i v_{i,k} Z_i^2}{2} = \sum_i v_{i,k} \psi_i \tag{aI-13}$$

$$b_k = \frac{w_k}{\psi_k} \cdot 10^{-11} \tag{aI-14}$$

$$y_i = \frac{\psi_i m_{t,i}}{I} = \frac{\psi_i \sum_k v_{i,k} m_k}{I} \tag{aI-15}$$

$$y_k = \frac{\psi_k m_k}{I} \tag{aI-16}$$

$\bar{y}_i$ is defined in the same way as y_i, but using $\bar{I}$ instead of I. Equations aI-12 and aI-15 can be applied to cations and anions. b is the Debye-Hückel B parameter, and $\mathring{a}_k$ is an ion size parameter for the electrolyte.

The equations summarized above permit calculation of activity coefficients in mixed as well as single electrolytes at 25°C and 1 bar. Complex equations depending on $T, P, T_0, P_0, a_i, \Theta,$

Ψ, w, Y, and c_i, among other variables, are used to calculate the short-range interaction parameters at any other temperature and pressure.

Calculations Performed

Most of the work performed by Helgeson is focused on binary systems. He did not report any result for ternary or higher order systems in the papers reviewed (Helgeson and Kirkham, 1974a, b, 1976, Shock and Helgeson, 1988, Helgeson et al., 1981, Pokrovskii et al., 1997a, b, Sverjensky et al., 1997). Some work was performed trying to reproduce some of those binary results, but the agreement between experimental and calculated data was not good. Figures aI-1 and aI-2 show the calculations for the binary systems NaCl-H_2O and NaOH-H_2O. DH-Helgeson refers to the first term of equation aI-10, while Helgeson refers to the addition of all the terms in equation aI-10.
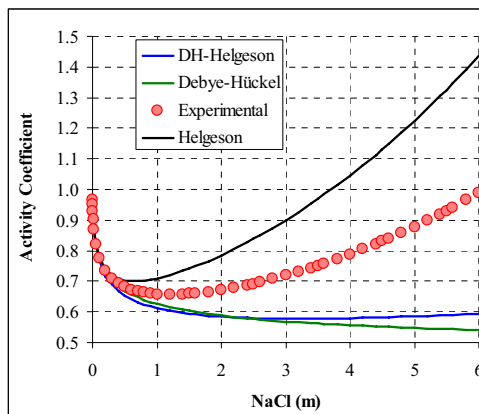

Figure aI-1. Mean activity coefficient for the system NaCl-H_2O at 25°C and 1 bar.
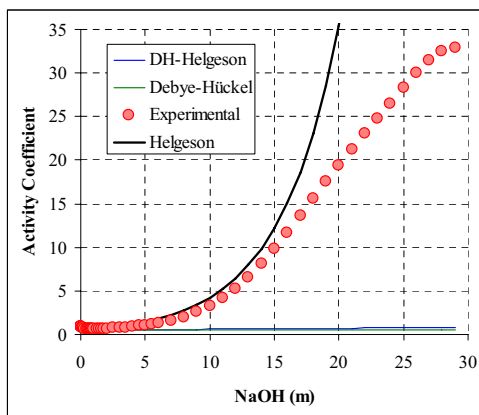

Figure aI-2. Mean activity coefficient for the system NaOH-H_2O at 25°C and 1 bar.

Apart from the impossibility to reproduce Helgeson's results, the final number of parameters required to implement Helgeson's approach is rather large. Such number increases considerably when the temperature and pressure are different from 25°C and 1 bar. Many of the required parameters were not available for most of the scaling minerals of interest in the present work. Therefore, the use of Helgeson's framework for the purpose of the present Ph.D. is not a recommendable choice, and it does not report any advantage when compared to extended UNIQUAC.

Bromley's Model

The great achievement of the model proposed by Bromley is the use of just one interaction parameter for each salt. Many of those parameters are reported in literature (Zemaitis et al., 1986, Borge et al., 1996, Belaustegi et al., 1998, Raposo et al., 1998).

Chaiko et al. (1988) assure that Bromley's method often works well for both single and multicomponent electrolyte solutions at ionic strengths lower than 6 m. Zhaoyue et al. (1995) compared Bromley's model with Pitzer's model for binary systems at temperatures in the range 15-25°C, and 1 bar. In general, Pitzer's method performs better, but in some systems the agreement between Bromley's estimations and experimental data was very close. Nonetheless, in many other systems Bromley's model can lead to significant over or under estimation.

The molal activity coefficient of ion i in a multicomponent solution at 25°C can be expressed as (Zemaitis et al., 1986).

$$\ln \gamma_i = -\frac{A z_i^2 I^{1/2}}{1 + I^{1/2}} + F_i \tag{aI-17}$$

where A is the Debye-Hückel constant, I the ionic strength, and z_i the charge of ion i. F_i is a summation of interaction parameters. The first term on the right hand side of equation aI-17 is the Debye-Hückel activity coefficient, used in a mol fraction scale, while the second term is given in a molal scale. Therefore, there is some incongruence related to the units chosen for equation aI-17.

$$F_i = \sum_l \dot{B}_{il} z_{il}^2 m_l \tag{aI-18}$$

$$F_l = \sum_i \dot{B}_{il} z_{il}^2 m_i \tag{aI-19}$$

where subscript i denotes cation and l anion

$$z_{il} = \frac{z_i + z_l}{2} \tag{aI-20}$$

The terms $\dot{B}$ are calculated as

$$\dot{B}_{il} = \frac{(0.06 + 0.6 B_{il}) |z_i z_l|}{\left(1 + \frac{1.5}{|z_i z_l|} I\right)^2} + B_{il} \qquad \textbf{(aI-21)}$$

B_{il} is a parameter accounting for ion-ion interactions.

The equations presented above do not take into account interactions between two ions with the same charge, or any higher order interactions.

For molecular species n, Setschénow equation is used:

$$\ln \gamma_n = \ln\left(\frac{m_n^0}{m_n}\right) = k m_s \qquad \textbf{(aI-22)}$$

where m_n^0 is the solubility of the gas in pure water, m_n the solubility of the gas in the multicomponent solution, k the salting out parameter, and m_s the molality of the salt in the solution.

The water activity for a single electrolyte solution can be calculated from the osmotic coefficient as

$$\ln a_w^0 = -\frac{M_s \nu m}{1000} \Phi \qquad \textbf{(aI-23)}$$

where M_s is the molecular weight of the solvent, m represents the electrolyte molality, and ν is the number of ions the electrolyte dissociates into. To calculate the water activity of a multicomponent solution it is necessary to apply equation aI-23 to each electrolyte present in the mixture. Once these values are obtained, the method suggested by Meissner and Kusik can be used (Zemaitis et al., 1986):

$$\log(a_w)_{mix} = \sum_i \sum_l W_{il} \log(a_w^0)_{il} + r \qquad \textbf{(aI-24)}$$

where $(a_w^0)_{il}$ is the hypothetical pure solution water activity for electrolyte il. Further information about the calculation of W_{il} and r can be found in Zemaitis et al. (1988).

The temperature dependence of the activity coefficient presented by Bromley is accounted by two terms: The Debye-Hückel A parameter, and the B parameter. Bromley presented two alternative equations to correlate the effect of temperature on B, including four additional parameters

$$B = B_1 \ln \frac{T - 243}{T} + \frac{B_2}{T} + B_3 + B_4 \ln T \qquad \textbf{(aI-25)}$$

$$B = \frac{B_1}{T - 230} + \frac{B_2}{T} + B_3 + B_4 \ln T \qquad \textbf{(aI-26)}$$

It is believed the use of Bromley's model is not adequate for multicomponent solutions, since it employs the concept "molality of the electrolyte" in equation aI-23 to calculate water activity. That term can lead to confussion and different results depending on the interpretation given to the system and the electrolytes considered to be formed (i.e., a system formed by K^+, Na^+, Cl^- and SO_4^- can be regarded as a mixture of NaCl and K_2SO_4; or Na_2SO_4 and KCl; or NaCl, K_2SO_4, and KCl, etc). Table aI-1 shows different result which can be obtained using the concept of "molality of the electrolyte" for a multicomponent solution formed by $CaCl_2$, $CaSO_4$, NaCl, and Na_2SO_4, even though the total concentrations of the species are constant (4 m Ca^{2+}, 2 m Na^+, 3 m Cl^-, and 3.5 m SO_4^-).

Table aI-1
Different "molality of the electrolyte" results for a common-ion solution

	Solution 1		Solution 2	
	Cation (m)	Anion (m)	Cation (m)	Anion (m)
$CaCl_2$	1	2	0.75	1.5
$CaSO_4$	3	3	3.25	3.25
NaCl	1	1	1.5	1.5
Na_2SO_4	1	0.5	0.5	0.25

References in Appendix I

Belaustegi, Y., Olazabal, M. A., Madariaga, J. M., 1999. Development of a Modified Bromley's Methodology for the estimation of ionic media effects on solution equilibria. Part 4. The chemical model of Fe(III) with the halide ligands in aqueous solution at 25ºC Fluid Phase Equilibria 155, 21-31.

Borge, G., Castaño, R., Carril, M. P., Corbillón, M. S., Madariaga, J. M., 1996. Development of a Modified Bromley's Methodology (MBM) for the estimation of ionic media effects on solution equilibria Part 1. Calculation of the interaction parameters in the molar and molal scales at 25ºC Fluid Phase Equilibria, 121, 85-98.

Bromley, L.A., 1973. Thermodynamic properties of strong electrolytes in aqueous solutions. AIChE Journal 19, 313-320.

Chaiko, D.J., Fredrickson, D.R., Reichley-Yinger, L., Vandegrift, G.F., 1988. Separation Science and Technology 23, 1435-1451.

Helgeson, H.C., 1967. Thermodynamics of complex dissociation in aqueous solutions at elevated temperatures. J. Phys. Chem. 71, 3121-3136.

Helgeson, H.C., 1969. Thermodynamics of hydrothermal systems at elevated temperatures and pressures. Amer. J. Sci. 267, 729-804.

Helgeson, H.C., 1970. Calculation of mass transfer in geochemical process involving aqueous solutions. Geochimica et Cosmochimica Acta 34, 569-592.

Helgeson, H.C., Kirkham, D.H., 1974 a. Theoretical prediction of the thermodynamic behaviour I. American Journal of Science 274, 1089-1198.

Helgeson, H.C., Kirkham, D., 1974 b. Theoretical prediction of the thermodynamic behaviour of aqueous electrolytes at high pressures and temperatures: II. Debye-Hückel parameters for activity coefficients and relative partial molal properties. Amer. J. Sci. 274, 1199-1261.

Helgeson, H.C., Kirkham, D.H., 1976. Theoretical prediction of the thermodynamic behaviour III American Journal of Science 276, 97-240.

Helgeson, H.C., Delany, J.M., Nesbitt, H., Wayne; B., Dennis, K., 1978. Summary and critique of the thermodynamic properties of rock-forming minerals. Pp 229

Helgeson H.C., Kirkham D.H., Flowers G.C., 1981. Theoretical prediction of the thermodynamic behaviour IV. American Journal of Science 281, 1249-1516.

Johnson, J.W., Oelkers, E.H., Helgeson, H.C., 1992. SUPCRT92: A software package for calculating the standard molal thermodynamic properties of minerals, gases, aqueous species, and reactions from 1 to 5000 bar and 0 to 1000ºC. Computers and Geosciences 18, 899-947.

Pokrovskii, V.A., Helgeson, H.C., 1997a. Thermodynamic Properties of Aqueous Species and the Solubilities of Minerals at High Pressures and Temperatures: The System Al_2O_3-H_2O-KOH. Chemical Geology 137, 221-242.

Pokrovskii, V.A., Helgeson, H.C., 1997b. Geochimica et Cosmochimica Acta 61, 2175-2183.

Raposo, J. C., Sanz, J., Borge, G., Olazábal, M. A., Madariaga, J. M., 1998. Fluid Phase Equilibria 155, 1-19.

Shock, E.L., Helgeson, H.C., 1988. Calculation of the thermodynamic and transport properties. Geochimica et Cosmochimica Acta 52, 2009-2036.

Sverjensky, D.A., Shock, E.L., Helgeson, H.C., 1997. Geochimica et Cosmochimica Acta 61, 1359-1412.

Tanger, J. C., Helgeson, H. C., 1988. American Journal of Science, 288, 19-98.

Zhaoyue, M., Seinfeld, J.H., Saxena, P., Kim, Y.P., 1995. Aerosol Science and Technology 23, 131-154.

Zemaitis, J. F. Jr., Clark, D. M., Rafal, M., Scrivner, N. C., 1986. Handbook of aqueous electrolyte thermodynamics, design institute for physical property data, New York.

Appendix II: Conductivity Measurements

In this Appendix, complementary data and results for the conductivity measurements performed for $SrSO_4$-H_2O solutions and presented in Chapter 8 are included.

The amount of initial salt and distilled water used in the preparation of the starting celestite ($SrSO_4$) solutions for the different conductivity measurements are reported in table aII-1. The added water flow rate can also be seen there.

Table aII-1
Experimental conditions

Experiment	$SrSO_4$ (g)	$V_{initial}$ (mL)	$rate$ (mL·min^{-1})
1	0.0711	500	0.2
2	0.0718	500	0.2
3	0.0787	500	0.2

Figure aII-1 and aII-2 show the results obtained for experiment 1. A relatively flat zone corresponding to a total solution volume around 510-530 mL is observed. From that point, the conductivity decreases continuously. This could be interpreted as the result of a dilution process. Nevertheless, the first measurements in figure aII-1 show an unexpected positive slope. The increasing conductivity with volume must be explained as a dissolution process, consequence of the lack of equilibrium in the original sample. This behaviour manifests the unsuitability of synthetic methods for our purposes as the time to attain equilibrium is too long.

To be completely sure the lack of equilibrium in the original sample was responsible of the positive slope in figure aII-1, a new experiment (experiment 2) was performed. In experiment 2, additional volumes of water were only added once the initial sample was at equilibrium (constant value of conductivity over the time). Stirring was used to accelerate the equilibrium, which was only observed after 20 hours. The results for experiment 2 are shown in figure aII-3.
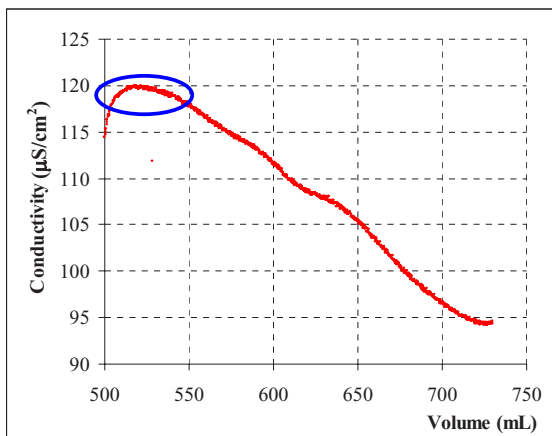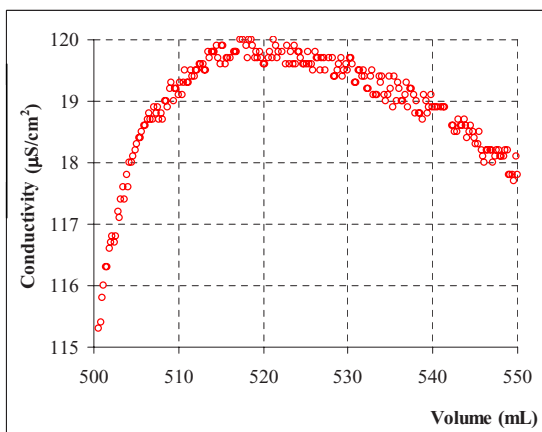
Figure aII-1. Results for experiment 1

Figure aII-2. Results for experiment 1: amplified section of figure aII-1
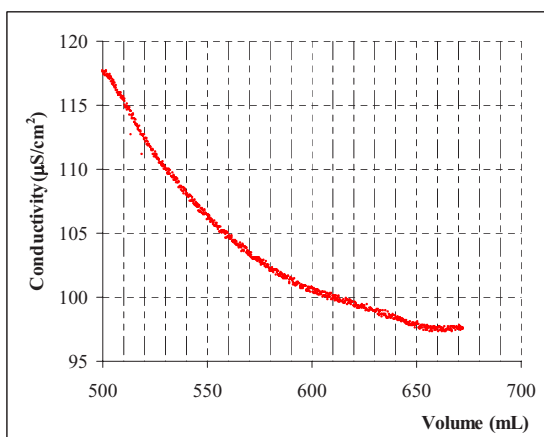
Figure aII-3. Results for experiment 2

Comparing figures aII-1 and aII-3, it is clear the initial increase in conductivity observed in experiment 1 is consequence of a dissolution process.

In figure aII-3, a continuous decrease in conductivity is observed. This can only be explained as a dilution process, meaning that either the original sample was undersaturated (very unlikely) or that the equilibrium is not reached for any of the measurements. The excess of $SrSO_4$ placed in the original sample was calculated according to literature data on the solubility of celestite in pure water. To verify whether undersaturation was the responsible cause of the shape of figure aII-3, a solution containing a rather larger amount of salt in the same initial volume of distilled water was prepared (experiment 3). The new solution was clearly saturated, and some solid particles could be observed at the bottom of the vessel after equilibrium was reached (constant conductivity after stirring the solution for several hours). The results for experiment 3 are shown in figure aII-4.
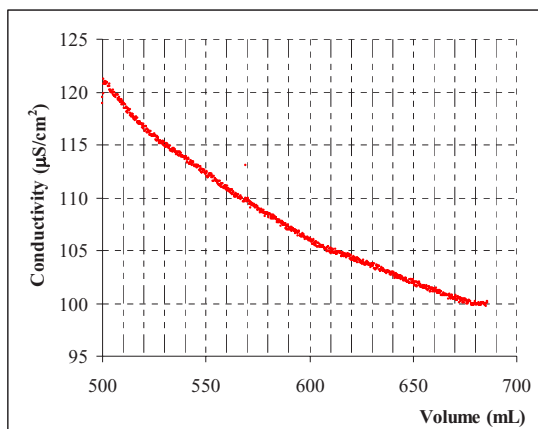
Figure aII.4. Results for experiment 3

Figure aII-4 proves the conductivity continuously decreases when adding more solvent, even though solid phase is present in the vessel. Therefore, this behaviour must be a consequence of kinetic impediments for the $SrSO_4$-H_2O system. It is reported by many authors that alkaline earth metal sulphates have slow dissolution kinetics. Thus, after adding an amount of water, even though such amount is very low, dissolution of solid particles takes several hours and the solution is not allowed to reach equilibrium before the next addition. So, the dilution effect is much faster than the dissolution process, and the former effect is the only one observable in the measurements performed.

References in Appendix II

Bock, J., Bestgen, H., Elschner, S., Preisler, E., 1993. Large shaped parts of melt cast BSCCO for applications in electrical engineering. IEEE Transactions of Applied Superconductivity 3 (1), 1659-1662.

Appendix III: BaSO₄ Solubility in NaCl at High Temperature and Pressure

Appendix III is a complement to Chapter 8 on the solubility of BaSO₄ in sodium chloride solutions at high temperatures and pressures. The experimental conditions used, volumes of solution filtrated, ICP-MS results, and BaSO₄ concentrations are given in tables aIII-1 to aIII-5. Results concerning the system NaCl-H₂O are reported in tables aIII-6 to aIII-9.

The calibration curves used for the ICP-MS measurements for samples 1 to 17 are shown in figure aIII-1. The results from the ICP-MS analysis performed at the Chemistry department of DTU for experiments 1 to 17 are reported in table aIII-1. *SD* stands for standard deviation, and *CV* is the variation coefficient:

$$CV = \frac{SD}{Mean} \cdot 100 \qquad\qquad \textbf{(aIII-1)}$$
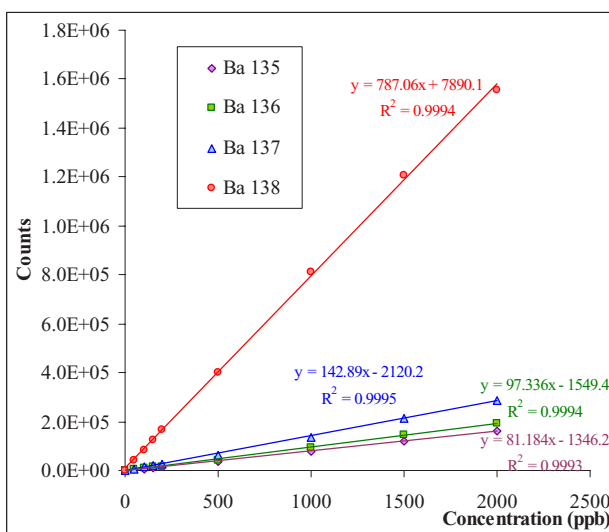
Figure aIII-1. Calibration curves for ICP-MS measurements for experiments 1 to 17

Table aIII-1
ICP-MS results for experiments 1 to 17

Exp.	^{135}Ba (ppb)	^{136}Ba (ppb)	^{137}Ba (ppb)	^{138}Ba (ppb)	Mean (ppb)	SD (ppb)	CV (%)
1	1543.44	1561.01	1550.65	1565.50	**1555.15**	9.98	0.64
2	2072.65	2074.04	2074.08	2021.59	**2060.59**	26.01	1.26
3	1775.02	1789.19	1783.58	1768.95	**1779.18**	8.97	0.50
4	1751.30	1759.40	1754.89	1748.29	**1753.47**	4.79	0.27
5	1353.23	1362.34	1357.52	1386.52	**1364.90**	14.88	1.09
6	1571.53	1574.12	1571.86	1586.50	**1576.00**	7.10	0.45
7	1374.91	1381.44	1381.86	1408.09	**1386.58**	14.69	1.06
8	2009.18	2018.96	2007.12	1957.34	**1998.15**	27.69	1.39
9	2110.26	2118.51	2104.78	2041.09	**2093.66**	35.49	1.70
10	1545.27	1539.47	1545.25	1567.64	**1549.41**	12.46	0.80
11	1412.89	1421.26	1421.17	1451.07	**1426.60**	16.78	1.18
12	2047.93	2041.17	2035.25	1992.80	**2029.29**	24.87	1.23
13	797.32	803.49	802.25	849.12	**813.05**	24.20	2.98
14	746.89	750.06	752.38	799.20	**762.13**	24.81	3.26
15	993.11	995.63	1000.68	1053.01	**1010.61**	28.44	2.81
16	1124.15	1124.57	1129.97	1176.33	**1138.76**	25.19	2.21
17	1289.64	1289.39	1293.20	1327.15	**1299.85**	18.29	1.41
100[a]	218.636677	218.535794	217.793408	223.234442	**219.55**	2.48	1.13

[a] Test-Standard containing 100 ppb Ba^{2+}

The calibration curves used for the second ICP-MS measurements for samples 10 to 17 are shown in figure aIII-2. The results from the second ICP-MS analysis performed at the Chemistry department of DTU for experiments 10 to 17 are reported in table aIII-2.
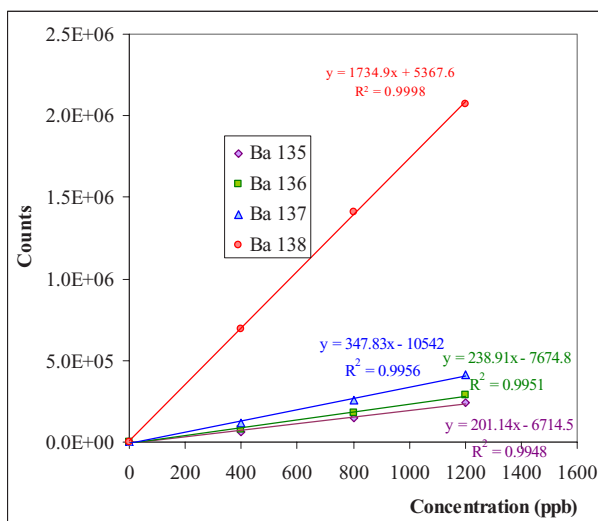

Figure aIII-2. Calibration curves for second ICP-MS measurements for experiments 10 to 17

Table aIII-2
Second ICP-MS results for experiments 10 to 17

Exp.	^{135}Ba (ppb)	^{136}Ba (ppb)	^{137}Ba (ppb)	^{138}Ba (ppb)	Mean (ppb)	*SD* (ppb)	*CV* (%)
10	1825.62	1817.95	1802.62	1564.02	1752.55	126.05	7.19
11	1507.72	1507.30	1486.31	1373.16	1468.62	64.42	4.39
12	1895.46	1886.21	1864.30	1618.33	1816.08	132.48	7.29
13	997.13	1000.65	999.37	1000.36	999.38	1.60	0.16
14	856.36	857.56	852.97	880.85	861.94	12.76	1.48
16	1087.37	1091.83	1089.58	1076.24	1086.26	6.92	0.64
16	1038.46	1035.54	1034.72	1031.45	1035.04	2.88	0.28
17	1137.17	1134.62	1127.53	1107.70	1126.75	13.34	1.18
100[a]	162.53	162.88	162.20	162.23	162.46	0.32	0.20
500[b]	646.86	651.46	650.38	690.01	659.68	20.32	3.08
1000[c]	1291.24	1298.00	1291.62	1230.42	1277.82	31.75	2.48
100_2[d]	188.83	188.82	189.57	194.02	190.31	2.50	1.31

[a] Standard containing 100 ppb of Ba^{2+} in 0.1% NaCl solution
[b] Standard containing 500 ppb of Ba^{2+} in 0.1% NaCl solution
[c] Standard containing 1000 ppb of Ba^{2+} in 0.1% NaCl solution
[d] Commercial standard containing 100 ppb of Ba^{2+}.

Table aIII-3
Laboratory ICP-MS results for experiments 1 to 17 and test-standards

Exp.	Ba (μg L^{-1})	*CV* (%)
1	1700	1.6
2	1400	1.6
3	1300	1.6
4	1300	1.6
5	1200	1.6
6	1300	1.6
7	1400	1.6
8	1200	1.6
10	3600	1.6
11	1300	1.6
12	2900	1.6
13	850	1.6
14	720	1.6
16	910	1.6
16	880	1.6
17	980	1.6
500[a]	1100	1.6
1000[a]	1600	1.6
1500[a]	2000	1.6
2000[a]	2400	1.6
2500[a]	3700	1.6

[a] Standards in 0.1 % NaCl. Their Ba^{2+} concentration corresponds to the value given in table aIII-3.

The sample volumes filtrated in the experiments, the mass of water placed in the dilution vessel and the final barite concentration calculated from the ICP-MS results is reported in table aIII-4 for experiments 1 to 8, and in table aIII-5 for experiments 10 to 18.

Table aIII-4
Experimental variables and calculated concentrations for experiments 1 to 9

Exp.	Time (h)	V$_{filtrated}$ (mL)	Dilution mass (g)	ICP-MS$_{DTU1}$ (ppb)	BaSO$_{4,DTU1}$ (m)	ICP-MS$_{Lab}$ (µg L^{-1})	BaSO$_{4,Lab}$ (m)
1	4	74.18	30.03	1555.15	6.34E-05	1700	6.92E-05
2	4[a]	74.43	30.11	2060.59	8.39E-05	1400	5.69E-05
3	6[a]	74.32	30.07	1779.18	7.25E-05	1300	5.29E-05
4	2[a]	74.81	30.20	1753.47	7.14E-05	1300	5.28E-05
5	3	74.81	30.22	1364.90	5.55E-05	1200	4.87E-05
6	2[b]	74.41	30.13	1576.00	6.41E-05	1300	5.28E-05
7	2	74.16	30.09	1386.58	5.64E-05	1400	5.68E-05
8	6[a]	74.67	30.23	1998.15	8.11E-05	1200	4.86E-05
9	9[a]	75.98	30.47	2093.66	8.52E-05	3600	1.46E-04

Table aIII-5
Experimental variables and calculated concentrations for experiments 10 to 18

Exp.	Time (h)	V$_{filtrated}$ (mL)	Dilution mass (g)	ICP-MS$_{DTU1}$ (ppb)	BaSO$_{4,DTU1}$ (m)	ICP-MS$_{DTU2}$ (ppb)	BaSO$_{4,DTU2}$ (m)	ICP-MS$_{Lab}$ (µg L^{-1})	BaSO$_{4,Lab}$ (m)
10	12[a]	74.88	30.30	1549.41	6.29E-05	1752.55	7.1096E-05	3600	1.46E-04
11	16[a]	74.72	30.28	1426.60	5.78E-05	1468.62	5.9539E-05	1300	5.26E-05
12	4[a]	74.93	30.34	2029.29	8.22E-05	1816.08	7.3582E-05	2900	1.17E-04
13	6[a]	89.90	22.12	813.05	6.18E-05	999.38	7.5961E-05	850	6.45E-05
14	6	102.05	23.04	762.13	5.96E-05	861.94	6.7399E-05	720	5.62E-05
15	6	106.01	23.01	1010.61	8.17E-05	1086.26	8.7837E-05	910	7.34E-05
16	9[a]	105.15	23.06	1138.76	9.11E-05	1035.04	8.2812E-05	880	7.02E-05
17	5	104.57	22.77	1299.85	1.06E-04	1126.76	9.1815E-05	980	7.97E-05
18	7	105.19	23.02			986.61	7.9207E-05	780	6.25E-05

[a] Apart form the agitation time reported in table aIII-5, the solution was kept at constant temperature and pressure with no agitation for another 16 h.
[b] Apart form the agitation time reported in table aIII-5, the solution was kept at constant temperature and pressure with no agitation for another 44 h.

Table aIII-6 reports the NaCl concentration found in samples that have been agitated for different periods of time. The experimental samples were diluted with distilled water (the dilution rate is reported in the third column of table aIII-6), and the concentration of NaCl (C_{NaCl}) was determined by titration with AgNO$_3$ 0.1 M:

$$C_{NaCl} = \frac{C_{AgNO_3} \cdot V_{AgNO_3}}{V'_{NaCl}} \tag{aIII-2}$$

where V_{AgNO_3} is the volume of AgNO$_3$ used in the titration, and V'_{NaCl} is the volume of the undiluted NaCl sample (i.e., if the dilution rate is 5:250, $V'_{NaCl} = 5V_{NaCl}/250$).

Table aIII-6
Determination of the time required to attain equilibrium for the system NaCl-H$_2$O at 30ºC and 1 atm using agitation (vibration)

Exp.	Time (min)	Dilution NaCl:H$_2$O	V_{AgNO3_1} (mL)	V_{AgNO3_2} (mL)	V_{NaCl} (mL)	NaCl (M)	SD (M)
NaCl_1	0	5:250	1.9	1.9	2	4.85	0.00
NaCl_2	15	5:250	2.2	2.2	2	5.61	0.00
NaCl_3	30	5:250	2.1	2.1	2	5.36	0.00
NaCl_4	60	4:250	1.7	1.7	2	5.42	0.00
NaCl_5	90	1:100	2.6	2.6	5	5.30	0.00
NaCl_6	120	2:500	0.4	0.45	2	5.42	0.45
NaCl_7	150	8:500	1.6	1.8	2	5.42	0.45
NaCl_8	270	5:250	5.4	5.3	5	5.51	0.07
NaCl_9	330	5:250	5.2	5.2	5	5.36	0.00

Table aIII-7
Determination of the time required to attain equilibrium for the system NaCl-H$_2$O at 30ºC and 1 atm without using agitation

Exp.	Time (h)	Dilution NaCl:H$_2$O	V_{AgNO3} (mL)	C_{AgNO3} (M)	V_{NaCl} (mL)	NaCl (M)
NaCl_10	1	10:100	91.2	0.05	15	3.04
NaCl_11	3	5:250	9.5	0.1	10	4.75
NaCl_12	5	5:250	9.0	0.1	10	4.50
NaCl_13	7	5:250	10.7	0.1	10	5.35
NaCl_14	23	5:250	5.4	0.1	5	5.40

Table aIII-8
NaCl solubility in pure water at 30ºC

Exp.	P (bar)	$V_{filtrated}$ (mL)	Dilution mass (g)	Dilution NaCl:H$_2$O	V_{AgNO3_1} (mL)	V_{AgNO3_2} (mL)	V_{AgNO3_3} (mL)	V_{NaCl} (mL)	NaCl (M)	SD (M)
NaCl_15	100	36.23	86.885	10:100	2.7	2.6	2.6	2	6.60	0.14
NaCl_16	300	45.05	60.035	10:100	4.4	4.4	4.3	2.5	5.52	0.07
NaCl_17	300	50.17	75.249	20:200	3.25	3.3	3.3	2	5.38	0.05
NaCl_18	400	45.14	75.487	10:100	3.0	3.1	3.1	2	5.53	0.10
NaCl_19	400	45.16	75.744	10:100	3.2	3.2	3.3	2	5.84	0.10
NaCl_20	400	41.03	75.113	10:100	2.9	3.0	2.9	2	5.80	0.11

Table aIII-9
NaCl solubility in pure water at 100ºC

Exp.	P (bar)	$V_{filtrated}$ (mL)	Dilution mass (g)	Dilution NaCl:H$_2$O	V_{AgNO3_1} (mL)	V_{AgNO3_2} (mL)	V_{AgNO3_3} (mL)	V_{NaCl} (mL)	NaCl (M)	SD (M)
NaCl_21	100	44.78	71.82	10:100	3.4	3.5	3.5	2	6.89	0.11
NaCl_23	100	40.49	74.92	5:100	1.9	1.9	1.9	2.5	6.87	0.00
NaCl_24	300	45.17	65.72	10:100	5.5	5.5	5.7	3	6.88	0.13
NaCl_25	300	41.24	75.72	5:100	0.7	0.8	0.8	1	6.80	0.47
NaCl_26	500	36.78	74.02	5:100	1.5	1.55	1.5	2	7.45	0.13
NaCl_27	500	42.08	75.45	5:100	2.35	2.3	2.3	3	6.65	0.08
NaCl_28	500	45.12	74.48	10:100	8.65	8.45	8.55	5	6.82	0.07
NaCl_29	500	45.18	74.42	10:100	9.05	9.1	9.3	5	7.28	0.09
NaCl_30	500	45.19	73.40	10:100	9.3	9.35	9.3	5	7.35	0.02
NaCl_31	500	36.47	74.20	10:100	3.45	3.4	3.4	2.5	6.79	0.05

Figure aIII-3. Experimental setup

Figure aIII-4. Experimental Setup II

Ada Villafáfila García

Measurement and Modeling of Scaling Minerals